-Programa de Doctorado en Neurociencias-

Instituto de Neurociencias UMH-CSIC

Role of PI3K/Akt/Pten in tumorigenesis:

A link between inflammation and reprogramming of the host metabolism

Memoria de Tesis Doctoral presentada por:

Lucía García López

-2020-

Directora de Tesis:

María Domínguez Castellano

Codirector de Tesis:

Santiago Nahuel Villegas

INSTITUTO DE NEUROCIENCIAS

EXCELENCIA SEVERO OCHOA

Centro de Excelencia «Severo Ochoa» 2014-2018

Sant Joan d'Alacant, 16 de Diciembre de 2020

To whom it may concern,

The doctoral thesis entitled "Role of PI3K/Akt/Pten in tumorigenesis: A link between inflammation and reprogramming of the host metabolism" has been developed by myself, Lucía García López. This thesis is presented in a conventional format. It is based on experimental studies undertaken at the Neuroscience Institute of Alicante during the PhD program in neuroscience of the Miguel Hernández University.

Yours sincerely,

Lucía García López

Sant Joan d'Alacant, 9 de Febrero de 2021

To whom it may concern,

The doctoral thesis entitled "Role of PI3K/Akt/Pten in tumorigenesis: A link between inflammation and reprogramming of the host metabolism" has been developed by myself, Lucía García López. This thesis includes the following publication, of which I am the third author. I declare that the publication has not been used and will not be used in any other thesis in agreement with my thesis director Dr. María Domínguez Castellano and my thesis co-director Dr. Santiago Nahuel Villegas Nieto:

- Santiago Nahuel Villegas, Rita Gombos, Lucia García-López, Irene Gutiérrez-Pérez, Jesús García-Castillo, Diana Marcela Vallejo, Vanina Gabriela Da Ros, Esther Ballesta-Illán, József Mihály and Maria Dominguez. "PI3K/Akt Cooperates with Oncogenic Notch by Inducing Nitric Oxide-Dependent Inflammation". (2018). Cell Reports 22, 2541–2549. doi.org/10.1016/j.celrep.2018.02.049

Yours sincerely,

Lucía García López

Dra. María Domínguez Castellano

Dr. Santiago Nahuel Villegas Nieto

Sant Joan d'Alacant, 16 de Diciembre de 2020

A quien corresponda:

Dña. María Domínguez Castellano, Profesora de Investigación del Consejo Superior de Investigaciones Científicas (CSIC),

AUTORIZA la presentación de la Tesis Doctoral titulada "Role of PI3K/Akt/Pten in tumorigenesis: A link between inflammation and reprogramming of the host metabolism", realizada por Dña. Lucía García López (DNI 74013330 C), bajo mi inmediata dirección y supervisión como directora de su tesis Doctoral en el Instituto de Neurociencias (CSIC-UMH) y que presenta para la obtención del grado de Doctor por la Universidad Miguel Hernández.

Y para que conste, a los efectos oportunos, firma el presente certificado.

Fdo. María Domínguez Castellano

m.dominguez@umh.es
www.ina.umh.es
Tel: +34 965 919390
Fax: +34 965 919561
Fax: +34 965 919561
Av Ramón y Cajal s/n
Campus de San Juan
03550 SAN JUAN DE ALICANTE– ESPAÑA

Sant Joan d'Alacant, 9 de Febrero de 2021

A quien corresponda:

D. Santiago Nahuel Villegas Nieto, Director Científico de My Personal Therapeutics (MPT),

AUTORIZA la presentación de la Tesis Doctoral titulada "Role of PI3K/Akt/Pten in tumorigenesis: A link between inflammation and reprogramming of the host metabolism", realizada por Dña. Lucía García López (DNI 74013330 C), bajo mi inmediata dirección y supervisión como codirector de su tesis Doctoral en el Instituto de Neurociencias (CSIC-UMH) y que presenta para la obtención del grado de Doctor por la Universidad Miguel Hernández.

Y para que conste, a los efectos oportunos, firma el presente certificado.

Fdo. Santiago Nahuel Villegas Nieto

nahuel@mypersonaltherapeutics.com
www.mypersonaltherapeutics.com
My Personal Therapeutics
The Westworks, White City Place
Unit 5, Part First Floor
195 Wood Lane
London W12 7FQ

Sant Joan d'Alacant, 9 de Febrero de 2021

A quien corresponda:

Dña. Elvira De la Peña García, Profesora titular de la Universidad Miguel Hernández (UMH) y Coordinadora del programa de doctorado en Neurociencias del Instituto de Neurociencias de Alicante, centro mixto de la Universidad Miguel Hernández (UMH) y de la Agencia Estatal Consejo Superior de Investigaciones Científicas (CSIC),

CERTIFICA:

Que la Tesis Doctoral titulada "Role of PI3K/Akt/Pten in tumorigenesis: A link between inflammation and reprogramming of the host metabolism" ha sido realizada por Dña. Lucía García López (DNI 74013330 C), bajo la dirección y supervisión de Dña. María Domínguez Castellano como directora y D. Santiago Nahuel Villegas Nieto como codirector, y da su conformidad para que sea presentada a la comisión de Doctorado de la Universidad Miguel Hernández.

Y para que conste, a los efectos oportunos, firma el presente certificado.

Fdo. Elvira De la Peña García

Coordinadora Programa de Doctorado en Neurociencias

elvirap@umh.es
www.ina.umh.es
Tel: +34 965 91 9540
Fax: +34 965 91 9549
Av Ramón y Cajal s/n
Campus de San Juan
03550 SAN JUAN DE ALICANTE–ESPAÑA

Financiación/Subvención/Beca:

Este trabajo de Tesis Doctoral ha sido posible gracias a una beca predoctoral de Formación de Personal Investigador (FPI), financiada por el Ministerio de Economía y Competitividad (MINECO) con referencia BES-2015-073796, un contrato de titulado superior en actividades técnicas y profesionales financiado por la Agencia Estatal de Investigación, y un contrato de apoyo técnico a la investigación financiado a través del programa PROMETEO. La investigación ha sido financiada por los siguientes proyectos:

"Neural mechanisms in Body Size Regulation" – SEV-2013-0317

"Mechanisms orchestrating the control of organ size and neurogenesis - BFU2016-76295-R.

"Cáncer mecanismos y posibles terapias (cancerMEC y TERAP)" – Prometeo/2017/146

A mis padres y hermanos,

A Dani y Alberto

Index

1. Abbreviations

2-DG: 2-Deoxy-D-glucose

3-HAA: 3-hydroxyanthranilic acid

3-HK: 3-hydroxykynurenine

5-HT: 5-hydroxytryptamine, serotonin

5-HTP: 5-hydroxytryptophan

acetyl-CoA: acetyl coenzyme A

ADP: adenosine diphosphate

AhR: aryl hydrocarbon receptor

Ala: alanine

AMP: adenosine monophosphate

AMPs: antimicrobial peptides

ATP: Adenosine triphosphate

ATPβsyn: beta subunit of the ATP synthase

CAT: catalase

cDNA: complementary DNA

cn: cinnabar

COX: citocrome *c* oxidase

COX: cyclo-oxygenases

D2HG: D-2-hydroxyglutarate

DHEA: dehydroepiandrosterone

***Dl**: delta*

DNA: deoxyribonucleic Acid

ETC: electron transport chain

***ey**: eyeless*

FACS: Fluorescence-activated Cell Sorting

$FADH_2$: flavin adenine dinucleotide

GC-MS: Gas Chromatography coupled to Mass Spectrometry

GFP: green fluorescent protein

GLUT: glucose transporter

GPCR: G Protein-coupled receptor

GSH: glutathione

GSIs: γ-secretase inhibitors

GSK3: glycogen synthase kinase-3

HIF-1: hypoxia-inducible factor–1

IA: indoleacrlylic acid

IAA: indoleacetic acid

IDH: isocitrate dehydrogenase 1 or 2

IDO indoleamine-2,3-dioxygenase

IGF-1: insulin growth factor 1

IHC: inmunohistochemistry

InR: insulin receptor

JNK: c-Jun N-terminal kinase; **pJNK**: JNK phosphorilated

K: kynurenine

KA: kynurenic acid

KMO: kynurenine 3-monooxygenase

KP: kynurenine pathway

KYAT: kynurenine aminotransferases

LC-MS: Liquid Chromatography coupled to Mass Spectrometry; **UHPLC:** ultra-high precision liquid chromatography

LOPAC1280: Library of Pharmacologically Active Compounds

LOX: lipoxygenase

LPS: lipopolysaccharide

Met: methionine

mTOR: mammalian target of rapamycin

NADPH: nicotinamide adenine dinucleotide

NF-κB: nuclear factor-κB

NICD: Notch intracellular domain

NMDA: N-methyl-D-aspartate receptors

NMDA: N-methyl-D-aspartate receptors

NO: nitric oxide**; NOS**: nitric oxide synthase

NSAIDs: nonsteroidal anti-inflammatory drugs

OXPHOS: oxidative phosphorylation

PBS: phosphate-buffered *saline*

PDK1: phosphatidyl inositoldependent kinase-1

PFA: paraformaldehyde

PH3: phospho-histone H3

PHGDH: phosphoglycerate dehydrogenase

PI3K: phosphatidylinositol 3-kinase

PIP3: phosphatidylinositol (3,4,5)-trisphosphate

PPO: prophenoloxidase

PPP: pentose phosphate pathway

PRRs: pattern recognition receptors

PTEN: phosphatase and tensin homolog

QA: quinolinic acid

qPCR: quantitative Polymerase Chain Reaction; **RT-qPCR**: Real Time qPCR

Rel: reticuloendotheliosis transcription factor

RFP: red fluorescent protein

RNA: ribonucleic Acid

RNAi: RNA interference

ROS: reactive oxygen species

RT: room ttemperature

RTK: tyrosin-kinase receptor

sima: similar

SOD1: superoxide dismutase 1

SREBP: sterol regulatory element–binding protein

ss: spineless

st: scarlet

T-ALL: T cell Acute Lymphoblastic Leukemia

TAMs: tumor-associated macrophages

TCA: tricarboxylic acid cycle

TDO: tryptophan-2,3-dioxygenase

Thr: threonine

Trh: tryptophan hydroxylase

Trp: tryptophan

v: vermilion

w: white

XanA: xanthurenic acid

2. Abstract

Although cancer begins locally, symptoms associated with disease progression can be manifested systemically and be extremely debilitating for the patient. Identifying the genes that drive and mediate both local and systemic effects of tumorigenesis is important not only for developing treatments aimed at targeting cancer, but also for maintaining and improving patient quality of life. Here we use a multidisciplinary approach to uncover new mechanisms underlying Notch-PI3K/Akt-driven tumorigenesis in a well-established cancer paradigm in *Drosophila melanogaster* with highly predictive value (Palomero *et al.,* 2007; Villegas *et al.*, 2018). First, we designed an unbiased *in vivo* chemical screen to identify drugs that can selectively dampen this oncogenic cooperation without side effects. We identified a novel nitric oxide-dependent inflammatory pathway that is associated with Notch/Pten-dependent oncogenesis and perhaps amenable to pharmacological intervention.

On the other hand, phospho-proteomic analysis of these tumors revealed that aberrant PI3K/Akt signaling fuels Notch tumorigenesis in part by triggering mitochondrial dysfunction and generating oxidative stress. Our results also indicate that stress-activated Jnk signal might be restricting tumor progression by inducing apoptosis, and therefore acting as a tumor suppressor in this context.

Surprisingly, we found that Notch-PI3K/Akt tumors not only consume high amounts of glucose, but also remotely alter whole-body metabolism. High throughput large-scale and tissue-specific metabolomics revealed an unexpected interplay between the tumor and the host tryptophan-kynurenine metabolism, especially in the fat body, which ultimately leads to a systemic inflammation. Moreover, we detected changes related to tryptophan metabolism in the hemolymph, gut microbiota and brain of tumor-bearing hosts, further confirming for the first time that tumors can induce a multi-organ metabolic reprogramming. Consequently, diet supplementation with tryptophan was sufficient to prevent tumor formation through different multi-layered mechanisms. These findings could have important implications, since dietary interventions may hold the promise for the development of better treatments against cancer.

Resumen

Aunque el cáncer comienza localmente, los síntomas asociados con la progresión de la enfermedad pueden manifestarse sistémicamente y ser extremadamente debilitantes para el paciente. Identificar los genes que impulsan y median tanto los efectos locales como sistémicos derivados de la tumorigénesis es importante no sólo para desarrollar tratamientos contra el cáncer, sino también para mejorar la calidad de vida del paciente. En este estudio hemos utilizado un enfoque multidisciplinario para descubrir nuevos mecanismos subyacentes a la tumorigénesis impulsada por Notch-PI3K/Akt en un paradigma de cáncer bien establecido en *Drosophila melanogaster* con valor altamente predictivo (Palomero *et al.*, 2007; Villegas *et al.,* 2018). Primero, diseñamos un cribado imparcial *in vivo* para identificar medicamentos que pudieran afectar selectivamente esta cooperación oncogénica sin efectos secundarios. Identificamos una nueva vía inflamatoria dependiente del óxido nítrico asociada a la oncogénesis de Notch/Pten, siendo susceptible de intervención farmacológica.

Por otro lado, el análisis fosfoproteómico de estos tumores reveló que la señalización aberrante de PI3K/Akt desencadena el potencial tumorigénico de Notch en parte al generar disfunciones en la mitocondria y estrés oxidativo. Nuestros resultados también indican que la señal Jnk, la cual se activa por estrés, podría estar restringiendo la progresión del tumor al inducir apoptosis y, por lo tanto, actúa como un supresor de tumores en este contexto.

Sorprendentemente, descubrimos que los tumores Notch-PI3K/Akt no sólo consumen grandes cantidades de glucosa, sino que también alteran de forma remota el metabolismo de todo el cuerpo. Llevando a cabo un estudio de metabolómica de alto rendimiento a gran escala y específico de tejido, encontramos una interacción inesperada entre el tumor y el metabolismo del triptófano-quinurenina del hospedador, especialmente en el cuerpo graso, que finalmente conduce a una inflamación sistémica. Además, detectamos cambios relacionados con el metabolismo del triptófano en la hemolinfa, la microbiota intestinal y el cerebro de los hospedadores con tumores, lo que confirma, por primera vez, que los tumores pueden inducir una reprogramación

metabólica en múltiples órganos. En consecuencia, la suplementación de la dieta con triptófano fue suficiente para prevenir la formación de tumores. Estos hallazgos podrían tener implicaciones importantes, ya que las intervenciones en la dieta prometen ser clave para el desarrollo de mejores tratamientos contra el cáncer.

3. Introduction

Cancer is a complex multifactorial process involving several genetic, molecular and cellular mechanisms that creates a hard-to-treat oncogenic network. Thus, the development of efficient therapeutic options requires sophisticated *in vivo* modelling in whole organisms.

3.1 Cancer, Metabolism and Inflammation

Cancer involves the accumulation of genetic mutations and epigenetic alterations that allow cells to proliferate uncontrollably (Merlo *et al.*, 2006; Laird, 2005; Stratton *et al.*, 2009; Janiszewska *et al.*, 2015). Over the course of evolution of these tumor cells, many diseases emerge, eventually resulting in the death of the host. Hanahan and Weinberg reviewed twenty years ago that malignant growth characteristic of cancer cells is the manifestation of six essential physiological alterations: self-sufficiency in growth signals, insensitivity to antigrowth signals, evasion of programmed cell death, limitless replicative potential, sustained angiogenesis, and tissue invasion and metastasis (Hanahan & Weinberg, 2000). Other features are: genomic instability, reprogramming of energy metabolism and tumor promotion by inflammation and evasion of the immune response (Fig. 1) (Hanahan & Weinberg, 2011).

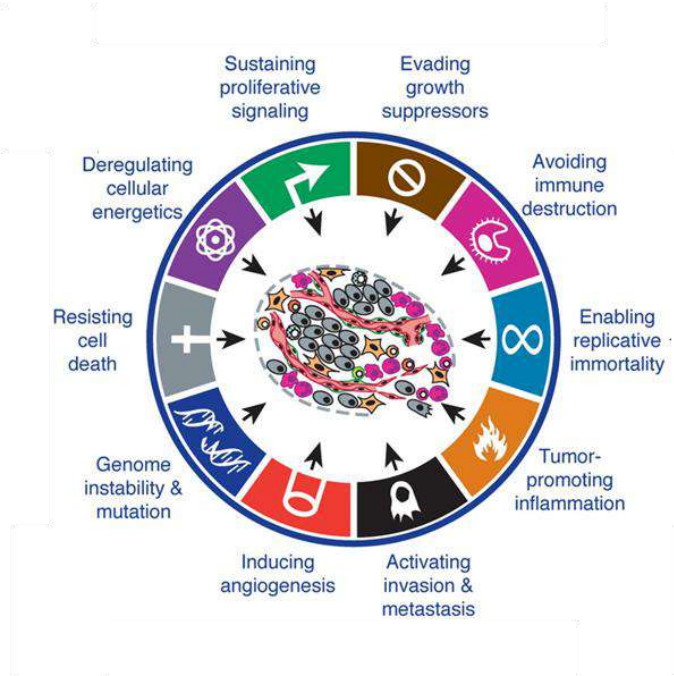

Figure 1. **Acquired capabilities of cancer cells** (taken from Hanahan & Weinberg, 2011).

3.2 *Drosophila* cancer models

Drosophila melanogaster has been used to understand the genetics of cancer since more than one hundred years ago (Villegas *et al.*, 2019). Pioneering works by Mary Stark described the presence of tumors in larvae (Stark, 1918) and first evidences of metastases in *Drosophila* (Stark, 1919b). Several years later, Elizabeth Gateff became a legend by discovering the first tumor suppressor gene (Gateff & Schneiderman, 1967, 1969, 1974) and further studies in *Drosophila* produced crucial knowledge about the genes and proteins relevant to human cancers (Duronio *et al.,* 2017; Villegas, 2019).

In fact, many genetic screens in flies have revealed genes that result in tumor growth and/or invasion, many of which have human homologues, contributing to the identification of pathways and mechanisms underlying the steps of cancer initiation (Villegas *et al.*, 2019). Furthermore, the powerful genetic toolkit available coupled with its short life span makes the fruit fly a simple and

effective animal to mimic some of the steps of mammalian tumorigenesis and performing high throughput genetic and pharmacological screens (Brumby *et al.,* 2005; Vidal & Cagan, 2006; Pendse *et al.*, 2013; Villegas *et al.*, 2018).

All these advantages led to groundbreaking works produced in different labs around the world during the last 15 years that helped to establish *Drosophila* as a potent model for cancer research (Edgar and Lehner, 1996; Milán *et al.*, 1996; Karim & Rubin, 1998; Milán *et al.*, 1997; Bilder *et al.*, 2000; Brumby and Richardson, 2003; Grifoni *et al.*, 2004; Read *et al.*, 2004; Caussinus & Gonzalez, 2005; Igaki *et al.*, 2006; Ferres-Marco *et al.*, 2006).

3.2.1 The PI3K/Akt/Pten signaling pathway

The PI3K/Akt pathway is a highly conserved signal transduction cascade that promotes survival and growth in response to many extracellular signals (Fig. 2). Activated Akt protein phosphorylates numerous substrates related to the regulation of cell proliferation, such as inactivation of glycogen synthase kinase-3 (GSK3) which induces cell cycle progression, membrane translocation of the glucose transporter (GLUT) and enhancement of protein synthesis by increasing the phosphorylation of mammalian target of rapamycin (mTOR), for example (Cross *et al.*, 1995; Wang *et al.*, 1999; Nave *et al.*, 1999; Sekulic *et al.*, 2000; Lawlor & Alessi, 2001). Another important function of activated PI3K/Akt is the inhibition of apoptosis, by phosphorylating and inactivating proapoptotic proteins. This results in a PI3K-dependent cell survival response, by means in a resistance to cell death (Franke *et al.*, 1997; Stocker & Hafen, 2000).

The critical regulator of this pathway is the tumor suppressor *Pten* (phosphatase and tensin homologue deleted on chromosome 10), which is evolutionary conserved from flies to humans. It is, therefore, required to modulate Akt activation, (Osaki *et al.*, 2004; Palomero *et al.,* 2007). As such, *Pten* loss of function alterations as inactivating mutations or epigenetic silencing result in an overactive PI3K/Akt pathway followed by increased cell proliferation and

resistance to apoptosis (Sulis *et al.*, 2003; Altomare & Testa, 2005; Georgescu, 2010), which creates a context for tumor development fueled by other oncogenes. Importantly, one-third of human cancers show loss of the tumor suppressor *PTEN* (Di Cristofano *et al.*, 1998; Hollander *et al.*, 2011), and the consequential chronic activation of the protein kinase AKT1 (Stambolic *et al.*, 1998; Song *et al.*, 2012).

Chronic activation of PI3K/AKT signaling is commonly associated with a poor prognosis and chemotherapy resistance (Lee *et al.*, 2001; Perez-Tenorio *et al.*, 2002; Nam *et al.*, 2003; Yamamoto *et al.*, 2004).

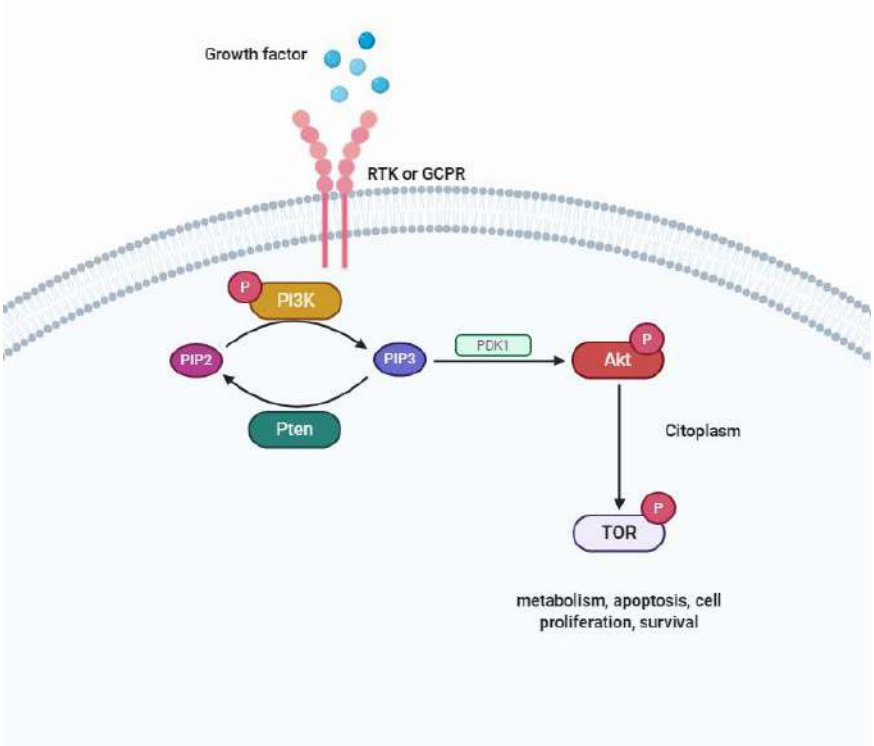

Figure 2. The PI3K/Akt/Pten pathway (diagram created with BioRender).

Schematic and simplified view: Different growth factors, hormones and cytokines can stimulate a tyrosin-kinase receptor (RTK) or a G Protein-coupled receptor (GPCR) triggering the phosphorylation of the enzyme phosphatidylinositol 3-kinase (PI3K). Activated PI3K then phosphorylates lipids on the plasma membrane, forming the second messenger phosphatidylinositol (3,4,5)-trisphosphate (PIP3). Akt, a serine/threonine kinase, is then translocated to the membrane by interaction through its phosphoinositide docking sites, so that it can be phosphorylated by phosphatidyl inositol-dependent kinase-1 (PDK1), which is constitutively activated, leading to stabilization of the Akt active conformation.

The pathway is negatively regulated by *Pten* gene, which encodes for a lipid phosphatase that is responsible for PIP3 dephosphorylation and clearance.

Although potent inhibitors of PI3K and Akt are available, the pleiotropic roles of this pathway during development and in adult tissue homeostasis point a challenge to target Pten tumors without side effects associated to these inhibitors, as well as overcome resistance caused by oncogenic addition of cooperating partners such as Notch (Knoechel *et al.*, 2014; Herranz *et al.*, 2015; Knoechel & Aster, 2015).

3.2.2 Notch signaling pathway in cancer

The Notch signaling pathway is a highly conserved cell signaling system present in most multicellular organisms. *Notch* gene was first described by John S. Dexter more than one century ago, who noticed the appearance of a notch in the wings of the fruit fly (Dexter, 1914). This gene encodes for a transmembrane receptor that is activated upon ligand binding and transduces extracellular signals into changes in gene expression (Fig. 3) that are important for organizer formation and cell-cell communication processes such as differentiation, self-renewal, proliferation and apoptosis during embryonic and adult life (Grabher *et al.*, 2006). While in mammals there are four *NOTCH* paralogs (*NOTCH1* to *NOTCH4*) that display both redundant and unique functions with multiple ligands (Delta-like-1, -3, -4 and Jagged-1 and-2), the fly genome contains only one *Notch* receptor and two ligands named *Delta* and *Serrate* (Artavanis-Tsakonas *et al.*, 1995; Domínguez, 2014).

Notch signaling is dysregulated in numerous types of human cancers such as leukemia, breast carcinomas, gliomas and neuroblastoma (Miele *et al.*, 2006; Palomero *et al.*, 2007), although its role in tumorigenesis was first discovered in studies in *Drosophila* (Artavanis-Tsakonas *et al.*, 1995).

In humans it was found that *NOTCH1* gene was found to be engaged in chromosomal translocations in a subset of T-cell acute lymphoblastic leukemia (T-ALL) (Ellisen *et al.,* 1991). Notch pathway has a role in normal T-cell development; thus, when NOTCH is hyperactivated, the differentiation process is halted and immature cells can become vulnerable for additional oncogenic mutations. Hence, deregulated NOTCH constitutes a very important aspect of T-ALL and mutations in the *NOTCH1* receptor are present in more than half of these tumors (Sjölund *et al.*, 2005; Palomero *et al.,* 2006).

Although the use of Notch inhibitors was proposed as a therapeutic option for many types of cancers, due to the broad spectrum of biological functions associated with Notch signaling, their utilization resulted in severe side effects and precluded its use in the clinic.

The discovery that single activated Notch, like most oncogenes, is insufficient for developing cancer *in vivo,* has motivated our laboratory to adopt genetic approaches to search for *Notch* partners in tumorigenesis. In 2006, the Dominguez group established a highly specific forward genetic screen in *Drosophila* to search for pairwise combinations of genes that functionally cooperate with Notch pathway to develop tumors *in vivo* (Ferres-Marco *et al.*, 2006; Palomero *et al.*, 2007). To this end, they coupled the UAS-Gal4 system (Brand & Perrimon, 1993) to overexpress the Notch ligand *Delta* specifically in the eye imaginal disc with the Gene Search method (Toba *et al.*, 1999) to systematically generate random gain or loss of function mutations. Like most oncogenes, single activation of Notch caused a ‘large eye’ phenotype. However, they found that a GS line inducing aberrant *Akt1* activity synergizes with Notch hyperactivation to promote tumor development *in vivo* (Palomero *et al.*, 2007).

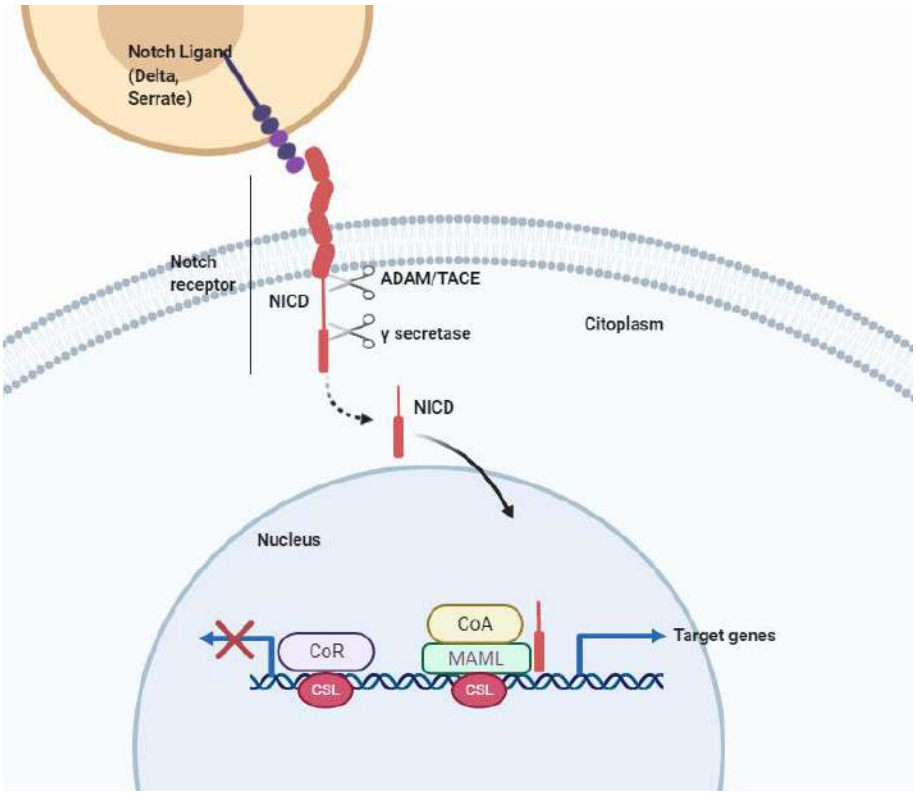

Figure 3. The core Notch signaling pathway (diagram created with BioRender).

Schematic and simplified view: the receptor is composed of an extracellular ligand-binding domain anchored to the membrane by its interaction with the transmembrane/cytoplasmic domain. When the Notch receptor is activated by one of its ligands, two proteolytic cleavage events are elicited: first by an ADAM-family metalloprotease and second by the γ-secretase complex, which results in the release of the Notch intracellular domain (NICD). The latter enters the nucleus and interacts directly with the DNA-binding protein CSL and the co-activator Mastermind to promote transcription of target genes (Zacharioudaki & Bray, 2014).

3.2.3 A brief overview of Notch-PI3k/Akt/Pten cooperation and challenge: the T-ALL paradigm

Cooperation between oncogenic Notch and PI3K/Akt/Pten pathways is highly prevalent in some human cancers (Rizzo *et al.*, 2008; Louvi *et al.*, 2012; Fruman *et al.*, 2014). For example, mutations or regulatory events leading to increased activation of the PI3K/Akt/Pten pathway are frequently found together with

activated NOTCH1 in T-ALL (Palomero *et al.*, 2007; Gutierrez *et al.*, 2009; Silva *et al.*, 2009), as well as in breast and lung carcinomas (Eliasz *et al.*, 2010; Muellner *et al.*, 2011; Gonzalez-Garcia *et al.*, 2012; Hales *et al.*, 2014).

Early studies using a *Drosophila* model of gain-of-function tumorigenesis and *in vitro* T-ALL studies have found that activated Notch and PI3K/Akt signaling cooperate to trigger malignancy. Later studies using cellular lines and mice demonstrated that cooperation and crosstalk between these signaling pathways enable heightened proliferative signaling, growth, survival, angiogenesis and therapy resistance (Palomero *et al.*, 2007; Efstratiadis *et al.*, 2007).

The prognosis of T-ALL has improved over the years (Van Vlierberghe & Ferrando, 2012), yet, the therapeutic options available are limited for patients with resistance to the current treatments or cases of relapse, where lethality is very high (Oudot *et al.,* 2008). Usually, the simultaneous inhibition of Notch and PI3K/Akt is necessary for maximal therapeutic response. Unfortunately, therapeutic targeting of developmental signaling pathways poses substantial challenges owing to their parallel roles in normal cells (Bray, 2006; Kopan & Ilagan, 2009, Fruman & Rommel, 2014), resulting in short- and long term severe side effects (van Es *et al.*, 2005; Micchelli *et al.*, 2003; Gore *et al.*, 2013; Hales *et al.*, 2014, Ntziachristos *et al.*, 2014; Hernandez Tejada *et al.*, 2014; Fruman & Rommel, 2014). Consecuently, the pharmacological inhibition of these signaling pathways not only effectively arrests the cell-cycle or kills the cancerous cells (Cullion *et al.*, 2009), but can also interfere with the normal development, growth, and maturation of many tissues (Micchelli *et al.*, 2003; van Es *et al.*, 2005; Ntziachristos *et al.*, 2014).

Notably, gamma-secretase inhibitors (GSIs) were proposed as potential therapy in T-ALL, since they effectively block Notch signaling (Palomero & Ferrando, 2008). However, the results of treatment with GSIs in relapsed/refractory T-ALL have shown no significant clinical responses and a high incidence of gastrointestinal toxicity (Deangelo *et al.*, 2006). In addition, Palomero and coworkers (2007) found that the aberrant activation of the PI3K/Akt

signaling pathway due to the mutational loss of *Pten* induces resistance to GSI therapy (Palomero *et al.*, 2007).

Therefore, the challenge now is identifying the different factors and the molecular events that underlie the disease in order to develop more effective and less toxic anti-neoplastic drugs.

3.2.4 Identification of drugs targeting oncogenic cooperation using high-throughput drug screening in *Drosophila*

In the past few years, *Drosophila* has been validated as a model used for living-organism-based chemical screenings (Vidal & Cagan, 2006; Chang *et al.*, 2008; Pandey & Nichols, 2011; Dar *et al.*, 2012; Gladstone *et al.*, 2012; Willoughby *et al.*, 2013; Gao *et al.*, 2014; Markstein *et al.*, 2014). However these studies tested already known antitumor drugs or drugs that target specific patways. The predictive value of *Drosophila* to identify novel compounds and the potential to target cooperative oncogenesis was understudied.

As explained previously, targeting Notch and/or PI3K/Akt pathways is highly effective *in vitro*, but inhibition of these crucial developmental pathways *in vivo* can have profound side effects with long-lasting impact in animal models and is inefficient in some cases with resistance due to oncogenic cooperation; this underscores the need for novel alternatives. Identification of drugs to target Notch and PI3K/Akt cooperation in cancer is an unmet medical need. Here, we used the *Drosophila* eye cancer paradigm of Notch and PI3K/Akt cooperative oncogenesis *in vivo* (Palomero *et al.*, 2007) (Fig. 4), to screen the Library of Pharmacologically Active Compounds (LOPAC1280) (Jones & Bunnage, 2017) with the aim to identify compounds capable to suppress tumorigenesis without causing side effects to the treated animals and evaluate their use for treating human T-ALL.

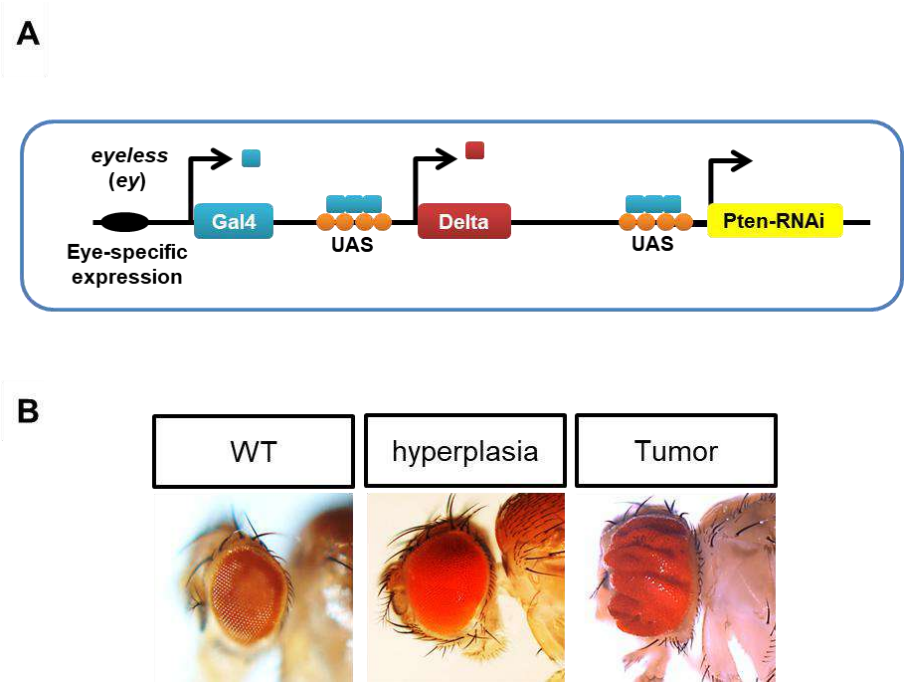

Figure 4. Hyperactivation of Notch and PI3K/Akt/Pten signaling induces tumorigenesis in *Drosophila*.

(A) Scheme of the eye cancer model in larvae carrying *eyeless*-Gal4 (*ey*-Gal4) to activate the constructs UAS-*Dl* and UAS-*Pten*-RNAi, inducing the simultaneous overactivation of Notch and Akt pathways, which triggers the formation of tumors in the eye imaginal disc of third instar larvae. **(B)** Tumor development can be monitored directly by visual observation in the adult fly eye. Representative phenotypes are shown as wild type (*ey*>), hyperplasia (*ey*>*Dl*) and tumor (*ey*>*Dl*>*Pten*-RNAi).

3.3 From inflammation to cancer

3.3.1 Definition of inflammation

Inflammation is, by definition, a defensive reaction involving the **innate immune system** in response to harmful stimuli, such as pathogens or injured tissue. The main function of inflammation is to eliminate the initial cause of cell injury, clear out necrotic cells and damaged tissues and initiate tissue repair (Ferrero-Miliani *et al.*, 2007).

Inflammation can be classified as acute or chronic. The process of acute inflammation is initiated by resident immune cells already present in the involved tissue, mainly macrophages. At the onset of an infection or other injuries, these cells undergo activation and release inflammatory mediators (Cotran *et al.,* 1998; Kumar *et al.,* 2004) such as vasoactive amines (histamine and serotonin), as well as eicosanoids (prostaglandin E2 and leukotriene B4) and nitric oxide (NO) to remodel the local vasculature (Fukumura *et al.*, 2006; Dennis & Norris, 2015). These mediators induce vascular changes such as vasodilation, increased permeability and increased blood flow, facilitating the movement of plasma fluid, containing important proteins such as fibrin and immunoglobulins (antibodies) into the inflamed tissue.

The cellular phase involves leukocytes which must extravasate from blood into the inflamed tissue. Some act as phagocytes, removing pathogens and ingesting cellular debris. If the inflammatory stimulus is a wound, different mediators can clot the injured area and provide hemostasis, the first step of wound healing (Herrington, 2014). The inflammatory response ceases when no longer needed to prevent chronic inflammation and cellular destruction. The anti-inflammatory program includes the production of mediators as lipoxins from arachidonic acid–derived prostaglandins and leukotrienes, among other mechanisms (Cotran *et al.*, 1998; Sato *et al.*, 1999; Serhan & Savill, 2005; Eming *et al.,* 2007). When this does not occur, a chronic inflammation and cellular destruction ensures, in some cases facilitating tumor formation (Coussens & Werb, 2002; Mantovani *et al.,* 2008; Colotta *et al.,* 2009; Wang & Dubois, 2010; Steinhilber *et al.*, 2010; Greene *et al.*, 2011; Chen *et al.*, 2009, 2014; Petkau *et al.,* 2017).

3.3.3 The innate immune response in *Drosophila*

Insects use an innate immune system that is homologous to mammals in order to build different responses against microorganisms. Innate immunity of *Drosophila melanogaster* consists first in physical barriers. If they succeed in entering the body cavity, the animal recognizes them as foreign and activates both humoral and cellular responses to kill and eliminate them.

Humoral secretion of antimicrobial peptides (AMPs) into the hemolymph by fat body cells is used as a weapon to lysate microbes as soon as they reach the epithelial barrier (Leclerc & Reichhart, 2004). The **cellular response** in *Drosophila* involves blood type cells called hemocytes, classified in: plasmatocytes, crystal cells, and lamellocytes (Meister & Lageux, 2003) (Fig. 5).

Equivalent to what occurs in mammals, in *Drosophila*, the inflammatory response consists on the recruitment of innate immune cells to the site of microbial infection or tissue damage. Injured cells lose their plasma membrane integrity and release endogenous components which can be recognized as pro-inflammatory molecules (Shen *et al.*, 2013). Those factors are collectively called alarmins that ultimately contribute to the downstream cellular and vascular manifestations of inflammation. Then hemocytes migrate to wound, a process that depends on PI3K (Wood *et al.*, 2006), and respond triggering a robust inflammatory response to both fight infection, if present, and clear wound debris (Razzell *et al.*, 2011). However, the inflammatory response can be also activated under certain circumstances without infection or tissue injury, for example by tumor cells (Asri *et al.*, 2019).

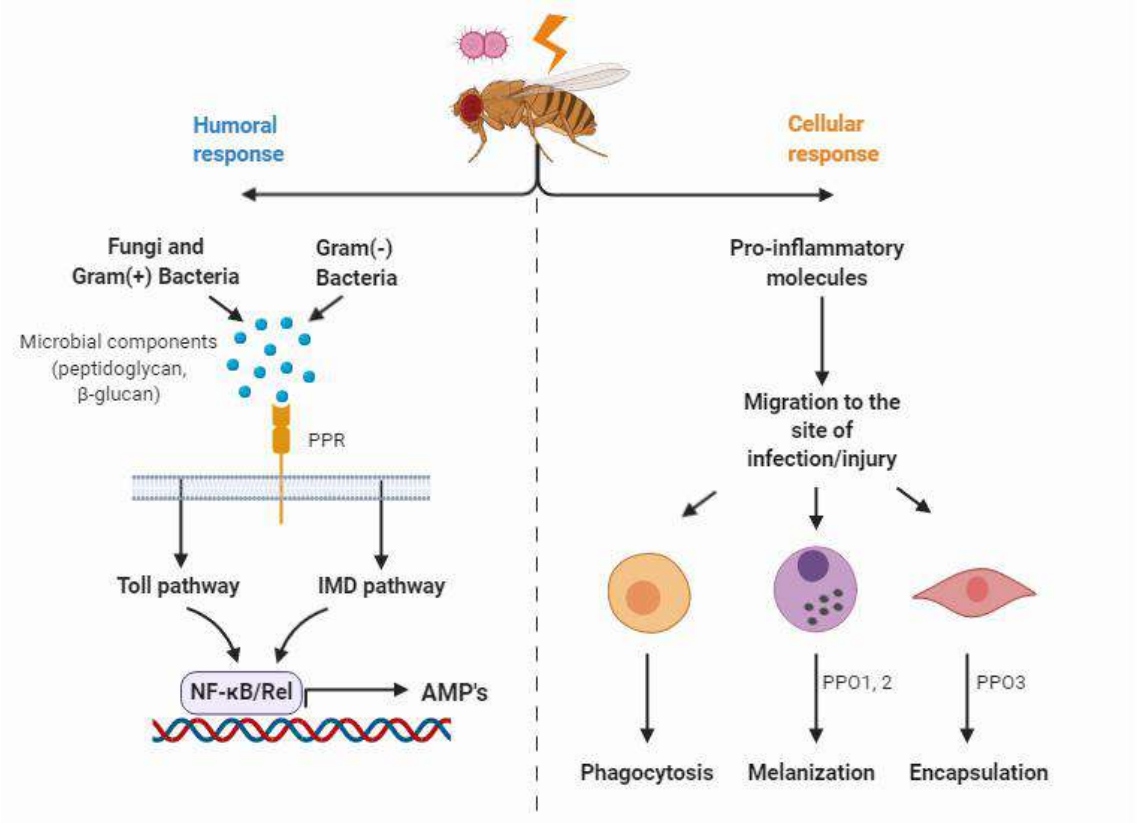

Figure 5. **Schematic view of the immune response in *Drosophila* against microbial infection or tissue injury** (diagram created with BioRender).

Left: Expression of AMPs: fungi and Gram-positive bacteria induce the expression of *drosomycin* and others genes through the Toll pathway, whereas Gram-negative bacteria induce the expression of *diptericin* and others genes through the IMD pathway (Lemaitre *et al.*., 1997; De Gregorio *et al.*., 2002; Irving P, *et al.*., 2001). The Toll and Imd pathways integrate the signals from pattern recognition receptors (PRRs), which are immune proteins able to recognize general microbial components (Janeway, 1989) and both pathways culminate in the activation of a nuclear factor-κB (NF-κB)/reticuloendotheliosis (Rel) family transcription factor, thus inducing the expression of the corresponding AMPs. **Right**: Plasmatocytes are equivalent to the mammalian monocytes/macrophages. Upon infection, they mediate phagocytosis of microorganisms and apoptotic cells (Pearson *et al.*., 2003). Crystal cells are required for melanization, which is an invertebrate-specific defense mechanism. Melanization produces the black pigment melanin, which is localized on the clot at the site of infection or injury in the hemocoele, and generates bactericidal reactive oxygen species (ROS) (Buchon *et al.*. 2014). The key enzyme to form melanin is phenoloxidase (PO) whose proenzyme is prophenoloxidase (PPO). PPOs are activated by recognition of microbial elicitors like LPS, peptidoglycan, or β-1,3-glucan (Ashida & Brey, 1997). The *Drosophila* genome possesses three different genes encoding *PPOs*. PPO1 and PPO2 are produced in crystal cells and have an important role in survival after infection. However, function of PPO3 is not clear yet, although some reports suggest that PPO3 is expressed in lamellocytes as a defense mechanism against parasitoid wasps (Soderhall & Cerenius, 1998; Dudzic *et al.*, 2015). Lamellocytes constitute a defense mechanism against parasites that is also typically restricted to invertebrates. They carry out a process named encapsulation, usually accompanied by melanization, killing the parasite. (Leclerc & Reichhart, 2004).

3.3. 2 Inflammation is a hallmark of cancer

Although the relationship between inflammation and cancer was first exposed long ago, in 1863 by Rudolf Virchow (Balkwill & Mantovani, 2001), the molecular mechanisms by which inflammatory signals help cancer cells to thrieve and form full blown tumors remains a mystery. Virchow hypothesized that cancer is originated at sites of chronic inflammation enhancing cell proliferation and nowadays is widely assumed that a pro-inflammatory environment is a risk factor for neoplastic growth in cells that acquire overproliferation capacity (Dvorak, 1986; Wu and Zhou, 2009; Grivennikov *et al.*, 2010).

Cancer cells produce a variety of cytokines that are mitogenic (stimulate cell division) and chemokines aimed at the recruitment of specific leukocyte populations that trigger an acute inflammatory response to resolve the neoplastic event (Homey *et al.*, 2002). However, while tumor-associated macrophages (TAMs) often have an anti-tumorigenenic roles, they can also be subverted by cancer cells in ways that are not fully understood to promote, rather that limit, neoplastic progression by further releasing cytokines and growth factors (Schoppmann *et al.*, 2002; De Palma and Lewis, 2013; Lee *et al.*, 2013b). Chronically inflamed tissues frequently also inhibit cell death programs, thus resulting in amplification of aberrant cells with unrepaired DNA defects that contribute to tumour growth (Coussens & Werb, 2002). Furthermore, tumor cells take advantage of the trophic factors made by inflammatory cells to migrate alone or with innate immune cells to spread and colonize distant tissues (Kim *et al.*, 1998; Coussens & Werb, 2002) (Fig. 6).

Less understood is how local inflammation evolves towards a systemic inflammation that ultimately leads to multiorgan failure and the death of the host. Recent epidemiological data suggest that treatments with anti-inflammatory drugs such as those used to treat ashma can have tumor-prevention activity, supporting the idea that a chronic systemic inflammation may facilitate tumorigenesis. In addittion, evidence from studies in long-term users of nonsteroidal anti-inflammatory drugs (NSAIDs) indicates that use of these drugs reduces cancer risk in different human cancers (Baron & Sandler, 2000; Garcia-Rodriguez *et al.*, 2001).

Therefore, it is evident that inflammatory cells have an important role on tumor development. Remains undefined if the tumor favors its own development by subverting immune cell functions and evading host defense mechanisms or if, by contrast, the recruitment of inflammatory cells may also represent an attempt by the host to suppress tumor growth.

For the development of new therapies is necessary to decipher the mechanisms involved in the immune response to tumors. Of particular importance is the use of animal models to test the efficacy of new drugs with fewer side effects in whole body organisms. Therefore, we have used our *Drosophila* tumor model to unravel how inflammation is causally related to Notch and PI3K/Ak-driven tumorigenesis.

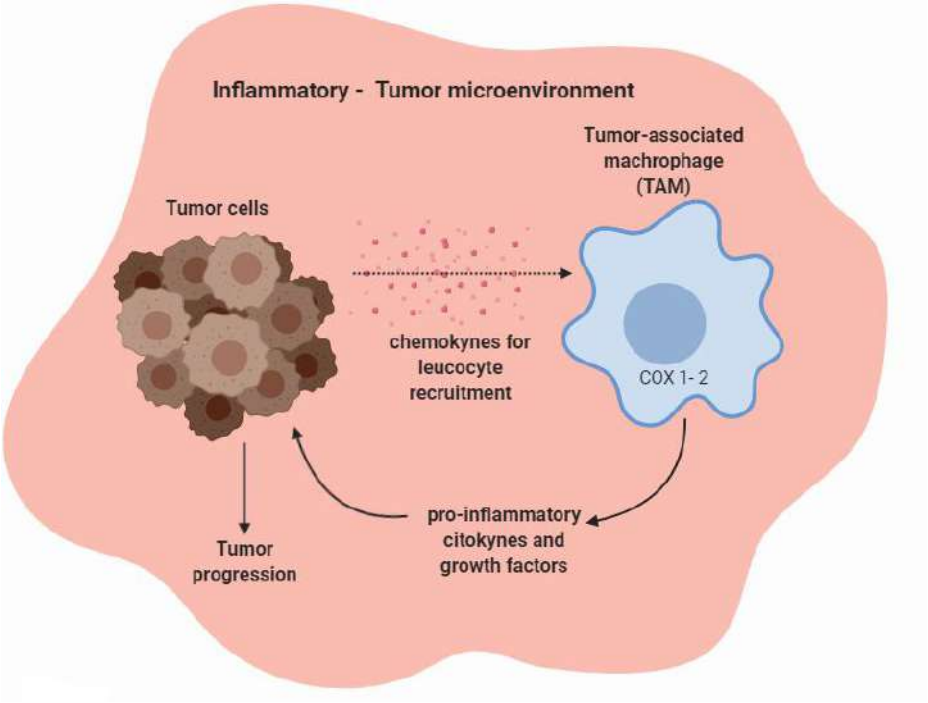

Figure 6. Diagram of tumor-inflammatory interplay (diagram created with BioRender).

Tumor cells produce chemokines to recruit macrophages and other leukocyte populations. Inflammatory cells release cytokines and growth factors to potentiate tumor progression.

3.4 Why and how cancer cells reprogram their metabolism

Tumor cells exhibit changes in their metabolic activities that are distinct compared to neighboring normal cells, but similar to high proliferative cells in early development in order to support their malignant growth. This process is referred to as **reprogramming of energy metabolism** (Hanahan & Weinberg, 2011; Pavlova & Thompson, 2016; Vander Heiden & DeBerardinis, 2017). These reprogrammed activities provide cancer cells a selective advantage by supporting cell survival under stressful conditions or allowing cells to grow uncontrollably and overproliferate (Fig. 7). Most classical examples are focused on highlighting the diversity of cell-autonomous metabolic changes on tumor cells and the microenvironment, such as altered bioenergetics, redox balance and enhanced biosynthesis (Vander Heiden & DeBerardinis, 2017).

The general changes of catabolism, anabolism and redox balance in tumors reflect the upregulation of signaling pathways that are commonly perturbed in cancer cells (Cantor & Sabatini, 2012), particularly the PI3K/Akt/mTOR pathway (Yuan & Cantley, 2008; Dibble & Manning; 2013).

3.4.1 Altered bioenergetics and biosynthesis of macromolecules

Otto Warburg in 1920 observed that cancer cells take up higher amounts of glucose and produce lactate regardless of oxygen availability (Warburg, 1925; Liberti & Locasale, 2016). This phenomenon known as “Warburg Effect” or aerobic glycolysis has been recognized in the last decade as a common cancer feature (Lunt & Vander Heiden, 2011; Koppenol *et al.*, 2011). Warburg proposed that cancer cells preferentially use glycolysis for energy production instead of the more effective pathway, the mitochondrial oxidative phosphorylation (OXPHOS) (Romero-Garcia *et al.*, 2011), to obtain their energy even under normoxic conditions, becoming greedy for glucose and increasing the uptake through up-regulation of glucose transporters (DeBerardinis & Cheng, 2010; Zheng, 2012). He added, some years later, that dysfunctional mitochondria are the root of aerobic glycolysis (Warburg, 1956). This classical view has been extensively challenged. Crabtree studied the heterogeneity of glycolysis in distinct tumor types and

confirmed Warburg's findings, corroborating that the tumors display a high rate of glucose consumption. However, he further discovered that mitochondrial respiration was variable, and many tumors exhibit a substantial amount of respiration (Crabtree, 1926). In addition, numerous studies failed to demonstrate defective respiration as a general feature of malignant cells (Galluzzi *et al.,* 2010; Koppenol *et al.*, 2011). By contrast, many studies have demonstrated that the great majority of tumor cells have the capacity to produce energy through mitochondrial glucose oxidation (Weinberg *et al.*, 2010; Martinez-Reyes *et al.*, 2016). Thus, despite their high glycolytic rates, most cancer cells generate the majority of ATP through mitochondrial function. The PI3K/Akt/Pten pathway plays an important role in the function of mitochondria and therefore identifying mitochondrial targets phosphorylated by oncogenic Akt is important to understand its role in cancer cell metabolism.

In addition, there is large evidence that mitochondria can support cancer cells through a progressive increase in mitochondrial ROS (a recognized inducer of genomic instability frequently involved in the malignant transformation process) or through mitochondrial biogenesis, since energy production also ensures the synthesis of many molecules indispensable for biosynthesis of macromolecules (Weinberg & Chandel, 2009; Sullivan & Chandel, 2014). Mitochondria are also involved in apoptotic and autophagic cell death and have a close relationship with oncogenes and tumor-suppressor genes.

Furthermore, anabolic pathways are essential to enable cells to produce the macromolecules required for cell division and malignant growth. Biosynthesis of proteins, lipids, and nucleic acids is under the control of the same signaling pathways that govern cell growth and are activated in cancer, such as the PI3K-mTOR signaling (Fig. 7). Therefore, cancer cells exhibit an incredible metabolic flexibility since they can respond to the changing microenvironment and the intermediates available during tumor evolution (Boroughs & DeBerardinis, 2015).

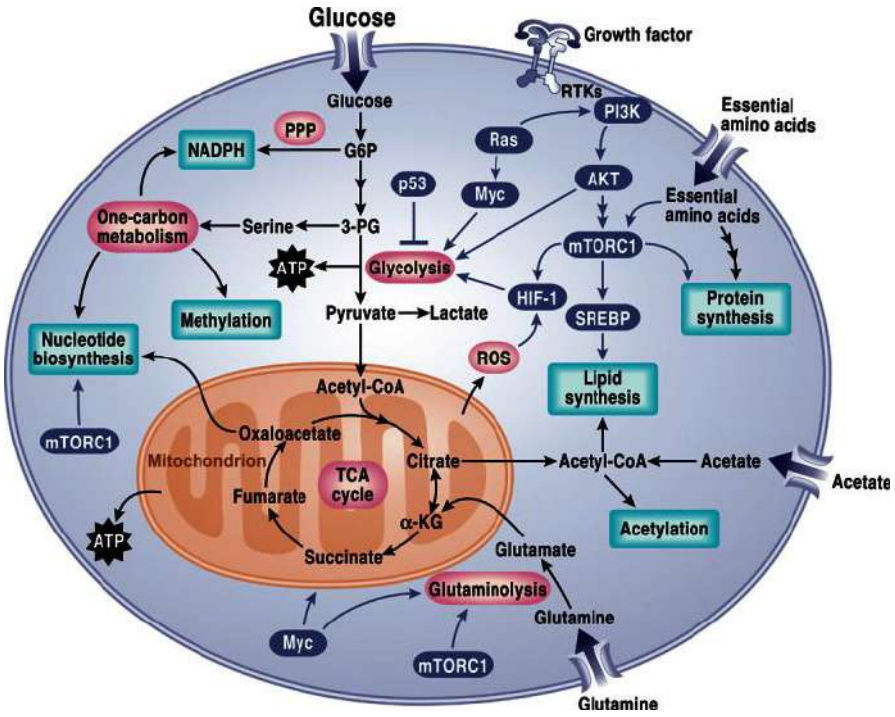

Figure 7. View of signaling pathways that regulate cancer metabolism (picture taken from DeBerardinis & Chandel, 2016).

TCA cycle intermediates are also used as precursors in biosynthetic pathways, which require that carbon be resupplied to the cycle. **Pyruvate carboxylation** produces oxaloacetate from glucose/pyruvate and **glutaminolysis** produces α-ketoglutarate from glutamine are commonly enhanced in cancer cells (Liem *et al.*, 2014). The **β-oxidation of fatty acids** also generates acetyl-CoA, NADH and $FADH_2$, which are used to produce mitochondrial ATP. **Protein biosynthesis** is highly regulated and requires the acquisition of amino acids from the extracellular space. The entry of amino acids stimulates mTORC1 exerts its effects on translation and ribosome biogenesis to synthesize new proteins (Laplante & Sabatini, 2012). Parallel to this, **degradation of intracellular proteins** and other macromolecules to supply amino acids in cancer cells have been characterized extensively. This can be reached by micropinocytosis, which supplies both nitrogen and carbon to central metabolic pathways (Commisso *et al.*, 2013). Fatty acids are required for membrane biosynthesis, lipidation reactions and cellular signaling, thus tumor cells need to rapidly produce them. **Fatty acid synthesis** requires acetyl-CoA and cytosolic NADPH. In most cultured cells, glucose is the most prominent acetyl-CoA source for fatty acid synthesis (Yoo *et al.*, 2004; DeBerardinis *et al.*, 2007) although glutamine and acetate could be an alternative carbon source (Schug *et al.*, 2015). On the other hand, it has been recently suggested that most NADPH used for fatty acid synthesis arises from the **pentose phosphate pathway (PPP),** which is frequently upregulated in tumors (Fan *et al.*, 2014; Lewis *et al.*, 2014). Finally, the **synthesis of RNA and DNA** requires the complex biosynthesis of nucleotides as purine and pyrimidine. The phosphoribosylamine backbone of these molecules is produced from ribose-5-phosphate, an intermediate of the PPP (Stincone *et al.*, 2014).

3.4.2 Redox balance and oxidative stress in cancer

The reactive oxygen and nitrite species, hereafter referred globally as ROS, are intracellular metabolites of oxygen that include the superoxide anion (O_2^-), hydrogen peroxide (H_2O_2), and the hydroxyl radical ($OH\cdot$), among others (Murphy, 2009). ROS are mainly generated by the mitochondrial respiratory chain and in the cytosol by NADPH oxidases (NOXs) (Brand, 2010). These free radicals are highly reactive and can cause oxidative damage to intracellular macromolecules such as proteins, lipids and DNA (Cross *et al.,* 1987; Trachootham *et al.,* 2008). However, recent studies have unveiled the physiological role of **ROS in cellular signaling**, working as redox messengers in several regulatory processes (Roy *et al.*, 2017). In normal conditions, the effect of ROS is balanced by non-enzymatic antioxidants as well as by antioxidant enzymes such as superoxide dismutase (Sod) and catalase (Cat), maintaining ROS homeostasis without causing collateral damage to cells (Kantner *et al.*, 2013) (Fig. 8). Notwithstanding, in cancer cells this balance can be broken owing to several mechanisms such as activation of oncogenes, aberrant metabolism and **mitochondrial dysfunction** (Trachootham *et al.*, 2009). The subsequent increase in ROS levels can contribute to cancer promotion in different manners. For example, mitochondrial ROS seem to affect the PI3K/Akt pathway (Nemoto & Finkel, 2002) and it is also able to stabilize hypoxia-inducible factor (HIF), one of the most important mechanisms involved in the induction of the glycolytic pathway (Hielscher & Gerecht, 2015). The increased levels of ROS in cancer cells need to be buffered; thus, tumor cells usually have higher levels of ROS scavenging enzymes, preventing ROS-mediated activation of pathways that induce cell death, like c-Jun N-terminal kinase (Jnk) and p38 MAPK, oxidation of lipids, proteins, and DNA (Chandel & Tuveson, 2014).

The dual role of oxidative stress in promoting cancer development provides two opposite therapeutic strategies. One one hand, increasing ROS-scavenging capacity using antioxidants can abrogate ROS signaling and suppress growth in some tumors. However, several antioxidants used in clinical trials were associated with increased risk of cancer. This adverse effect of antioxidants might be related to the inhibition of ROS-mediated apoptosis and the prevention of oxidative damage in tumors that are already established and may therefore promote tumor-cell survival. An opposite strategy is to use pharmacological agents that have prooxidant properties. Nevertheless, ROS can

modulate the activities and expression of many transcription factors and signaling proteins that are involved in the stress response, cell survival and inhibition of apoptosis through multiple mechanisms. Furthermore, it is also possible that such approach might promote mutations in normal cells (Trachootham *et al*, 2009). Therefore, information of the redox status of cancer cells before treatment and predicting outcome relies on the use of animal models and *avatars*.

Moreover, tumors and cultured cancer cells exhibit different metabolic phenotypes. In fact, while many cancer cell lines can quantitatively convert glucose to lactate, glucose oxidation is prevalent in tumors (Marin-Valencia *et al.*, 2012; Hensley *et al.*, 2016). The microenvironment can also affect the efficacy of drugs targeting metabolism (Vander & DeBerardinis, 2017). Although new therapeutic targets are often discovered by using simple models like cultured cells, it is essential to define their context-specific roles *in vivo*, which underscores the need of using accurate whole-organism models that mimic the genetic events that occur during tumor initiation and progression in humans and, importantly, that mimic responses. In this study we used our *Drosophila* tumor model, with an extensively validated predictive value (Villegas *et al.,* 2018), to identify the key downstream mechanisms that underlie the Notch-PI3K/Akt/Pten oncogenic cooperation using a phospho-proteomic approach and diverse functional assays, further revealing an important role of mitochondrial dysfunction and ROS in tumor initiation.

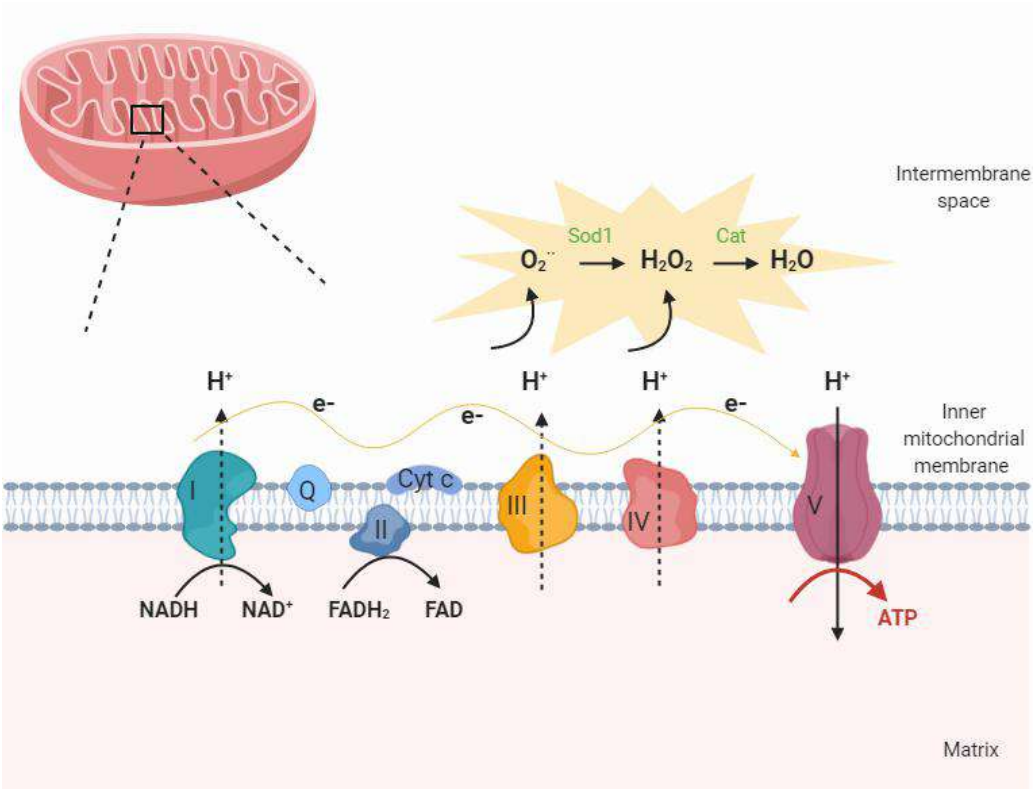

Figure 8. Generation of ROS in the mitochondria (diagram created with BioRender).

Mitochondrial electron transport chain (ETC) is located at the mitochondrial inner membrane and comprises four protein complexes acting as electron donors and acceptors. Electrons are transferred from NADH and $FADH_2$ through the different complexes until electrons are passed to oxygen, which is reduced to water. This process releases energy, which is used to generate a proton gradient by actively pumping protons into the intermembrane space. Then, Complex V (ATP synthase) uses this electrochemical gradient to phosphorylate ADP and form ATP. A small percentage of electrons directly leak to oxygen, resulting in the formation of the free-radicals (ROS) that contribute to oxidative stress. Antioxidant enzymes as Sod and Cat maintain ROS homeostasis in physiological conditions; however cancer cells often present mitochondrial dysfunction, which ultimately results in higher levels of ROS.

3.5 Diet and cancer: the connection between dietary restriction, immunity and Pten tumors

Cancer is not merely a cell problem, since interactions not only occur within cancer-containing tissues, but also within normal cells in distant tissues. Consequently, having a cancer affects other tissues/organs of the host in manners that are not fully understood. Whereas metabolic reprogramming has been widely studied at cellular level and extended to the microenvironment of the tumor, the complex association between whole-body metabolic changes, diet and cancer outcomes remains an open question.

Diet has a recognized benefit on the longevity of the animals. Indeed, numerous studies in different animal models suggest that **caloric restriction** prolongs life span of the tumor-bearing host (Hursting *et al,.* 2010; Longo and Fontana 2010) and reduces the incidence and growth rates of various types of tumors (Tannenbaum & Silverstone, 1949; Tannenbaum & Silverstone, 1953; Weindruch & Walford, 1982; Zhu *et al.*, 1997; Pugh *et al.*, 1999; Thompson *et al.*, 2003; Sell, 2003). However, as first observed by Rous "some spontaneous and transplantable tumor grafts are not affected by the more rigorous diet" (Rous, 1914; Tannenbaum, 1954).

In 2009, Kalaany and Sabatini reported that cancer cells carrying mutations that cause constitutive activation of the PI3K/Akt pathway are resistant to the anti-tumorigenic effects of dietary restriction (Kalaany & Sabatini, 2009), confirming first observations of diet-resistant tumors by Rous in 1914. Remarkably, the beneficial effects of dietary restriction in cancer incidence and longevity (Kritchevsky, 2001; Lien & Vander Heiden, 2019) are mediated in large part by the reduction of systemic insulin/IGF-1/PI3K/AKT and TOR pathways (Vellai *et al.*, 2003; Kapahi *et al.*, 2004; Kaeberlein *et al.*, 2005; Powers *et al.*, 2006). In mammals, mTOR induces protein synthesis (Guertin & Sabatini, 2007) and can be activated by Akt. Animals exposed to dietary restriction show a reduction in the levels of circulating insulin and insulin-like growth factor-1 (IGF-1) (Kalaany & Sabatini, 2009), well-known activators of PI3K/Akt pathway, further providing a feasible explanation of how those tumors with overactivating mutations in PI3K/Akt/Pten pathway can overcome resistance to caloric restriction.

In *Drosophila melanogaster*, restriction of dietary yeast (the fly's main source of protein and amino acids) to 5% of the *ad libitum* food intake significantly extends lifespan of wild type animals (Grandison *et al.*, 2009). However, this intervention also enhances the proliferative potential of cells lacking *Pten*, promoting tumorigenesis and leading to the death of the host through an unknown non-autonomous mechanism (Britton *et al.*, 2002; Nowak *et al.*, 2013).

Importantly, the mechanistic links between metabolism and inflammation between in the host with cancer is still missing. In *Drosophila* the fat body is the major organ for nutrient sensing and immune function. Indeed, immune defense is energetically costly (Lazzaro & Galac, 2006), thus must draw resources from other physiological processes (Zerofsky *et al.*, 2005; DiAngel *et al.*, 2009). Therefore, low-protein diet can also impact immune functions that are highly dependent on the adequate availability of amino acids and can lead to vulnerability to infection (Kim *et al.*, 2007).

Moreover, modulating the amino acid composition of the diet can also slow cancer growth. For example, serine depletion from the diet has a potential role in the treatment of p53-deficient tumors (Maddocks *et al.*, 2013). Besides, kynurenine, a breakdown product of the amino acid tryptophan, can modulate both the innate and adaptive immune system and has been implicated in cancer-associated immunosuppression (Platten *et al.*, 2014). Drug inhibition of this pathway can help break immune tolerance and potentiate chemotherapy (Muller *et al.*, 2005). Nevertheless, investigations into how diet affects tumor growth remain an underexplored area.

To conclude, diet directly affects tumor growth and the immune response through several complex mechanisms and tumor cells compete with the host cells for essential nutrients such as glucose, lipids and amino acids. We hypothesize that different dietary components may exert different functions and responses in tumor cells and the host depending on the genetic composition of the tumor. Since malnutrition is a common accompaniment of cancer patients and tumor cells may have heterogeneous nutritional requirements, it is important to determine whether such behaviors are protective or detrimental to the host and what and how different dietary components affect the host with cancer.

However, the mechanisms by which cancer cells negative influence the host metabolism are largely unknown. This area of research holds the promise for the development of new therapeutic strategies that implement the pharmacological inhibition of metabolic targets and dietary interventions against cancer. Here, we use an innovative approach to evaluate the impact of Notch-Akt tumors in the whole-body metabolism. By performing large-scale and tissue-specific metabolomics we discovered a novel mechanism by which tumors in the eye imaginal disc of *Drosophila* can reprogram the tryptophan-kynurenine pathway in distal organs as the fat body. Our findings confirm for the first time that tumors can rewire the metabolism of the whole-organism.

4. Objectives

Oncogenic cooperation between Notch and PI3K/Akt pathways is associated with aggressiveness and treatment resistance in many human cancers. Although selective inhibitors of each pathway are available, targeting each pathway separately fails to induce a therapeutic response, since together they have potent anticancer effect but also produce adverse side effects. To identify new ways to specifically target their cooperative tumorigenesis, we need to understand how activated PI3K/Akt/Pten cooperates with activated Notch to initiate tumorigenesis and evade the innate anti-tumor response. To this aim, we have used an unbiased, multidisciplinary approach, which I hereby present in three sections with their specific objectives:

Section 1:

1.1 Identify compounds that *in vivo* suppress Notch-PI3K/Akt-induced tumorigenesis as efficiently as the available Notch and PI3k/Akt inhibitors, but without their side effects by screening the Library of Pharmacologically Active Compounds (LOPAC1280).

1.2 Unravel the role of top hit compounds targeting the NOS and LOX-inflammatory pathways in the Notch-PI3K/Akt-driven tumorigenesis.

1.3 Validate top hit compounds in human T-ALL cells with activated NOTCH and loss of *PTEN*.

Section 2:

2.1 Identify phosphorylation targets of oncogenic Akt by performing phospho-proteomics analysis.

2.2 Elucidate the role of ATP-β-synthase and mitochondrial dysfunction in Notch-PI3K/Akt tumorigenesis.

2.3 Determine the role of stress-activated Jnk signaling in this tumorigenic context.

2.4 Characterize the alterations related to glucose catabolism in Notch-PI3K/Akt tumors.

Section 3:

3.1 Characterize whole-body metabolic reprogramming associated with Notch/PI3K/Akt/Pten eye tumours using large-scale and tissue-specific metabolomics.

3.2 Characterize the role of tryptophan-kynurenine pathway in the fat body of tumor-bearing animals.

3.3 Identification of tryptophan-kynurenine pathway inhibitors with potential to suppress Notch-PI3K/Akt tumorigenesis.

3.4 Determine if tryptophan starvation in hosts with Pten-loss tumors contributes to dietary restriction resistance and the associated host lethality.

5. Material and methods

Fly husbandry

All crosses were carried out at 26.5ºC and stocks were maintained at 25ºC in standard fly food and a 12-hr light/dark cycle unless otherwise noted. We used the following strains: w^{1118}; *ey*-Gal4/Cyo twist-GFP; *ey*-Gal4>UAS-*Dl*/CyO twist-GFP; *tubulin*-Gal4>UAS-GFP/TM6b. Other stocks used were: GstD1-GFP (a gift from D. Bohmann), TRE40-RFP (a gift from Baena-Lopez) and Hml-dsRed.Δ (FBtp0069700) (a gift from K. Brueckner). The rest of fly stocks used is listed in Table 1.

Symbol	Annotation symbol	Stock number	Genotype
RNAi			
ATP syn α	CG3612	V34664	w^{1118}; P{GD11030}v34664
ATP syn δ	CG2968	V100621	P{KK108804}VIE-260B
ATPsynβ	CG11154	B28056	y^1 v^1; P{TRiP.JF02892}attP2
Bsk	CG5680	V34138	w^{1118}; P{GD10555}v34138
Bsk	CG5680	B32977	y^1 sc* v^1 sev^{21}; P{TRiP.HMS00777}attP2
Bsk	CG5680	B31476	y^1 v^1; P{TRiP.JF01274}attP2/TM3, Ser^1
Bsk	CG5680	B31323	y^1 v^1; P{TRiP.JF01275}attP2
cn	CG1555	B65029	y^1 sc* v^1 sev^{21}; P{TRiP.HMC05903}attP40
Glut1	CG43946	V101365	P{KK108683}VIE-260B
Ldh	CG10160	B33640	y^1 v^1; P{TRiP.HMS00039}attP2
ND42	CG6343	B28894	y^1 v^1; P{TRiP.HM05104}attP2
ND75	CG2286	V10733	P{KK108222}VIE-260B
ND-ASHI	CG3192	V108745	P{KK108448}VIE-260B
Pten	CG5671	B25967	y^1 v^1; P{TRiP.JF01987}attP2/TM3, Sb^1
sima	CG45051	B26207	y^1 v^1; P{TRiP.JF02105}attP2
Sod1	CG11793	V31551	w^{1118}; P{GD7385}v31551
ss	CG6993	V108732	P{KK107561}VIE-260B
st	CG4314	B60134	y^1 sc* v^1 sev^{21}; P{ TRiP.HMC05128}attP40
Trh	CG9122	B25842	y^1 sc* v^1 sev^{21}; P{TRiP.HMC05128}attP40
v	CG2155	B50641	y^1 v^1; P{TRiP.HMC03041}attP2
w	CG2759	B25785	y^1 v^1; P{y[TRiP.JF01786}attP2
UAS (Gain of Function)			
Bsk	CG5680	B9310	w*; P{UAS-bsk.B}2
Cat	CG6871	B24621	w^1; P{UAS-Cat.A}2
Gtpx1	CG12013	Missirlis *et al.*, 2003	P{UAS-PHGPx.M}

Ldh	CG10160	B16829	y^1 w^{67c23}; P{EPgy2}EY07426
Nos	CG6713	B56830	w*; P{w[+mC]=UAS-Nos.L}2; P{w[+mC]=UAS-Nos.L}3
sima	CG45051	B9582	w*; P{UAS-sima.B}2
Sod1	CG11793	B33605	w^{1118}; P{UAS-Sod1}12.1
Alleles and other lines			
Bsk	CG5680	B6409	w^{1118} P{UAS-bsk.DN}2
cd	CG6969	B3052	cd^1
cn	CG1555	B263	cn^1
P35	-	B8421	P{UAS-p35.H}
sima	CG45051	B60222	y^1 w*; Mi{PT-GFSTF.2}simaMI05111-GFSTF.2C
ss	CG6993	B2973	ss^1
Trh	CG9122	B10531	w^{1118}; PBac{PB}Trhc01440
UAS-mitoGFP	-	B8442	w^{1118}; P{UAS-mito-HA-GFP.AP}2/CyO
v	CG2155	B137	v^1

Table 1. List of fly stocks used in this study.

All the lines were obtained from either the Bloomington Drosophila Stock Center (B) or the Vienna Drosophila Research Centre (V).

Drosophila image acquisition

Drosophila eye images were captured on a ZEISS Axiophot optical microscope and a MicroPublisher 5.0 Camera (QImaging). Different focal planes are taken using a 5X objective with 1.5 zoom and composite images are generated with AutoMontage Essentials 5.0 software.

Identification of phosphoproteins by liquid chromatography coupled to mass spectrometry

To identify activated proteins downstream of Notch-PI3K/Akt overexpression we combined a standard two-dimensional gel electrophoresis (2-DE) protocol with subsequent post-staining of gels with phosphospecific fluorescent Pro-Q Diamond dye, a fluorophore that recognizes phosphate groups on proteins and peptides directly on gels. The combination of these two methods for fluorescence detection of proteins allows quantitative detection of phosphoproteins in 2-DE gels. Following, we employed MALDI-TOF-MS for protein identification. We used eye imaginal discs from L3 larvae

of the following genotypes: wild type (*ey*>Gal4) and the tumorigenic combination Notch-PI3K/Akt overexpression (*ey>Dl>Pten*-RNAi). For each condition we dissected out 900 eye imaginal discs (for triplicate biological samples comprising 300 discs each). The following steps were carried out by the Proteomics Laboratory CSIC/UAB. The soluble protein fraction was obtained after homogenization in 10 mM HEPES/NaOH buffer (pH 7.0) containing 10 mM PMSF supplemented with 10 mM NaF and 1 mM Na_3VO_4. Then purified and concentrated by acetone precipitation and 2-DE gels were carried out as follows: in the first dimension, 300 mg protein were separated on IPG (immobilized pH gradient) strips (18 cm, pH 4- 7; GE Healthcare) followed by SDS-PAGE (12.5 % acrylamide, 0.75 mm) in the second dimension. Gels were stained with Pro-Q Diamond phosphoprotein stain (Life Technologies), and SYPRO Ruby used for total protein stain (Life Technologies). Images of the gels following fluorescent staining were acquired using a FLA 3000 laser scanner (Fuji Photo Film) with 532 nm excitation and 580 nm longpass emission filter for Pro-Q Diamond, and 473 nm excitation and 580 nm longpass emission filter for SYPRO Ruby. For 2-DE gel image analysis we used the software Delta 2D (Decodon). To cut out putative phosphoproteins for the mass spectrometric identification, the 2-DE gels were stained with colloidal Coomassie. The resulting spot pattern coincides with that of SYPRO Ruby staining and, thus, the information from the Pro-Q Diamond/SYPRO Ruby dual views can be used to define the positions of the phosphoproteins in the Coomassie-stained gels. Finally, interesting protein spots were excised manually from Coomassie-stained gels, and processed for MALDI-TOF-Mass Spectrometry protein identification.

Immunostaining

Imaginal discs were dissected in cold PBS 1X, fixed in 4% PFA for 20 minutes and washed three times in 0,4% PBT at RT. Incubation with primary antibodies was performed in a wet chamber overnight at 4ºC, followed by three washes in 0,4% PBT at RT. Secondary antibodies were added and incubated for 120 minutes in gentle agitation at RT and rinsed thrice in 0,4% PBT. DNA was stained with DAPI (1 μg/ml in PBS) for 7 minutes. Three final washing steps were performed with PBT for 5 minutes each before imaginal discs were finally mounted in mounting medium (Fluoromount-G®, ref.# 140626).

The following primary antibodies were diluted in PBS at final concentrations (1:100): rabbit anti-Caspase (CST, ref.# 9661); mouse anti-phospho-histone H3 (CST, ref.# 9706); rat anti-Elav (DSHB, ref.#7E8A10); rabbit anti-GFP (Abcam, ref.# ab290, Polyclonal) and anti-RFP (Evrogen, ref.# ab234).

The following secondary antibodies were used at 1 μg/ml in PBS final concentrations (1:200): donkey anti-rabbit Alexa Fluor® 488 (Invitrogen, ref.# A21206); donkey anti-mouse Alexa Fluor 647 (Life Tech, ref.# A31571); goat anti-rat Cy3® (Life Tech, ref.# A10522) and donkey anti-rabbit Alexa Fluor 555 (Life Tech, ref.# A31572). Acquisition of confocal microscopy images was performed in a vertical confocal microscope (LEICA SPEII) and processed with ImageJ software.

Cell proliferation analysis

Fixed eye imaginal discs from third instar larvae were immunolabeled with antibodies against mouse anti-phospho-histone H3 (CST, ref.# 9706). Image stacks were acquired with a 20x/0.75 objective and average projections from fourteen sections were generated using ImageJ software. By visual analysis of the image stack, all mitotic cells within each imaginal disc were counted. The absolute total number of mitotic cells per disc was quantified and also the relative number normalized by area.

ROS levels visualization

The transgenic strain GstD1-GFP was generously provided by Dirk Bohmann (Sykiotis & Bohmann, 2008). Fixed eye imaginal discs from third instar larvae with GstD1-GFP reporter line were mounted in Fluoromount-G™ with DAPI (Invitrogen, ref.# 00-4959-52) and visualized directly with a Leica SPEII confocal microscope. For direct determination of ROS levels, the CellROX® Deep Red Reagent kit (Life Technologies, ref.# C10422) was used. Eye imaginal discs were dissected in Schneider's Drosophila Medium (Gibco, ref.# 21720024) and incubated with CellROX reagent (1:500) in agitation at room temperature for 15 minutes. Samples were washed three times with PBS, fixed in 4% PFA for five minutes, washed and mounted as described before.

Serotonin immunostaining

Larval brains were dissected in cold PBS 1X, fixed in 4% PFA for 20 minutes and washed thrice in 0,3% PBT at RT. A 30 minute blocking step with 1% PBT-BSA was performed before adding the primary antibody. The mouse monoclonal serotonin antibody (ThermoFisher, ref.#MA5-12111) was diluted in 1% PBT-BSA at a final concentration of 1:80 and incubated in a wet chamber overnight at 4ºC, followed by three washes in 0,3% PBT at RT. Samples were incubated with the donkey anti-mouse-488 (1:1000 in 1% PBT-BSA) secondary antibody for 120 minutes in gentle agitation at RT. Three final washing steps were performed with PBT for 10 minutes each before the tissue was finally mounted in Vectashield® Antifade Mounting Medium with DAPI (Vectorlabs, ref.# H-1200-10). Quantification of serotonin signal was performed using ImageJ software.

In vitro ROS determination by Fluorescence-activated Cell Sorting (FACS)

T-ALL cells from human donors were treated with CellROX® reagent to detect basal ROS levels and after treatment with the drug BW B70C (20 μg/ml). The reagent was added to the medium at a final concentration of 5 μM and cells were incubated in a CO_2 incubator for 30 min, followed by three washes with PBS. Cells were re-suspended in PBS and analyzed by Fluorescence-activated Cell Sorting (BD FACS Aria III) without delay.

Protein co-immunoprecipitation assays

Cell culture

To detect the interaction between Akt and ATPsynβ *in vitro*, Kc167 cells were grown in flasks with Schneider's Drosophila Medium (Gibco, ref.# 21720024) supplemented with L-Glutamine, 10% fetal bovine serum and 0,5% gentamycin. $2x10^6$cells were collected

from the plate with a serological pipette, centrifuged for 5 minutes at 2000 r.p.m. and washed once with sterile PBS. The resulting cell pellets were stored at -80ºC.

Lysate preparation

To extract protein content from cell pellets, 2ml of cold lysis buffer were added. Lysis buffer is prepared supplementing RIPA buffer, which contains 20 mM Tris-HCl [pH 7.4], 150 mM NaCl, 1% Triton and 5mM EDTA, with protease and phosphatase inhibitor: 2 mM Pefabloc (Sigma-Aldrich, ref.#11873601001), 1X cOmplete Mini EDTAfree protease inhibitor cocktail (Sigma-Aldrich, ref.#11836170001), 1mM Na_3VO_4 and 1mM NaF. After this step, the samples were sonicated using a Biorruptor sonicator (Diagenode). In order to completely break the cells, the samples underwent 4 cycles of 30 second ON/OFF at maximum power. After sonication, the lysates were centrifuged 10 minutes at 4ºC and maximum speed. Supernatants were collected and total protein concentration measured.

Bradford protein assay

Total protein concentration of the lysate was determined using the Pierce BCA Protein Assay Kit (Thermo scientific, ref.# 23227) following manufacturer's instructions. Absorbance at 562nm was measured by a Biochrom EZ Read Microplate Reader.

Pre-clearing

Pre-clearing the lysate reduces non-specific binding and background. For that, lysates were cleared adding magnetic beads conjugated with Protein A or G depending on the species immunoglobulin isotype of the antibody (Millipore, ref. #16-661), followed by and incubation at 4ºC in a rotating shaker during 6 hours.

Immunoprecipitation

The cleared lysates were incubated with the primary antibody rabbit anti-ATP5B (Sigma-Aldrich, ref.#HPA001528) (1:50) at 4ºC overnight in a rotating shaker. After the incubation, 60 µl of magnetic beads conjugated with Protein A or G were added to each sample and incubated for 1 hour at 4ºC in a rotating shaker. The samples were then

washed four times with lysis buffer. Finally, all the samples were resuspended in 30 µl of 3X SDS Red Loading Buffer (NEB, ref.#B7703) with 1,25M DTT Reducing Agent (1 µl for each 10 µl of 3X SDS buffer) and boiled for 10 minutes at 95ºC. Using a magnet, the magnetic beads were separated from the sample to be analyzed by Western Blot as described below.

Western blot

Protein samples were separated in 8-16% SDS-PAGE gels (Bio-Rad, ref. #4561105) and transferred to a PVDF membrane (Inmovilon-P Transfer membranes, Millipore, ref. #IPVH00010) previously activated with methanol. Membranes were blocked in PBS with 0.1% Tween-20 and 3% BSA (TBS-BSA) for 1 hour at room temperature. After that, membranes were incubated overnight with the primary antibody at 4ºC: mouse anti-pospho-Ser473-Akt (Cell Signalling, ref.#1294) (1:1000). After incubation, membranes were washed thrice with TBS and incubated during 1 hour at room temperature with secondary antibody: HRP-conjugated mouse anti-IgG (Jackson, ref. #115-035-062, 1:20 000) diluted in TBS-BSA and followed by three washes with TBS. Proteins were detected using the chemiluminescent substrate Immobilon Western (Millipore, ref. #WBKLS0050) and the detector Amersham Imager 680 blot and gel imager (GE Healthcare Life Sciences).

RT-qPCR

Sample extraction

Tissues from third instar larvae were dissected in cold 1X PBS and stored in RNA*later*® Stabilization Reagent (QIAGEN) at -80°C. For RNA extraction from whole larvae, these were directly collected (5 larvae per sample), washed in PBS and stored at -80ºC. Each condition was represented thrice.

RNA extraction and purification

Either tissue or whole larva was disrupted using TissueLyser LT (QIAGEN). RNA was isolated using the RNeasy Mini Kit (QIAGEN, ref.# 74106), according to the manufacturer's protocol. After that, RNA samples were treated with DNase (TURBO DNA-free Kit, Applied Biosystems, ref.# AM1907) to eliminate the remaining DNA from the samples, as indicated in the manufacturer's protocol. Total RNA concentration (ng/µl) was measured using NanoDrop ND-1000 spectrophotometer.

Reverse transcription

To synthesize first-strand cDNA, 1 µg of RNA was reverse-transcribed adding the following components: 500 ng of oligo(dT)12-18, 500 ng of random hexamers and 1 µl 10 mM dNTP Mix per reaction, reaching a final volume of 13µl. The mixtures were heated at 65°C for 5 minutes and incubated on ice for at least 1 minute. Then, 4 µl 5X First-Strand Buffer, 1 µl 0.1 M DTT, 1 µl RNaseOUT™ Recombinant RNase Inhibitor (Invitrogen, ref.#10777-019) and 1 µl of SuperScript™ III RT (Invitrogen, ref.#18080-093) were added per reaction (20µl final volume) followed by an incubation at 50°C for 60 minutes. Finally, the reactions were inactivated by heating at 70°C for 15 minutes. To remove RNA complementary to the cDNA, 1 µl of RNase H were added and incubated at 37°C for 20 minutes.

Quantitative PCR

Quantitative PCRs were performed using Power SYBR Green PCR Master Mix (Applied Biosystems, ref.# 4367659), 10ng of template cDNA and gene-specific primers, under the following conditions: 10 minutes at 95°C, 40 cycles of 15 seconds at 95°C and 40 seconds at 60°C. Real-time PCR reactions were performed using a 7500 Real-Time PCR system (Applied Biosystems), according to the manufacturer's recommendations. The results were normalized to endogenous Rp49 expression levels (Table 2). Three separate samples were collected from each condition and triplicate measurements were conducted. Data are presented as mean ± standard error of the mean; statistical analyses were performed using two tailed Student's t-test.

Target gene	Forward primer	Reverse primer	Comments
RP49	TGTCCTTCCAGCTTCAAGATGACCATC	CTTGGGCTTGCGCCATTTGTG	Housekeeping
puc	TCCGGCGGTCTACGATATAGAAA	AGCAATAGATGCGGGAAAA	Jnk/Bsk pathway
Glut1	TGATGCAGCTGAGCCAGCAA	TCCAGGGCAGTCTTCATGCT	Glycolytic pathway
HK-A	GGTGCACGAGTTATGTCAGC	GTGCGATGGCATCCTTTAGC	
Pfk	CGAGCCTGTGTCCGTATGG	AGTTGGCTTCCTGGATGCAG	
Ald	CATTCTGGGCATCAAGGTCG	GGATCGACTGGTAGGATGGG	
Tpi	ATCAGGCTCAAGAGGTCCAC	GCGTTGATGATGTCCACGAA	
Gapdh1	TAAATTCGACTCGACTCACGGT	CTCCACCACATACTCGGCTC	
Eno	CCCGTCAGATCTACGACTCC	GATTGGCCTTGATCAGCTCG	
PyK	GGTCTTGGTGACTGGCTGAA	TTCTTTCCGACCTGCAGACC	
ImpL3	AGATCCTGACTCCCACCGAA	GCCTGGACATCGGACATGAT	
Pgi	GGCAAACCCGTCAAGTACAG	GCCATTAAAGCCTCCGTCTG	PPP
Pgd	ATGAGCGGACAAGCGGATATT	TAGGCGCACACCACGAATC	
zw	AGGAGGTGACTGTCAACATCA	CGAAAGGCTTCTCGATAATCACG	
sima	AGCCCAATCTGCCGCCAACC	TGGAGGCCAGGTGGTGGGAC	HIF1α/sima transcriptional factor
Spermine oxidase	GCATGGTTGGAGGATGTCTT	TCTGGGATTTTCCACCTCAG	Sima targets
Sequoia	TCGCAGTACACCTTCACGAC	AGCAGCTCGTTCTTCAGCTC	
fgaB	CACCCTTTCTCTGCACAACA	TGTCCAAAAGTTCCCGAAAG	
v	TCGATGAAACCAAGACGCTGGAGA	GAAACCAGATGCGGGTGCCAGG	Kynurenine pathway
cn	CGGTTATTGGAGCAGGACTTG	TGCGAAAGAGCCAGGTTAATAC	
CG6050/Kyat	GTGCCCCGCTTTGTTCCCCT	TGCGGCAGAGCTCGGCTATC	
dNOS	AACGTTCGACAAATGCGCAA	GTTGCTGTGTCTGTGCCTTC	Nitric oxide synthase
4E-BP	GAAGGTTGTCATCTCGGATCC	ATGAAAGCCCGCTCGTAG	Insulin signaling
InR	GCTGTCAAGCAAGCAGTGAA	TCTTTTTACCCGTCGTCTCC	

Table 2. Primer sequences used to perform RT-qPCR experiments. Notice that RP49 is the housekeeping gene for fly samples.

Glucose uptake assays

For *in vivo* assessment of glucose uptake, tissues from dissected larvae were incubated in PBS with 0.25 mM 2-NBDG (Abcam, ref.# ab146200) for 45 min at room temperature, washed twice in PBS for 10 min, fixed 20 min in PBS + 4% PFA, and washed again twice for 10 min in PBS. All washes and the fixation were done with precooled PBS. Tissues were mounted in Fluoromount-G™ with DAPI (Invitrogen, ref.# 00-4959-52), and images were immediately collected with a Leica SPEII confocal microscope. 2-NBDG fluorescence was excited at 488 nm and detected at 500–520 nm.

UHPLC-Q-TOF-MS-based Nontargeted Metabolomics

Metabolite Extraction

Methanol: chloroform: water (3:1:1 v/v/v) at 0ºC was used for sample quenching extraction. Larvae were then homogenized for 30 seconds at 6m/s speed by using 220mg of glass beads (QIAGEN, ref.#13116-400) and the TissueLyser-LT cell disruptor (QIAGEN, ref.# 85300). The homogenates were then briefly centrifuged and removed from the cell debris and glass beads. Finally, extracts were stored at -20ºC until required. Three replicates were carried out for each condition.

UHPLC-Q-TOF/MS

This step was carried out by the CIAL-Metabolomics Platform core facility (Universidad Autónoma de Madrid). The samples were analyzed in positive mode by an Agilent 1290 Infinity UHPC equipment coupled to an Agilent 6540 UHD exact mass spectrometer with quadrupole-time-of-flight analyzer (Q-TOF) and an ESI Jet Stream interface.

Metabolic fingerprinting

To obtain the *metabolic fingerprint*, the M/Z signals corresponding to the metabolites present in the samples were acquired. Subsequently, through a statistical analysis of the

signals acquired, relationships based on differences and/or significant similarities of the "metabolic fingerprint" were established between the groups of study. Those M/Z signals that allow to classify the groups of samples were identified tentatively using databases to compare experimental and theoretical exact mass, as explained in more detail below.

i. Data processing

The processing of the chromatograms obtained was carried out using the Agilent MassHunter Qualitative software (v. 8.0) together with the Mass Profiler Professional software (v. 14.5). All the samples, as well as the injection and extraction blanks, were analyzed simultaneously using the same procedure. A recursive analysis was carried out to obtain the list of metabolites, with the area of each of them, its exact mass and its retention time. For the detection of the peaks, the "Find by Molecular Feature" algorithm of the MH Qualitative software was used. Once the list of peaks for each sample has been obtained, they are aligned, using the Mass Profiler Professional software. The integration of this list of aligned peaks is done with the "Find by Formula" algorithm of the MH Qual platform.

In the post-processing of the samples, the median of the areas of each of the technical triplicates was taken (triplicate injections of the same sample). Then, all the peaks whose area was less than 3 times the peak area in the extraction targets were filtered, as well as all those that are not in at least 66% of all the samples belonging to the same group. A total of 437 metabolites were found in the samples. To conclude the processing, the normalization of the areas of each peak was carried out, assuming that the total sum of the areas of the peaks of each sample must be equal within the same group and the peaks not found (those that have not been found in any sample due to the automatic peak detection process) were filled by a value equal to half the lowest value, with the objective of not showing artifacts in the statistical analysis later.

ii. Statistical analysis

The normal distribution of the data was verified and scaled using the Pareto algorithm. The statistical analysis was carried out using the software implemented in the

Metaboanalyst 3.0 tool and is divided into two parts. On the one hand, an analysis of the 4 groups is carried out at the same time, to have an initial look and to detect possible outliers. On the other hand, once the outliers have been checked, a comparison is made two to two, that is, between the Notch^{+}, Pten^{-} and Tumor versus the Wild Type. The results of the significant metabolites in each of the comparisons are summarized in Table 6 and Suppl. Table 1. Finally, for the comparison of all the groups, a Principal Components Analysis (PCA) was carried out (Fig. 9).

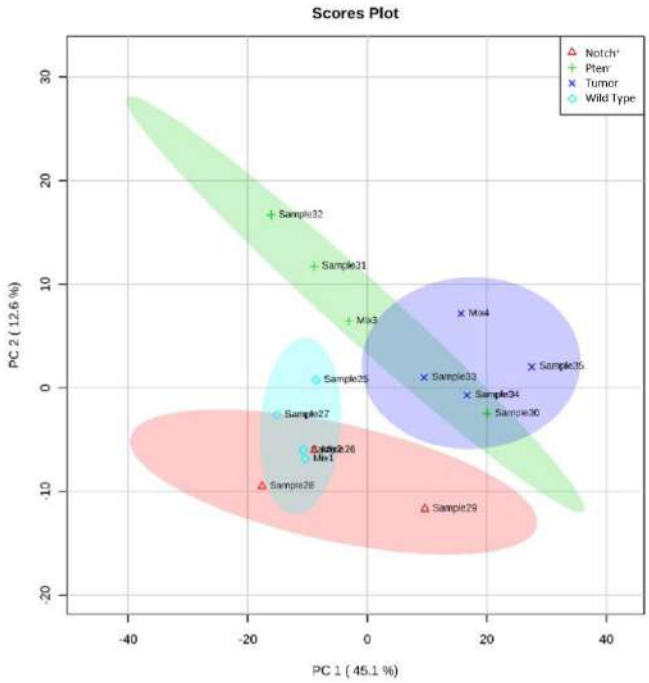

Figure 9. PCA of all the study samples ("mix" corresponds to the pools of each group). Each sample is grouped with those of its own group. A greater variability (greater variation in the first component) is seen in the Pten^{-} and Notch^{+} samples, but no outlier was observed, as the diagrams represent a limit of 95% confidence for each group. The different genotypes correspond to: *ey>* (wild type), *ey>Dl* (Notch), *ey>Pten*-RNAi (Pten) and *ey>Dl>Pten*-RNAi (tumor).

iii. Metabolites identification

The metabolites that present discriminant values in the different comparisons were identified using the Metlin and KEGG databases. This identification was tentative, since it simply uses the values of mass, isotopic pattern and retention time as orientation.

Gas Chromatography-Mass Spectrometry (GC-MS)-based Targeted Metabolomics

Sample collection

For whole larvae assays, 15 wandering L3 larvae were collected in 1.5mL microcentrifuge tubes, washed thrice in cold PBS to remove the remaining food and centrifuged at 2,000×g for 1 min at 4 °C. The residual PBS was removed, samples were freezed in liquid nitrogen and immediately stored at -80ºC freezer.

For hemolymph extraction, 50 third instar larvae were carefully punctured in the thorax using a needle. Punctured flies are placed in a 0.5 ml microfuge tube that contains a hole at the bottom of the tube. This tube was then placed within a 1.5 ml collection tube and centrifuged at 9,000 × g for 5 minutes at 4°C, yielding approximately 10 µl of hemolymph per sample. Fat bodies of 30 larvae per sample were dissected in PBS and collected in eppendorfs placed in a -20ºC freezer to preserve tissue integrity. Finally, all tissue samples were freezed in liquid nitrogen and immediately stored at -80ºC freezer.

Transfer of Samples to Bead Tubes

Each larval or tissue sample was transferred to a 2 mL screwcap tubes containing 1.4 mm ceramic beads (Fisherbrand™, ref.# 15-340-153) and quickly weighed using an analytical balance. The larval/tissue pellet mass was used to normalize the metabolomic data and sample tubes were keeped in liquid nitrogen prior and after the transfer.

Metabolite Extraction

All sample tubes were placed in a -20 °C cooler during the following steps. We added 0.8 mL of prechilled (-20 °C) 90% methanol containing 2 µg/mL succinic-d4 acid (internal standard) into each tube. NOTE: for this technique is only used HPLC grade H_2O and methanol. Samples were homogenized for 30 second at 6.45 m/s using the Omni Bead Ruptor Homogenizer (OMNI, ref.#19-040) at 4 °C. The homogenized samples were incubated in a -20 °C freezer for 1 h. After that, tubes were centrifuged at maximum speed for 5 min at 4 °C and 600 µL of the supernatant were transferred into a

new 1.5 mL tube. To remove all the solvent, sample tubes with open lid were placed in a vacuum centrifuge at room temperature overnight.

Chemical Derivatization

A solution of 40 mg/mL methoxylamine hydrochloride (MOX) (Sigma-Aldrich, ref.# 226904) in anhydrous pyridine (Millipore Sigma, ref.#PX2012-7) was prepared daily. Both MOX and pyridine are extremely sensitive to H_2O, therefore these chemicals must be stored in a desiccator. The MOX in the pyridine solution was incubated in a thermal mixer at 35 °C for 10 min at 600 rpm. Hereafter, 40 µL of MOX-anhydrous pyridine solution was added to each dried sample, vortexed and incubated at 35 °C for 1 h at 600 rpm in a thermal mixer. All samples were centrifuged at maximum speed for 5 min to remove the particle matter. After that, 25 µL of supernatant were transferred into an autosampler vial (Thermo ref.#PD199740) with a 250 µL deactivated glass microvolume insert (Agilent, ref.#51818872). Finally, 40 µL of N-methyl-N-trimethylsilyltrifluoracetamide (MSTFA) containing 1% TMCS (Thermo, ref.#PD199740) was added to each vial. A crimper tool was used to place a cap on the autosampler vial and the samples were incubated at 37 °C for 1 hour at 250 rpm.

GC-MS Detection

We conducted this step with the assistance of the Mass Spectroscopy Core Facility of Indiana University (IN, USA). The GC-MS detection was carried out in a 7890B Gas Chromatograph + 5977 Single Quadrupole instrument (Agilent Technologies). The mass spectrometer was set to execute a SIM/SCAN acquisition mode over a mass range of 50–500 m/z, allowing to the high sensitivity identification of the metabolites of interest.

Data Analysis

Targeted analysis was focused on measuring the abundance of a defined set of metabolites that we describe below (Table 4). For each compound of interest, the retention time and the representative peaks of the ion profile were used for the rapid

identification and subsequent quantification in our samples. Note: the retention time values detailed in Table 3 are specific for these samples in this instrument. A list of aminoacids and some intermediates of glycolysis and krebs cycle was already available in the lab, whereas for compounds related with the kynureine pathway was necessary the pre-analysis of pure standards (Table 4). Qualitative Analysis B.07.00 and MS Quantitative Analysis for GC-MS (Agilent MassHunter) software were used for qualitative and quantitative detection of metabolites, respectively. NIST Mass Spectral Library allowed the validation of the different compounds.

Metabolite	Retention time (min)	Representative ion(s) (Thompsons)
d4-succinate (internal standard)	8.45	251
D-Glucose	22.05	319
Pyruvate	3.69	174
Lactate	3.87	219
Citrate	20.25	273
α-ketoglutarate	14.77	198
Succinate	8.52	247
Fumarate	9.26	245
Malate	12.79	245
2-hydroxyglutarate	14.75	247
Alanine	4.44	190
Valine	6.49	218
Leucine	7.62	158
Isoleucine	8.16	218
Proline	8.22	216
Glutamine	19.07	347
Glycine	8.45	276
Serine	9.75	218
Threonine	10.40	218
Methionine	13.36	176
Pyroglutamate	13.40	258
Aspartate	13.50	232
Cysteine	14.27	220
Glutamate	15.75	348
Phenylalanine	15.79	218
Asparagine	16.89	231
Lyisine	22.10	317
Tyrosine	22.42	218
Tryptophan	27.56	291
3-hydroxykynureine	31.24	395
Kynureine	27.17	424
Xanthurenic Acid	28.31	406
Serotonin	31.58	290
Kynurenic acid	24.73	231

Table 3. List of metabolites analyzed by GC-MS in whole larvae, fat body and hemolymph and their respective retention times (min) and representative ions (Thompsons).

Compound/standard	Ref.#		Solvent	Final concentration (µg/µl)
L-Tryptophan	Fisher Scientific	BP395	60% Methanol in water	4
Serotonin hydrochloride	Sigma-Aldrich	H9523		4
L-Kynurenine		K8625		4
Xanthurenic acid		D120804	pyridine	1
3-Hydroxy-DL-kynurenine		H1771	Water for HPLC	1
Kynurenic acid		K3375		1

Table 4. List of the standard metabolites. Table shows solvents and final concentrations of each metabolite to proces by GC-MS.

Protein restriction analysis

According to Bjordal *et al*, a corn-flour-based food without yeast is deficient in protein content (~60% less than normal food) and specially poor in tryptophan and lysine essential aminoacids. Therefore, to assess the effect of protein restriction in tumorigenesis levels, our standard food recipe was prepared reducing the amount of yeast to a final concentration of 5g/L (Table 5).

Ingredient	Amount
Water	1L
Agar	9,5g
Sucrose	63g
Yeast	31,5g (5g in low yeast diet)
Wheat flour	47g
Nipagin	4,4mL
Propionic acid	8,2mL

Table 5. Standard and low-yeast food recipes.

Feeding experiments

2-deoxyglucose (Sigma-Aldrich, ref. #D8375) was dissolved in water and added to the standard food at 100 μg/ml final concentration. Tryptophan (Sigma-Aldrich, ref. #T0254) was dissolved in water and added to the standard/low yeast food at 0,09 and 0,2 mg/ml final concentration (Grandison *et al.*, 2009). TDO inhibitor 680C91 (ref. #4392) and KMO inhibitor UPF 648 (ref. #4926/10, Tocris Bioscience, Bristol, UK) were dissolved in dimethyl sulfoxide (DMSO; 0.001% final) and in 100% ethanol respectively and subsequently added to the standard food at several concentrations (30, 100, 300 and 500 μM). 3-hydroxykynurenine (Sigma-Aldrich, ref. #H1771) and Xanthurenic acid (Sigma-Aldrich, ref. #D120804) were dissolved in water and DMSO respectively, and then mixed with standard maize food at the concentrations of 1 and 2 mg/ml. All crosses were set up on the supplemented media, and tumor incidence was scored in emerged adult flies.

6. Results

Section 1. PI3K/Akt cooperates with oncogenic Notch by inducing Nitric Oxide-dependent inflammation

Section 2. PI3K/Akt/Pten-induced mitochondrial dysfunction cooperates with Notch in tumorigenesis

Section 3. Notch-PI3K/Akt/Pten tumors reprogram whole-body metabolism via the Tryptophan-Kynurenine pathway

Section 1. PI3K/Akt cooperates with oncogenic Notch by inducing Nitric Oxide-dependent inflammation

Report

Cell Reports

PI3K/Akt Cooperates with Oncogenic Notch by Inducing Nitric Oxide-Dependent Inflammation

Graphical Abstract

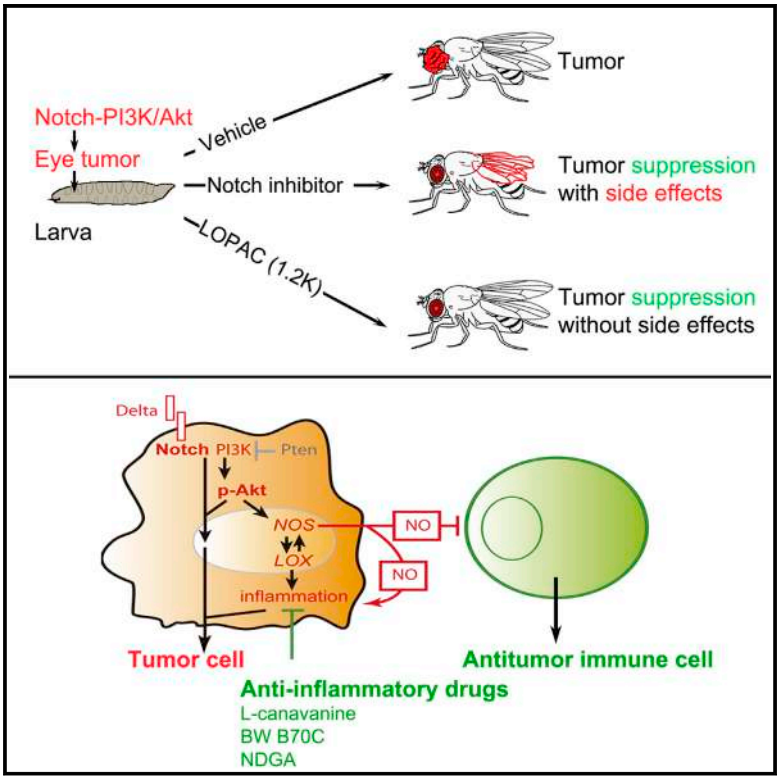

Highlights

- An effective drug screening platform in flies for targeting oncogenic cooperation
- Specific anti-inflammatory drugs block Notch-PI3K/Akt oncogenesis
- Activated PI3K/Akt induces inflammation and immunosuppression via NO synthase
- NO synthase and immunosuppression fuel tumorigenesis by activated Notch

Authors

Santiago Nahuel Villegas, Rita Gombos, Lucia García-López, ..., Esther Ballesta-Illán, József Mihály, Maria Dominguez

Correspondence

svillegas@umh.es (S.N.V.), m.dominguez@umh.es (M.D.)

In Brief

Villegas et al. devised a high-throughput screen for compounds targeting oncogene cooperation without side effects. The screen revealed that a nitric oxide- and LOX-dependent inflammatory environment induced by activated PI3K/Akt facilitates Notch-driven cancer promotion.

Villegas et al., 2018, Cell Reports *22*, 2541–2549
March 6, 2018
https://doi.org/10.1016/j.celrep.2018.02.049

CellPress

Cell Reports
Report

PI3K/Akt Cooperates with Oncogenic Notch by Inducing Nitric Oxide-Dependent Inflammation

Santiago Nahuel Villegas,[1,*] Rita Gombos,[2] Lucia García-López,[1] Irene Gutiérrez-Pérez,[1] Jesús García-Castillo,[1,3] Diana Marcela Vallejo,[1] Vanina Gabriela Da Ros,[1,4] Esther Ballesta-Illán,[1] József Mihály,[2] and Maria Dominguez[1,5,*]

[1]Instituto de Neurociencias, Consejo Superior de Investigaciones Científicas-Universidad Miguel Hernández (CSIC-UMH), Avda. Ramón y Cajal s/n, 03550 Sant Joan d'Alacant, Alicante, Spain

[2]Institute of Genetics, Biological Research Centre, Hungarian Academy of Sciences, MTA-SZBK NAP B Axon Growth and Regeneration Group, Temesvári krt. 62, H-6726 Szeged, Hungary

[3]Present address: Instituto Murciano de Investigación Biosanitaria (IMIB), 30120 Murcia, Spain

[4]Present address: Instituto de Biología y Medicina Experimental (IBYME-CONICET), Vuelta de Obligado 2490, C1428ADN Buenos Aires, Argentina

[5]Lead Contact

*Correspondence: svillegas@umh.es (S.N.V.), m.dominguez@umh.es (M.D.)

https://doi.org/10.1016/j.celrep.2018.02.049

SUMMARY

The PI3K/Akt signaling pathway, Notch, and other oncogenes cooperate in the induction of aggressive cancers. Elucidating how the PI3K/Akt pathway facilitates tumorigenesis by other oncogenes may offer opportunities to develop drugs with fewer side effects than those currently available. Here, using an unbiased *in vivo* chemical genetic screen in *Drosophila*, we identified compounds that inhibit the activity of proinflammatory enzymes nitric oxide synthase (NOS) and lipoxygenase (LOX) as selective suppressors of Notch-PI3K/Akt cooperative oncogenesis. Tumor silencing of *NOS* and *LOX* signaling mirrored the antitumor effect of the hit compounds, demonstrating their participation in Notch-PI3K/Akt-induced tumorigenesis. Oncogenic PI3K/Akt signaling triggered inflammation and immunosuppression via aberrant *NOS* expression. Accordingly, activated Notch tumorigenesis was fueled by hampering the immune response or by *NOS* overexpression to mimic a protumorigenic environment. Our lead compound, the LOX inhibitor BW B70C, also selectively killed human leukemic cells by dampening the NOTCH1-PI3K/AKT-eNOS axis.

INTRODUCTION

Tumorigenesis requires cooperative action among two or more signaling pathways or genes, but the basis of cooperation often remains undefined. Concurrent activation of Notch and phosphatidylinositol 3-kinase (PI3K)/Pten/Akt pathways can trigger tumorigenesis in flies and mice (Palomero et al., 2007; Piovan et al., 2013; Hales et al., 2014; Kwon et al., 2016). This oncogenic combination is also prevalent in aggressive cancers in humans (Eliasz et al., 2010; Kwon et al., 2016; Muellner et al., 2011), such as pediatric T cell acute lymphoblastic leukemia (T-ALL) (Palomero et al., 2007; Gutierrez et al., 2009). Although Notch and PI3K/Akt inhibitors effectively kill cancer cells, only their combination can bypass single-agent pathway inhibitor resistance (Hales et al., 2014). Unfortunately, these pathways have many physiological functions (Bray, 2016; Engelman, 2009; Fruman and Rommel, 2014; Kopan and Ilagan, 2009), so the systemic inhibition of Notch or PI3K/Akt results in severe and lasting side effects (Akinleye et al., 2013; Ntziachristos et al., 2014). Therefore, to minimize side effects, drugs that dampen oncogenic interactions more selectively are needed.

The fruit fly *Drosophila* is a suitable genetic model for exploring the molecular mechanisms of cancer (Bangi, 2013; Pagliarini and Xu, 2003; Ferres-Marco et al., 2006; Vidal and Cagan, 2006; Palomero et al., 2007) and for developing drugs using phenotype-based screening approaches (Dar et al., 2012; Gladstone and Su, 2011; Gonzalez, 2013; Markstein et al., 2014; Willoughby et al., 2013; Bangi et al., 2016). Here, using a *Drosophila* cancer model (Palomero et al., 2007) to screen the Library of Pharmacologically Active Compounds (LOPAC^{1280}), we have identified compounds capable of suppressing Notch-PI3K/Akt cooperative tumorigenesis. Notch inhibitors impeded the development of these tumors, but this was accompanied by high animal mortality and notched wings—two effects characteristic of Notch deficiency. However, we found many other compounds capable of blocking tumor formation by this oncogene cooperation without side effects. These include the anti-inflammatory drug BW B70C (our top hit compound, which suppressed tumorigenesis with the lower dose), a lipoxygenase (LOX) inhibitor, and drugs inhibiting nitric oxide (NO) production.

NO is generated by nitric oxide synthase (NOS) and is a key signaling molecule in inflammation, immune response, and cancer (Fukumura et al., 2006). Arachidonate metabolites produced by LOX enzymes are also primary mediators of inflammation (Dennis and Norris, 2015) and cancer (Chen et al., 2009, 2014; Wang and Dubois, 2010; Greene et al., 2011; Steinhilber et al., 2010). Inflammation is an important contributing factor to solid cancer associated with infection and autoimmunity (Coussens and Werb, 2002) and with certain oncogenes (e.g., Myc and Ras) (Mantovani et al., 2008). Therefore, it is particularly important to understand the interplay between these inflammatory mediators and Notch-PI3K/Akt cooperative oncogenesis.

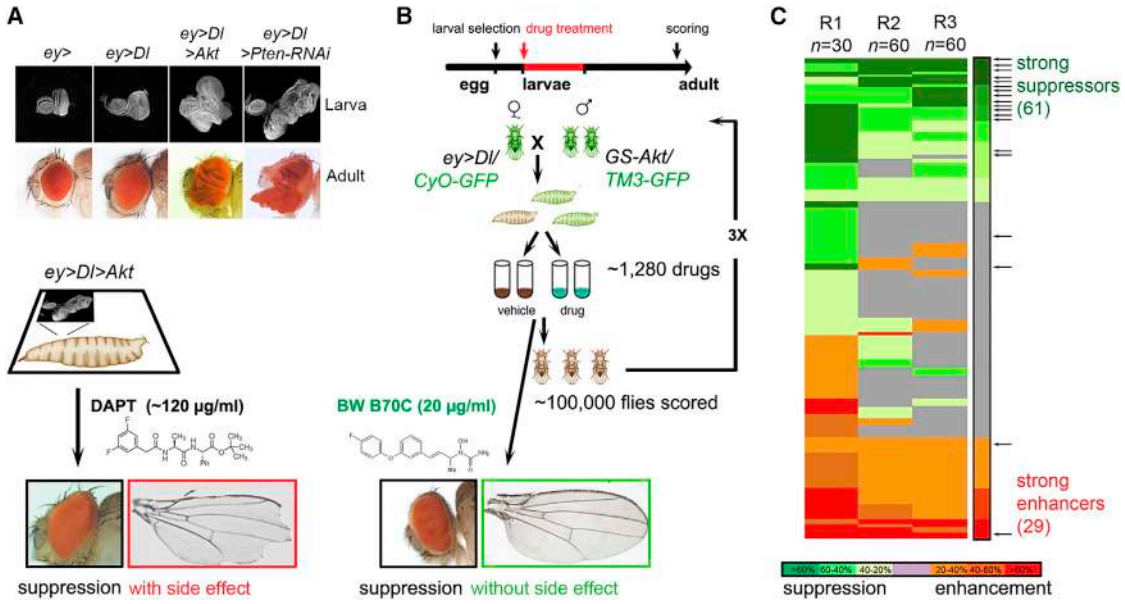

Figure 1. Drug Screen Selectively Targeting Notch-PI3K/Akt Cooperative Oncogenesis

(A) Larval eye imaginal discs (upper row) and adult eyes (lower row) of the control and two tumor models, involving co-overexpression of *Dl* and either *Akt* or *Pten-RNAi* (*BL25967*) using *ey-Gal4* (*ey* >). Below: example of the adult resulting from GSI (DAPT)-treated, tumor-bearing larva. The side effect (notched wings) mimics genetic Notch pathway inhibition.

(B) Schematic of the screen design. Tumor-bearing larvae (non-GFP) were treated with compounds (100 µg/mL in the food) or vehicle. Below: representative adult fly *ey* > *Dl* > *Akt* treated with the top hit compound BW B70C during the larval stage.

(C) Heatmap of the screen results (right column, mean effect). Green, suppression; red, enhancement; gray, no significant change. Arrows point to anticancer drugs in the LOPAC^{1280}. n, number of larvae per drug per round (R).

In vertebrates, the expression of inflammatory markers such as reactive oxygen species, NO, and macrophage infiltration are hallmarks of inflammation in cancer (Colotta et al., 2009; Mantovani et al., 2008). In *Drosophila*, inflammation contributes to adult gut tumorigenesis (Petkau et al., 2017), and both LOX (Miller et al., 1994; Merchant et al., 2008; Stanley, 2006) and NO (Nappi et al., 2000) pathways participate in general inflammatory responses to infection and/or epithelial tissue repair (Wood and Martin, 2017). However, whether *Drosophila* NOS and LOX have a role in tumorigenesis was unknown. To address this, we genetically validated the contribution of the NOS and LOX pathways and inflammation in Notch-PI3K/Akt-driven tumorigenesis. Furthermore, we provide proof-of-concept evidence that BW B70C blocks tumorigenesis in human T-ALL cells by dampening a conserved NOTCH1-PI3K/AKT-eNOS axis.

RESULTS

Unbiased Drug Screen for Targeting Notch-PI3K/Akt Oncogenic Cooperation

We devised a phenotype-based chemical screen to identify agents that block Notch-PI3K/Akt oncogenic cooperation without harming normal cells. We used our *Drosophila* eye cancer model, which captures the molecular features of Notch-PI3K/Akt cooperative oncogenesis (Figures 1A and S1A) (Palomero et al., 2007). The Notch ligand *Delta* (*Dl*) is co-expressed with *Akt* or with an RNAi transgene to silence *Pten*, a PI3K-negative regulator, using the eye-specific promoter *eyeless* (*ey*)-*Gal4*. The cooperative action of these pathways is what causes the development of eye tumors, and the activation of either pathway alone is not sufficient to promote tumorigenesis (Figure 1A) (Ferres-Marco et al., 2006; Palomero et al., 2007). The *ey* > *Dl* > *Akt* and *ey* > *Dl* > *Pten-RNAi* models yield a similar robust eye tumor phenotype (tumor incidence, 70%) (Figures 1A and S1A), allowing the identification of compounds that suppress or further enhance the tumor phenotype. Systemic inhibition of Notch using the γ-secretase inhibitor N-[N-(3,5-difluorophenacetyl)-l-alanyl]-S-phenylglycine t-butyl ester (DAPT) not only blocks tumorigenesis but also interferes with normal growth, resulting in smaller notched wings and lethality (Figures 1A and S1B). Systemic inhibition of PI3K/Akt signaling using LY294002 or wortmannin also resulted in high lethality (Figure S1B), indicating toxic side effects comparable to those seen in mice and humans (Muellner et al., 2011).

We screened the LOPAC^{1280} library of 1,280 small molecules, including a set of U.S. Food and Drug Administration (FDA)-approved anticancer drugs as internal controls. An annotated list of the known targets of the LOPAC^{1280} drugs is readily available, enabling the transformation of phenotypic screening results into a target-based drug discovery approach (Jones and Bunnage, 2017). We administered each drug in food during the larval period at a concentration of 100 µg/mL in three double-blind rounds (Rs) and then assessed the impact on tumorigenesis and normal tissue growth in adults (Figure 1B). This allowed us to directly evaluate responses and side effects. Antitumor response was calculated as the ratio of non-tumor eyes to tumor eyes in treated flies, normalized to the vehicle control

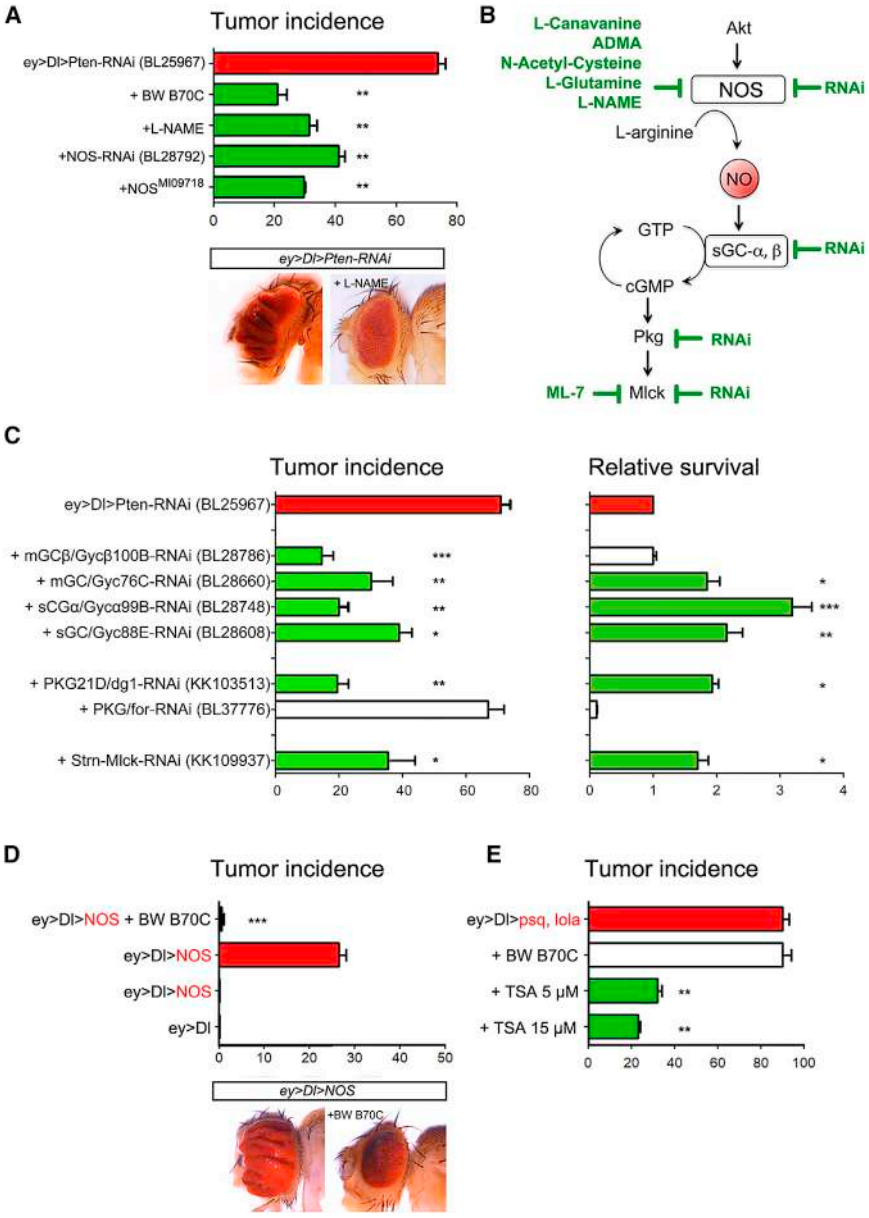

Figure 2. NOS Facilitates Notch-Induced Tumorigenesis

(A) Tumor incidence (as a percentage) in control flies and after pharmacological or genetic inhibition or activation of *NOS*. Below: representative images of control and L-NAME-treated eyes.

(B) Schematic of NO pathway and antitumorigenic drugs identified in our screen and RNAi-based validation.

(C) Tumor incidence (as a percentage, left graph) and normalized survival (right graph) in RNAi-silenced flies (n = 50–100 eyes/genotype).

(D) Tumor incidence (as a percentage) in flies co-expressing *Dl* and *NOS*. Below: representative images of control and BW B70C-treated animals.

(E) Tumor incidence (as a percentage) in Notch-pipsqueak (psq) lola (eyeful cancer) flies with or without trichostatin A (TSA) or BW B70C treatment.

Mean ± SD. *$p < 0.05$, **$p < 0.01$, ***$p < 0.001$ (one-way ANOVA followed by Bonferroni's multiple comparisons test).

group (Figure S1C). Compounds that showed a lethal effect in R1 (n = 30 larvae/drug) were re-tested at lower doses (20 μg/mL).

After R1, any compound causing a response greater than 20% was re-screened (198 suppressor and 276 enhancer compounds) (Figure S1D) using a larger number of animals (n = 60 larvae/drug/R). This significantly reduced the number of false positives and increased reproducibility (>80%) between R2 and R3 (Figure 1C). After screening approximately 100,000 tumor-bearing flies, we found 90 compounds (Figure 1C) that strongly (>60% response) suppressed (61) or enhanced (29) tumorigenesis (see representative eyes and wings in Figures 1A and 1B to compare responses and side effects of DAPT and BW B70C) (Tables S1 and S2). All positive hits were counter-screened in larvae with single oncogene overexpression; none of them rescued single *Dl*- or Akt-induced phenotypes (data not shown), indicating that the identified drugs target the cooperative action of Notch and Akt.

Our screen identified 15 of the 21 known anticancer compounds included in the library (Figure 1C; Table S3) as strong (13) and moderate (2) suppressors of tumorigenesis. Of the remaining 6, 2 were strong enhancers, 2 were lethal, and 2 had no effect. We were able to single out these anticancer drugs, some of which are approved by the FDA for the treatment of leukemia and solid cancers, thus confirming the validity of our screen. These results show a strong positive correlation with the response observed in human cells.

RNAi-Based Validation of Drug Screen Results

The remaining 48 strong suppressors (excluding the 13 known anticancer drugs) are previously unappreciated modulators of Notch-PI3K/Akt-driven tumorigenesis. Because most compounds have a known human molecular target, we validated these results genetically by examining whether tumor-specific RNAi downregulation of candidate target genes (Figures S2A and S3A) mimicked the action of the corresponding compounds. We targeted 92 RNAi lines corresponding to 77 ortholog genes of the annotated and predicted molecular targets of the hit compounds (Table S4). We reasoned that an antineoplastic effect would also rescue tumor-associated lethality. *PI3K-RNAi* was used as a blind positive control, and effects were assessed in adult flies. As a result, we confirmed that 64% of the compounds act through conserved targets rather than indirect side effects (Figures S2B and S2C). This indicates that despite the evolutionary distance of *Drosophila* from humans, we can use our

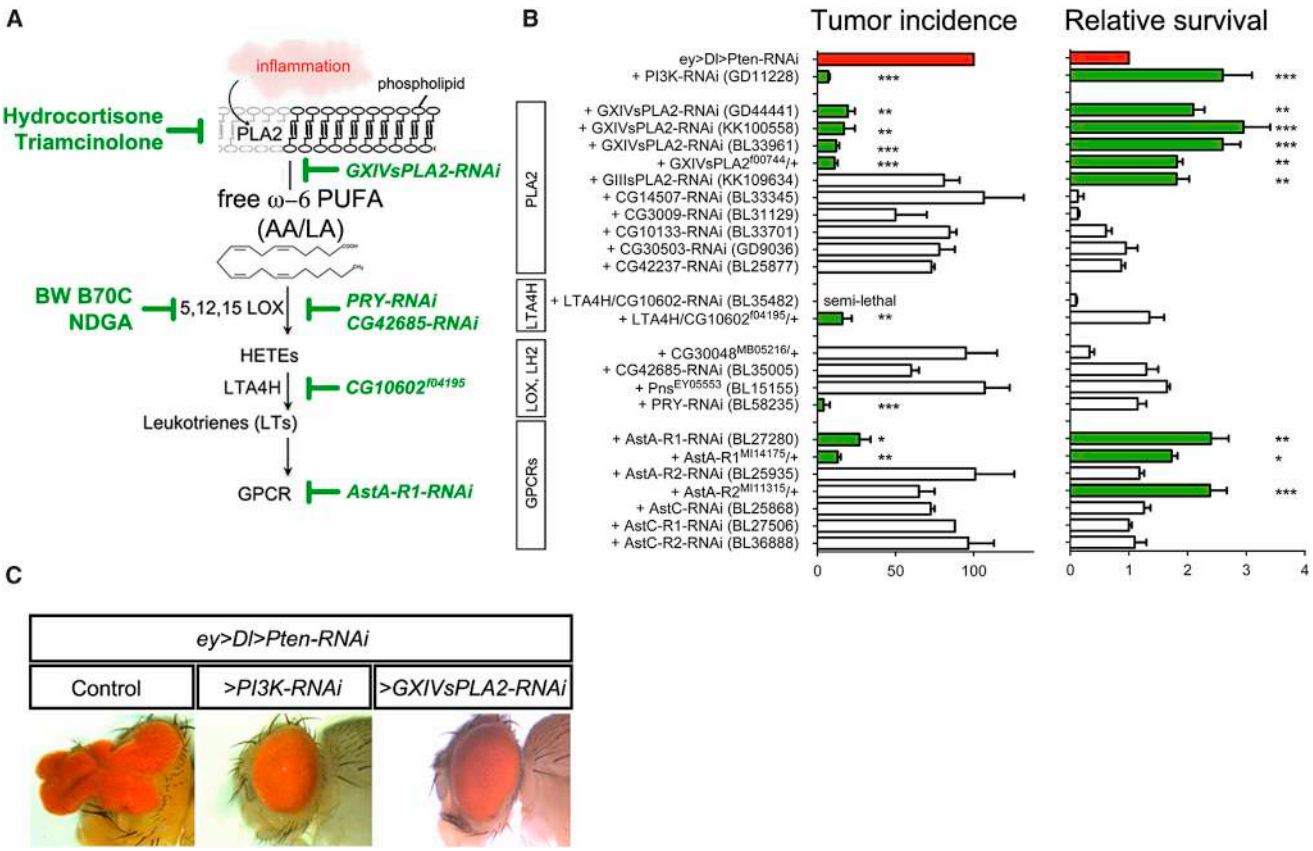

Figure 3. Genetic Targeting of LOX Signaling Blocks Notch-PI3K/Akt Cooperative Oncogenesis

(A) Schematic LOX signaling pathway. Left labels: antitumorigenic drugs identified in our screen and RNAi-based silenced genes. Right labels: homologous *Drosophila* genes. In response to inflammatory stimuli, PLA2 releases arachidonic acid (AA) and/or linoleic acid (LA) from the membrane phospholipids, which are converted to a variety of bioactive lipids via LOX enzymes.

(B) Tumor incidence (left) and normalized survival to adulthood (right) of control and *ey > Dl > Pten-RNAi* flies after depleting the indicated genes via RNAi or mutation. *PI3K92E-RNAi* is the internal positive control. n = 50–100 eyes/genotype.

(C) Example eyes of *ey > Dl > Pten-RNAi* without or with depleted *PI3K92E* or *GXIVsPLA2* via RNAi.

Mean ± SD. *p < 0.05, **p < 0.01, ***p < 0.001 (one-way ANOVA followed by Bonferroni's multiple comparisons test).

Drosophila-based strategy to identify anticancer drugs, as well as their clinically relevant targets.

PI3K/Akt Fuels Notch-Driven Tumorigenesis through NOS

A survey of the hit compounds classified as strong to moderate suppressors revealed the presence of numerous anti-inflammatory agents targeting the NO/NOS and LOX signaling pathways (Table S1), including BW B70C and nordihydroguaiaretic acid (NDGA), each of which inhibits 5- and 12/15-LOX enzymes (Payne et al., 1991; Hussey and Tisdale, 1996; Rudhard et al., 2015). BW B70C drew considerable attention because it blocked tumorigenesis at a very low dose (20 μg/mL) (Figure 1B; Table S1), especially compared with DAPT (Figures 1A and S1A).

We first investigated how NO signaling contributes to Notch-PI3K/Akt-induced tumorigenesis. Using the *NOS* reporter $NOS^{MI09718}$ (Venken et al., 2011), we observed aberrant expression of *NOS* within the tumor eye tissue (Figure S3B), an action induced by *Pten* depletion (Figures S3A and S3C). Treatment of *ey > Dl > Pten-RNAi* larvae with N(G)-nitro-L-arginine methyl ester (L-NAME), a selective NOS inhibitor with documented activity in *Drosophila* (Mukherjee et al., 2011), significantly suppressed tumor growth (Figure 2A). Similarly, genetic silencing of the single *Drosophila NOS* gene (*ey > Dl > Pten-RNAi > NOS-RNAi*) or a *NOS* endogenous mutation (*ey > Dl > Pten-RNAi;* $NOS^{MI09718/+}$) selectively suppressed tumorigenesis (Figures 2A and S2C).

Moreover, targeting the NO canonical pathway within tumor cells by RNAi silencing of genes encoding soluble guanylyl cyclases (*sGC-α* and *sGC-β*), cyclic guanosine monophosphate (cGMP)-*PKG21D*, and its target, myosin light-chain kinase (*Mlck*), suppressed tumorigenesis (Figures 2B and 2C). These results validate another of the top hit compounds that we identified in our screen: ML-7, an inhibitor of Mlck (Figures 2B and 2C). Altogether, we found that *NOS* was aberrantly expressed in tumor cells and that tumor cell-specific knockdown of NO signaling suppressed tumorigenesis. These results highlight the importance of the NO-sGC/cGMP/PKG (cGMP-dependent protein kinase G) pathway in Notch-PI3K/Akt-driven tumorigenesis.

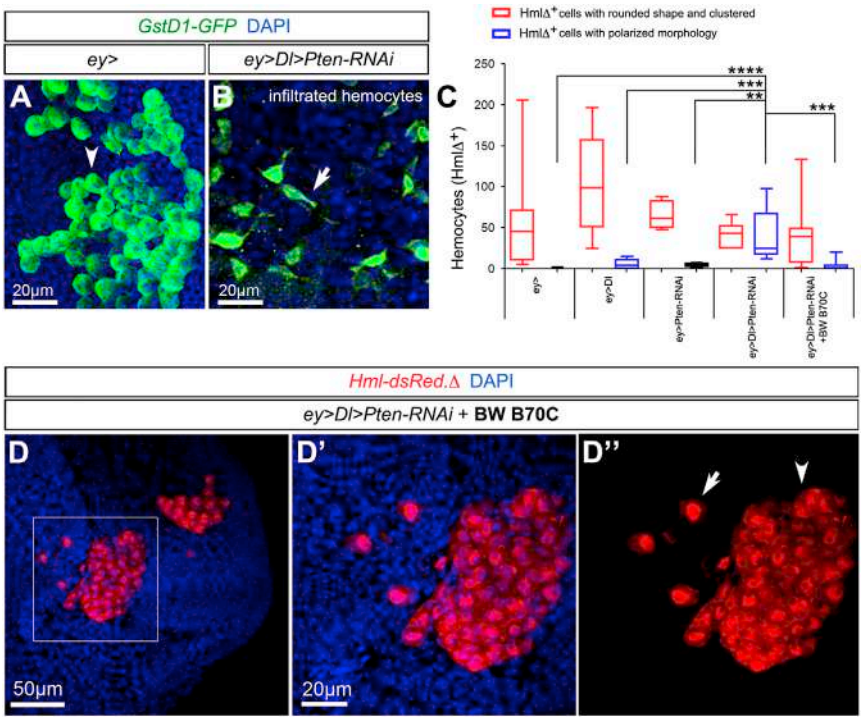

Figure 4. Tumor-Associated Hemocytes and Response to LOX Inhibitor

(A) Hemocytes (arrowhead) in control eye discs (*ey* >) are rounded and form clusters attached to the disc epithelium.

(B) Representative hemocytes in a neoplastic tumor disc with a migratory spindle shape (arrow).

(C) Hemocyte counts in the indicated genotypes (n = 14 eye discs/genotype). Mean ± SD. **p < 0.01, ***p < 0.001, ****p < 0.0001 (one-way ANOVA followed by Bonferroni's multiple comparisons test).

(D) Hemocytes in a Notch-PI3K/Akt eye disc treated with BW B70C (20 μg/mL, 63.2 μM). Right: magnifications of the outlined area. Arrow and arrowhead point to round (pancake-like) and clustered hemocytes, respectively.

Tissue and tumor resident hemocytes are labeled with GstD1-GFP (green, A and B), *Hml-dsRed.Δ* (red, D), and DAPI (blue). For co-localization of GstD1-GFP with the pan-hemocyte marker *Hml-dsRed.Δ*, see Figure S4.

Overexpression of *NOS*, together with overexpression of *Dl*, induced tumorigenesis in the absence of further hyperactivation of PI3K/Akt (*ey* > *Dl* > *NOS*) (Figure 2D). Eye-specific silencing or overexpression of the *NOS* gene alone is inconsequential for eye growth (Cáceres et al., 2011; Jaszczak et al., 2015). BW B70C treatment blocked Notch-NOS-driven tumorigenesis (Figure 2D), suggesting that this process involves an axis with LOX/NOS interdependency. Conversely, tumors induced by the cooperation of Notch with the epigenetic regulators Pisqueak and Lola (Ferres-Marco et al., 2006) were not sensitive to BW B70C, even though they could be suppressed using the epigenetic drug trichostatin A (Figure 2E). Hence, BW B70C does not generally suppress Notch-driven tumorigenesis but dampens a tumor formation process orchestrated by inflammatory NOS.

LOX Pathway Inhibition Blocks Notch-PI3K/Akt-Driven Tumorigenesis

LOX enzymatic activity and LOX-derived lipids have been detected in *Drosophila* extracts and other insects, but the *LOX* gene or genes remained undefined (Pagés et al., 1986; Tan et al., 2016). We therefore searched for *Drosophila* LOX pathway homologs that could be suitable for further validation of our screen results.

Leukotriene A4 hydrolase (LTA4H) catalyzes the production of leukotriene B4 (LTB4), a major lipid product of LOX enzymes that is highly expressed in some cancers (Steinhilber et al., 2010). The *Drosophila* gene *CG10602* encodes an LTA4H homolog (Figure 3A). Halving its gene dosage (*ey* > *Dl* > *Pten-RNAi* > *CG10602*$^{f04195/+}$) markedly suppressed tumorigenesis and rescued tumor-associated lethality (Figures 3B and S3A). Leukotrienes act through G protein-coupled receptors (Wang and Dubois, 2010), and we silenced the allatostatin receptors, the structural orthologs of leukotriene receptors in *Drosophila* (Figure 3A; Table S4). Inactivation of *AstA-R1* suppressed tumorigenesis, whereas silencing *AstA-R2*, *AstC-R1*, and *AstC-R2* did not affect it (Figure 3B).

The most upstream step in LOX-mediated production of proinflammatory lipid metabolites is the release of arachidonic acid from the plasma membrane, mediated by phospholipase A2 (PLA2) (Dennis and Norris, 2015) (Figure 3A). Five suppressor drugs identified in our screen target this step (Figure 3A; Table S1). We tested the seven predicted *Drosophila PLA2* genes (Renault et al., 2002) and found that tumor-specific RNAi silencing of *GXIVsPLA2*, as well as halving its gene dosage (*GXIVsPLA2*$^{f00744/+}$), strongly suppressed tumorigenesis (Figures 3B and 3C), mirroring the antitumor effect of the identified drugs. This confirmed that LOX-generated lipids are required for Notch-PI3K/Akt-driven tumors.

Protumorigenic Immune Inflammation Underlies Notch-PI3K/Akt Cooperation

The participation of the NO/NOS and LOX pathways in Notch-PI3K/Akt-promoted tumorigenesis hints at an unanticipated connection between inflammation and this oncogenic cooperation. Work in vertebrates has implicated macrophage infiltration and expression of inflammatory markers such as NO as key hallmarks of inflammation in solid cancer (Colotta et al., 2009; Mantovani et al., 2008), and immune cells that infiltrate tumors facilitate tumor growth or survival (Grivennikov et al., 2010). In *Drosophila*, macrophage-like hemocytes (Lemaitre and Hoffmann, 2007) have been implicated in the immune response against epithelial tumors (Pastor-Pareja et al., 2008; Cordero et al., 2010).

We examined the hemocytes associated with these tumors using the hemocyte-specific marker *Hml-dsRed.Δ* (Makhijani

et al., 2011) and the oxidative stress reporter *GstD1-GFP*, which we found is expressed in hemocytes (Figure S4A). Wild-type and hyperplastic eye disc-associated hemocytes typically form aggregates with a rounded morphology (Figures 4A, S4B, and S4C) and are attached to the basal membrane (Cordero et al., 2010). We observed that hemocytes within Notch-PI3K/Akt discs were dispersed and became polarized (spindle shaped) (Figures 4B, S4D, and S4E), infiltrating the tumor epithelium (Figures 4C, S4F, and S4G). This suggests that hemocytes change their morphology in response to signals from tumor cells. Consistent with this idea, these morphological changes were suppressed in mutant discs treated with BW B70C (Figures 4C and 4D), suggesting that NOS/LOX activity shapes the inflammatory response in Notch-PI3K/Akt tumors. Altogether, these data link inflammation to tumorigenesis driven by these oncogenes.

Genetic Depletion of Prophenoloxidase in Immune Cells Fuels Notch-Mediated Tumorigenesis

A salient feature of cancer-related inflammation is immunosuppression (Coussens and Werb, 2002; Mellman et al., 2011). In *Drosophila*, melanization—a process mediated by the enzyme phenoloxidase (PO) encoded by the prophenoloxidase (PPO) genes—is a critical innate immune response to tumor cells (Minakhina and Steward, 2006). Platelet-like crystal cells, another class of hemocytes present in larval stages, are the site of *PPO* gene synthesis (Binggeli et al., 2014). We examined *PPO* expression and function to further investigate the participation of inflammation and immunosuppression in Notch-PI3K/Akt tumorigenesis. Larvae with single Notch pathway overactivation (*ey > Dl*) showed robust stimulation of *PPO1* and *PPO2* expression in immune cells (Figure 5A). Conversely, tumor-bearing (*ey > Dl > Pten-RNAi*) and single PI3K/Akt (*ey > Pten-RNAi*) larvae did not show this response (Figure 5A), suggesting that activated PI3K/Akt signaling dampens a secreted signal required in crystal cells to activate the immune response. To ascertain the role of immune cell-derived PPO/PO in single *Dl*-induced overgrowth, we created a genetic immunosuppressed condition using a triple *PPO1, PPO1, PPO3* knockout (Binggeli et al., 2014). Halving *PPO* gene dosage resulted in 55% of the emerging adults bearing full-blown tumors (*ey > Dl*, $PPO1^{-/+}$, $PPO2^{-/+}$, $PPO3^{-/+}$) (Figure 5B), equal to the effect of *NOS* overexpression (Figure 2D). Reducing *PPO* in Notch-PI3K/Akt larvae with already-low *PPO* levels did not enhance tumorigenesis. Furthermore, we found that aberrant *NOS* expression was sufficient to dampen *PPO* expression (Figure 5C) and the immune response triggered by the PO-activating cascade manifested as a strong reduction of melanized crystal cell response after heat stress (Neyen et al., 2015) (Figures 5D and 5E) (see Supplemental Experimental Procedures). Altogether, these observations indicate that immunosuppression is driven by aberrant NOS promoted by activated PI3K/Akt in the tumor cells, which explains how activated PI3K/Akt unleashes the oncogenic potential of Notch.

Validation in Human T Cell Acute Lymphoblastic Leukemic Cells

We validated the antitumor effect of BW B70C in well-established human T-ALL cell models that depend on NOTCH1 and PI3K/AKT signaling (Palomero et al., 2007). We observed that BW B70C treatment killed T-ALL cells (Palomero et al., 2007) that were resistant to Notch inhibitors (*PTEN*-negative, γ-secretase inhibitor [GSI]-resistant T-ALL cell lines RPMI8402, CCRF-CEM, P12-ICHIKAWA, JURKAT, and MOLT-3), as well as *PTEN*-positive, GSI-sensitive T-ALL lines (CUTLL1, ALL-SIL, and DND-41) (Figure 5F). BW B70C treatment had little or no toxicity against normal T lymphocytes (peripheral blood mononucleated cells [PBMCs]) derived from healthy donors (Figure 5F). Moreover, paralleling the results obtained in *Drosophila* tumors, we found that one of the three *NOS* genes, endothelial NOS (*eNOS*), was aberrantly enriched in AKT/NOTCH1-driven T-ALL cells (Figure 5G). Healthy PBMCs did not show *eNOS* expression (Figure 5H). Finally, we found that BW B70C selectively killed T-ALL cells associated with suppression of the aberrant *eNOS* in leukemic cells (Figure 5H).

DISCUSSION

Several Notch and PI3K/Akt inhibitors with potent antineoplastic activity are available, but their progress toward clinical use is hindered by side effects associated with the inhibition of physiological signaling and by drug resistance (Andersson and Lendahl, 2014; Chia et al., 2015; Fruman and Rommel, 2014). The characterization of the targets and mechanisms downstream of Notch-PI3K/Akt in tumorigenesis that are distinct from their targets in normal cells is crucial for identifying cancer vulnerabilities that could be exploited therapeutically. Using an *in vivo* drug screen in *Drosophila* we have identified pharmacologically active compounds that block Notch-PI3K/Akt-driven tumors in flies and validated the top hit compound in human T-ALL cells with NOTCH1 and PI3K/AKT mutations. In addition, BW B70C and compounds inhibiting specific inflammatory pathways were found to elicit potent and selective antitumorigenic responses in Notch-PI3K/Akt tumors by blocking a hitherto unsuspected NOS/LOX axis. Our screen identified 15 of the 21 well-known anticancer compounds included as internal controls; some of them have anti-inflammatory properties (Table S3), but most act mainly by blocking cell proliferation non-specifically through DNA damage.

Genetic studies further highlighted a strong requirement for tumor-specific inflammation driven by LOX- and NOS-dependent Notch-PI3K/Akt cooperation. Human LOX signaling (Chen et al., 2009; Hussey and Tisdale, 1996) and NO signaling (Fukumura et al., 2006; Lim et al., 2008) have been linked to specific cancers as both tumor suppressors and tumor enhancers. Here we linked these inflammatory pathways to tumor initiation by Notch-PI3K/Akt cooperation. The oncogenes Ret, Myc, and Ras can trigger an intrinsic inflammatory response that creates a protumorigenic microenvironment (Mantovani et al., 2008), which accelerates cancer development (Grivennikov et al., 2010). We found that activated PI3K/Akt signaling triggers inflammation and immunosuppression via aberrant *NOS* expression. Overexpressing *NOS* or diminishing the endogenous immune response is sufficient to facilitate tumor initiation via the activated Notch pathway, supporting the notion that inflammation is a key mechanism to unleash the oncogenic potential of

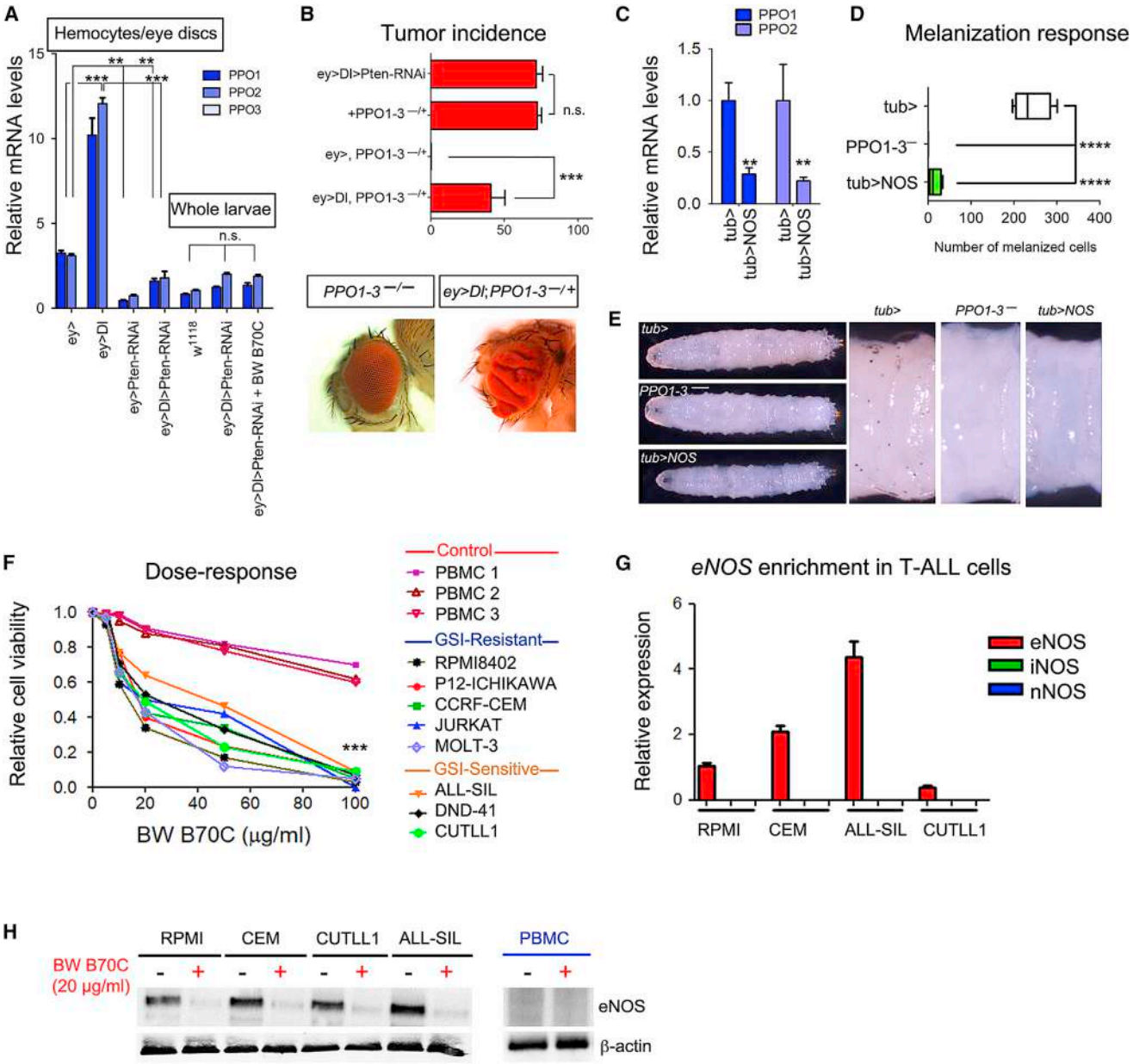

Figure 5. Immunosuppression Releases Notch Oncogenic Potential

(A) *PPO* gene expression in immune cells attached to eye discs (n = 30/genotype) and whole larvae (n = 5/genotype). *PPO3* was undetected in these assays. Experiments were performed in triplicate.

(B) Relative tumor incidence (as a percentage) in *ey > Dl; PPO1–PPO2*$^{-/+}$ (n = 50–100 eyes). Below: representative eyes.

(C) *PPO1* and *PPO2* expression in control and *tub > NOS* larvae.

(D and E) Melanized crystal cell counts (D) and images (E, right, magnifications) of larvae with crystal cell-mediated PPO/PO activity (black cells) response to heat shock. Negative control was *PPO1–3*$^{-}$.(F) BW B70C treatment in a panel of T-ALL cell lines and healthy PBMCs. Data represent three independent experiments and are expressed as mean ± SD. Student's t test for each T-ALL cell line response was ***p < 0.001. Mean ± SD. *p < 0.05, **p < 0.01, ***p < 0.001 (one-way ANOVA followed by Bonferroni's multiple comparisons test in B and Student's t test in D).

(G) qRT-PCR analysis of the three *NOS* genes in T-ALL cells (relative to *GADPH*). Graph shows pooled data from three independent experiments and represents mean ± SD.

(H) Representative western blots of three independent analyses showing eNOS levels in PBMCs and T-ALL cells treated with BW B70C (20 μg/mL, 48 hr) or DMSO (vehicle).

Notch. LOX/NOS inhibition did not harm normal cells, which suggests that these pathways represent promising, safe, druggable targets for human cancers.

Validation of the anti-inflammatory drug BW B70C in a panel of human T-ALL cells dependent on NOTCH1 and PI3K/AKT yet resistant to Notch inhibitors (Palomero et al., 2007) further

highlights the considerable value of unbiased chemical screens in *Drosophila* when it comes to deciphering targets and potential therapeutic approaches relevant to human cancers.

EXPERIMENTAL PROCEDURES

Drosophila Husbandry

The list of RNAi transgenes used is in Table S4. Other fly stocks used were w^{1118}, *ey-Gal4*, *UAS-Dl, CyO twist-GFP, CyO tub-Gal80, Pten-RNAi* (BL25967), *UAS-NOS* (BL56830 and BL56823), $GXIVsPLA2^{f00744}$, $CG10602^{f04195}$, $Pns^{EY05553}$, $AstA\text{-}R1^{MI14175}$ (y^1 *w*; Mi{MIC}AstA-*$R1^{MI14175}$), $NOS^{MI09718}$ (y^1 *w*; Mi{MIC}* $Nos^{MI09718}$), and $PKG/dg2^{MI02855}$ (y^1 *w*; Mi{MIC}dg2*^{MI0285}), all from the Bloomington Drosophila Stock Center; *PI3K92E-RNAi* (*GD11228*, *v38985*) from the Vienna Drosophila RNAi Center; *GS(2)1D233C* (*dAkt1*) (Palomero et al., 2007); $GS(2)88A8^{lola\ pipsqueak}$ (the eyeful cancer strain) (Ferres-Marco et al., 2006); $PPO^{\Delta 1-2,3}$ (a gift from B. Lemaitre); GstD1-GFP (a gift from D. Bohmann); and *Hml-dsRed.Δ* (FBtp0069700) (a gift from K. Brueckner). Flies were reared and maintained in standard fly food at 27°C on a 12-hr light/dark cycle.

Statistical Methods

All statistical analyses were performed in GraphPad Prism 6. qPCR data and melanized crystal cell counts were analyzed using unpaired Student's t tests. For tumor incidence and hemocyte counts, p values were calculated using one-way ANOVA followed by Bonferroni's multiple comparison tests.

All research and human cell procedures were conducted in strict compliance with the European Community Council Directives and Spanish legislation. The protocols were approved by the Universidad Miguel Hernández (2017/VSC/PEA/00154) at the Institute of Neuroscience.

SUPPLEMENTAL INFORMATION

Supplemental Information includes Supplemental Experimental Procedures, five figures, and four tables and can be found with this article online at https://doi.org/10.1016/j.celrep.2018.02.049.

ACKNOWLEDGMENTS

We thank B. Lemaitre and K. Brueckner for mutant flies and D. Ferres-Marco for the analysis of trichostatin A in the eyeful flies. We thank I. Oliveira, M.C. Martinez-Moratalla, L. Mira, C.A. Rehák, S. Bozsó, and A. Berente for technical assistance. We also thank the Bloomington Drosophila Stock Center (NIH P40OD018537) for fly stocks, the Drosophila Genomics Resource Center (NIH 2P40OD010949) for reagents, the Transgenic RNAi Project (TRiP) at Harvard Medical School (NIH/NIGMS R01-GM084947), and the Vienna Drosophila Resource Center (VDRC, http://www.vdrc.at) for providing transgenic RNAi fly stocks. L.G.-L. was supported by a predoctoral Formación Personal Investigador (FPI) fellowship from the Spanish Ministry of Economy and Competitiveness (BES-2015-073796) and R.G. by a postdoctoral fellowship from the Hungarian Scientific Research Foundation (OTKA) (PD-121193). This work was supported by grants from the Hungarian Brain Research Program (KTIA_NAP_13-2-2014-0007), the Hungarian Scientific Research Foundation (OTKA) (109330) to J.M., the European Commission ("CancerPathways", reference FP7-HEALH-F22-2008-201666), the Fundación Botín, the Generalitat Valenciana (PROMETEO/2017/146), the Fundación Española Contra el Cancer (AECC) (CICPF16001DOMÍ), the Spanish Ministry of Economy and Competitiveness (BFU2015-64239-R), and the Spanish State Research Agency, through the "Severo Ochoa" Program for Centers of Excellence in R&D (SEV-2013-0317) to M.D.

AUTHOR CONTRIBUTIONS

S.N.V., R.G., I.G.-P., J.G.-C., D.M.V., and V.G.D.R. performed the drug screen; S.N.V. and L.G.-L. performed the functional experiments; E.B.-I. provided technical support; J.M. contributed to supervision of the *Drosophila* drug screening; M.D. contributed by providing the general concept, study design, and supervision; and S.N.V. and M.D. performed data analyses and interpretation and wrote the manuscript.

DECLARATION OF INTERESTS

The authors declare no competing interests.

Received: August 28, 2017
Revised: December 29, 2017
Accepted: February 12, 2018
Published: March 6, 2018

REFERENCES

Akinleye, A., Avvaru, P., Furqan, M., Song, Y., and Liu, D. (2013). Phosphatidylinositol 3-kinase (PI3K) inhibitors as cancer therapeutics. J. Hematol. Oncol. *6*, 88.

Andersson, E.R., and Lendahl, U. (2014). Therapeutic modulation of Notch signalling—are we there yet? Nat. Rev. Drug Discov. *13*, 357–378.

Bangi, E. (2013). *Drosophila* at the intersection of infection, inflammation, and cancer. Front. Cell. Infect. Microbiol. *3*, 103–110.

Bangi, E., Murgia, C., Teague, A.G., Sansom, O.J., and Cagan, R.L. (2016). Functional exploration of colorectal cancer genomes using *Drosophila*. Nat. Commun. *7*, 13615.

Binggeli, O., Neyen, C., Poidevin, M., and Lemaitre, B. (2014). Prophenoloxidase activation is required for survival to microbial infections in *Drosophila*. PLoS Pathog. *10*, e1004067.

Bray, S.J. (2016). Notch signalling in context. Nat. Rev. Mol. Cell Biol. *17*, 722–735.

Cáceres, L., Necakov, A.S., Schwartz, C., Kimber, S., Roberts, I.J., and Krause, H.M. (2011). Nitric oxide coordinates metabolism, growth, and development via the nuclear receptor E75. Genes Dev. *25*, 1476–1485.

Chen, Y., Hu, Y., Zhang, H., Peng, C., and Li, S. (2009). Loss of the Alox5 gene impairs leukemia stem cells and prevents chronic myeloid leukemia. Nat Genet. *41*, 783–792.

Chen, Y., Peng, C., Abraham, S.A., Shan, Y., Guo, Z., Desouza, N., Cheloni, G., Li, D., Holyoake, T.L., and Li, S. (2014). Arachidonate 15-lipoxygenase is required for chronic myeloid leukemia stem cell survival. J Clin Invest *124*, 3847–3862.

Chia, S., Gandhi, S., Joy, A.A., Edwards, S., Gorr, M., Hopkins, S., Kondejewski, J., Ayoub, J.P., Califaretti, N., Rayson, D., and Dent, S.F. (2015). Novel agents and associated toxicities of inhibitors of the pi3k/Akt/mtor pathway for the treatment of breast cancer. Curr. Oncol. *22*, 33–48.

Colotta, F., Allavena, P., Sica, A., Garlanda, C., and Mantovani, A. (2009). Cancer-related inflammation, the seventh hallmark of cancer: links to genetic instability. Carcinogenesis *30*, 1073–1081.

Cordero, J.B., Macagno, J.P., Stefanatos, R.K., Strathdee, K.E., Cagan, R.L., and Vidal, M. (2010). Oncogenic Ras diverts a host TNF tumor suppressor activity into tumor promoter. Dev. Cell *18*, 999–1011.

Coussens, L.M., and Werb, Z. (2002). Inflammation and cancer. Nature *420*, 860–867.

Dar, A.C., Das, T.K., Shokat, K.M., and Cagan, R.L. (2012). Chemical genetic discovery of targets and anti-targets for cancer polypharmacology. Nature *486*, 80–84.

Dennis, E.A., and Norris, P.C. (2015). Eicosanoid storm in infection and inflammation. Nat. Rev. Immunol. *15*, 511–523.

Eliasz, S., Liang, S., Chen, Y., De Marco, M.A., Machek, O., Skucha, S., Miele, L., and Bocchetta, M. (2010). Notch-1 stimulates survival of lung adenocarcinoma cells during hypoxia by activating the IGF-1R pathway. Oncogene *29*, 2488–2498.

Engelman, J.A. (2009). Targeting PI3K signalling in cancer: opportunities, challenges and limitations. Nat. Rev. Cancer *9*, 550–562.

Ferres-Marco, D., Gutierrez-Garcia, I., Vallejo, D.M., Bolivar, J., Gutierrez-Aviño, F.J., and Dominguez, M. (2006). Epigenetic silencers and Notch collaborate to promote malignant tumours by Rb silencing. Nature *439*, 430–436.

Fruman, D.A., and Rommel, C. (2014). PI3K and cancer: lessons, challenges and opportunities. Nat. Rev. Drug Discov. *13*, 140–156.

Fukumura, D., Kashiwagi, S., and Jain, R.K. (2006). The role of nitric oxide in tumour progression. Nat. Rev. Cancer *6*, 521–534.

Gladstone, M., and Su, T.T. (2011). Chemical genetics and drug screening in *Drosophila* cancer models. J. Genet. Genomics *38*, 497–504.

Gonzalez, C. (2013). *Drosophila melanogaster*: a model and a tool to investigate malignancy and identify new therapeutics. Nat. Rev. Cancer *13*, 172–183.

Greene, E.R., Huang, S., Serhan, C.N., and Panigrahy, D. (2011). Regulation of inflammation in cancer by eicosanoids. Prostaglandins Other Lipid Mediat. *96*, 27–36.

Grivennikov, S.I., Greten, F.R., and Karin, M. (2010). Immunity, inflammation, and cancer. Cell *140*, 883–899.

Gutierrez, A., Sanda, T., Grebliunaite, R., Carracedo, A., Salmena, L., Ahn, Y., Dahlberg, S., Neuberg, D., Moreau, L.A., Winter, S.S., et al. (2009). High frequency of PTEN, PI3K, and AKT abnormalities in T-cell acute lymphoblastic leukemia. Blood *114*, 647–650.

Hales, E.C., Taub, J.W., and Matherly, L.H. (2014). New insights into Notch1 regulation of the PI3K-AKT-mTOR1 signaling axis: targeted therapy of γ-secretase inhibitor resistant T-cell acute lymphoblastic leukemia. Cell. Signal. *26*, 149–161.

Hussey, H.J., and Tisdale, M.J. (1996). Inhibition of tumour growth by lipoxygenase inhibitors. Br. J. Cancer *74*, 683–687.

Jaszczak, J.S., Wolpe, J.B., Dao, A.Q., and Halme, A. (2015). Nitric oxide synthase regulates growth coordination during *Drosophila melanogaster* imaginal disc regeneration. Genetics *200*, 1219–1228.

Jones, L.H., and Bunnage, M.E. (2017). Applications of chemogenomic library screening in drug discovery. Nat. Rev. Drug Discov. *16*, 285–296.

Kopan, R., and Ilagan, M.X. (2009). The canonical Notch signaling pathway: unfolding the activation mechanism. Cell *137*, 216–233.

Kwon, O.J., Zhang, L., Wang, J., Su, Q., Feng, Q., Zhang, X.H., Mani, S.A., Paulter, R., Creighton, C.J., Ittmann, M.M., and Xin, L. (2016). Notch promotes tumor metastasis in a prostate-specific Pten-null mouse model. J. Clin. Invest. *126*, 2626–2641.

Lemaitre, B., and Hoffmann, J. (2007). The host defense of *Drosophila melanogaster*. Annu. Rev. Immunol. *25*, 697–743.

Lim, K.H., Ancrile, B.B., Kashatus, D.F., and Counter, C.M. (2008). Tumour maintenance is mediated by eNOS. Nature *452*, 646–649.

Makhijani, K., Alexander, B., Tanaka, T., Rulifson, E., and Brückner, K. (2011). The peripheral nervous system supports blood cell homing and survival in the *Drosophila* larva. Development *138*, 5379–5391.

Mantovani, A., Allavena, P., Sica, A., and Balkwill, F. (2008). Cancer-related inflammation. Nature *454*, 436–444.

Markstein, M., Dettorre, S., Cho, J., Neumüller, R.A., Craig-Müller, S., and Perrimon, N. (2014). Systematic screen of chemotherapeutics in *Drosophila* stem cell tumors. Proc. Natl. Acad. Sci. USA *111*, 4530–4535.

Mellman, I., Coukos, G., and Dranoff, G. (2011). Cancer immunotherapy comes of age. Nature *480*, 480–489.

Merchant, D., Ertl, R.L., Rennard, S.I., Stanley, D.W., and Miller, J.S. (2008). Eicosanoids mediate insect hemocyte migration. J. Insect Physiol. *54*, 215–221.

Miller, J.S., Nguyen, T., and Stanley-Samuelson, D.W. (1994). Eicosanoids mediate insect nodulation responses to bacterial infections. Proc. Natl. Acad. Sci. USA *91*, 12418–12422.

Minakhina, S., and Steward, R. (2006). Melanotic mutants in *Drosophila*: pathways and phenotypes. Genetics *174*, 253–263.

Muellner, M.K., Uras, I.Z., Gapp, B.V., Kerzendorfer, C., Smida, M., Lechtermann, H., Craig-Mueller, N., Colinge, J., Duernberger, G., and Nijman, S.M. (2011). A chemical-genetic screen reveals a mechanism of resistance to PI3K inhibitors in cancer. Nat. Chem. Biol. *7*, 787–793.

Mukherjee, T., Kim, W.S., Mandal, L., and Banerjee, U. (2011). Interaction between Notch and Hif-alpha in development and survival of *Drosophila* blood cells. Science *332*, 1210–1213.

Nappi, A.J., Vass, E., Frey, F., and Carton, Y. (2000). Nitric oxide involvement in *Drosophila* immunity. Nitric Oxide *4*, 423–430.

Neyen, C., Binggeli, O., Roversi, P., Bertin, L., Sleiman, M.B., and Lemaitre, B. (2015). The Black cells phenotype is caused by a point mutation in the *Drosophila* pro-phenoloxidase 1 gene that triggers melanization and hematopoietic defects. Dev. Comp. Immunol. *50*, 166–174.

Ntziachristos, P., Lim, J.S., Sage, J., and Aifantis, I. (2014). From fly wings to targeted cancer therapies: a centennial for notch signaling. Cancer Cell *25*, 318–334.

Pagés, M., Roselló, J., Casas, J., Gelpí, E., Gualde, N., and Rigaud, M. (1986). Cyclooxygenase and lipoxygenase-like activity in *Drosophila melanogaster*. Prostaglandins *32*, 729–740.

Pagliarini, R.A., and Xu, T. (2003). A genetic screen in *Drosophila* for metastatic behavior. Science *302*, 1227–1231.

Palomero, T., Sulis, M.L., Cortina, M., Real, P.J., Barnes, K., Ciofani, M., Caparros, E., Buteau, J., Brown, K., Perkins, S.L., et al. (2007). Mutational loss of PTEN induces resistance to NOTCH1 inhibition in T-cell leukemia. Nat. Med. *13*, 1203–1210.

Pastor-Pareja, J.C., Wu, M., and Xu, T. (2008). An innate immune response of blood cells to tumors and tissue damage in *Drosophila*. Dis. Model. Mech. *1*, 144–154, discussion 153.

Payne, A.N., Jackson, W.P., Salmon, J.A., Nicholls, A., Yeadon, M., and Garland, L.G. (1991). Hydroxamic acids and hydroxyureas as novel, selective 5-lipoxygenase inhibitors for possible use in asthma. Agents Actions Suppl. *34*, 189–199.

Petkau, K., Ferguson, M., Guntermann, S., and Foley, E. (2017). Constitutive immune activity promotes tumorigenesis in *Drosophila* intestinal progenitor cells. Cell Rep. *20*, 1784–1793.

Piovan, E., Yu, J., Tosello, V., Herranz, D., Ambesi-Impiombato, A., Da Silva, A.C., Sánchez-Martín, M., Perez-Garcia, A., Rigo, I., Castillo, M., et al. (2013). Direct reversal of glucocorticoid resistance by AKT inhibition in acute lymphoblastic leukemia. Cancer Cell *24*, 766–776.

Renault, A.D., Starz-Gaiano, M., and Lehmann, R. (2002). Metabolism of sphingosine 1-phosphate and lysophosphatidic acid: a genome wide analysis of gene expression in *Drosophila*. Mech. Dev. *119* (*Suppl 1*), S293–S301.

Rudhard, Y., Sengupta Ghosh, A., Lippert, B., Böcker, A., Pedaran, M., Krämer, J., Ngu, H., Foreman, O., Liu, Y., and Lewcock, J.W. (2015). Identification of 12/15-lipoxygenase as a regulator of axon degeneration through high-content screening. J. Neurosci. *35*, 2927–2941.

Stanley, D. (2006). Prostaglandins and other eicosanoids in insects: biological significance. Annu. Rev. Entomol. *51*, 25–44.

Steinhilber, D., Fischer, A.S., Metzner, J., Steinbrink, S.D., Roos, J., Ruthardt, M., and Maier, T.J. (2010). 5-lipoxygenase: underappreciated role of a pro-inflammatory enzyme in tumorigenesis. Front. Pharmacol. *1*, 143.

Tan, L., Xin, X., Zhai, L., and Shen, L. (2016). *Drosophila* fed ARA and EPA yields eicosanoids, 15S-hydroxy-5Z,8Z, 11Z, 13E-eicosatetraenoic acid, and 15S-hydroxy-5Z,8Z,11Z,13E,17Z-eicosapentaenoic acid. Lipids *51*, 435–449.

Venken, K.J., Schulze, K.L., Haelterman, N.A., Pan, H., He, Y., Evans-Holm, M., Carlson, J.W., Levis, R.W., Spradling, A.C., Hoskins, R.A., and Bellen, H.J. (2011). MiMIC: a highly versatile transposon insertion resource for engineering *Drosophila melanogaster* genes. Nat. Methods *8*, 737–743.

Vidal, M., and Cagan, R.L. (2006). *Drosophila* models for cancer research. Curr. Opin. Genet. Dev. *16*, 10–16.

Wang, D., and Dubois, R.N. (2010). Eicosanoids and cancer. Nat. Rev. Cancer *10*, 181–193.

Willoughby, L.F., Schlosser, T., Manning, S.A., Parisot, J.P., Street, I.P., Richardson, H.E., Humbert, P.O., and Brumby, A.M. (2013). An *in vivo* large-scale chemical screening platform using *Drosophila* for anti-cancer drug discovery. Dis. Model. Mech. *6*, 521–529.

Wood, W., and Martin, P. (2017). Macrophage functions in tissue patterning and disease: new insights from the fly. Dev Cell. *40*, 221–233.

Cell Reports, Volume *22*

Supplemental Information

PI3K/Akt Cooperates with Oncogenic Notch by Inducing Nitric Oxide-Dependent Inflammation

Santiago Nahuel Villegas, Rita Gombos, Lucia García-López, Irene Gutiérrez-Pérez, Jesús García-Castillo, Diana Marcela Vallejo, Vanina Gabriela Da Ros, Esther Ballesta-Illán, József Mihály, and Maria Dominguez

Supplemental Figures

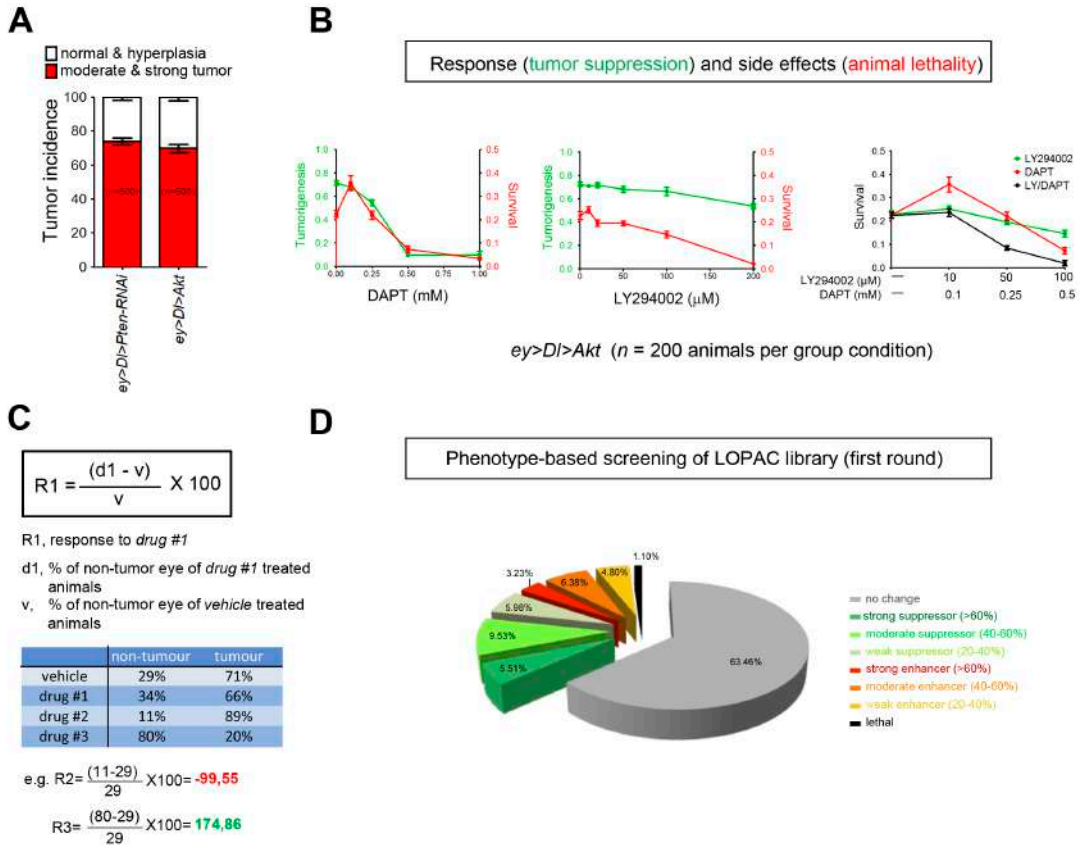

Figure S1. Proof-of-Concept, and Formula to Calculate Drug Response, Related to Figure 1

(A) Graphs show the tumor incidence of each fly models of Notch-PI3K/Akt cooperative oncogenesis. (B) Proof-of-concept of efficacy versus toxicity of drugs directly targeting individual Notch or PI3K/Akt signaling. The γ-secretase inhibitor DAPT {N-[N-(3,5-difluorophenacetyl)-l-alanyl]-S-phenylglycine t-butyl ester} and the PI3K inhibitor LY294002 work effectively in flies (Bjedov et al., 2010; Danilov et al., 2013; Micchelli et al., 2003). The graphs show the efficacy (tumor incidence) and toxicity (survival to adulthood) of adults emerging from drug fed tumor-bearing larvae overexpressing *Delta* and *dAkt1* by *ey-Gal4* at increasing doses (n = 100 flies per drug and concentration). The mortality rate of untreated animals co-overexpressing *Delta* and *Akt* (or *Pten-RNAi*) by *ey-Gal4* is 79% (i.e. survival rate of 21%). Low-dose of DAPT rescued partially this tumor-associated mortality without reducing tumor burden. Doses of DAPT that suppressed tumorigenesis were highly lethal. PI3K inhibitors caused 100% larval lethality, while non-lethal doses failed to suppress tumorigenesis. Combination of DAPT and LY294002 led to synergistic toxicity, resulting in high lethality even in the low-dose DAPT groups. (C) Formula to calculate response (R). The eye tumor phenotype can be influenced by culturing conditions such as humidity, temperature, and variation in the fly food. As such, vehicle-control groups grown in parallel were used to normalize the response. (D) Summary of results after first round (R1) of screening. 37% of the compounds (474/1280) showed a suppressor/enhancer response equal or higher than 20% and were selected for re-screening.

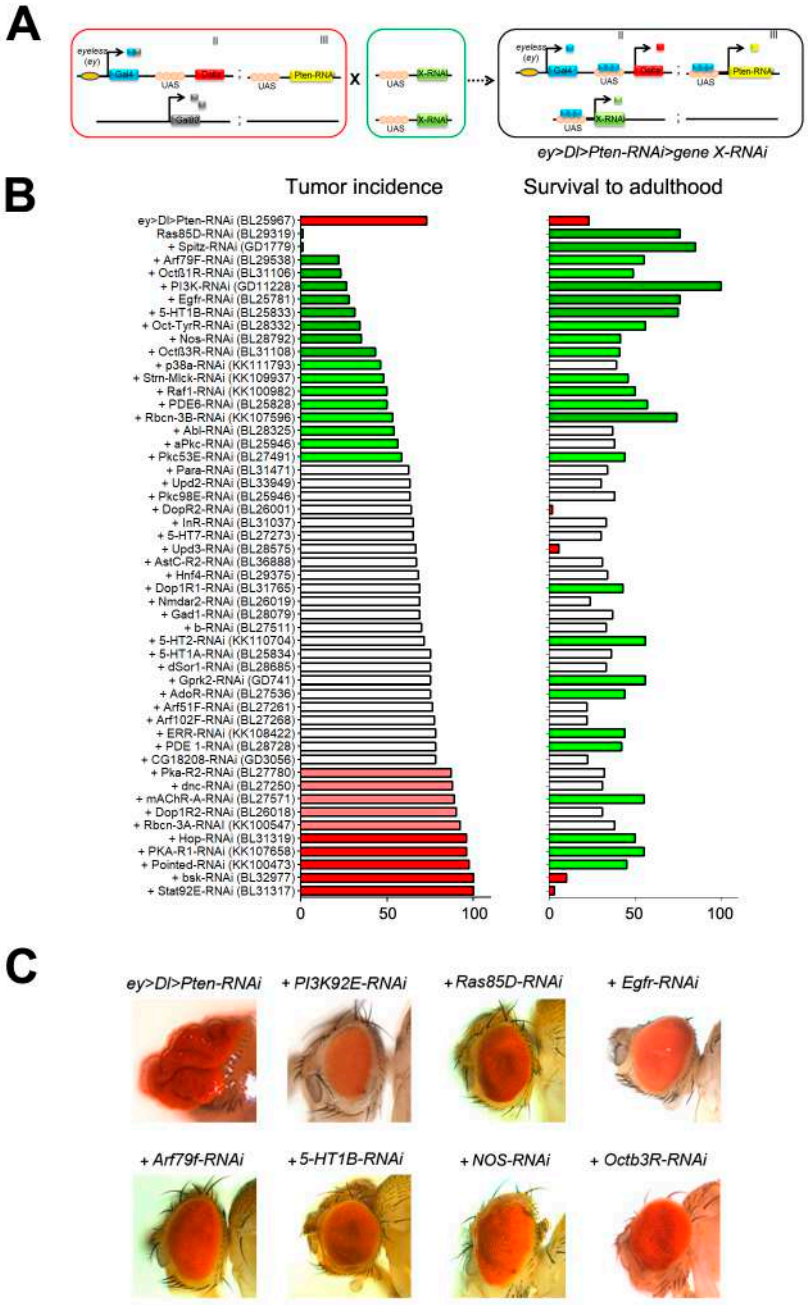

Figure S2. *In Vivo* RNAi-Based Validation of Drug Screen Results, Related to Figure 1

(A) Scheme of the genetic crosses to test *UAS-RNAi* transgenes of candidate drug targets *in vivo* in larvae carrying *UAS-Dl* and *UAS-Pten-RNAi* and *ey-Gal4*. F1 offspring was scored for the tumor burden and animal mortality. (B) Left: Bar graph shows tumor incidence. Right: Relative survival to adulthood after RNAi-mediated depletion of the predicted molecular drug target in the *ey>Dl>Pten-RNAi>gene-RNAi* animals. (C) Representative eye tumor rescued phenotype carrying the indicated *UAS-RNAi* transgenes against the candidate targets. We used the orthologs search tools from FlyBase, which includes Compara, eggNOG, Inparanoid, OMA, Panther, Phylome, RoundUp, TreeFam ortholog prediction algorithms.

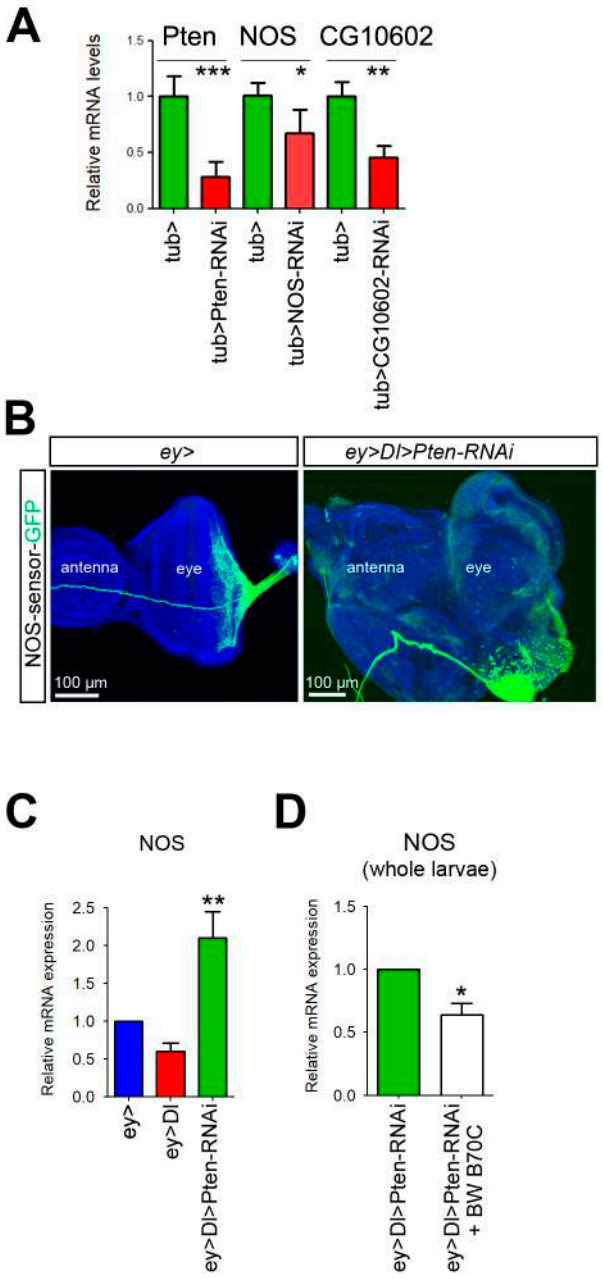

Figure S3. *NOS* Aberrant Expression Induced by Activated Akt Signaling, Related to Figure 2

(A) Validation of indicated transgenic RNAi fly lines using qRT-PCR. (B) $NOS^{MI09718/+}$ (GFP reporter of *NOS*, green) in control *ey-Gal4* eye discs is restricted to the postmitotic retinal cells and the optic nerve. Eye tumor discs show aberrant *NOS* in the undifferentiated proliferative eye region where *ey-Gal4* is expressed. (C) Graph shows the relative levels of *NOS* mRNA, normalized to *Rp49* of the indicated genotypes (n = 30 eye discs *per* genotype). (D) Discs from larvae treated with BW B70C or control. *P* values were calculated using one-way ANOVA test, using Bonferroni multiple comparison tests.

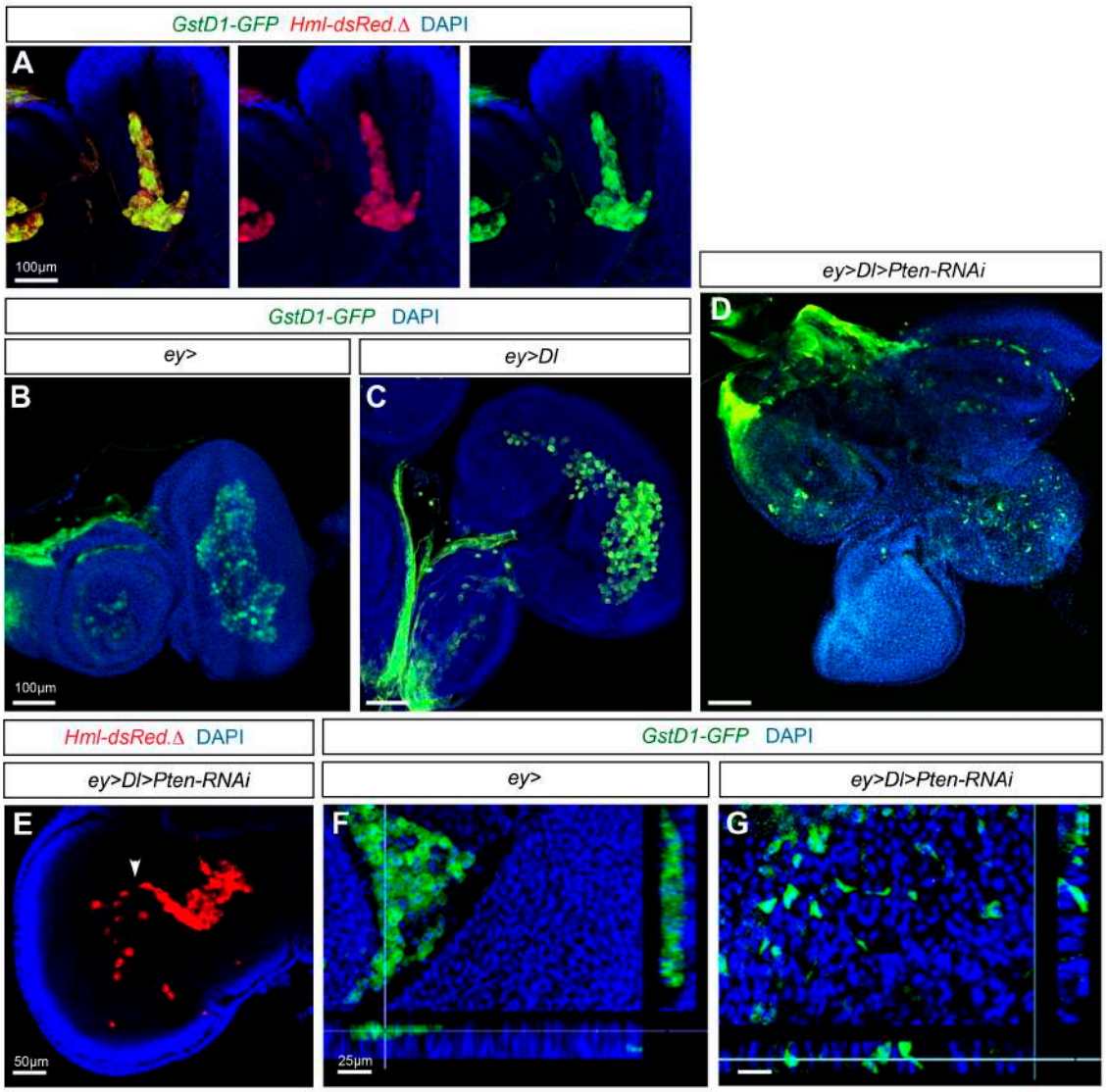

Figure S4. Tissue and Tumor-Associated Hemocytes, Related to Figure 4

(A) Tissue resident hemocytes (macrophage-like cells) are double labeled by *GstD1-GFP* (green), a sensitive oxidative stress reporter and by the pan-hemocyte marker *Hml-dsRed.Δ* (red). Single channel images are also shown. Discs are counterstained with DAPI (blue). (B) Tissue resident hemocytes in control eye disc (*ey>*). (C) Hyperplastic eye disc (*ey>Dl*). (D) Neoplastic eye disc Notch-PI3K/Akt (*ey>Dl>Pten*-RNAi) in which the dispersed migratory spindle shape of hemocytes can be see. Number of hemocytes associated with imaginal discs is highly variable among discs, for quantification see **Figure 4C**. (E) Hemocytes with polarized migratory phenotype labeled by *Hml-dsRed.Δ* (red) originating from the clusters of tissue resident hemocytes (arrowhead) are shown. (F) The confocal image and vertical sections of control eye imaginal disc epithelium, and (G) tumor eye disc epithelium (*ey>Dl>Pten*-RNAi). Hemocytes are labeled by ROS sensor (green). Note that hemocytes infiltrate the tumor epithelial disc (see vertical section in G) but remain at the surface of the wild type eye disc epithelium (F). In F, basal is up.

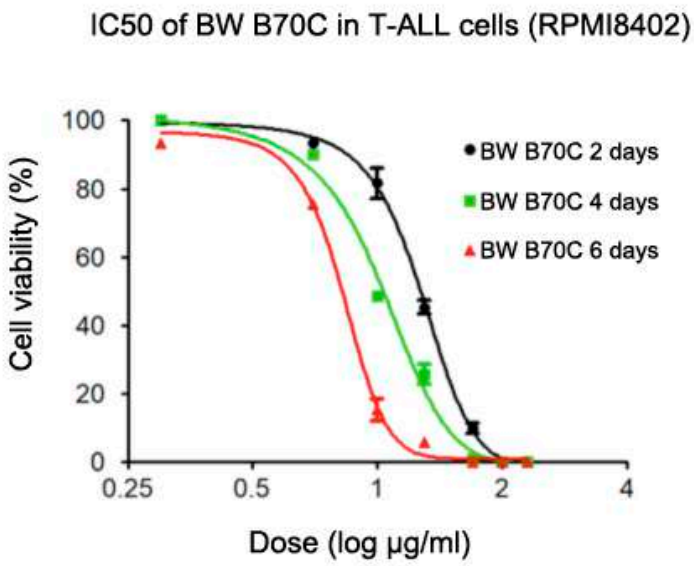

Figure S5. BW B70C Half Maximal Inhibitory Concentration (IC50), Related to Figure 5

The IC50 of the LOX inhibitor BW B70C in human T-ALL cell line RPMI8402, which is NOTCH1-PI3K/AKT dependent but resistant to Notch inhibitors owing to the mutation in *PTEN*. The graph shows dose response curves measured as a function of time and drug concentration. Cytotoxic effect is measured in RPMI8402 T-ALL cells (IC50 are 3.92, 5.89 and 19.93 µg/ml, corresponding to 12.3, 18.6 and 63.2 µM, respectively) at days 2, 4, and 6. Means ± S.D (n= 3).

Supplemental Experimental Procedures

High-Throughput Screening Approach, Compound Treatment Procedure, and Optimization

The HTS approach differs in various aspects from previous drug screens in flies. First, the screening used a larger number of larvae (n=30 in R1 and n=60 in R2 and R3) and response is measured by scoring tumor burden in treated adult animals and simultaneously measuring toxicity and side effects. We used the eye-specific *ey-Gal4* driver for spatial and temporal control of transgene expression in larva (juvenile stages in insects). Targeted expression of *Delta* (*UAS-Dl*) and its cooperating partner, *Akt1* using our *GS1D233C-Akt1* (Palomero et al., 2007) or the silencing of *Pten* (*UAS-Pten-RNAi*) yielded ~70% of the flies developing eye tumors. Both cancer models are quite lethal, with a survival rate of ~21%. In addition, ~3-7% of the survival mutant flies display metastasis (Palomero et al., 2007). The incidence of metastasis is too low to be statistically significantly scored in the drug screen.

For the HTS, we generated stocks of flies with GFP-labeled balancer chromosomes: (1) *ey>Dl/CyO twist-GFP*, (2) *GS1D233C-Akt/TM3 twist-GFP* and (3) *UAS-Pten-RNAi/TM3 twist-GFP*. Offspring of the cross of virgin females *ey>Dl/CyO twist-GFP* with males *GS1D233C-dAkt1* or *UAS-Pten-RNAi/TM3, twist-GFP* were selected (as GFP^{-} L2 larvae) for drug treatment or vehicle control group.

For genetic validation via RNAi transgene expression, we generated a stock carrying three transgenes *ey-Gal4 UAS-Dl* and *UAS-Pten-RNAi* along with the Gal4 repressor (*tub-Gal80*) in the balancer chromosome (*ey>Dl/CyO tub-Gal80; UAS-Pten-RNAi/TM3 twist-GFP*).

Extensive small-scale 'pilot' screens preceded the HTS to provide the basis and guidance of potential problems arising from variability of the phenotype-based assays, impact of environment (temperature, humidity, diet), and optimization of compound preparation and suitable solvents for the HTS in *Drosophila*. In these preliminary tests, we also defined empirically an operational dose of **100µg/ml** for the HTS based on experiments with Notch inhibitors and pilot screens of a set of 100 randomly selected drugs from the Sigma Life Science's Lopac^{1280} library of pharmacologically active compounds. The LOPAC^{1280} library comprises highly pure and diverse annotated collection of inhibitors, receptor ligands, pharma-developed tools, and approved drugs for various diseases including cancer (see, http://www.sigmaaldrich.com/life-science/cell-biology/bioactive-small-molecules/lopac1280-navigator.html).

We found that the γ-secretase inhibitor DAPT {N-[N-(3,5-difluorophenacetyl)-l-alanyl]-S-phenylglycine t-butyl ester} effectively suppressed tumorigenesis at a dose ranging from 0.5-1 to mM (~230 µg/ml; concentration of the drug in the food) but was also very toxic for the larvae (n = 100 animals scored *per* drug concentration). The PI3K inhibitors, LY294002 and wormannin, which had been shown to work effectively in flies (Bjedov et al., 2010; Danilov et al., 2013), caused 100% lethality and sub-lethal doses did not suppress tumorigenesis.

Based on these observations, an initial operational concentration of 200-250 µg/ml was assayed with the random set of 100 drugs. These tests unveiled high toxicity of DMSO vehicle itself and of the majority of drugs tested (see below). In contrast, several drugs modified tumorigenesis without showing overall toxicity at a ~2.5-fold lower concentration (100 µg/ml), thus, we choose this dose for the HTS.

Drug Treatment and Internal Controls

GFP^{-} L2 (48 h after egg laying, AEL) larvae were transferred to drug (or vehicle) containing food vials (2 ml of food) and raised at 27º C until adulthood. Response was determined by direct measurement of tumor burden and potential side effects, calculated using the formula in Figure S1C. Adult wing defects were chosen as a direct measurement of side effects of drugs in non-transformed tissues.

We prepared stock solutions (1, 2, 10 mg/ml) using DMSO, EtOH, MeOH, H2O or chloroform according to manufacturer instructions. Drug concentration was limited by the toxicity of DMSO in flies. For example, doses of DMSO higher than 0.4% provoked toxicity that could confound or mask drug response, setting the maximal concentration used for DMSO dissolved drugs. The small compounds were mixed with warm (45° C) Iberian fly food (see below) and left to solidify at room temperature. For

experiments using EtOH, MeOH or chloroform as vehicle, the food mixed with the drug or vehicle alone was prepared 24 h before transferring the larvae to allow evaporation of these solvents. Standard 'Iberian' fly food was made by mixing 15 l of water, 0.75 kg of wheat flour, 1 kg of brown sugar, 0.5 kg yeast, 0.17 kg agar, 130 ml of a 5% nipagin solution in ethanol, and 130 ml of propionic acid.

Drugs were screened blindly, and the first round of screening was done in the laboratories of Dominguez in Alicante (Spain) and Mihály in Szeged (Hungary) using both the same Iberian fly food recipe and a standardized protocol. The subsequently re-screening R2 and R3 used $n = 60$ animals per drugs and were performed over several months in the laboratory in Alicante (Spain). In this first round of testing, most drugs except 14 did not results in animal lethality at the dose of 100µg/ml. These 14 drugs were re-tested at lower dose (20µg/ml) but only BW B70C was non-lethal and was selected as a suppressor drug.

The eye tumor burden was measured under the scope manually and using the formula in Figure S1C, compounds were classified as 'suppressors' or 'enhancers' according to their effect (strong, moderate and weak: see Tables S1 and S2). Compounds showing an average effect (suppression or enhancement) higher than 20%, 40% and 60% were classified as weak, moderate or strong, respectively.

Of the 21 well-established anticancer compounds included in LOPAC^{1280} library (internal control of the screen), hydroxyurea (HY) and retinoic acid p-hydroxyanilide were found to fuel Notch-PI3K/Akt-associated tumorigenesis significantly (Table S3), and the anticancer agent nimustine hydrochloride used to treat malignant glioma caused complete larval lethality even at a low concentration (20 µg/ml). These findings suggest that *Drosophila* cancer models can also help provide clues about the potential detrimental (tumor enhancement) effects of candidate drugs. However, we do not rule out the possibility that the lethality and/or tumor enhancement properties of some compounds may reflect the differences in pharmacokinetics and pharmacodynamics between flies and mammals.

Validation: Secondary *In Vivo* RNAi –Based Analysis

A large majority of library compounds identified as suppressors in the HTS have one or more known molecular target in humans (Table S4). Other candidate drug targets were defined based on predicted drug-protein interaction using STITCH software according to the drug chemical architecture. Additionally, signaling components or effectors associated with specific targets were also selected for further tests via RNAi analyses. Several, independently generated RNAi transgenes were tested when available.

In such a way, 54 molecular targets of the 48 strong suppressor compounds identified in our HTS were identified. By performing a protein homology search, a total of 77 *Drosophila* homologues of the 54 human genes were identified and each gene was knockdown using tumor-specific *in vivo* RNAi transgene expression. All candidate genes were assayed in the progeny of the cross of virgin females from the stock *ey>Dl/CyO, tub-Gal80; UAS-Pten-RNAi/TM3, tub-Gal80* with males of the corresponding *UAS-RNAi* line. *PI3K-RNAi* served as a blind, positive control (related to Figures S2A-C and Table S4).

Many of the RNAi of candidate drug targets also increased the survival to adulthood rate. In particular, 25 RNAi lines increased survival significantly along with suppressed tumorigenesis, including Ras85D, Spitz, Arf79, Octß1R, PI3K, EGFR, 5-HT1B, Oct-TyR, Nos, Octß3R, Strn-Mlck, Raf1, Rbcn-3B, and Pkc53E. Additionally, some candidate genes when silenced tumor-specifically increased animal survival without suppressing tumorigenesis (e.g. *AstC-R2*), suggesting that the two phenotypes could be uncoupled. The larval lethality was linked to over-activation of PI3K/Akt signaling and the systemic inflammation, and overexpression of *PI3K*, *Akt*, *UAS-Pten-RNAi* alone or *NOS* overexpression was all sub-lethal.

COX inhibitors and Non-Steroidal anti-Inflammatory Drugs (NSAIDs), which target COX-1 and COX-2, were found to act as enhancers (Table S2) and RNAi-silencing of the *Drosophila* cyclooxygenase genes, *Pxt* and *CG10211* also enhanced tumorigenesis (Related to Table S4), consolidating the effect seen after pharmacological inhibition of COX.

Monoamine Oxidase Inhibitors (*MAOis*) significantly worsened Notch-Pten-Akt-induced tumorigenesis in *Drosophila* (Table S2) MAOis increase the levels of amides such as octopamine and serotonin, which are produced by neurons and immune cells. Consistent with this drug screen results, RNAi silencing of

the amide receptors, 5-HT1B, Octß1R, Octß1R and OctTyrR (Table S4) in the tumor cells using *ey-Gal4* (*ey>Dl>Akt>receptor-RNAi*) significantly decreased tumorigenesis (see Figures S2B and S2C) and Table S4.

Epidermal Growth Factor Receptor (EGFR) Inhibitors were found as enhancers of Notch-Pten-Akt-driven tumors (Table S2) but strong depletion via RNAi silencing of *EGFR* gene, and other pathway components, effectively suppressed tumorigenesis in our experimental set-up (Figures S2B and S2C).

Immunostaining and Imaging of Larval, Adult Eyes, and Wings

For assessing tumor suppression/enhancement, batches of late third instar larvae imaginal eye-antennal discs of treated or vehicle-control groups were dissected in PBS and collected in ice-chilled PBS. The tissue was fixed in 4% PFA at RT for 20 min and then washed three times with PBT (PBS buffer and 0.3% Triton). The tissue was incubated with DAPI (Invitrogen) for 15 min at RT (0.3 µg/ml), and washed again three times with PBT and a final wash with PBS. Discs were staining with anti-GFP, anti-DsRed, and counterstaining with DAPI, and mounted in Vectashield (Vector Labs), and images were obtained using a Leica TCS SP2 Confocal microscope.

For adult wing notches analysis, adult wings from female flies were dissected and mounted on slides in 80% glycerol in phosphate-buffered saline solution. For imaging of adult eyes, flies were fixed and kept in 70% ethanol until imaging. Images were captured on an optical microscope ZEISS Axiophot, using a MicroPublisher 5.0 camera (QImaging) and the QCapture software (QImaging). All pictures were taken using a 5X objective with 1.5X zoom. Each eye image is a composite of 15 to 25 images of the same sample focused at different heights of the specimen. The in-focus composites were generated using the software AutoMontage Essentials 5.0.

Quantitative Real-Time PCR

Primers for real-time (RT)-PCR were obtained from Applied Biosystems. Comparative RT-PCRs were performed in triplicates, and relative expression was calculated using the comparative Ct method. Primers were designed using the Primer3 online tool (http://bioinfo.ut.ee/primer3-0.4.0/primer3/). Data are presented as mean ± standard deviation (S.D.); statistical analyses were performed using two-tailed Student's *t*-test.

Primer sequences are:

Drosophila Rp49	Forward 5'-CATCCGCCCAGCATACAG-3' Reverse 5'-ACCGTTGGGGTTGGTGAG-3'
Drosophila NOS	Forward 5'-AACGTTCGACAAATGCGCAA-3' Reverse 5'-GTTGCTGTGTCTGTGCCTTC-3'
Drosophila PPO1	Forward 5'-TGAGCGTAATCAGGCTTTGA-3' Reverse 5'-GTTCTCACCAGGCACCAAAT-3'
Drosophila PPO2	Forward 5'-CTGGTGCCAAAGGGTCTG-3' Reverse 5'-ACCAATTGCTGGTCAATCCT-3'
Drosophila PPO3	Forward 5'-CATCCATCAGGGCTACGTTT-3' Reverse 5'-GGATGTCGATGCCCTTAGC-3'
Drosophila Pten	Forward 5'-TGATCATAACCCTCCAACGA-3' Reverse 5'-TCAATCGGCAAGGTTTTCAG-3'
Drosophila CG10602	Forward 5'-AGTGCTCTCAACTGGAAGATCG-3' Reverse 5'-GCAGTCAACACCTTGAAGCG-3'
Human *eNOS*	Forward 5'-CCCGCTTCCTGTTTCTTAGT-3' Reverse 5'-GGCACAGTCCCTTATGGTAAA-3'
Human *iNOS*	Forward 5'-GTCAGAGTCACCATCCTCTTTG -3'

	Reverse 5'-GCAGCTCAGCCTGTACTTATC-3'
Human *nNOS*	Forward 5'-CCCTCTCGCCAAAGAGTTTATT-3' Reverse 5'-CTTGAGCTGGTAAGTGCTAGTG-3'
Human *β-actin*	Forward 5'-CCAACCGCGAGAAGATGA-3' Reverse 5'-CCAGAGGCGTACAGGGATAG-3'

Crystal Cell Phenoloxidase Activity Assay

Crystal cells are characterized by crystalline inclusions that contain the zymogen pro-PO encoded by the *PPO1-3* genes and can be visualized due to specific blackening upon heating larvae at 60°C for 10 min. Third instar wandering stage larvae were heat treated to visualize crystal cells and imaged using Leica microscope. Melanised crystal cell counts were done in 5 larvae per condition and genetic background. Error bars represent the standard deviation. *P* values were calculated using one-way ANOVA.

T-ALL Cells Culture and *In Vitro* Drug Analysis

RPMI8402, P12-ICHIKAWA, CCRF-CEM, MOLT-3, JURKAT (*PTEN*-negative, GSI-resistant) and ALL-SIL, DND-41 and CUTLL1 (*PTEN*-positive, GSI-sensitive) T-ALL cell lines were obtained from Dr. Adolfo A. Ferrando (Columbia University, NY, US). Genetic alterations of these cell lines are described in (Palomero *et al*, 2007). The T-ALL cell lines were cultured in RPMI 1640 medium supplemented with 100 U/mL penicillin, 100 µg/mL streptomycin, and 10% fetal calf serum (FCS; GIBCO) at 37°C and 5% CO2. Peripheral blood samples were taken from healthy volunteers with full ethical consent in the Hospital Universitari Sant Joan d'Alacant, University Miguel Hernandez, Spain. Briefly, PBMC suspension was prepared from fresh whole blood diluting the blood samples in RPMI 1640 medium (GIBCO, Life Technologies) containing 20 U/mL heparin and obtained after a 30 minute centrifugation at 400 *g* on Ficoll Hypaque gradient.

For viability assays (MTT) T-ALL and PBMC cells were plated in 96-well plates at a density of $2.5x10^3$ and $5x10^3$ cells per well respectively. Cells were exposed to BW B70C for the indicated concentrations and duration at 37°C and 5% CO2 and then incubated with Thiazolyl blue tetrazolium bromide (MTT) reagent (Sigma-Aldrich) for an additional 3 h. Each well was washed one time with HBSS then DMSO was added to dissolve the formazan crystals. Cell media was removed and replaced with MTT-containing media (1 mg ml^{-1} final concentration) and cells were allowed to grow at 37 °C for another 3.5 h. MTT media was removed and MTT precipitate dissolved in 4 mM HCl, 0.1% NP40 in isopropanol, solvent by shaking for 1 h. Absorbance values were then measured at 570 nm with a EZ Read 400 microplate spectrophotometer (Biochrom) using a 96-well-plate reader were used to establish growth and viability of cells. The absorbance values were background subtracted and normalized to vehicle. Each drug dose was tested in triplicates. Dose-response curves were generated using non-linear regression with the GraphPad Prism®6 software package to generate IC50 values.

Western Blotting

T-ALL and PBMC cells were cultured and treated with inhibitors or vehicle in 6 well-plates under the conditions previously stated. Protein concentration of the samples was determined using BCA Protein Assay Kit (Pierce). 25 µg of protein sample were re-suspended in 6X SDS loading buffer (300 mM Tris-HCl [pH 8.8], 12% SDS, 0.6% bromophenol blue and 30% glycerol) with β-mercaptoethanol (1 µl for each 50 µl of 6X SDS buffer), and boiled for 5-10 minutes at 95ºC. Protein samples were separated in 8, 10 or 16 % SDS-PAGE gels and transferred to a nitrocellulose membrane (Inmovilon-P Transfer membranes, Millipore). Membranes were blocked in PBS with 0.1% Tween-20 and 3% BSA for 1 h at RT. After that, membranes were incubated with the primary antibodies: anti-eNOS, anti-β-actin HRP conjugated (Sigma, 1:50000); all diluted in PBS with 0.1% Tween-20 and 3% BSA. After overnight incubation at 4ºC, membranes were incubated during 1 h at RT with secondary antibodies: HRP-conjugated rabbit anti-IgG (Sigma, 1:10000) or HRP-conjugated mouse anti-IgG (Jackson, 1:5000); all diluted in PBS with 0.1% Tween-20 and 3% BSA. Proteins were detected using the chemiluminescent substrate ECL (Pierce), the detector LAS-100 (Fujifilm) and the Image Reader LAS-1000 software (FujiFilm).

Summary

This part of my thesis was done in collaboration with other members of Dr. Maria Dominguez group. I actively contributed to this article by performing some of the functional experiments together with Dr. Villegas, my thesis co-director and first author of this publication. These experiments involved all the RT-qPCRs, the heat shock assays, assays with Notch inhibitor DAPT, experiments with cell lines and other experiments that were not finally included in the manuscript but were necessary to the project to progress.

As exposed in the introduction, the cooperative interaction of Notch and PI3K/Akt signaling pathways is associated with aggressiveness in human cancer. Here, we devised an unbiased high-throughput chemical screen in *Drosophila* to identify compounds capable of targeting this oncogenic cooperation without side effects.

We found 61 and 29 compounds that strongly suppressed or enhanced Notch-PI3K/Akt tumorigenesis, respectively. Our screen also identified 15 of the 21 known anticancer FDA-approved compounds included in the library, thus validating our screen. These results were genetically validated using tumor-specific RNAi downregulation of candidate target genes to mimic the action of those compounds with known human molecular targets. Despite the evolutionary distance between *Drosophila* and humans, we confirmed that 64% of the compounds act through conserved targets, making evident that our Drosophila-based strategy is useful to identify anticancer drugs as well as their clinically relevant targets.

Some of the suppressor hit compounds are known anti-inflammatory agents targeting the NO/NOS and LOX signaling pathways. Of particular interest was the drug BW B70C, a 5-LOX inhibitor, since it blocked tumorigenesis at a very low dose. We observed that *Pten* depletion induces aberrant expression of NOS in tumor eye imaginal discs. As expected, treatment with L-NAME (a selective NOS inhibitor) and genetic silencing of NOS gene either by RNAi or an endogenous mutation selectively suppressed tumorigenesis. Furthermore, simultaneous overexpression of *NOS* and *Dl* induced tumorigenesis. Treatment with our drug candidate BW B70C blocked Notch-NOS-driven tumorigenesis, but not other Notch-driven tumors, suggesting that this drug dampens a tumor formation process orchestrated by PI3K/Akt-induced inflammatory NOS.

We also investigated the contribution of LOX pathway to Notch-PI3K/Akt-driven tumorigenesis and for that purpose, we searched for *Drosophila* LOX pathway homologs to validate our screen results. Genetic inactivation of leukotriene 4 hydrolase homolog, allatostatin receptors (the structural orthologs of leukotriene receptors in flies) and phospholipase A2, which is necessary for LOX-mediated production of proinflammatory lipid metabolites, strongly suppressed tumorigenesis, mirroring the antineoplastic effect of the identified drugs. These results confirmed that LOX-generated lipids are required for Notch-PI3K/Akt-driven tumors.

In vertebrates, macrophage infiltration and expression of inflammatory markers such as NO are hallmarks of cancer. We observed that macrophage-like hemocytes were dispersed, polarized and infiltrated in the tumor epithelium, whereas in physiological conditions they remain rounded-shaped and aggregated. These morphological changes were suppressed under the treatment with BW B70C, suggesting that the inflammatory response in Notch-PI3K/Akt tumors is shaped by NOS/LOX activity.

Another feature of cancer-related inflammation is immunosuppression. In *Drosophila*, melanization is a critical innate immune response to tumor cells and is mediated by the enzyme phenoloxidase, encoded by the prophenoloxidase genes (*PPO*). We examined *PPO* expression and found that larvae with Notch overactivation alone showed robust stimulation of *PPO1* and *PPO2* expression. In contrast, tumor-bearing larvae and *ey>Pten*-RNAi larvae did not show this response. Halving *PPO* gene dosage together with *Dl* overexpression resulted in half of the emerging adults bearing tumors. Furthermore, aberrant *NOS* expression was sufficient to dampen *PPO* expression and the immune response triggered by the PO-activating cascade under heat stress, visualized as a reduction of melanized crystal cells. Altogether, these observations indicate that activated PI3K/Akt drives aberrant NOS, which in turn promotes immunosuppression. This could explain how activated PI3K/Akt unleashes the oncogenic potential of Notch.

We also validated the antitumor effect of BW B70C in well-established human T-ALL (T-cell Acute Lymphoblastic Leukemia) cell lines with aberrant NOTCH1 and PI3K/AKT signaling. We observed that BW B70C treatment killed T-ALL cells that were resistant to Notch inhibitors and had little or no toxicity against healthy T lymphocytes. Moreover, as obtained in *Drosophila* tumors, we found that endothelial

NOS (eNOS) was aberrantly enriched in these T-ALL cells. Finally, we found that BW B70C selectively killed T-ALL cells associated by suppressing aberrant eNOS.

Section 2. PI3K/Akt/Pten-induced mitochondrial dysfunction cooperates with Notch in tumorigenesis

A phospho-proteomic approach reveals a role for ATPsynβ in tumorigenesis

In order to get further insight on oncogenic Notch-PI3K/Akt molecular network and to identify downstream activated targets that may be involved in tumor initiation/progression, we employed quantitative phospho-proteomic analysis. To this end, we collected eye imaginal discs from wild type and Notch-PI3K/Akt third instar larvae and performed 2D-gel electrophoresis combined with phospho-protein staining (Fig. 10A). Specific spots showing significant differential phosphorylation were identified based on their reproducibility among three replicate gels and further selected for mass spectrometry hit identification. Representative overlapped 2D gels from wild type and Notch-PI3K/Akt tumor samples are shown in Figure 10B.

Most notably, we found that the top hit in our assay corresponded to the protein ATP synthase β subunit (*ATPsynβ*, CG11154), which appeared highly phosphorylated in Notch-PI3K/Akt tumor samples. ATPsynβ is a subunit of the mitochondrial F1-ATPase complex V responsible for ATP production and is highly conserved from flies to humans (*Hm* ATP5B). Moreover, co-immunoprecipitation analysis confirmed that pAKT physically interacts with ATPsynβ in *Drosophila* Kc cells (Fig. 10C). Notice that a band appears in the negative control of the second Co-IP (below). A possible explanation could be that the molecular weight of ATPsynβ is 52KDa, same as the heavy chain of the polyclonal antibody, which might be masking the region where the band of interest is expected. These results coincide with previous studies in human cell lines showing that Akt present in mitochondria can phosphorylate the β-subunit of ATP synthase and other proteins (Bijur & Jope, 2003).

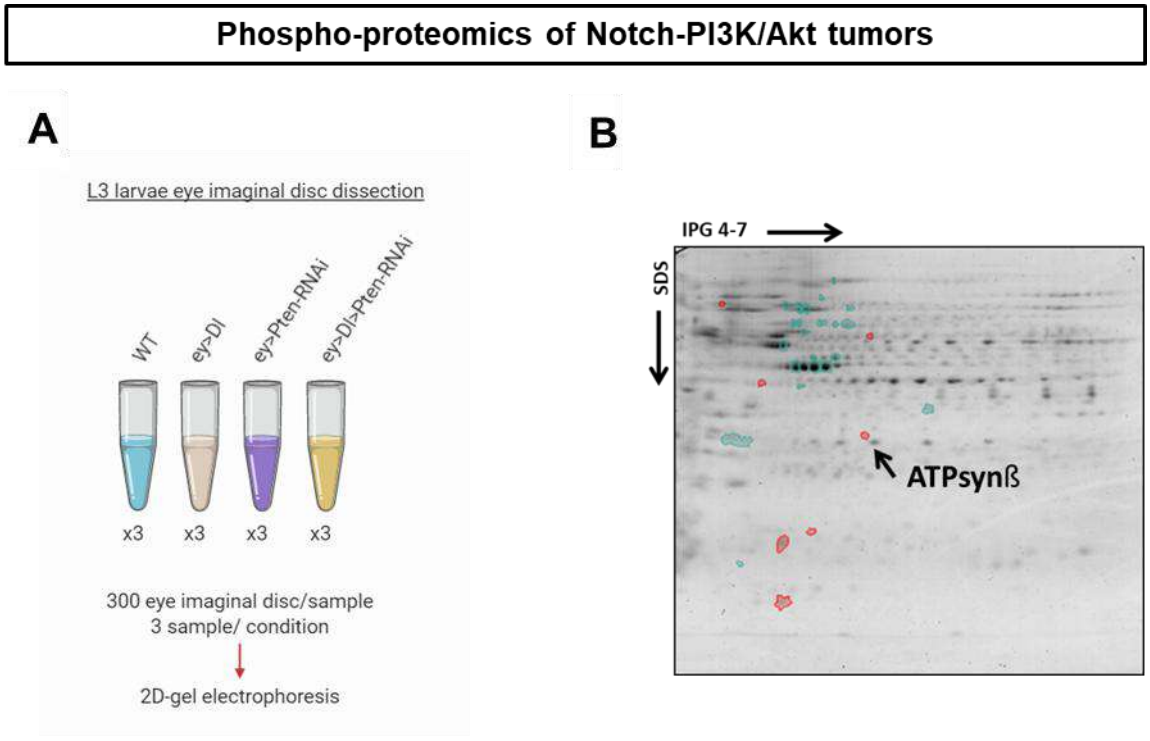

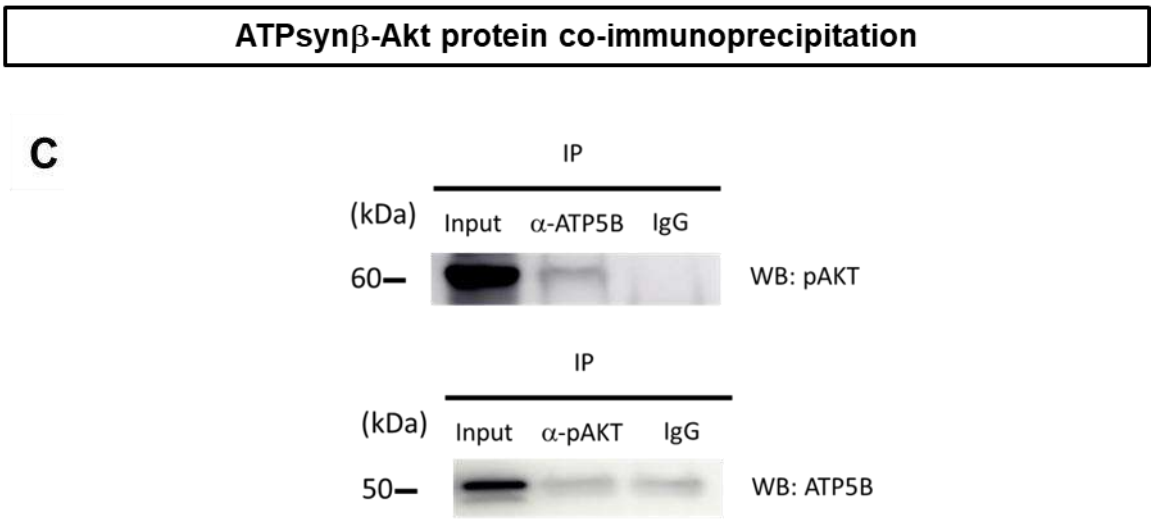

Figure 10. Notch-PI3K/Akt combination triggers downstream phosphorylation of ATP synthase β subunit.

(A) Brief scheme of the phospho-proteomic assay strategy. **(B)** Overlapped 2D-gels. Proteins highly phosphorylated in the wild type (green dots) or in the Notch-PI3K/Akt condition (red dots). **(C)** Co-immunoprecipitation assay of Kc cells: Western blot analysis of protein extracts from Kc167 cells containing input, IP of ATP5B, or IgG using antibody to pAKT (on top). Western blot analysis of protein extracts from Kc167 cells containing input, IP of pAKT, or IgG using antibody to ATP5B (below).

ROS generated by mitochondrial dysfunction is a key driver of Notch-PI3K/Akt-induced tumorigenesis

ATP synthesis requires conformational changes in the nucleotide-binding sites of the three β-subunits that are coupled to the catalytic activity of F_1-ATP synthase. Evidence from human skeletal muscle suggest that phosphorylation of ATPsynβ contributes to mitochondrial dysfunction by promoting its association with 14-3-3 proteins in the cytosol (Højlund *et al.*, 2003).

Therefore, we reasoned that knocking down *ATPsynβ* expression by using RNA interference (*ATPsynβ*-RNAi) would mimic the loss of function generated by its phosphorylation. We found that *ATPsynβ*-RNAi, when co-expressed together with *Notch* overexpression (*ey>Dl>ATPsynβ*-RNAi), also generated tumors (Fig. 11A). We then analyzed the phenotypes generated by knocking down other members of the F1-Complex V alongside Notch and observed a similar tumorigenic effect. Interestingly, down-regulation of several components of the Complex I, together with activated Notch resulted in a similar outcome (Fig. 11B).

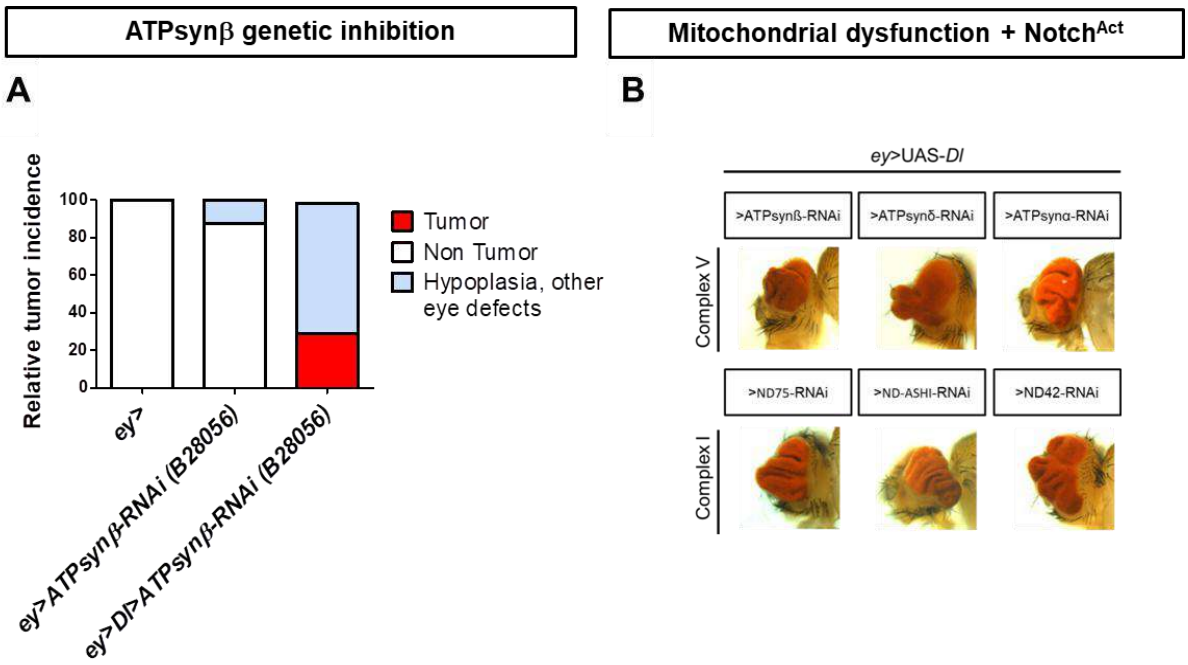

Figure 11. Mitochondrial dysfunction cooperates with Notch to promote tumorigenesis.

(A) Tumor incidence (as a percentage) in control flies and after genetic inhibition of *ATPsynβ*. Bars shown represent

the mean of total (n > 100) flies scored. Crosses were repeated twice. **(B)** Knock-down of other members of the complex I and V together with *Notch* up-regulation and representative phenotypes.

ATP synthase deficiency results in proton misbalance, which provokes an increase in the mitochondrial membrane potential leading to the slowdown of the electron transport chain (ETC). Therefore, more electrons are diverted from their normal pathway resulting in an elevated production of reactive oxygen species (ROS), such as peroxide and superoxide (Martínez-Reyes & Cuezva, 2014), both largely associated with cancer disease (see introduction).

To examine if generation of ROS might be implicated in Notch-PI3K/Akt tumor induction, we monitored the expression of GstD1, a prototypical ROS response gene that encodes for a detoxification enzyme (Sawicki *et al.*, 2003).

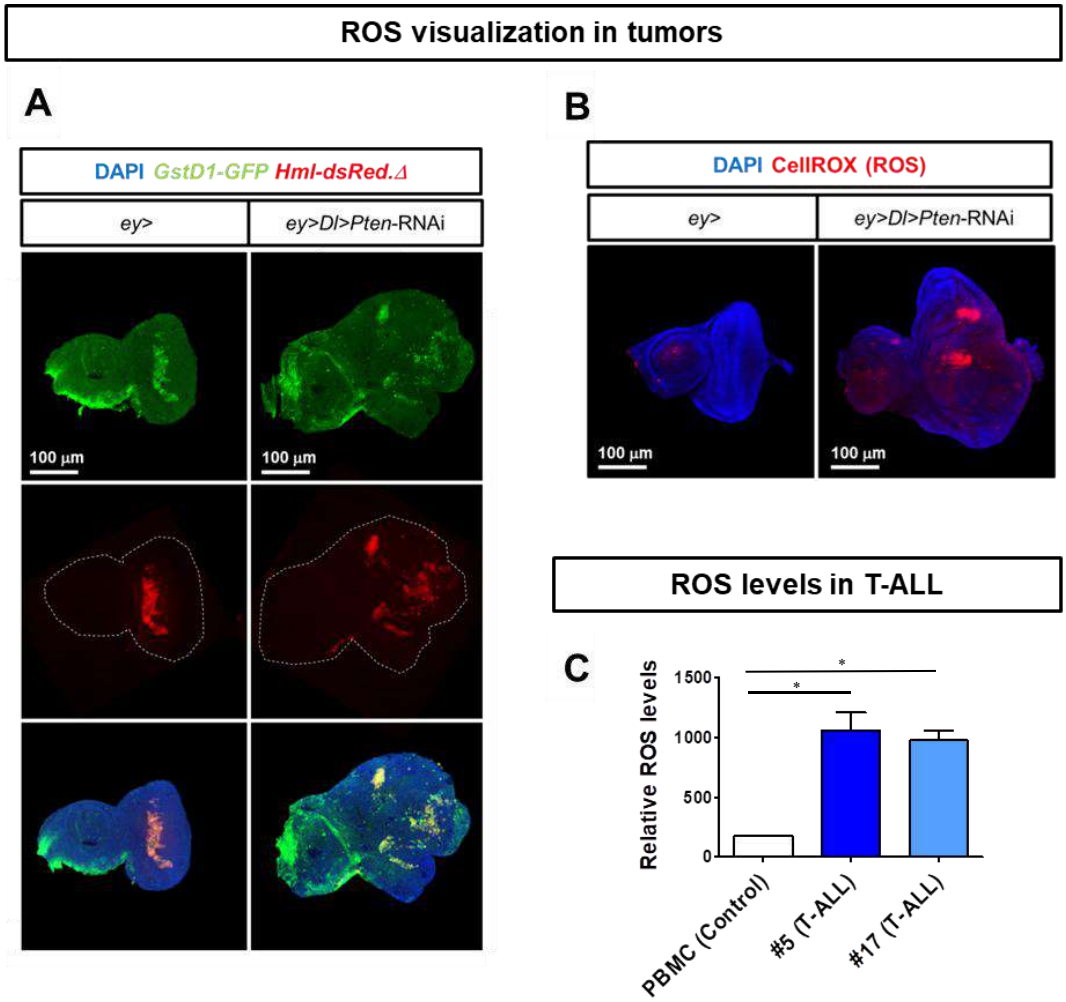

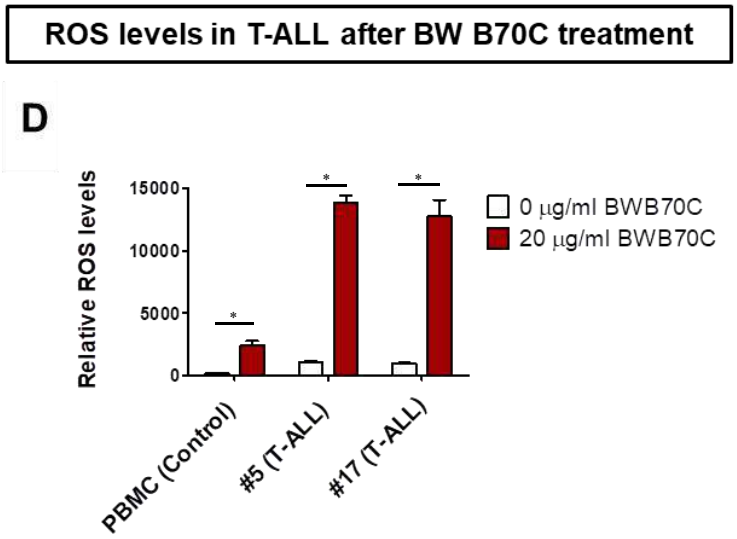

Figure 12. Notch-PI3K/Akt tumorigenic combination triggers ROS production.

(A) ROS levels and tissue resident hemocytes are visualized by *GstD1-GFP* (green), a sensitive oxidative stress reporter, and by the pan-hemocyte marker *Hml-dsRed.Δ* (red), respectively (merge in yellow). **(B)** Direct measurement of ROS by CellROX reagent in eye imaginal discs. **(C)** Measurement of basal ROS levels by FACS sorting in #5 and #17 cells taken from T-ALL patients compared to healthy PBMCs. **(D)** ROS levels in T-ALL cells after treatment with BW B70C.

We used a GstD1-GFP reporter line (Sykiotis & Bohmann, 2008) to evaluate oxidative stress *in vivo* and we found that tumor eye discs exhibit higher amounts of ROS (Fig. 12A). This observation was confirmed by direct measure of oxidative stress with CellROX reagent (Fig. 12B). Interestingly, *Drosophila* multipotent haematopoietic progenitors display increased levels of ROS under *in vivo* physiological conditions (Owusu-Ansah & Banerjee, 2009). Here we show that ROS signal co-localizes totally with hemocytes in the wild type eye imaginal disc, whereas in the tumor is disseminated along the whole tissue (Fig. 12A).

In addition, we evaluated the levels of ROS in human T-ALL cells from patients (#5 and #17) compared to healthy T and B lymphocytes (PBMC). For that purpose, we used fluorescence-activated cell sorting (FACS) combined with CellROX. We found that the levels of ROS were significantly higher in T-ALL cells compared to PBMC healthy counterpart, validating our previous results in the Notch-PI3K/Akt tumors of *Drosophila* (Fig. 12C). Markedly, BW B70C treatment increased ROS levels suggesting a cell death inducing mechanism (Fig. 12D).

Hyperactivation of the ROS-scavenging system prevents tumor formation

We reasoned that if ROS production is involved in Notch-PI3K/Akt tumor induction, then removing ROS excess would reduce the tumor burden. Consequently, we amplified the intracellular levels of ROS scavengers in the Notch-PI3K/Akt context by means of the up-regulation of the detoxification enzymes Superoxide dismutase 1 (Sod1), Catalase (Cat) and Glutathione peroxidase (GTPx). We found that over-expression of *Catalase* and *GTPx* significantly reduced oncogenesis while over-expression of *Sod1* suppressed almost completely the tumorigenic phenotype (Fig. 13A). Moreover, knock-down of *Sod1* together with Notch hyperactivation also generated eye tumors, indicating that elevated levels of ROS act together with increased Notch signaling to trigger tumorigenesis. Yet, *ey>Dl>Sod1*-RNAi yielded lower levels of tumorigenesis than Notch-PI3K/Akt, suggesting that compensatory mechanisms are involved (Fig. 13B).

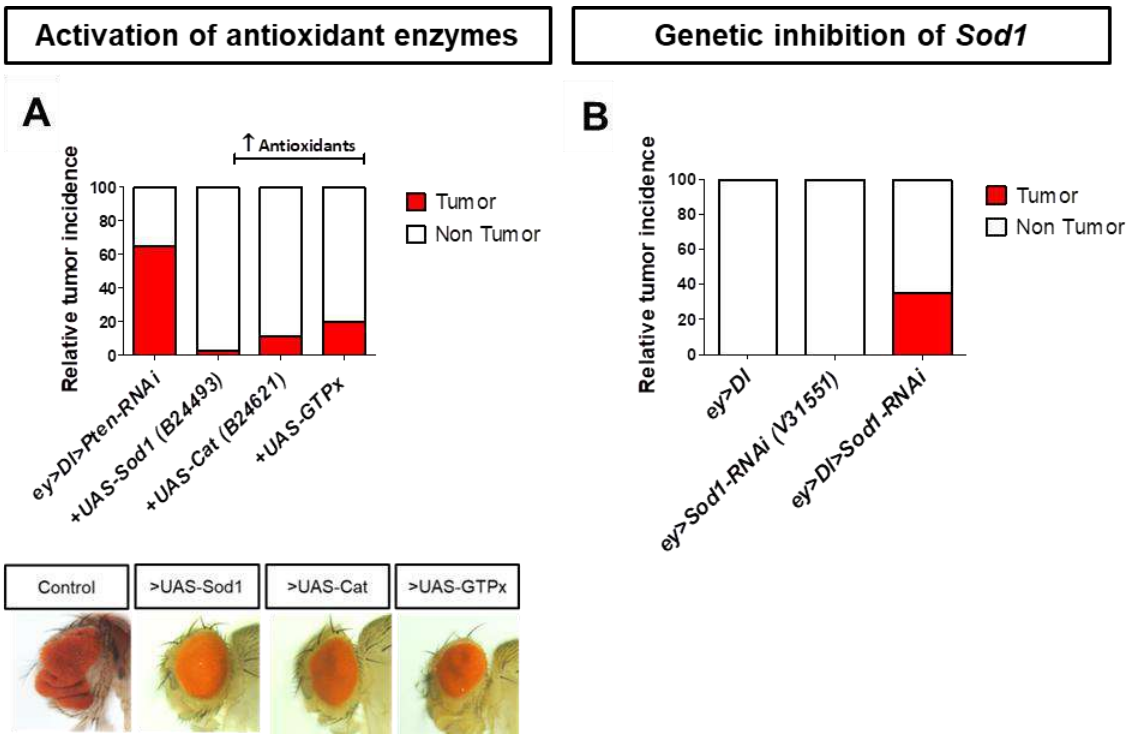

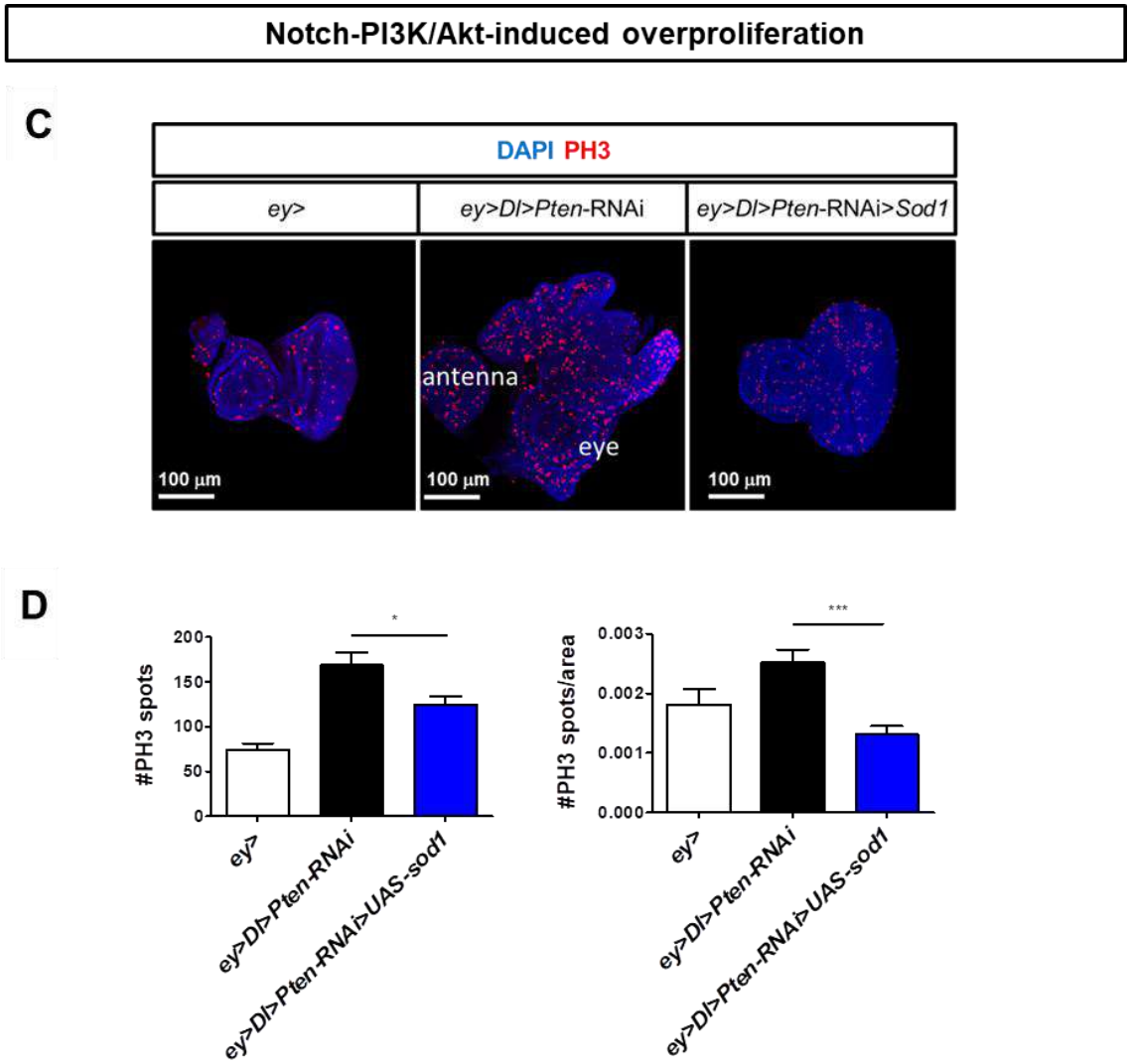

Figure 13. Hyperactivation of the ROS scavenging system reduces tumorigenesis.

(A) Tumor incidence (as a percentage) in control flies and after overexpression of different components of the ROS scavenging system in the context of Notch-PI3K/Akt. The construct P{UAS-PHGPx.M} was used to overexpress GTPx (Missirlis *et al.*, 2003). Below are shown representative phenotypes (Control: *ey>Dl>Pten*-RNAi). **(B)** Tumor incidence after down-regulation of *Sod1* together with overexpression of *Dl*. Bars shown represent the mean of total (n > 100) flies scored. Crosses were repeated twice. **(C)** On top, visualization of Notch-PI3K/Akt-induced overproliferation in wild type, tumors and after *Sod1* overexpression. Left: Average total number of PH3-positive cells in eye imaginal discs. Right: normalized per area.

Next, we analyzed the proliferation rate by measuring the number of PH3-positive cells within the imaginal disc. Our results indicate that Sod1 might be controlling the overproliferation induced by Notch-PI3K/Akt (Fig. 13C, left).

Normalization of PH3-positive cells per area revealed no statistical differences between wild type and the tumorigenic context, indicating that proliferating cells increase their biomass before going through the division, as expected for cancer cells (Fig. 13C, right). All together, these data indicate that changes in mitochondrial metabolism with the subsequent increase in ROS levels are at the center of Notch-PI3K/Akt-driven tumorigenesis.

Notch-PI3K/AKT combination triggers activation of JNK stress signaling cascade

ROS are known to act as second messengers that activate diverse redox-sensitive signaling transduction cascades. *Jnk* (*Bsk* in *Drosophila*) is a well-known stress response gene mainly activated in response to oxidative stress and proinflammatory cytokines. It has been widely described that increased ROS levels activate Jnk signaling pathway in other cancer models (Dhanasekaran & Reddy, 2008; Chambers *et al*, 2011). Therefore, we checked activation of Jnk in order to analyze if it is involved in Notch-PI3K/Akt-induced tumorigenesis. Thus, to monitor Jnk activation (phospho-Jnk) we used a fly line with an RFP fluorescent construct that reports the expression of a phospho-Jnk downstream gene (Jnk::TRE40-RFP). We observed that Jnk is activated in the tumor condition and partially co-localizes with ROS signal (Fig. 14A).

In addition, ROS and oxidative stress are known to trigger and modulate apoptosis, a well-characterized biological process by which cells undergo a programmed death. ROS-induced apoptosis requires the participation of other cell death signaling pathways, such as Jnk. Thus, we measured apoptosis levels by immunostaining of cleaved caspase 3, an essential mediator of the apoptotic process. The wild type does not show any Jnk signal, neither apoptosis, whereas in the tumor, apoptosis widely co-localizes with Jnk activation (Fig. 14A). Interestingly, tumors display intratumor heterogeneity, since some Jnk-positive cells do not co-localize with ROS or caspase, which may reflect different patterns of temporal expression.

Despite the researcher's efforts, the contribution of Jnk in both tumor promotion and suppression reflects our little understanding of the role of Jnk in the tumor microenvironment. There is great evidence that Jnk, besides controlling cell-autonomous functions, can drive the expression of cytokines that can act in a paracrine manner to sustain the proliferation of cancer cells (Sakurai *et al.*, 2006). Moreover, studies in mice have demonstrated that the contribution of Jnk is specific for cell type and isoform. Therefore, the paradoxical role of Jnk in cancer might be unraveled by elucidating the impact of Jnk signaling in inflammation that operates downstream of each oncogenic mutation.

In the present study, we hypothesized that if Jnk signaling is involved in Notch-PI3K/Akt-driven tumorigenesis, then its down-regulation may rescue the wild type phenotype. Thus, we used different RNAi lines to knock-down Jnk signaling in the context of the tumor. In support of this hypothesis, we found that one line (B31323) reduced the tumorigenic index; however, two other lines assessed did not showed any clear difference (V34138) or even increased percentages of tumors (B32977) (Fig. 14B). A feasible explanation is that the different *Jnk*-RNAi lines could be regulating *Jnk* in a different way. To answer this question, we measured the expression levels of *Puckered* (*Puc*), a very well-known Jnk target gene, (Wu *et al.*, 2009) by RT-qPCR for each *Jnk*-RNAi line. We found that two of the *Jnk*-RNAi lines effectively down-regulated *Jnk* levels, however and unexpectedly, the line B31323 produced the opposite effect (Fig. 14C). Interestingly, this RNAi was responsible for the partially rescued tumor phenotype, suggesting that high levels of Jnk may have a tumor suppressor role.

To improve our understanding of Jnk role in our cancer model, we blocked completely Jnk activity using a dominant negative *Jnk* construct, UAS-*Jnk*.DN. Results showed that the complete Jnk loss of function not only does not have anti-tumor activity in the Notch-PI3K/Akt context, but also it was oncogenic when expressed together with Notch, indicating that lack of Jnk signaling converts Notch into an oncogenic signal (Fig. 14D). Consequently, *Jnk*-RNAi lines that efficiently down-regulate *Jnk* also showed different degrees of hyperplasia, hypoplasia and tumorigenesis when co-expressed with *ey>Dl*, whereas the line that augments *Jnk* levels did not have any effect (Fig. 14E).

To corroborate the idea that *Jnk* is behaving as a tumor suppressor signal, we performed *Jnk* gain of function experiments by using UAS-*Jnk* transgenic flies. The

resulting phenotypes were variable, since the levels of tumorigenesis clearly decreased but almost all individuals showed hypoplasic phenotype (small eyes instead of the overgrowth that characterizes Notch hyperactivation) (Fig. 14D).

Finally, inhibition of apoptosis by overexpression of the protein P35, known to block the action of a wide range of caspases, revealed a reduction in tumorigenesis levels (Fig. 14F). All together, these results suggest that Jnk signal might be restricting the tumor burden by inducing apoptosis, which further suggests a tumor suppressor role in this context, as described in other cancer models (Whitmarsh & Davis, 2007; Shramek *et al.*, 2011; Ahn *et al.*, 2011; Tournier, 2013).

ROS, *Jnk* and apoptosis in tumors

A

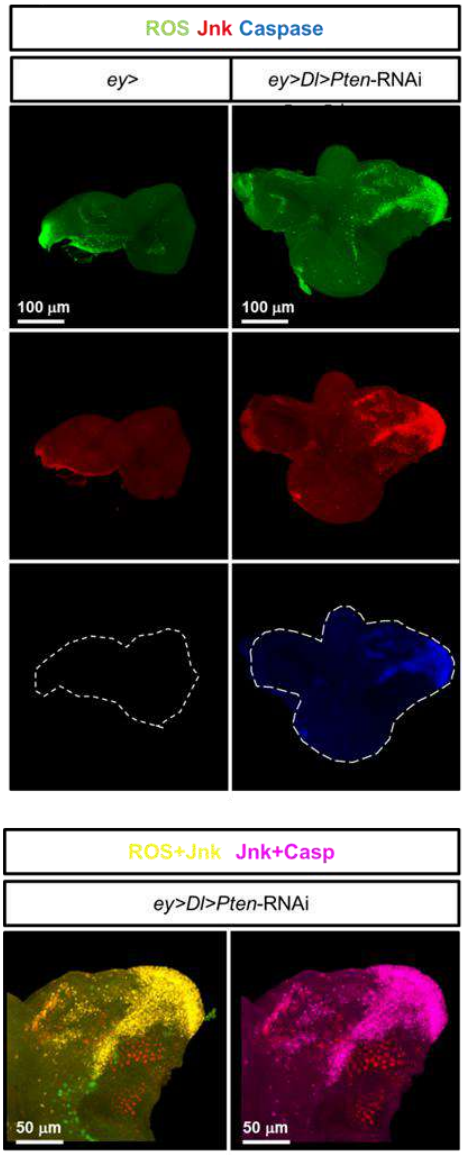

Jnk downregulation by RNAi

B

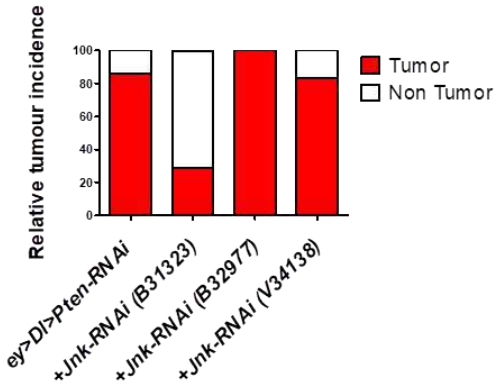

Jnk – RNAi validation

C

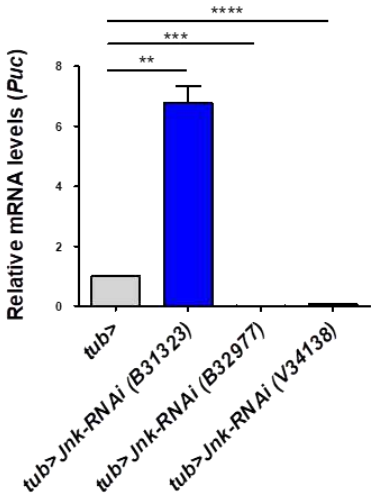

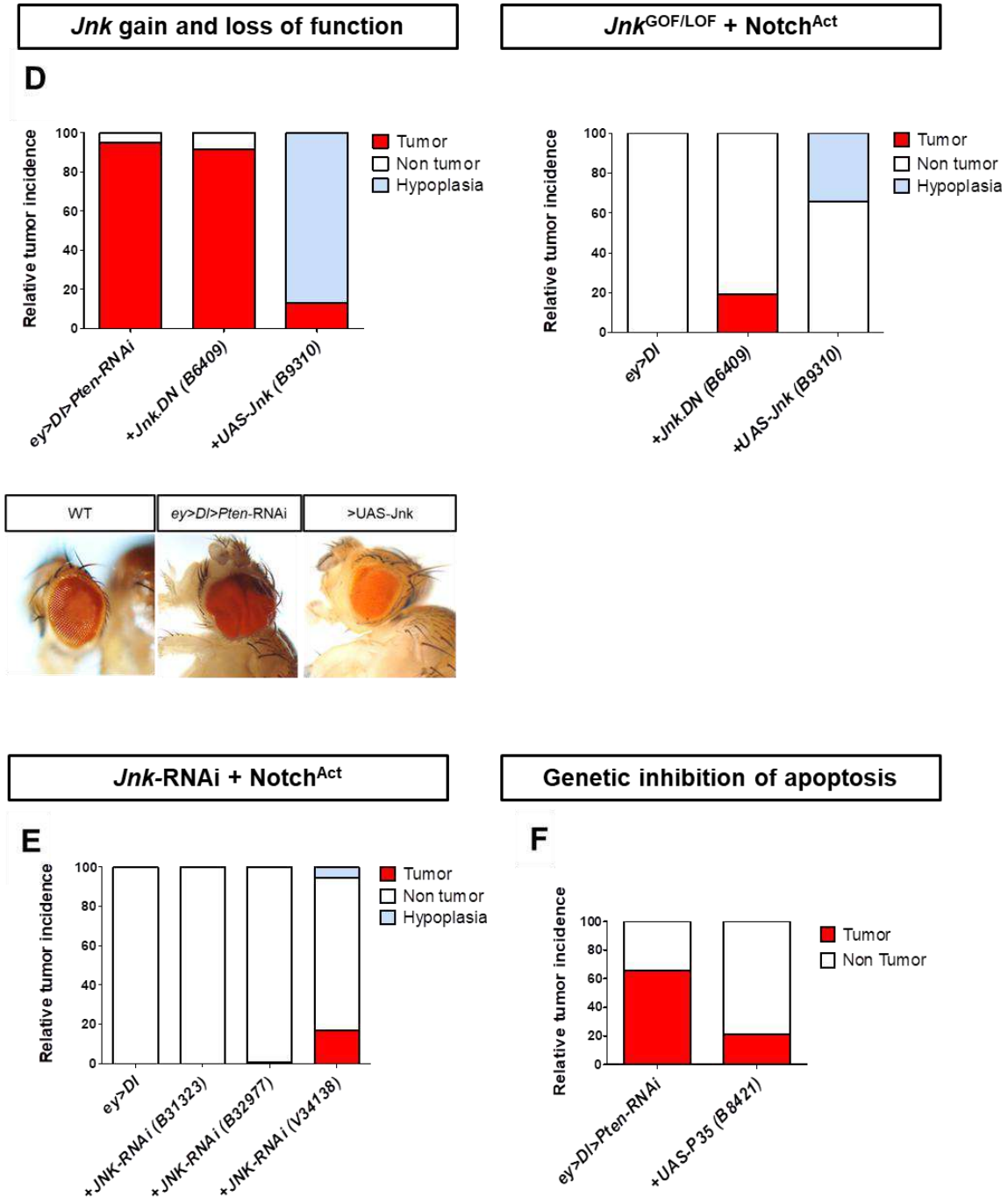

Figure 14. ROS-induced Jnk signaling triggers apoptosis as an anti-tumor response.

(A) *GstD1*-GFP, Jnk:TRE40-RFP reporter lines and immunostaining of cleaved caspase 3 show signal from ROS, Jnk and apoptosis respectively. **(B)** Tumor incidence (as a percentage) in control flies and after *Jnk* knock-down using different RNA of interference. **(C)** Efficiency of the different *Jnk*-RNAi lines by RT-qPCR. Data were analyzed by a two-tailed unpaired t-test and values represent the mean ± SD of three independent replicates.$p<0.05$ **(D)** Tumor incidence after total *Jnk* loss/gain of function. **(E)** Tumor incidence of *Jnk* knock-down combined with *ey>Dl*. **(F)** Tumor levels after inhibition of caspases by overexpression of *P35* in Notch-PI3K/Akt context. Bars shown represent the mean of total (n > 100) flies scored. Crosses were repeated twice.

Mitochondria induces apoptosis through cytochrome *c* oxidase hyperactivation in Notch-PI3K/Akt tumors

Many studies have shown that mitochondrial activities play a pathogenic role in cancer development and progression, in particular by its regulation of apoptosis. Mitochondria participate in apoptosis through different mechanisms, being the most important the release of cytocrome *c* to promote caspase activation (Wang & Youle, 2009) (Fig. 15A). Here we use the recombinant line P{UAS-mito-HA-GFP.AP} that targets the mitochondrial protein COX8A (8A is a subunit of the cytochrome *c* oxidase, the terminal enzyme of the mitochondrial respiratory chain) to visualize this organelle.

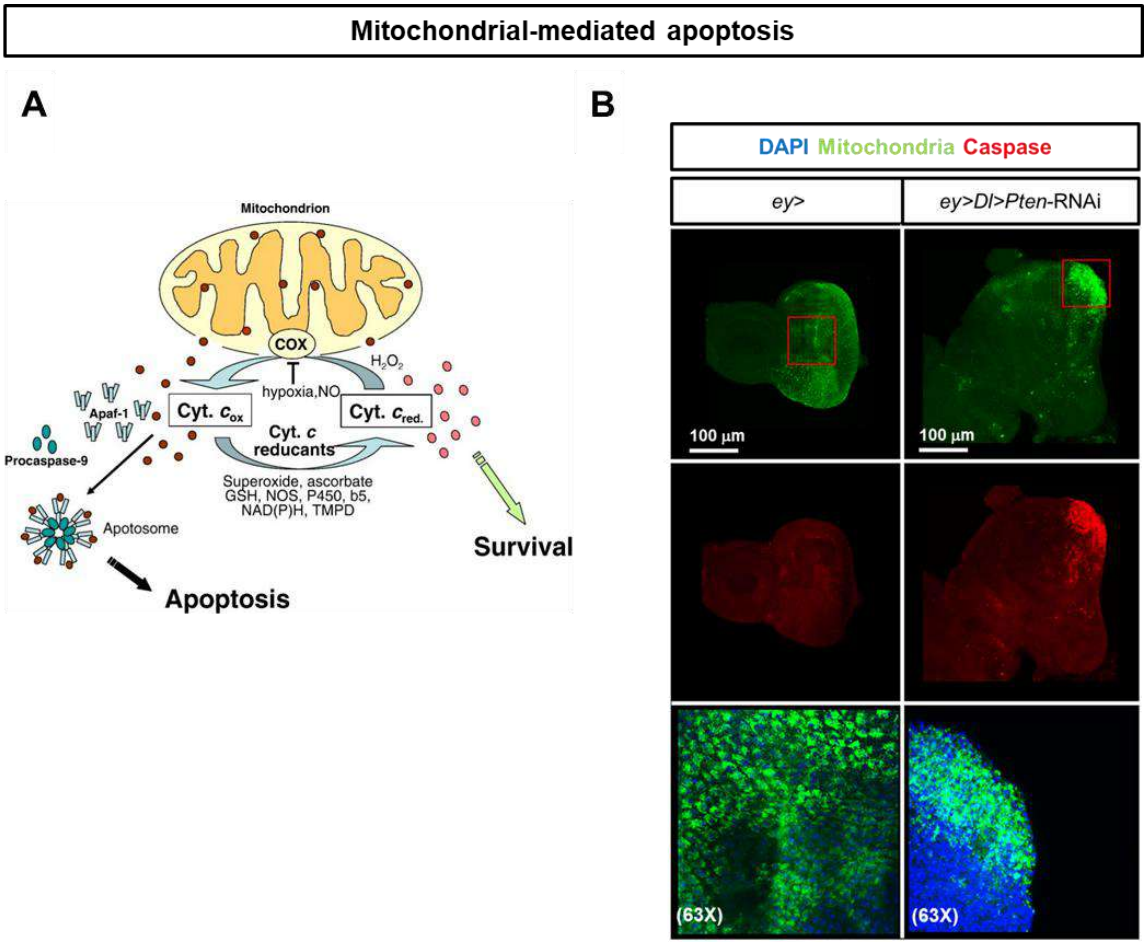

Figure 15. Mitochondria with higher cytochrome *c* oxidase activity induce apoptosis in Notch-PI3K/Akt tumors.

(A) Cytochrome *c* (Cyt.*c*) is oxidized by mitochondrial cytochrome *c* oxidase (COX) and then binds to Apaf-1 forming the apoptosome which activates pro-caspase-9, thus leading to apoptosis (adapted from Brown & Borutait, 2008). **(B)** UAS-mito-GFP reporter line and immunostaining of cleaved caspase 3 show signal from mitochondria and apoptosis, respectively.

Interestingly, we can appreciate a more intense signal in a particular region of the tumor where expression of COX8A gene is higher and co-localizes with cleaved caspase staining (Fig. 15B). Mechanisms that disable apoptosis occur in several cancer types and is generally correlated with worse outcome (Kim *et al.*, 2006), thus, we hypothesize that some regions of the tissue might be fighting against the tumor through mitochondrial-induced apoptosis.

Notch-PI3K/Akt tumors rely on enhanced glucose uptake

The PI3K/Akt pathway not only has an important role in mitochondrial function, but also is involved in metabolic reprogramming of cancer cells as many other oncogenes and tumor-suppressor genes (Iurlaro *et al.,* 2014). Particularly, the activation of Akt signaling leads to an increase in glucose metabolism by increasing the expression and translocation of glucose transporters (GLUT) to the plasma membrane and by phosphorylating key glycolytic enzymes. It also increases translation of HIF1α (hypoxia inducible factor 1 alpha) through activation of mTOR even under normal oxygen levels.

Here we use a glucose fluorescent analog to monitor the glucose uptake *ex vivo*. Glucose consumption was significantly higher in Notch-PI3K/Akt tumors compared to wild type (Fig. 16A), *ey>Dl* or *ey>Pten*-RNAi eye imaginal discs (Suppl. Fig. 2), which is in line with the fact that the predominant glycolytic phenotype observed in cancer cells is likely to be the result of complex cooperative interactions between several pathways. Surprisingly, the expression of glucose transporter 1 (GLUT1) is not affected (Fig. 16B) which might indicate that the protein is modified at post-translational level. This appears to protect against neoplasia. Indeed tumor-specific down-regulation of Glut1 by RNAi strongly reduced tumor incidence, as happens in other models (Fig. 16C) (Eichenlaub *et al.*, 2018). Moreover, treating tumor-bearing animals with 2-deoxyglucose, a glucose analog that inhibits glycolysis, also reduced tumor incidence (Fig. 16D).

These data highlight the need of high rates of glucose uptake to sustain growth in Notch-PI3K/Akt tumors.

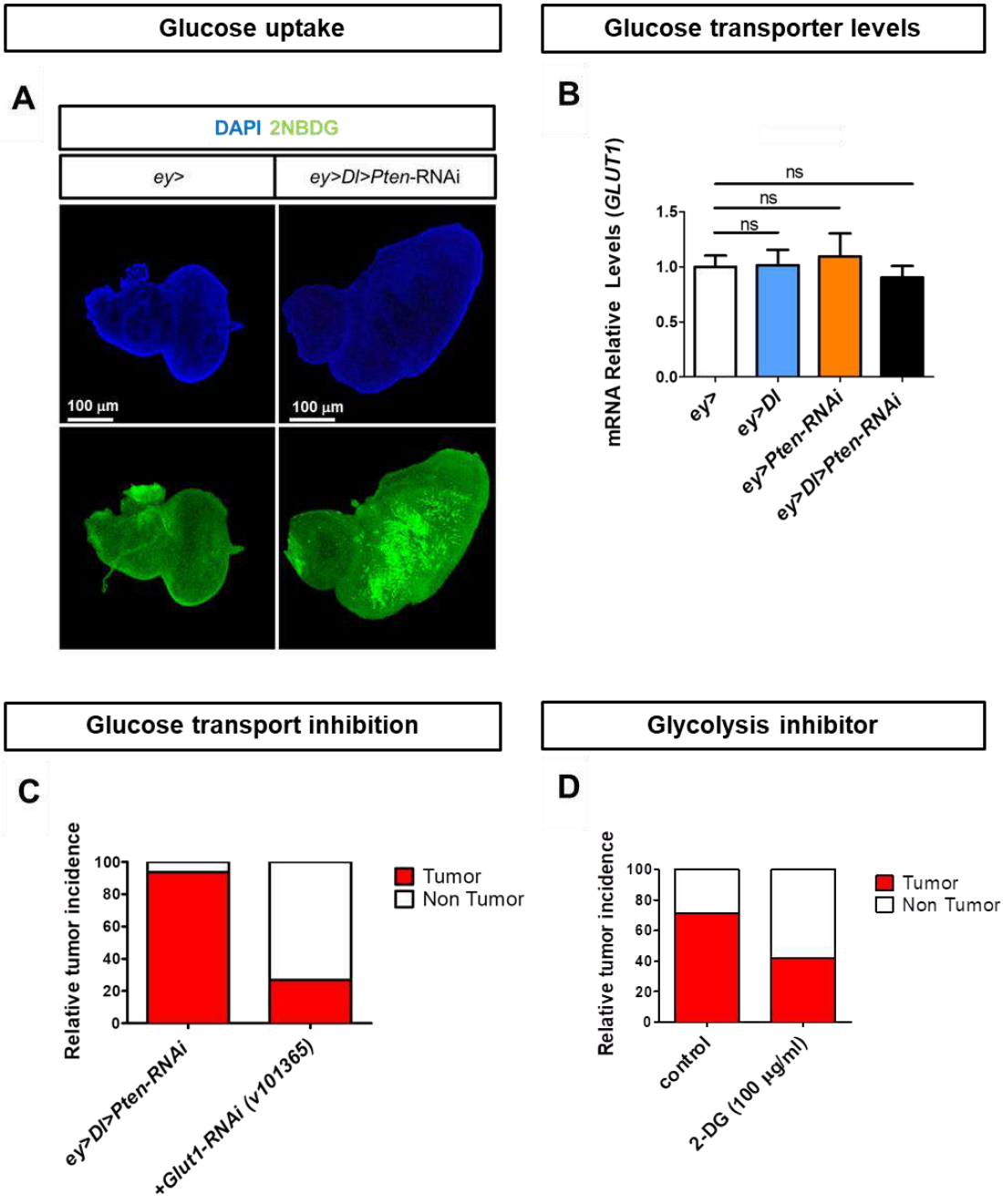

Figure 16. Glucose uptake is enhanced in Notch-PI3K/Akt tumors.

(A) Monitoring of glucose consumption *ex vivo* in *ey>* and *ey>Dl>Pten*-RNAi eye imaginal discs by using 2-NBDG. **(B)** mRNA levels of GLUT1in eye imaginal discs by RT-qPCR. Data were analyzed by a two-tailed unpaired t-test and values represent the mean ± SD of three independent replicates.$p<0.05$. **(C)** Tumor incidence (as a percentage) in control flies and after *Glut1* knock-down RNA of interference. **(D)** Tumor incidence (as a percentage) of *ey>Dl>Pten*-RNAi flies in *ad libitum* food (control) and after treatment with 2-Deoxy-D-glucose, a glycolysis inhibitor. Bars shown represent the mean of total (n > 100) flies scored. Crosses were repeated twice.

Hipoxia inducible factor 1 is stabilized in Notch-PI3K/Akt tumors

HIF1α, *sima* in flies, is a transcription factor that forms a complex together with HIF1β (*tango* in flies) and initiates the expression of genes that enhance survival during hypoxia (low oxygen environment), such as glycolytic enzymes and the glucose transporters (Semenza, 2012). Furthermore, it has been described that moderate levels of ROS can mediate the stabilization of the HIF1α (Kaelin & Ratcliffe, 2008).

Previous studies in *Drosophila* have shown that stimulation of the transcriptional response induced by Akt-mTOR involves upregulation of sima protein but not *sima* mRNA (Dekanty *et al.*, 2005). Sima protein has a very short half-life and its stability is highly regulated by posttranscriptional modifications. Direct observation of protein stabilization by using a GFP reporter revealed the presence of *sima* in tumors but not in wild type eye imaginal discs (Fig. 17A). However, as expected, we found that *sima* is slightly down-regulated at transcriptional level in Notch-PI3K/Akt tumors (Fig. 17B). Moreover, knockdown of *sima* with RNA interference led to a decrease in tumor incidence, whereas its overexpression resulted in lethality and no-head phenotype, as previously described (Centanin *et al.*, 2005) (Fig. 17C).

We also measured the expression levels of some of the known target genes of sima (Bertolin *et al.*, 2016). One of these genes is *fatiga,* which encodes for the HIF prolyl hydroxylase (hydroxylates sima and leads to its degradation under normoxia). We observed that *fatiga* is down-regulated in the tumor as expected, since activation of sima is mediated by lowering the expression of *fatiga* (Samenza, 2010; Li *et al.*, 2013). We also measured other reported genes that are regulated by sima in the fly, such as *spermine oxidase* (*smox*) and *sequoia* that appear down-regulated and up-regulated, respectively (Fig. 17D).

On the other hand, the enhanced expression of glycolytic enzymes is also mediated by sima. Lactate dehydrogenase (Ldh), the enzyme that converts pyruvate to lactate (Li *et al.*, 2013), is transcriptionally up-regulated in the tumor, as happens in most cancer models (Fig. 17E), although the tumorigenic process is Ldh-independent (Fig. 17F). We also observed that the glycolytic enzymes *Pgi* and *Pfk* were upregulated, but strikingly the other glycolytic enzymes remained unchanged (Fig. 17G).

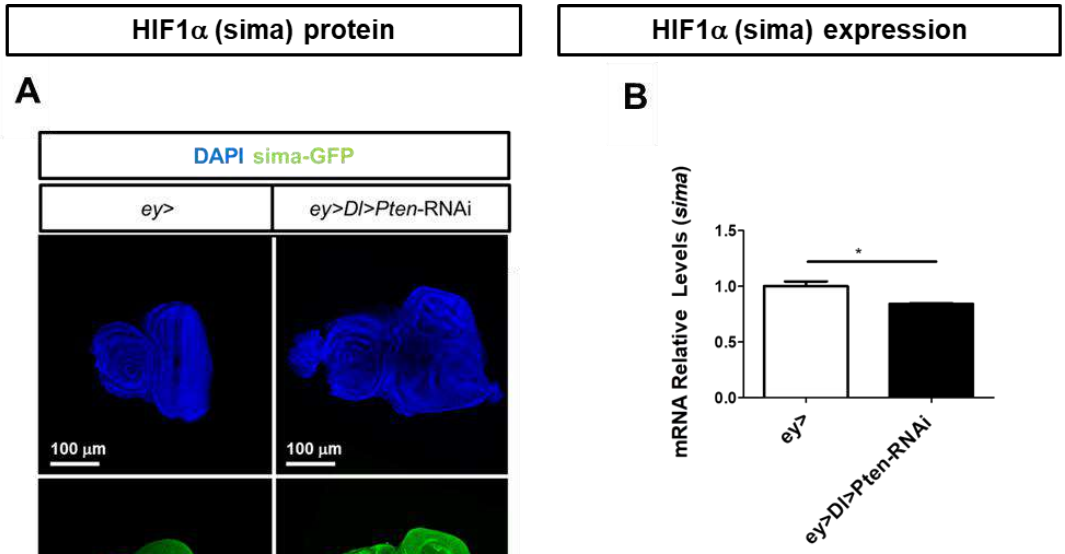
HIF1α (sima) protein
HIF1α (sima) expression
A
B
DAPI sima-GFP
ey>
ey>Dl>Pten-RNAi
100 µm
100 µm
mRNA Relative Levels (sima)
1.5
1.0
0.5
0.0
*
ey>
ey>Dl>Pten-RNAi

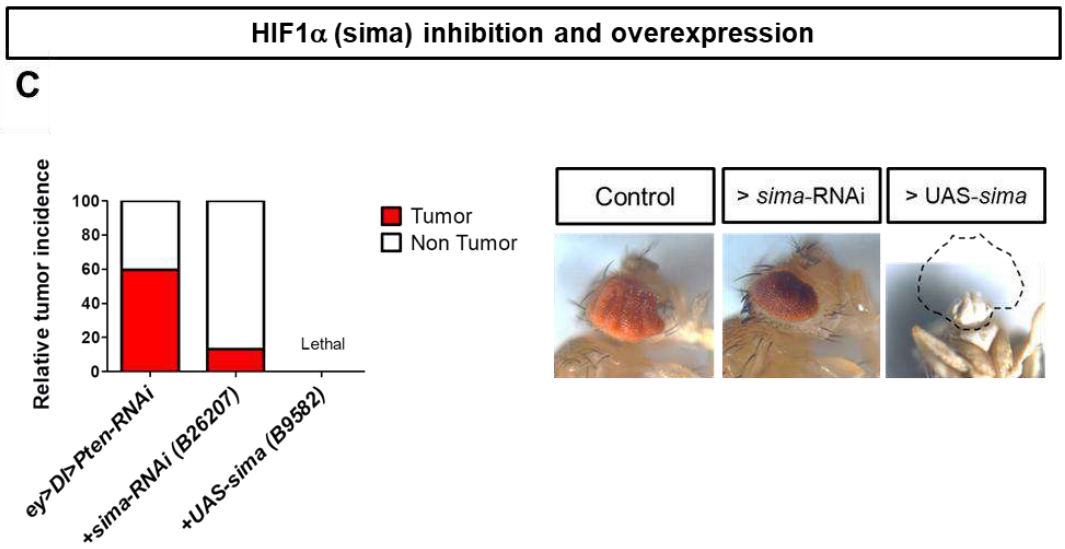
HIF1α (sima) inhibition and overexpression
C
Relative tumor incidence
100
80
60
40
20
0
Tumor
Non Tumor
Lethal
ey>Dl>Pten-RNAi
+sima-RNAi (B26207)
+UAS-sima (B9582)
Control
> sima-RNAi
> UAS-sima

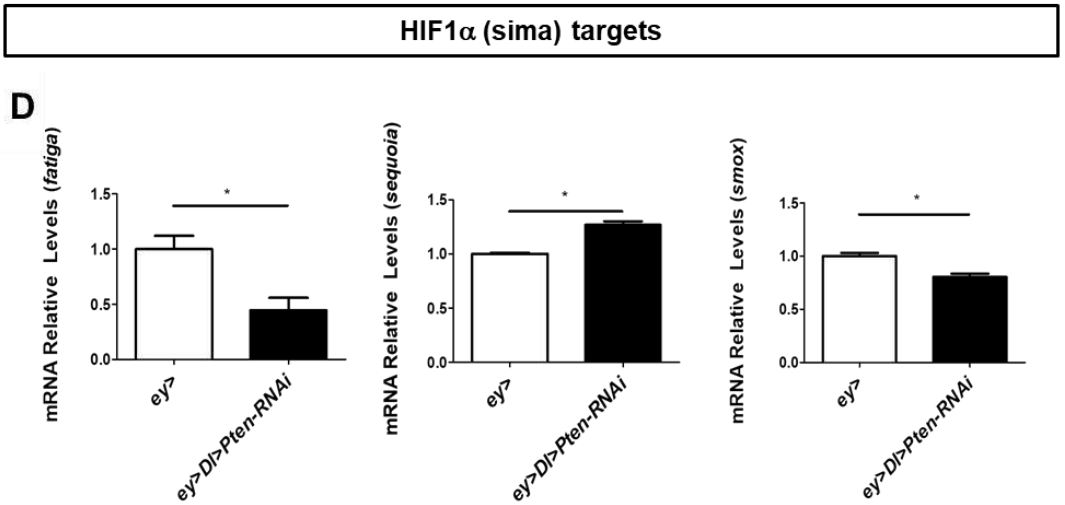
HIF1α (sima) targets
D
mRNA Relative Levels (fatiga)
mRNA Relative Levels (sequoia)
mRNA Relative Levels (smox)
1.5
1.0
0.5
0.0
*
ey>
ey>Dl>Pten-RNAi

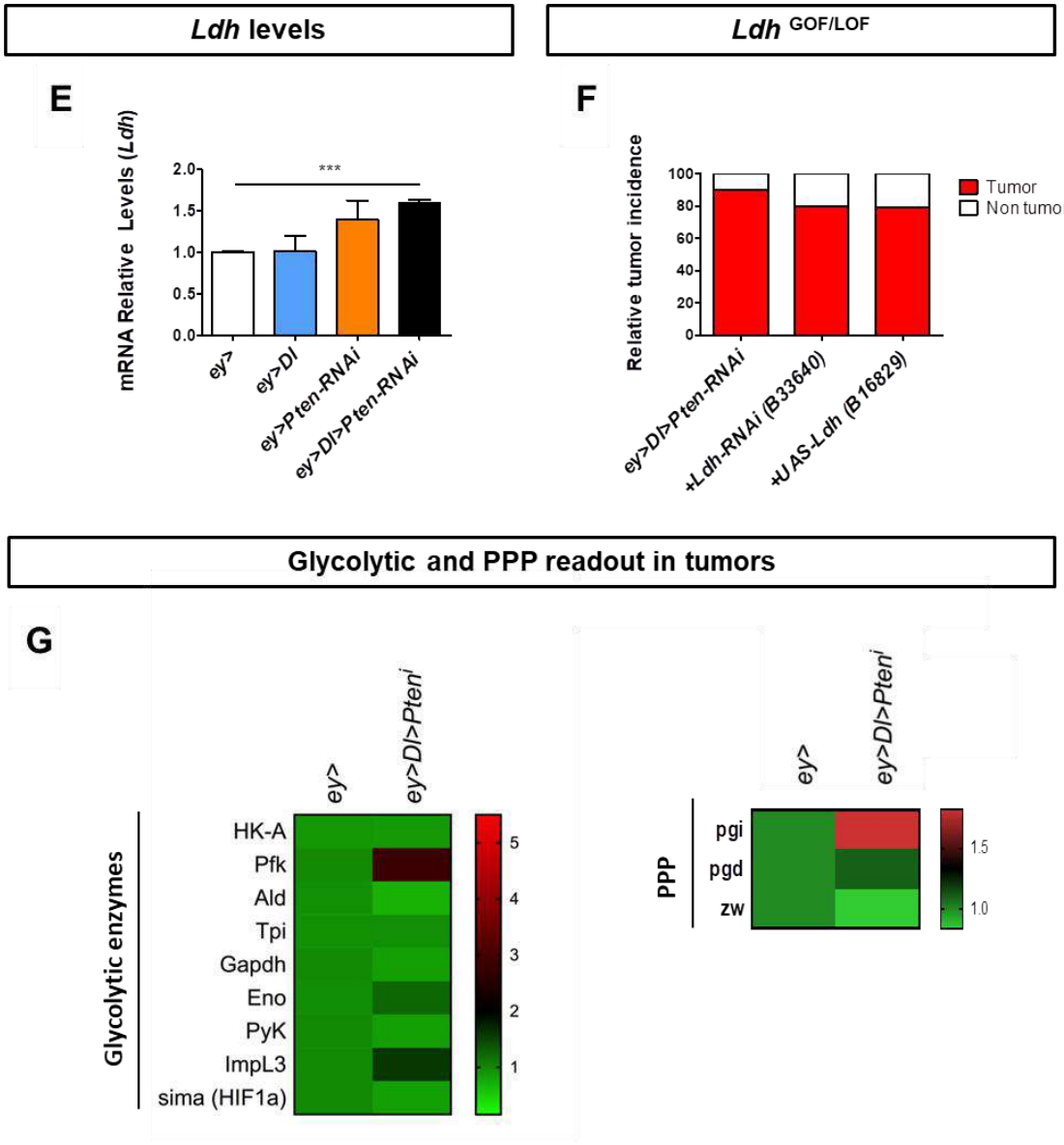

Figure 17. Sima stabilization is implicated in Notch-PI3K/Akt tumorigenesis.

(A) A mimic construct for *sima* (sima$^{MI05111\text{-}GFSTF.2}$, B60222) shows sima protein stabilization. **(B)** mRNA levels of *sima* in eye imaginal discs by RT-qPCR. Data were analyzed by a two-tailed unpaired t-test and values represent the mean ± SD of three independent replicates.$p<0.05$. **(C)** Tumor incidence (as a percentage) in control flies and after *sima* knock-down or overexpression in Notch-PI3K/Akt context and representative phenotypes. Bars shown represent the mean of total (n > 100) flies scored. Crosses were repeated twice. Notice that UAS-*sima* is lethal, thus pharates were dissected to show the no-head phenotype. **(D)** Expression levels of sima targets in eye imaginal discs by RT-qPCR. **(E)** Expression levels of *Ldh* in eye imaginal discs by RT-qPCR. **(F)** Tumor incidence (as a percentage) in control flies and after *Ldh* knock-down and overexpression. **(G)** Heatmap illustrating the expression levels of glycolytic and PPP enzymes in eye imaginal discs by RT-qPCR. Data were analyzed by a two-tailed unpaired t-test and values represent the mean ± SD of three independent replicates. $p<0.05$. HK-A: hexokinase A; Pfk: phosphofructokinase; Ald: aldolase; Tpi: topoisomerase; Gapdh: Glyceraldehyde-3-Phosphate Dehydrogenase; Eno: enolase; PyK: pyruvate kinase; ImpL3: latate dehydrogenase; sima: similar; pgi:phosphoglucoisomerase; pgd: 6-phosphogluconate dehydrogenase; zw: Zwischenferment (Glucose-6-phosphate dehydrogenase).

Glycolysis is tightly connected to the pentose phosphate pathway (PPP). Proliferating cells have a high need for PPP activity to provide ribose-5-phosphate needed for generating nucleotides and NADPH. Thus, the regulatory network of PPP flux is part of the important metabolic adaptations in human cancer (Cho *et al.*, 2018). Here we found that the key enzymes of this pathway remain unchanged, although *pgi* is upregulated.

Taken together, these data suggest that Notch-PI3K/Akt tumors rely on *sima* activation expectably through NOS and ROS signals. Interestingly, despite an increase in *Ldh* and increased glucose uptake, these tumors do not show a clear increase in glycolytic and PPP flux commonly associated with cancer cells.

Section 3. Notch-PI3K/Akt/Pten tumors reprogram whole-body metabolism via the Tryptophan-Kynurenine pathway

Loss of Pten drives whole-body metabolic shift towards upregulation of Glycolysis and Pentose Phosphate Pathway

As explained in section 2, Notch-PI3K/Akt eye disc tumors have increased needs for glucose than normal growing imaginal disc cells. Excess of glucose can enter the glycolytic pathway to provide biosynthetic precursors and energy to sustain the rapid and high proliferation rate of aggressive cancer cells (Boros *et al.*, 2002). On the other hand, the pentose phosphate pathway (PPP) represents an alternative route for anaerobic glucose degradation commonly upregulated in cancer cells. PPP contributes to cancer cell proliferation by supplying cells with ribose-5-phosphate and the reductant NADPH, important for detoxification of ROS (Jiang *et al.,* 2014).

To clarify the mechanism by which *Pten* impacts host metabolism and cancer outcome we evaluated the effect of Notch-PI3K/Akt tumors in the whole-body carbohydrate metabolism of tumor-bearing larvae. To that end, we quantified changes in the expression levels of key metabolic enzymes of glycolysis and the PPP by qRT-PCR. We compared non-tumor and tumor-bearing hosts at third instar wandering larvae, the period where tumors are generated. At this stage, we also dissected the fat body, since it functions as energy storage, immune response and nutritional sensor, being the equivalent to the vertebrate adipose tissue and liver. The fat body can also interplay with other tissues to coordinate metabolism during development by monitoring and responding to the physiological needs of the growing body (Zhang & Xi, 2014). Notwithstanding, its role in tumor growth is understudied.

Remarkably, whereas eye tumors display almost normal expression for most genes involved in the glycolytic and PPP pathways related to wild type eye imaginal discs (Fig. 17G), in stark contrast, these pathways are upregulated in larvae with tumors (Fig. 18A). We also measured the relative abundance of different metabolite intermediates of these pathways by GC-MS (Gas Chromatography coupled to Mass Spectrometry) and found that none of these metabolites are accumulated in the tumor-bearing larvae (Fig. 18B). Similarly, the dissected fat bodies from tumor-bearing larvae showed a dramatic upregulation of the glycolytic and the PPP pathways (Fig. 18C) and no accumulation of intermediate metabolites (Fig. 18D). These data suggest that both glycolysis and PPP pathways are highly active and their intermediate metabolites are

highly consumed, further revealing that the presence of the tumor in the eye imaginal disc is accelerating the host energy/glucose metabolism.

Our findings indicate that Notch-PI3K/Akt-driven tumors trigger non-autonomously and remotely disturbances in the host metabolism, particularly in a distal tissue as the fat body. Notably, the metabolic changes observed in the fat body are likely to account for the majority of the observed changes in whole larvae, thereby diluting the strong effect when the whole animal is dissected. The systemic enhancement of the PPP may reflect a state of high oxidative stress and an attempt of the fat body to counteract it by increasing the intracellular redox power through NADPH overproduction. Interestingly, treatment of Notch-PI3K/Akt tumor-bearing larvae with NADPH tetra sodium salt improved the survival of those animals (Villegas *et al.,* 2018). To identify the source of such oxidative stress in the fat body we next used a high throughput metabolomics approach.

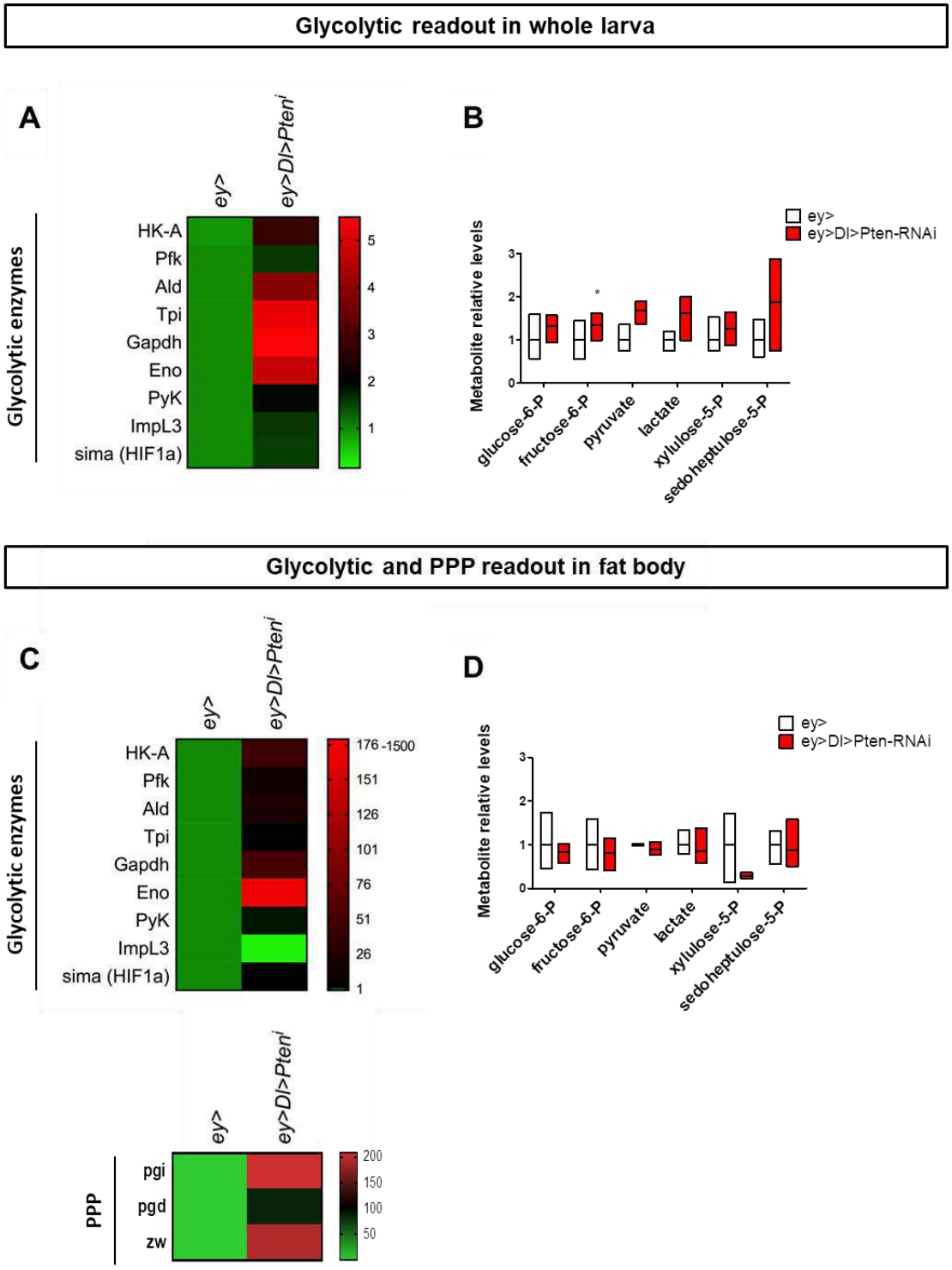

Figure 18. Glycolytic and PPP pathways are dramatically increased in the fat body of Notch-PI3K/Akt tumor-bearing larvae.

(A) Heatmap illustrating the expression levels of glycolytic enzymes in whole larvae by RT-qPCR. Data were analyzed by a two-tailed unpaired t-test and values represent the mean ± SD of three independent replicates. $p<0.05$. **(B)** Relative abundance of key glycolytic and PPP metabolites in wild type and tumor-bearing larvae. **(C)** Heatmap illustrating the expression levels of glycolytic and PPP enzymes in fat body of third instar larvae by RT-qPCR **(D)**

Relative abundance of key glycolytic and PPP metabolites in the fat body of wild type and tumor-bearing larvae. HK-A: hexokinase A; Pfk: phosphofructokinase; Ald: aldolase; Tpi: topoisomerase; Gapdh: Glyceraldehyde-3-Phosphate Dehydrogenase; Eno: enolase; PyK: pyruvate kinase; ImpL3: latate dehydrogenase; sima: similar; pgi:phosphoglucoisomerase; pgd: 6-phosphogluconate dehydrogenase; zw: Zwischenferment (Glucose-6-phosphate dehydrogenase).

Large-scale metabolomics reveals metabolic changes linked to the tryptophan catabolism in tumor-bearing larvae

To better characterize the systemic metabolic changes in tumor-bearing larvae, we performed a large-scale metabolomics assay using UHPLC-MS (Ultra High Precision Liquid Chromatography coupled to Mass Spectrometry, hereafter LC-MS). A representation of all the compounds that were detected comparing wild type larvae versus Notch-PI3K/Akt tumor-bearing larvae is in Figure 19A. Of all compounds, 58 of them present statistical differences between tumor and wild type samples (log10(p)>1), although the identity of some of them was not established. Of those identified, some are enriched in the tumor condition and others show a deficiency (Table 6; Suppl. Table 1).

We observed the most dramatic change in the 3-hydroxykynurenic acid, which is ~56 times higher in larvae with tumors (Fig. 19A), thus we focused our efforts on elucidating its role in this tumorigenic context. This metabolite is formed as a breakdown molecule of tryptophan (Trp) metabolism.

Tryptophan is an essential amino acid which is converted into several bioactive molecules, such as serotonin (~1-2%), a monoamine neurotransmitter and hormone that controls mood and immune reactions. A small percentage of tryptophan (~5%) is degraded by gut microbiota through the indole pathway. The remaining ~95% enters in the kynurenine pathway (KP), which is responsible for the detoxification of excess tryptophan, the control of plasma tryptophan availability and the production of kynurenine metabolites. The last ones have an important role in neuronal and immunomodulatory function (Bender, 1983; Badawy, 2002; Badawy *et al.*, 2016).

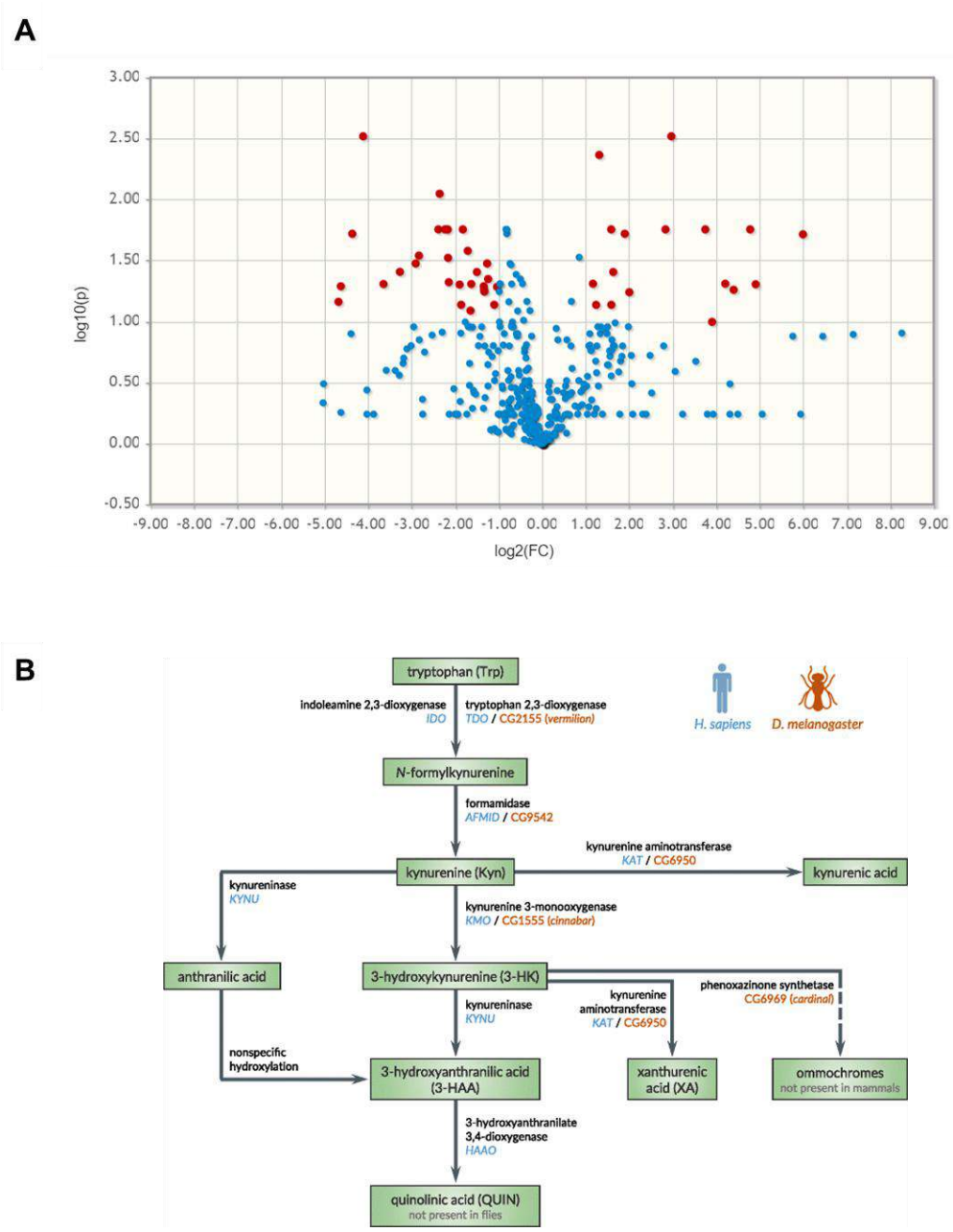

Figure 19. Tryptophan-kynurenine metabolism is altered in tumor-bearing larvae.

(A) Volcano plot of LC-MS quantification of metabolites identified between Notch-PI3K/Akt/Pten tumor-bearing larvae versus wild type larvae. Y-axis indicates −log10 (p value) while the horizontal axis indicates base 2 logarithmic value of mean metabolite abundance ratio (Tumor/Wild type). The horizontal dashed line represents the Benjamini-Hochberg FDR threshold of significance assigned for subsequent analysis of metabolites. Compounds that show significant changes are indicated in red. **(B)** Kynurenine metabolism in *Homo sapiens* and *Drosophila melanogaster* (picture from Navrotskaya *et al.,* 2018).

Tentative ID	Fold Change (Tumor/WT)	p. adjusted	Biological process
Hydroxykynurenic acid	55,85	0,019	Tryptophan metabolite/kynurenine pathway, Immune system
Methyladenosine	27,96	0,040	Modification in mRNA and DNA by methyltransferase complex
DHEA Sulfate	19,74	0,043	Dehydroepiandrosterone sulfate, steroid hormone
Acetylhistamine	12,99	0,031	N-acetylation of histamine; degradation pathway primarily important in microbial degradation
Tumonoic Acid	3,69	0,022	Cyanobacteria
Histamine	2,42	0,000	Hormone, neurotransmitter and messenger; immune response
Hydroxyisoleucine	2,28	0,045	Plant amino acid; insulinotropic activity
LysoPE (18:2)	0,65	0,035	Lysophospholipid
Acetylarginine	0,64	0,013	L-arginine in which one of the hydrogens attached to the nitrogen is replaced by an acetyl group.
Decanoylcarnitine	0,63	0,042	Fatty ester lipid derivative of L-carnitine; group of acyl carnitines
Indoleacrylic acid	0,62	0,023	Tryptophan metabolite from microbiota: promotes intestinal epithelial barrier function, mitigates inflammatory responses
Phenylalanine	0,57	0,004	Essential amino acid and precursor of the amino acid tyrosine.
inosine/arabinosylhipoxanthine	0,54	0,031	Nucleoside formed when hypoxanthine is attached to a ribose ring; purine derivative
PC(13:0)/PE(16:0)	0,49	0,037	Phosphatidylcholine (PC),phosphatidylethanolamine(PE), phospholipids
PC(11:0)/PE(14:0)	0,49	0,035	Phospholipid
PC(o-11:1)/LysoPE(16:1)	0,47	0,045	Lysophospholipid
PC(15:1)/LysoPE(18:1)	0,44	0,049	Phospholipid
Oleoylserine/tetradecenoylcarnitine	0,41	0,015	Fatty ester lipid derivative of L-carnitine; group of acyl carnitines
Methionine	0,41	0,013	Amino acid
Methylniveusin	0,35	0,043	Secondary metabolite from sunflower
Methyltyrosine/Homotyrosine	0,34	0,031	Tyrosine homolog; inhibits the Tryptophan indole-lyase PLP-dependent bacterial enzyme
beta-glucan	0,32	0,045	Sugars of bacterial cell walls, boosts immune system
stearoylglutamic acid	0,19	0,000	Glutamic acid derivative
Palmitoylglutamic acid	0,11	0,031	Glutamic acid derivative
Oxoproline/pyroglutamic acid	0,08	0,042	Cyclized derivative of L-glutamic acid.
PC(32:1)/PE(35:1)	0,06	0,033	Phospholipid
Thiomorpholine 3-carboxylate	0,04	0,040	Unknown biological function

Table 6. List of compounds identified by LC-MS with statistically significant effect.

In orange: metabolites more abundant in the tumor-bearing larvae (Fold Change > 1). In blue: metabolites less abundant in the tumor-bearing larvae (Fold Change < 1).

In humans, the kynurenine pathway (KP) exists mainly in the liver, where Trp is degraded by the enzyme tryptophan dioxygenase (TDO, *vermilion* in flies) to form kynurenine (K) and later its many breakdown products, which include: redox factors as nicotinamide adenine dinucleotide/phosphate (NAD+, NADP+), niacin (also known as nicotinamide, nicotinic acid or vitamin B3), the NMDA receptor agonist quinolinic acid (QA) and antagonist kynurenic acid (KA); and immunosuppressive metabolites such as 3-hydroxykynurenine (3-HK) and 3-hydroxyanthranilic acid (3-HAA). Kynurenine is

oxidized to 3-HK by the enzyme kynurenine monooxygenase (KMO, encoded by *cinnabar* in flies). Both K and 3-HK can also be transaminated to form KA and xanthurenic acid (XanA) by kynurenine aminotransferases (KYAT), respectively (Fig. 19B) (Badawy, 2017).

Tissue-specific targeted metabolomics points at the fat body as the origin of major metabolic changes observed in tumor-bearing larvae

To confirm and expand the data of LC-MS, we performed targeted GC-MS (Gas Chromatography coupled to Mass Spectrometry) of tumor-bearing host (Fig. 20A), the fat body (Fig. 20B) and the circulating hemolymph (Fig. 20C) compared with non-tumor hosts and hosts with single *Delta* overexpression or *Pten* knockdown. I carried out this technique in the lab of Dr. Tennessen in Indiana University (USA).

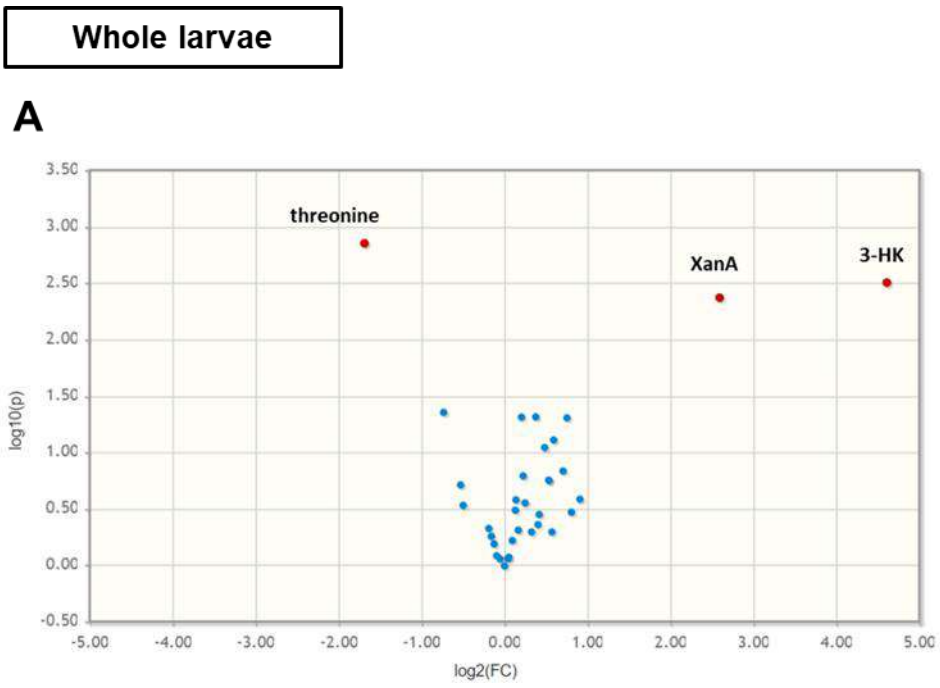

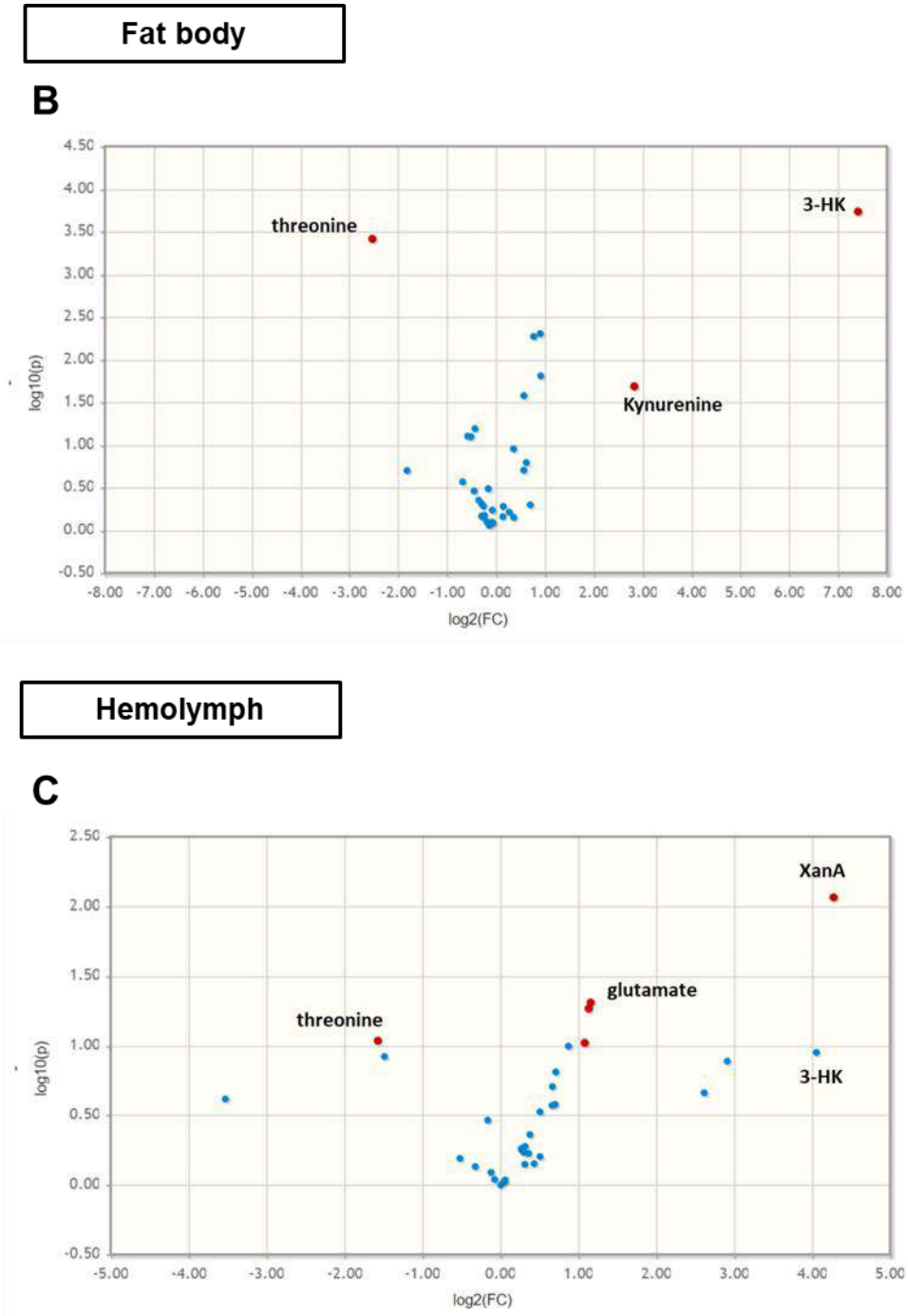

Figure 20. KP metabolites production is increased in tumor-bearing hosts.

Volcano plot representing GC-MS quantification of metabolites identified between **(A)** whole larvae **(B)** fat bodies and **(C)** hemolymph of Notch-PI3K/Akt/Pten tumor bearing-larvae versus wild type larvae. Y-axis indicates −log10 (p value) while the horizontal axis indicates base 2 logarithmic value of mean metabolite abundance ratio (Tumor/Wild type). The horizontal dashed line represents the Benjamini-Hochberg FDR threshold of significance assigned for subsequent analysis of metabolites. Compounds that show significant changes are indicated in red.

Targeted GC-MS corroborated the positive correlation of the tryptophan-kynurenine pathway in hosts with ey>*Dl*>*Pten*-RNAi tumors. These analyses also showed similar changes in larvae with single ey>*Pten*-RNAi expression, albeit less severe (Suppl. Fig 3). This data indicates that these metabolic alterations are brought about by the Pten deficiency rather than being a consequence of tumorigenesis, since *ey>Pten*-RNAi does not lead to overgrowth in fed hosts (Palomero *et al.*, 2007; Villegas *et al.,* 2018). Interestingly, besides the increase in 3-HK observed by LC-MS, xanthurenic acid (XanA), a breakdown product of 3-HK was also enriched in tumor-bearing larvae (Fig. 20A). Notably, the KP pathway is highly active in the fat body of tumor-bearing larvae and is presumably the main source of 3-HK changes observed in the host (Fig. 20B). Hemolymph analyses also revealed high levels of circulating K, 3-HK, and XanA metabolites in larvae with ey>*Dl*>*Pten*-RNAi tumors (Fig. 20C). Finally, a second targeted analysis of UHPLC-MS data confirmed the changes in the different KP metabolites identified by targeted GC-MS, specially 3-HK which was ~209 times higher (Suppl. Table 1).

Tryptophan-Kynurenine pathway is transcriptionally up-regulated in the fat body of tumor-bearing hosts

To verify that genes encoding the enzymes that produce kynurenine metabolites were altered in tumor-bearing hosts, we measured mRNA levels of the tryptophan-kynurenine pathway key enzymes in the tumor tissue (Fig. 21A), whole larvae (Fig. 21B) and fat bodies (Fig. 21C) by qRT-PCR. Expression levels of the main KP enzymes are increased in the fat body of Notch-PI3K/Akt larvae, as expected (Fig. 21C). These data corroborate that tryptophan-kynurenine pathway is elevated significantly in the fat body, albeit there is mild but significant up-regulation of KMO/*cn* in the eye tumors compared wild type controls (Fig. 21A). Consequently, we observe systemic tryptophan depletion ought to the huge increment in the activity of the KP in the fat body (Fig. 21D).

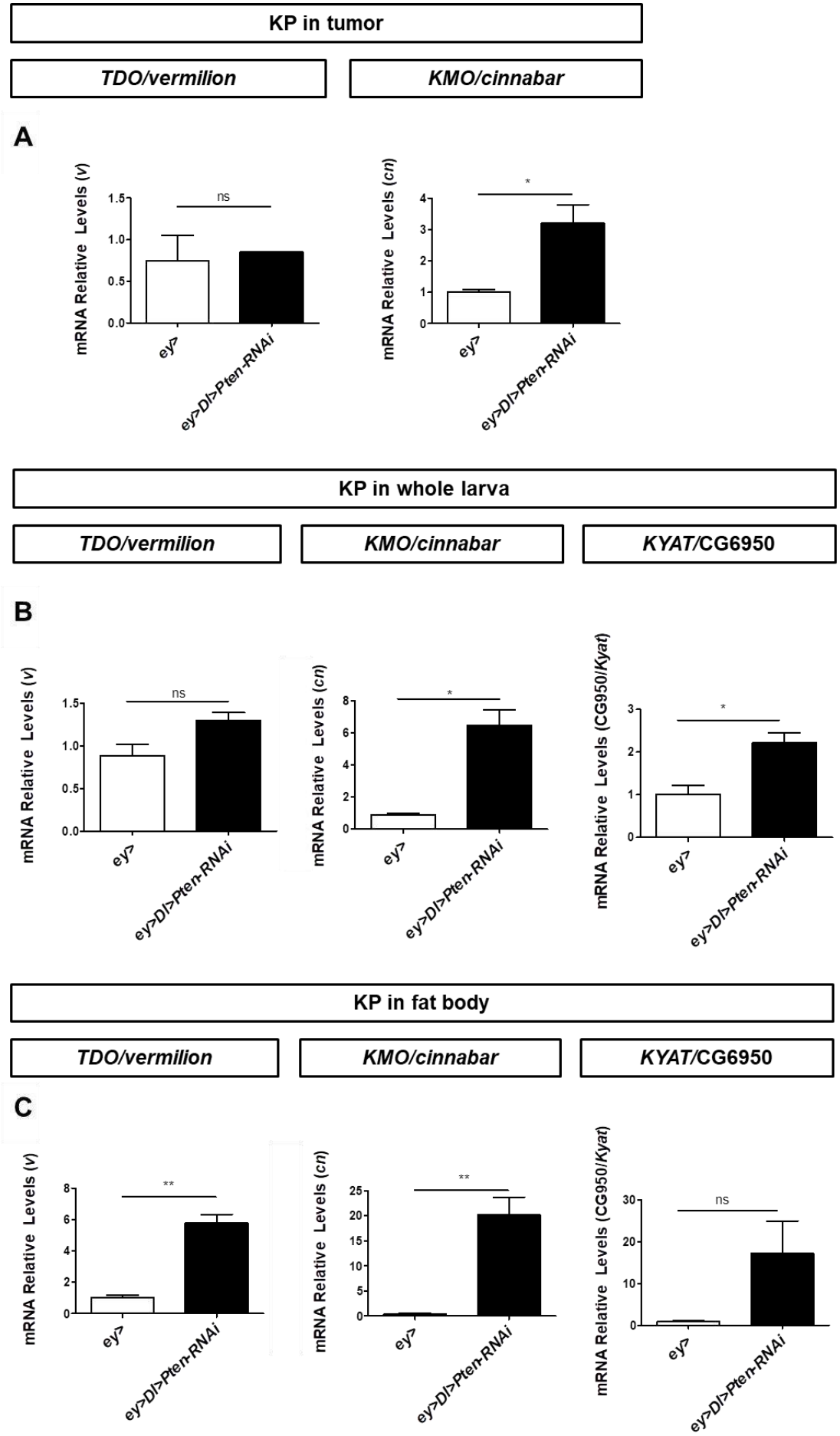
KP in tumor
TDO/vermilion
KMO/cinnabar
A
mRNA Relative Levels (v)
ns
mRNA Relative Levels (cn)
*
ey>
ey>Dl>Pten-RNAi
KP in whole larva
TDO/vermilion
KMO/cinnabar
KYAT/CG6950
B
mRNA Relative Levels (v)
ns
mRNA Relative Levels (cn)
*
mRNA Relative Levels (CG950/Kyat)
*
ey>
ey>Dl>Pten-RNAi
KP in fat body
TDO/vermilion
KMO/cinnabar
KYAT/CG6950
C
mRNA Relative Levels (v)
**
mRNA Relative Levels (cn)
**
mRNA Relative Levels (CG950/Kyat)
ns
ey>
ey>Dl>Pten-RNAi

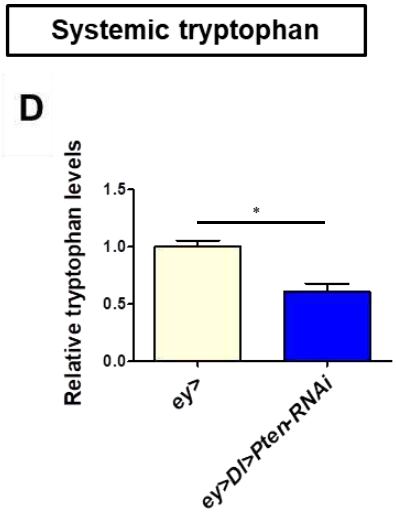

Figure 21. KP is shifted towards a higher production of 3-HK in fat body of Notch-PI3K/Akt tumor-bearing larvae.

mRNA levels of *vermilion* (*v*) and *cinnabar* (*cn*) in **(A)** eye imaginal discs**, (B)** fat body and **(C)** whole larva by RT-qPCR. Data were analyzed by a two-tailed unpaired t-test and values represent the mean ± SD of three independent replicates.$p<0.05$. **(D)** LC-MS quantification of tryptophan levels in Notch-PI3K/Akt/Pten tumor-bearing larvae versus wild type larvae.

Interestingly, levels of XanA are higher in the whole animal and hemolymph of Notch-PI3K/Akt tumor-bearing larvae (Fig. 20A, 20C). We measured the expression levels of KYAT/CG6950, the enzyme that produces XanA, and observed that is increased in the whole larva (Fig. 21B), but not in the fat body (Fig. 21C). All together, these data suggest that this metabolite is secreted to the hemolymph, as happens in humans, where is secreted to the plasma and urine (Keda *et al.*, 1986; Oxenkrug, 2015).

Carbohydrate metabolism could also be influenced by XanA, since it binds and inactivates insulin, having a diabetogenic effect in humans. In fact, high plasma levels of XanA are associated with insulin resistance, increased glycemia and higher probability of having diabetes **(**Reginaldo *et al.,* 2015; Pasco and Leopold, 2012). Here we measured the expression levels of FOXO targets, *4E-BP* and *insulin receptor* (*InR*). Whereas *4E-BP* expression levels are higher in the whole larva (Fig. 22A), *InR* and *4EBP* were markedly down-regulated in the fat body from tumor-bearing larvae (Fig. 22B), which allows the fat body cells to use glucose more effectively, reducing glycemia (Fig. 22C). We therefore hypothesize that whereas the fat body might be insulin sensitive, the whole animal might be insulin resistant.

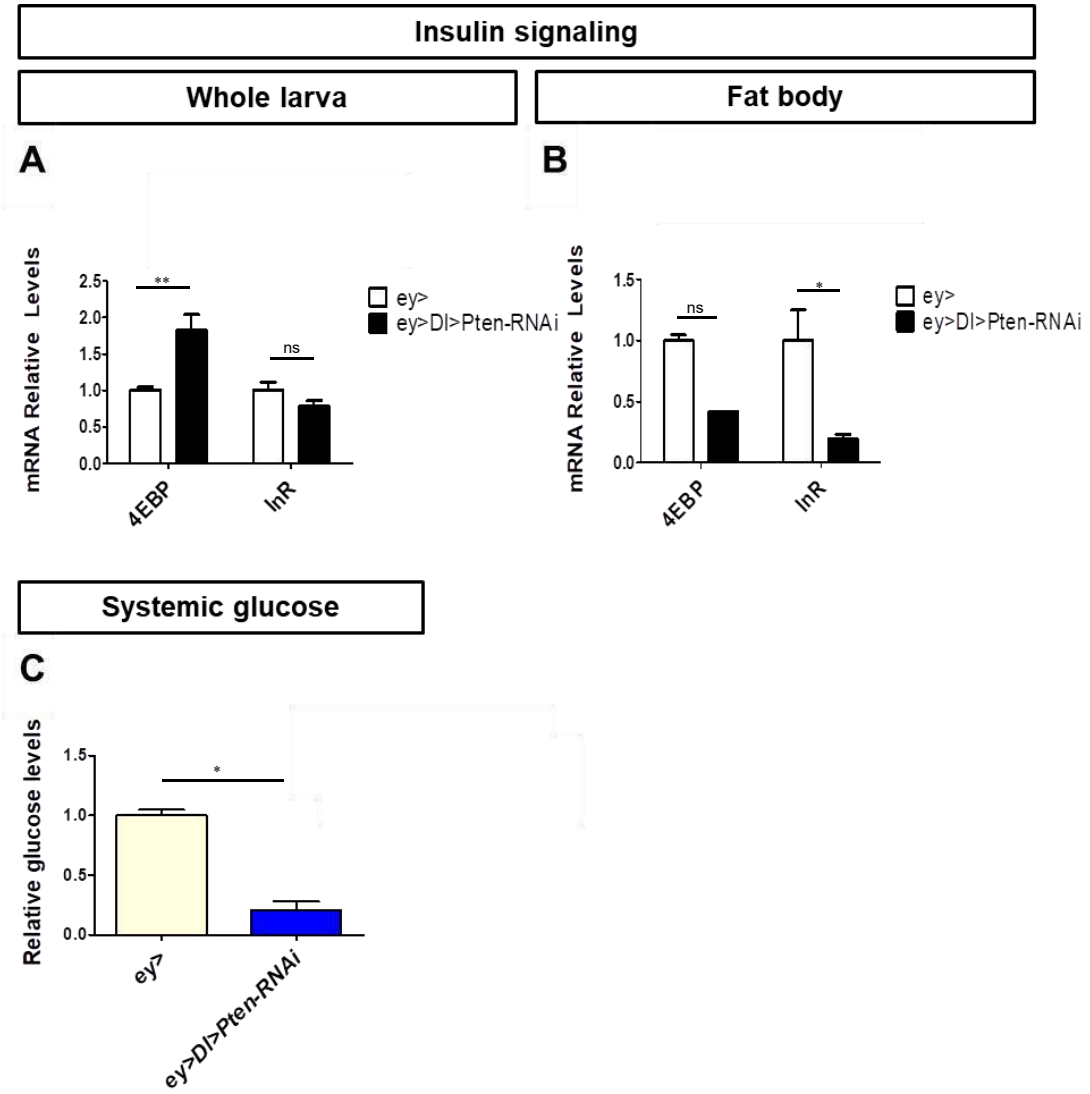

Figure 22. Fat body cells from tumor-bearing larvae are insulin sensitive.

(A) mRNA levels of FOXO targets, *4E-BP* and insulin receptor (*InR*) in whole larvae and **(B)** fat body by RT-qPCR. Data were analyzed by a two-tailed unpaired t-test and values represent the mean ± SD of three independent replicates.$p<0.05$. **(C)** LC-MS quantification of glucose levels in Notch-PI3K/Akt/Pten tumor-bearing larvae versus wild type larvae.

Overexpression of *Kynurenine 3-monooxygenase* (*KMO/cinnabar*) is the main contributor to Pten tumorigenesis

Disturbances in the function of KP could have clinical and therapeutic implications. The cancer-promoting role of KP was first reported in 2005 by Prendergast group. They showed that IDO promotes tumor formation through inhibition of T-cell immunity (Muller *et al.*, 2005). Furthermore, in some types of cancers, TDO is constitutively expressed and is capable of suppressing antitumor immune responses (Platten *et al.,* 2012). On the other hand, KMO overexpression is also a poor prognosis of cancer malignancy (Chiu *et al.,* 2019). However, despite the immunosuppressive role of the kynurenine metabolites has been widely investigated in cancer and the microenvironment, little is known about their systemic effects in cancer outcome.

In order to expand the pathophysiological roles of tryptophan-kynurenine pathway in tumorigenesis, we performed functional studies depleting each of the tryptophan catabolic genes TDO/*vermilion*, KMO/*cinnabar* and kynurenine metabolite transporters by both endogenously reducing the expression using mutations and by tumor-specifically knockdown via transgenic RNAi expression.

Drosophila TDO/*vermilion* is preferentially expressed in the fat body in normal growing larvae. Because we observed a fat body-specific upregulation of TDO/*vermilion* and KMO/*cinnabar* in ey>*Dl*>*Pten*-RNAi tumor-bearing hosts (Fig. 21B), consistent with the metabolomics data, we hypothesized that these genes may contribute to tumorigenesis by fat-body production of kynurenine and 3-HK, respectively. Tumor-specific knockdown of TDO/*vermilion* and KMO/*cinnabar* induced a decrease in tumor incidence, indicating a local role of KP in the tumor tissue, as happens in some cancers. The systemic effect of halving gene dosage of TDO/*v* or KMO/*cn* using endogenous mutations resulted in a drastic reduction of tumor incidence, suggesting that the presence of the tumor can rewire the host tryptophan-kynurenine metabolism (Fig. 23A). In line with these findings, diet supplementation with 3-HK in tumor-bearing larvae lacking KMO/*cn* rescued tumorigenesis, indicating that the production of this metabolite is causative of the tumor phenotype (Fig. 23B).

On the other hand, besides TDO, the rate-limiting factor of tryptophan conversion into kynurenine is the ATP-binding cassette (ABC) transporter (Sullivan *et*

al., 1980; Mackenzie *et al.*, 1999). The white, brown and scarlet genes encode ABC proteins that act as tryptophan transporters (Ewart *et al.*, 1994), but can also export 3-HK from cytoplasm into the pigment granules of eye cells (Mackenzie *et al.*, 2000). Tumor-specific downregulation of *white* and *scarlet* genes by transgenic RNAi to limit Trp/K cellular uptake resulted in a reduction of tumor incidence, indicating that either tryptophan and/or kynurenine metabolites are necessary for the Notch-PI3K/Akt cancer cells to grow (Fig. 23C).

In humans, IDO2 is regulated by the Aryl hydrocarbon receptor (AhR), a ligand-activated transcription factor that functions as xenobiotic sensor and also plays an important role in the control of immune response and tolerance (Stevens *et al.*, 2009). Kynurenine and some of its breakdown metabolites are endogenous ligands of the AhR. Binding of kynurenine or kynurenic acid to the AhR dampens the immune response to prevent excessive inflammation and autoimmunity (Juliard *et al.*, 2014). Studies on human lung cancer cells have shown that kynurenine activates IDO via AhR, which is associated with a poor prognosis, since IDO-mediated immunosuppression enables the immune escape of tumor cells (Litzenburger *et al.*, 2014).

Here we downregulate the *Drosophila* homolog of AhR, *spineless* (*ss*), tumor-specifically, which results in a significant reduction in tumor incidence. Halving gene dosage by introducing an endogenous mutation also has anti-tumor effect, albeit less strong (Fig. 23D). This data suggests that high levels of kynurenine metabolites found in tumor-bearing hosts trigger an immunosuppressive effect through binding to AhR and the subsequent activation of TDO/IDO/vermilion, generating a loop that reinforces tumor cell immune escape. Thus, fat body- and tumor-derived kynurenine metabolites contribute in a multifactorial manner to Notch-PI3K/Akt-driven tumorigenesis.

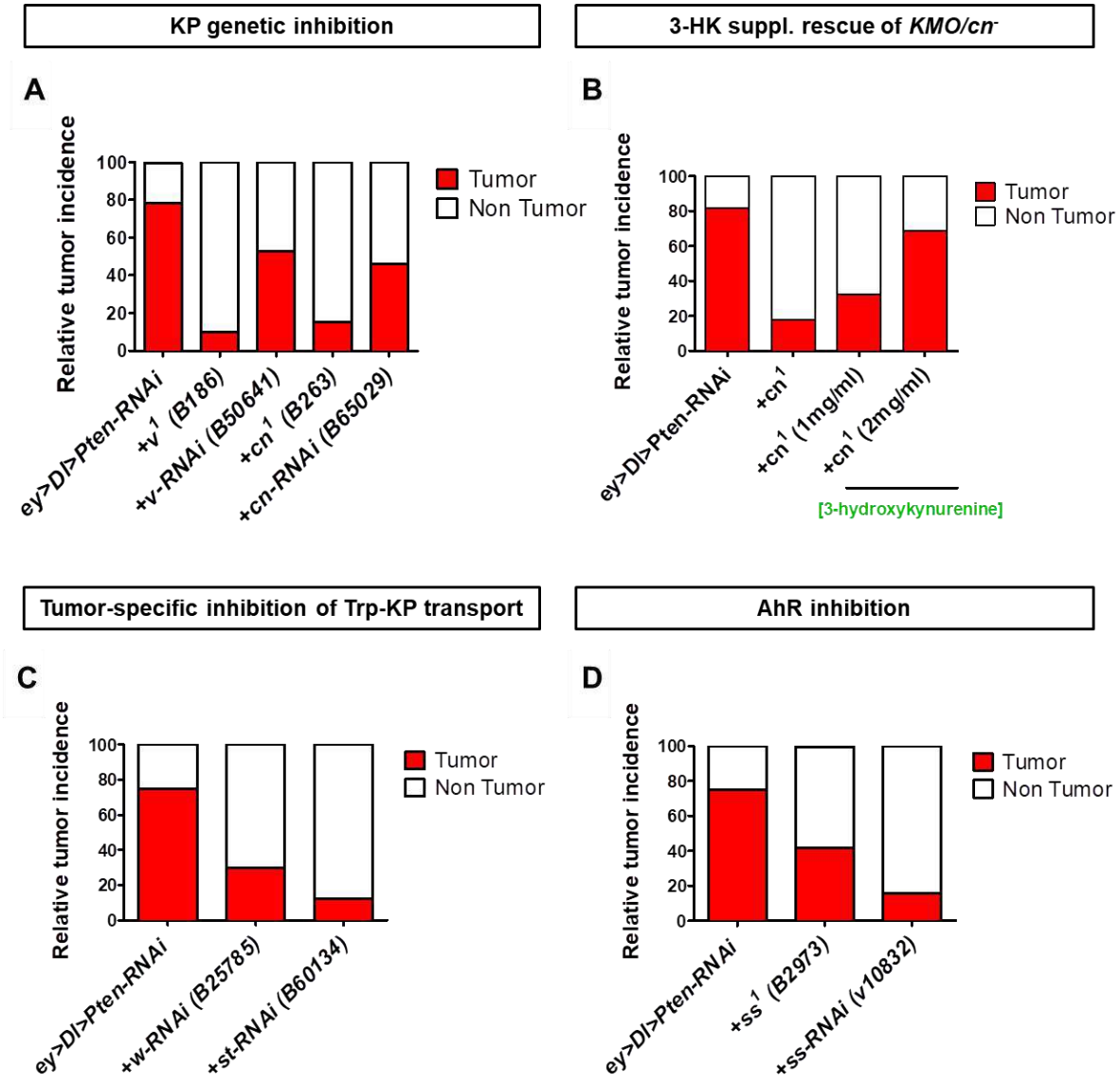

Figure 23. Fat body 3-HK overproduction is causative of the Notch-PI3K/Akt tumor phenotype.

(A) Tumor incidence (as a percentage) in control flies and after halving gene dosage of *vermilion* and *cinnabar* and after tumor-specific knock-down with RNA of interference. **(B)** Tumor incidence in tumor-bearing larvae lacking KMO/*cn* after diet supplementation with different concentrations of 3-HK**. (C)** Tumor incidence after tumor-specific knock-down of the tryptophan transporters *white* (*w*) and *scarlet* (*st*) and **(D)** after halving gene dosage or tumor-specific knock-down of the Aryl hydrocarbon receptor, *spineless* (*ss*). Bars shown represent the mean of total (n > 100) flies scored. Crosses were repeated twice.

Systemic pharmacologic inhibition of KMO/cn exerts an antineoplastic effect

Constitutive IDO expression has been reported in most human tumors and systemic pharmacological inhibition of IDO has been shown to reverse immune resistance mechanisms in several animal models (Uyttenhove *et al.*, 2003). In fact, IDO inhibitors (Prendergast *et al.* 2017) have entered clinical trials with the aim to dampen tumour immune escape (Sheridan *et al.* 2015). In addition, overactivation of liver-specific TDO in cancer (Cheong *et al.*, 2018) suggests that this enzyme also contributes to drive immune escape. Consistently, systemic TDO inhibition restored tumor rejection in a preclinical model (Opitz *et al.* 2011; Stroobant *et al.*, 2012).

Hence, we administrated a TDO/IDO/vermilion and KMO/cinnabar drug inhibitors to tumor-bearing hosts. TDO/v inhibitor was not effective at any of the tested doses (Fig. 24A) and it was lethal at doses >100µM due to vehicle toxicity (data not shown). In stark contrast, KMO/cn inhibitor exerted a potent antineoplastic effect (Fig. 24B). These data provide proof-of-concept evidence that KMO inhibitors block tumorigenesis by dampening the formation of the toxic 3-HK metabolite not only in tumor cells, but also in the whole organism.

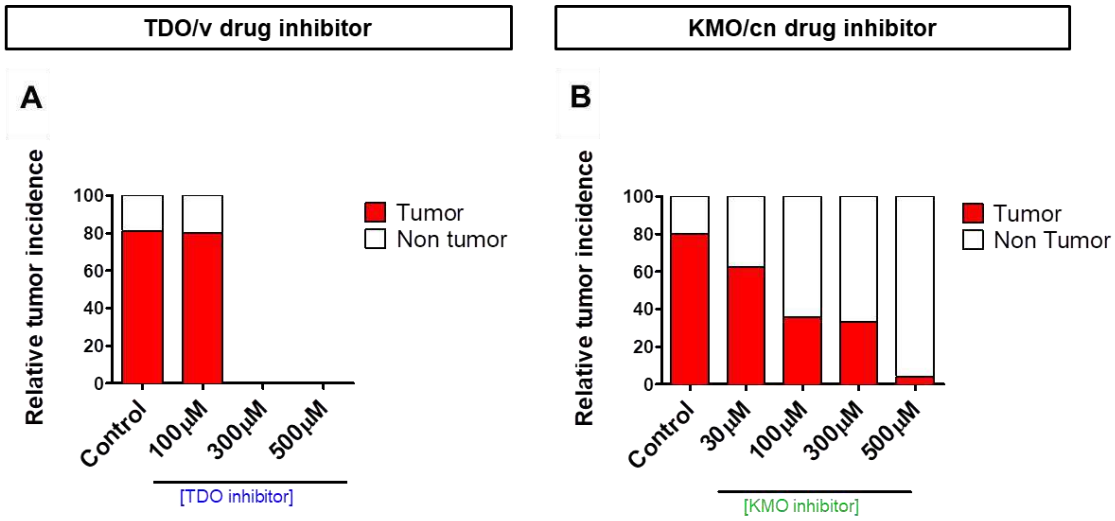

Figure 24. Drug inhibition of KMO/cn has antineoplastic effects.

(A) Tumor incidence (as a percentage) in tumor-bearing flies after treatment with drug inhibitors of TDO/vermilion and **(B)** KMO/cinnabar at different doses. The control is the absence of drug treatment. Bars shown represent the mean of total (n > 100) flies scored. Crosses were repeated twice.

Notch-PI3K/Akt-driven tumors trigger higher brain serotonin synthesis despite systemic tryptophan depletion

Tryptophan can be also converted into serotonin (5-hydroxytryptamine, 5-HT). Notably, we previously showed that serotonin exerts a positive effect on *ey>Dl>Pten*-RNAi tumors via its receptor 5HT1B (Villegas *et al.*, 2018). Moreover, previous works have demonstrated that Trp degradation along the KP leads to decreased availability of Trp for cerebral serotonin synthesis (Badawy and Evans, 1983). To provide new insights about the role of serotonin in Notch-PI3K/Akt driven tumorigenesis, we quantified the amount of brain serotonin synthesis, which revealed an increase of this neurotransmitter in tumor-bearing larvae (Fig. 25A, 25B), albeit the reduction in the pool of Trp (Fig. 21D). Furthermore, systemic levels of the serotonin precursor 5-HTP were significantly higher in these animals (Fig. 25C), although we could not detect any peak corresponding to serotonin neither by LC-MS nor by GC-MS. In addition, halving the amount of serotonin production by inhibiting tryptophan hydroxylase (Trh), the enzyme that converts Trp to 5-hydroxytryptophan (5-HTP) using a pBacTRH null mutation (Neckameyer *et al.*, 2007), resulted in a reduced tumor incidence (Fig. 25D).These results provide evidence that Notch-PI3K/Akt tumors rely on serotonin through an unknown mechanism.

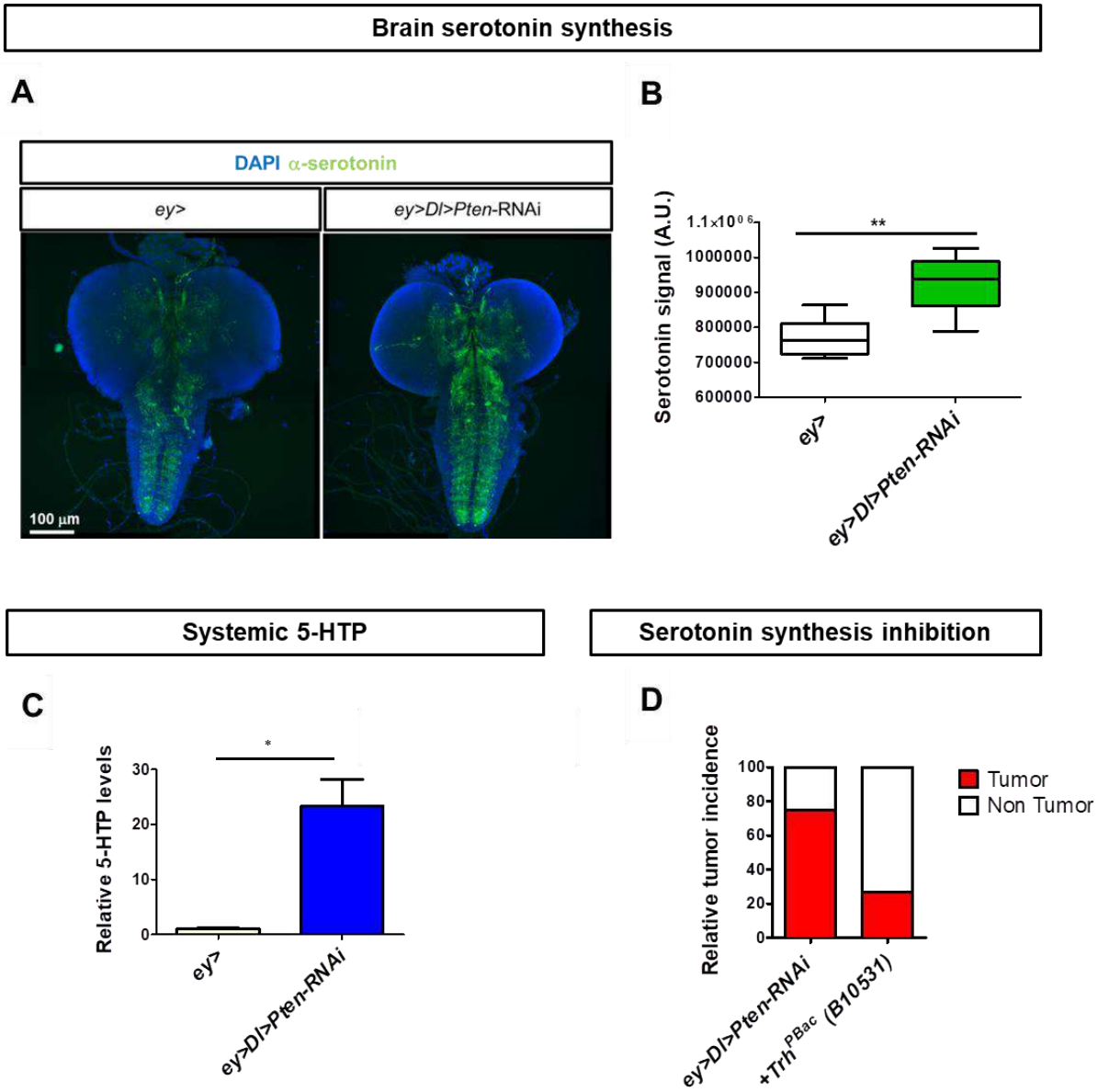

Figure 25. Serotonin synthesis is increased in the brain of tumor-bearing larvae.

(A) Serotonin neurotransmitter is visualized by anti-serotonin (green) in the brain. **(B)** Quantitative measurement of serotonin signal. **(C)** LC-MS quantification of 5-HTP levels in Notch-PI3K/Akt/Pten tumor-bearing larvae versus wild type larvae. **(D)** Tumor incidence (as a percentage) in tumor-bearing flies after inhibition of tryptophan hydroxylase (Trh). Bars shown represent the mean of total (n > 100) flies scored. Crosses were repeated twice.

Tryptophan degradation by gut microbiota is hampered in Notch-PI3K/Akt hosts

Tryptophan from the diet is also converted into various metabolites by the gut microbiota through the indole pathway. Here we detected by LC-MS reduced levels of indoleacrylic acid (IA) and indoleacetic acid (IAA) in tumor-bearing larvae (Fig. 26A).

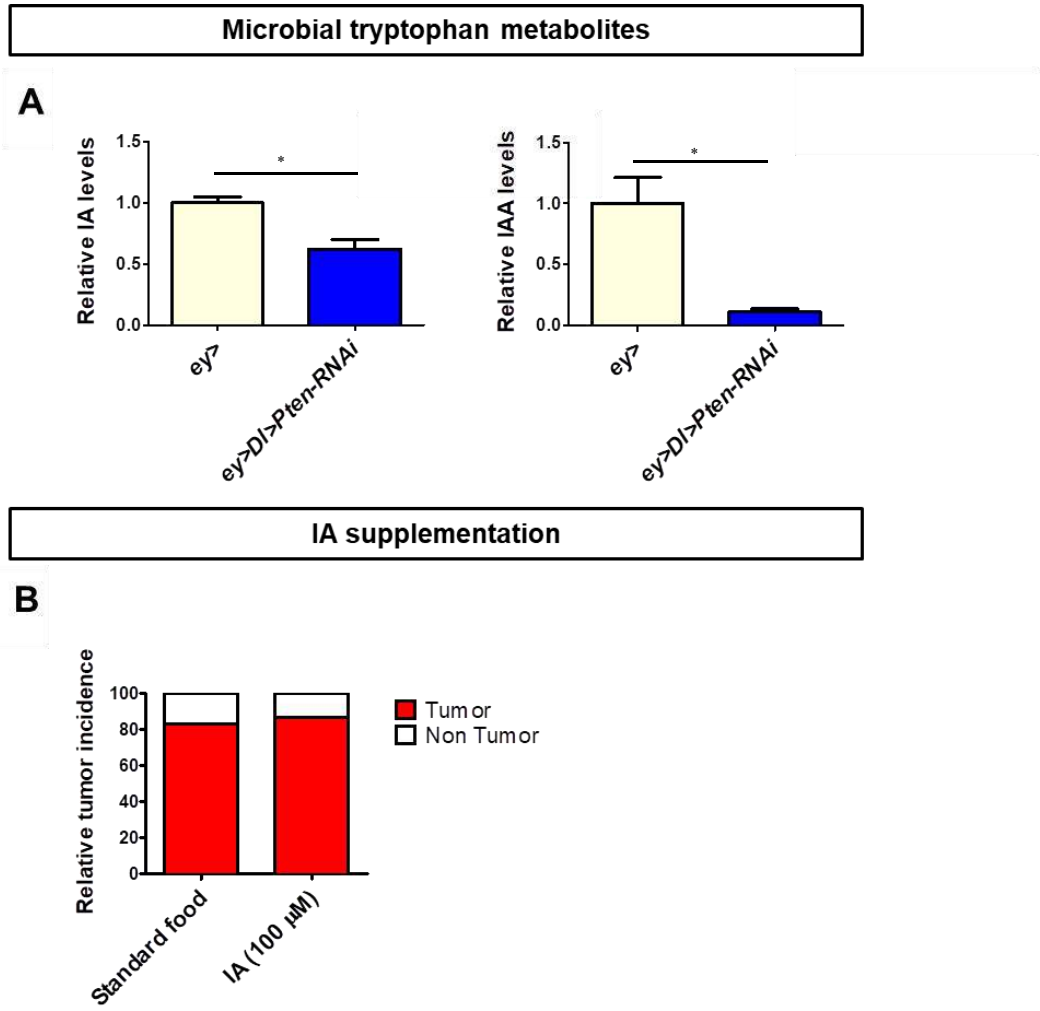

Figure 26. Amount of microbial-derived tryptophan metabolites is reduced in tumor-bearing hosts.

(A) LC-MS quantification of indoleacrylic acid (IA) and indoleacetic acid (IAA) levels in Notch-PI3K/Akt/Pten tumor-bearing larvae versus wild type larvae**. (B)** Tumor incidence (as a percentage) in tumor-bearing flies after treatment diet supplementation with indoleacrylic acid at different doses. Bars shown represent the mean of total (n > 100) flies scored. Crosses were repeated twice.

Trp degradation is shifted towards kynurenine pathway and serotonin synthesis. It is reasonable to think that the amount of tryprophan available for the microbiota to produce indole metabolites, which are known to have antiinflamatory and antioxidant properties, is reduced. Diet supplementation with IA did not have any effect on tumorigenesis at 100µM (Fig. 26B). Increasing doses were deleterious to the animal due vehicle toxicity (data not shown).

Tryptopham diet supplementation prevents lethality and tumorigenesis associated to protein restriction in *Pten*-deficient hosts

Modulation of the amino acid composition of the diet can influence cancer growth (Maddocks *et al.*, 2013). Here we have observed a systemic Trp depletion due to the fat body overproduction of KP metabolites and the increase in brain serotonin synthesis. It is well described that excess of tryptophan is one of the key regulatory mechanisms of the kynurenine pathway through reverse binding sequence (Badawy, 2017). As expected, adding a Trp supplement to the standard food was sufficient to drastically reduce the tumor phenotype (Fig. 27A). This result supports the notion that KP is involved in the tumorigenic process, since its inhibition by excess of Trp prevents tumor formation.

Moreover, as exposed in the introduction, tumors with Pten deficiency are resistant to protein restriction, but this dietary intervention also induces hypersensitivity and lethality in the host through an unknown non-autonomous mechanism (Kalaany *et al.*, 2009; Nowak *et al.*, 2013).

To ascertain whether reducing dietary amino acids in the host has a negative impact on larvae bearing Notch-PI3K/Akt tumors, we reared *ey>Dl>Pten*-RNAi hosts in a diet with 85% reduction of yeast. While non tumor-bearing hosts (*ey>*) and hyperplastic-bearing hosts (*ey>Dl*) survived this starvation condition (Suppl. Fig. 6), both *ey>Pten*-RNAi and tumor-bearing larvae (*ey>Dl>Pten*-RNAi) did not (Fig. 27B, Suppl. Fig 6). These data are in line with previous works pointing that Pten deficient tumors are diet-resistant, albeit the hosts are hypersensitive to semi-starvation of amino acids.

However, supplementation of the low-protein food with tryptophan not only rescued the host lethality associated to Pten inactivation (Fig. 27B), but also dramatically reduced the tumor phenotype, rendering wild type-like eyes (Fig. 27C). These data further reveal that this amino-acid is essential to overcome caloric restriction resistance.

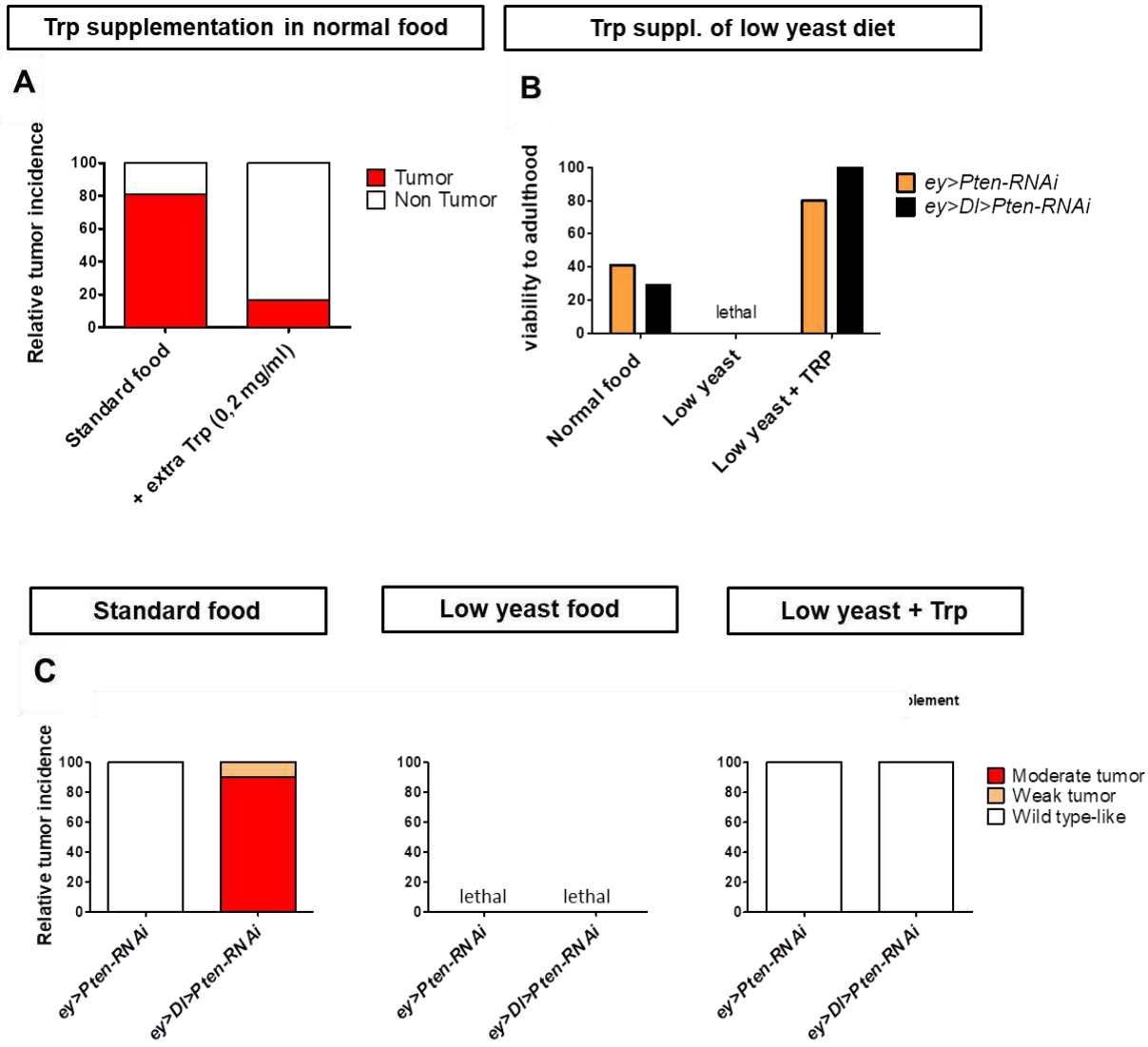

Figure 27. Tryptophan supplementation rescues viability associated to *Pten* loss under protein restriction conditions.

(A) Relative viability to adulthood in standard food (control) or in low yeast diet. **(B)** Tumor incidence as a percentaje and **(C)** relative viability to adulthood of ey>Pten-RNAi and ey>Dl>Pten-RNAi flies reared in standard food, low yeast food and low yeast food supplemented with 0,09mg/ml of tryptophan. Bars shown represent the mean of total (n > 100) flies scored. Crosses were repeated twice.

1. Discussion

The developmental outcome of a signaling pathway depends on how signals are integrated with other pathways within and between cells. Given the pleiotropic roles of Notch and Akt signaling pathways in multiple cellular processes during development, the interactions between both pathways and other signals is very complex. Disruption of these interactions by dysfunctional signaling is at the center of tumorigenesis. Tumor initiation involves a complex genetic, molecular and cellular network, which explains the poor efficiency of current treatments. Thus, for the discovery of better therapeutic options is necessary to address the complexity of Notch-PI3K/Akt context-dependent oncogenic interactions.

In the present thesis, we used *Drosophila* to model this oncogenic cooperation and induce eye tumors, since the sole activation of either the Notch or PI3K/Akt pathway is not sufficient to promote tumorigenesis (Ferres-Marco *et al.*, 2006; Palomero *et al.*, 2007). We employed a multidisciplinary approach to identify the underlying mechanisms of Notch-PI3K/Akt-driven tumorigenesis with the aim to find downstream targets that could be exploited therapeutically.

An unbiased drug screen in *Drosophila* reveals a conserved Nitric oxide-dependent inflammation in Notch-PI3K/Akt tumors

Notch and PI3K/Akt drug inhibitors exert a potent antineoplastic activity, but their use in clinics provokes side effects and drug resistance (Andersson & Lendahl, 2014; Fruman & Rommel, 2014; Chia *et al.*, 2015). Using an unbiased, phenotypic-based chemical screen we identified drug candidates that suppress Notch-PI3K/Akt-driven tumors without harming normal cells in flies, along with causal mechanisms underpinning this oncogenic cooperation.

We found that compounds inhibiting the production of LOX-derived lipid metabolites (such as the drug BW B70C) or the nitric oxide pathway elicit potent and selective antitumorigenic responses in Notch-PI3K/Akt tumors. LOX enzymes convert

linoleic and arachidonic acids into potent lipid mediators of inflammation (Dennis & Norris, 2015) and contribute to certain cancers (Chen *et al*, 2009a; 2014; Wang & DuBois, 2010; Steinhilber *et al.*, 2010; Greene *et al.*, 2011). NO, which is generated from L-arginine by NO synthase (NOS), is also a key signaling molecule in inflammation, the immune response, and cancer (Fukumura *et al.*, 2006).

In vertebrates, hallmarks of inflammation in cancer include the expression of inflammatory markers and macrophage infiltration (Mantovani *et al.*, 2008; Colotta *et al.*, 2009). In *Drosophila*, inflammation is linked to adult gut tumorigenesis (Petkau *et al.*, 2017), although a role of NOS and LOX in tumorigenesis was not described. Our results highlight an unanticipated connection between inflammation and tumorigenesis promoted by Notch-PI3K/Akt cooperation. We genetically validated the contribution of the NOS and LOX inflammatory pathways in Notch-PI3K/Akt-driven tumorigenesis. Our data indicate that activated PI3K/Akt signaling promotes inflammation and immunosuppression via aberrant NOS expression and unleashes the oncogenic potential of Notch.

In humans, NO is synthesized by three NOS isozymes. Endothelial NOS (eNOS) is a well-known direct target of AKT (Dimmeler *et al.*, 1999; Fulton *et al*, 1999), which suggests a conserved control of eNOS and Nos in flies (dNOS) by Akt through protein phosphorylation. We demonstrate that human T-ALL cells have elevated eNOS, whereas normal PBMCs did not show expression of this enzyme. Finally, we validated the top hit compound of our screen in human T-ALL cells with NOTCH1 and PI3K/AKT mutations resistant to Notch inhibitors (Palomero *et al.*, 2007). Curiously, treatment with BW B70C decreased aberrant eNOS expression and resulted toxic for human T-ALL cells, but spared normal lymphocytes, which represents a promising and safe therapeutic option. These results highlight the considerable value of drug screens in *Drosophila* to decipher potential druggable targets relevant to human cancers.

Mitochondrial dysfunction and elevated ROS levels are at the center of Notch-PI3K/Akt-induced tumorigenesis

Tumor initiation and progression is the result of a misbalance between cell proliferation and survival and the PI3K-Akt signaling pathway regulates both processes, thus playing an important role in tumor growth and treatment response. By employing a phospho-proteomic analysis on Notch-PI3K/Akt-induced tumors, we have identified the beta subunit from the ATP synthase as a specific downstream target that results phosphorylated and inactivated by Akt upon this oncogenic cooperation. The impairment of the electron transport chain owing to the ATP synthase deficiency leads to the disruption of normal mitochondrial function and increases the production of reactive oxygen species (ROS), a metabolic hallmark of cancer cells. Moreover, knocking down several members of the complex I and V alongside activated Notch yielded a neoplastic phenotype. These results provide evidence that PI3K-Akt hyperactivation fuels Notch tumorigenic potential by triggering a tumorigenic cascade of events through mitochondrial dysfunction.

Under physiological conditions these highly reactive molecules play an important role in cellular signaling (Roy *et al.*, 2017) and are counterbalanced by a natural antioxidant system, maintaining ROS homeostasis (Kantner *et al.*, 2013). In addition, increased generation of ROS and an altered redox status have long been observed in cancer cells. Indeed, a moderate increase in ROS can promote cell proliferation and cause oxidative damage to macromolecules, whereas excessive amounts of ROS can result cytotoxic by promoting apoptosis (Trachootham *et al.,* 2009).

Given the possibility that high ROS levels could induce tumor growth through stimulation of cell proliferation, it is not surprising that when the activity of the antioxidant enzyme Sod1 is enhanced in the context of Notch-PI3K/Akt flies, proliferation rate and tumor incidence decrease. In line with these results, upregulation of other ROS-scavenging enzymes also prevents tumorigenesis. By contrast, knock-down of Sod1 together with Notch hyperactivation generates eye tumors, indicating that high levels of ROS are causative of the tumor phenotype. Our results provide evidence

that *Pten* down-regulation can cooperate with activated Notch signal to modulate cellular proliferation through ROS generation.

At the onset of tumor progression, the metabolic activity of cancer cells is increased, resulting in higher ROS levels and the subsequent activation of signaling pathways that support cancer cell proliferation, metabolic adaptation and survival (Chandel & Tuveson, 2014). Accordingly, tumor cells increase their antioxidant capacity to prevent ROS-mediated activation of pathways that induce cell death, like c-Jun N-terminal kinase (JNK), further allowing for cancer progression (Chandel & Tuveson, 2014; Saito *et al.*, 2015). Strikingly, we observed that transcriptional levels of antioxidant enzymes remain intact in Notch-PI3K/Akt tumors (Suppl. Fig. 1). Consequently, the very high levels of accumulated ROS observed towards the end of the tumorigenic process in some regions of the tumor co-localize with an intense apoptotic signal.

Therefore, it is important to note that the role of ROS in cancer cell biology is, at least, controversial. Oxidative stress may inhibit or promote apoptosis. This sort of differential behavior depends on the cell redox status, which displays different spatial and temporal patterns; thus, in cells with high ROS levels, such as tumor cells, the increase in ROS may be inducing apoptosis, whereas in cells that display normal ROS levels, such increase may be promoting overproliferation and the switch to tumor phenotype.

The dual role of oxidative stress in cancer provides two opposite therapeutic approaches. Targeting redox metabolism by using drugs with prooxidant properties can increase ROS levels and induce cancer cell death (Saito *et al.*, 2015). The opposite strategy is the use of antioxidant agents to reduce ROS levels and their harming effects. However, both strategies can present inconveniences, since the first one might promote oncogenic mutations in normal cells, and the second one can inhibit ROS-mediated apoptosis and prevent oxidative damage in already established tumors, thus promoting tumor-cell survival (Trachootham *et al.*, 2009). Here we show that human T-ALL cells display higher ROS levels than healthy PBMCs and BW B70C treatment triggers ROS production. We provide proof-of-concept evidence that BW B70C could account for apoptotic cell death in human T-ALL cells by increasing oxidative stress, thereby coinciding with the results obtained *in vivo* in flies.

Activation of Jnk by oxidative stress exerts an antitumor response through induction of apoptosis in Notch-PI3K/Akt tumors

Understanding the mechanisms of how ROS levels can modulate different tumorigenic events has profound implications for both normal development and disease. The increase in ROS levels can contribute to cancer promotion in different manners. For example, it has been previously proposed that increased ROS levels can activate the Jnk signal transduction pathway, a classical cell stress mediator, in several cancer models (Dhanasekaran & Reddy, 2008; Chambers & LoGrasso, 2011) and it is also able to stabilize hypoxia-inducible factor (HIF), one of the most important mechanisms involved in the induction of the glycolytic pathway (Hielscher & Gerecht, 2015).

A large amount of effort has been spent to unravel the molecular complexity of the Jnk signaling pathway, owing to its seemingly contradictory role in promoting cell survival and proliferation on one hand and cell death on the other. At present, there is substantial evidence supporting that Jnk serves as an important proapoptotic mechanism in oxidatively stressed cells (Dhanasekaran & Reddy, 2008). Here we corroborate that notion, since those cells with elevated ROS levels highly co-localize in both, activation of Jnk signal and apoptosis in Notch-PI3K/Akt fly tumors.

However, different cancer models have produced conflicting findings, thus Jnk has been proposed to act as an oncogene or as a tumor suppressor depending on the context (Tournier, 2013). To better understand the role of Jnk in tumor initiation in our cancer model, we performed gain and loss of function genetic experiments. We observed that blocking Jnk signal does not affect tumorigenesis levels. In contrast, *Jnk* overexpression resulted in a significant decrease of tumor incidence and a prevalent hypoplasic phenotype, indicating that Jnk signaling may be either controlling cell proliferation or inducing apoptosis in the whole imaginal disc.

Additionally, we found that *Jnk* inhibition combined with activated Notch synergizes *in vivo* to promote tumorigenesis, although tumor incidence was not as high as in presence of *Pten*-inactivating mutations. In light of the above results, we presumed that *Pten* inhibition may be enhancing tumorigenesis through ROS generation and that

the subsequent Jnk activation observed may not be involved in the process of tumorigenesis, but rather is a response to face the oxidative stress produced by a malignant lesion.

All these results suggest that Jnk might act as a tumor suppressor signal by inducing apoptosis in tumor cells with high oxidative stress, as described in other cancer models (Whitmarsh & Davis, 2007; Shramek *et al.*, 2011; Ahn *et al.*, 2011; Tournier, 2013), including a *Pten* gene deletion mouse model (Hübner *et al.*, 2012).

Besides Jnk signaling pathway, ROS-induced apoptosis requires the participation of other cell death signaling pathways. Here we also show that oxidatively stressed tumor cells release the cytocrome *c* protein to respond against the tumor through mitochondrial-induced apoptosis, suggesting a tumor suppressor function for the mitochondria (Vyas *et al.*, 2016). If Jnk/mitochondrial-induced apoptosis is a protective mechanism to limit tumor progression, it is reasonable to think that blocking this process should enhance, or at least maintain, tumor incidence. However, in contrast to expectations, overexpression of the protein P35, which blocks the action of caspases, revealed a reduction in tumorigenesis levels. There is great evidence in several model organisms that apoptotic cells are able to stimulate neighboring surviving cells to undergo proliferation, a phenomenon named apoptosis-induced proliferation (AiP) with important implications for normal development and tumorigenesis. Jnk activity is both necessary and sufficient to induce AiP by expression of potent mitogens and is well studied in *Drosophila* (Ryoo *et al.*, 2004; Perez-Garijo *et al.*, 2009; Smith-Bolton *et al.*, 2009; Bergantinos *et al.*, 2010; Shlevkov & Morata G, 2012; Fan *et al*, 2014). In a mouse model of liver cancer, hepatocytes with accumulation of ROS result in cell death. Dying hepatocytes increase JNK activity that initiates the process of AiP, promoting proliferation of surviving hepatocytes and cancer (Maeda *et al.* 2005; Sakurai *et al.* 2008; Fan *et al*, 2014).

Therefore, we could hypothesize that Jnk, despite its protective role, may also have a cancer-promoting activity through AiP. Such an interesting possibility, however, awaits experimental corroboration and additional analysis. At present, many intriguing questions about the functions of ROS and Jnk activation remain to be further explored.

Future research work should focus on how tumor cells affect the surrounding cells under an *in vivo* microenvironment.

Our results point ROS as a key driver of Notch-PI3K/Akt-induced tumorigenesis, a fact that has obvious potential implications for therapeutic approaches. Accumulation of toxic levels of ROS in specific regions of the tumor leads to an apoptotic protective response through Jnk activation and release of cytochrome *c*, but highlights the possibility of compensatory cell proliferation mechanisms in the surrounding cells. Tumors display high cell heterogeneity, since every cell within a tumor is the result of the failure of numerous molecular events and biological mechanisms; therefore, each cancer cell can behave different respect to their neighbors. The genetic complexity and the subsequent intratumor heterogeneity are difficult to reproduce in experimental models, which hamper the design of effective therapies. We propose that the administration of BW B70C in Notch-PI3K/Akt flies enhances ROS production and reduces tumorigenesis levels by inducing cell death of the whole tissue. However, in our experiments, genetic crosses are set in food with drug, which means that such approach might be only effective at the onset of tumor formation by preventing accumulation of oncogenic ROS. The pro-oxidant capacity of this compound could result self-defeating in already stablished tumors with cells displaying different ROS levels within the tumor, by means of helping to sustain AiP and/or generating more oxidative damage.

Notch-PI3K/Akt tumors rely on enhanced glucose uptake and activation of hipoxia inducible factor 1

Metabolic reprogramming is a hallmark of cancer cells controlled by oncogenic signaling and complex transcriptional networks. It is widely assumed that cancer cells display higher rates of glucose consumption and glycolysis, a process called Warburg effect (Warburg, 1956). Contrary to first observations, today is accepted that this metabolic shift provides anabolic precursors necessary to tumor growth, but is not enough to supply the huge energy demand of cancer cells (Dang, 2012). Aberrant activation of the PI3K/Akt pathway, a feature commonly found in cancer cells, affects glucose metabolism by increasing expression and translocation of glucose transporters (GLUT) to the plasma membrane in order to increase glucose consumption and phosphorylating key glycolytic enzymes (Buzzai *et al.*, 2005; Hoxhaj & Manning, 2020). Here we corroborate that glucose uptake is higher in tumor eye imaginal discs compared to wild type tissue. Consequently, inhibition of glucose transport by knocking down of GLUT1 reduces tumor incidence, indicating that Notch-PI3K/Akt tumors need high amounts of glucose to sustain their growth. Moreover, administration of 2-deoxyglucose, a glucose analog that enters the cell and but can not be metabolized, reduced tumor incidence. Similarly, 2-chloro-2-deoxyglucose, another glycolittic inhibitor used in Villegas *et al.*, 2018, yielded same results.

Furthermore, Akt also promotes a robust anabolic program through activation of hypoxia-inducible factor–1 (HIF-1) via mTOR, even under normal oxygen levels (Yuan & Cantley, 2008; Dibble & Manning; 2013). The enhanced transcription of several key glycolytic enzymes and transporters, accompanied by augmented protein synthesis, is regulated by the evolutionary conserved transcription factors HIF-1 and MYC, the master inducers of glycolysis in cancer cells (Yeung *et al.*, 2008; Zwaans & Lombard, 2014).

HIF-1 is a heterodimer formed by one labile oxygen-sensitive subunit, the HIF-1α and one stable constitutively expressed subunit, the HIF-1β (Wang & Semenza, 1995; Ivan *et al.*, 2001; Kaelin & Ratcliffe, 2008; Semenza, 2012) encoded by the gene homologues *similar* (*sima*) and *tango* (*tgo*), respectively, in *Drosophila* (Bruick &

McKnight, 2001; Centanin *et al.*, 2005). The expression of *HIF-1α/sima* is controlled at multiple levels, such as transcription, nuclear transport, protein stability, and transactivation. Under normoxia, HIF-1α/sima is hydroxylated by the prolyl-4-hydroxylase/PHD (*fatiga* in flies), which acts as an oxygen sensor. The von Hippel-Lindau (VHL) E3 ubiquitin ligase recognizes and binds to the hydroxylated HIF-1α/sima subunit to target it for proteasomal degradation (Kaelin & Ratcliffe, 2008). In hypoxia, HIF-1α/sima is not degraded, because it cannot be hydroxylated by *fatiga* due to the lack of oxygen. Consequently, HIF-1α/sima binds to HIF-1β/tgo forming the HIF1 heterodimer, which translocates to the nucleus and controls the expression of hypoxia-inducible genes involved in the hypoxic response, metabolism, cell proliferation, cell survival and angiogenesis (Manalo *et al.*, 2005; Kaelin & Ratcliffe, 2008). We observed that *fatiga* is down-regulated in the tumor, which is in line with previous studies showing that activation of HIF-1α is mainly mediated by reduced expression of *PHD/fga* (Semenza, 2010).

Besides the lack of oxygen, other factor that plays a critical role in HIF-1α/sima stabilization is the availability of Fe(II), necessary for the hydroxylation step. Moreover, metabolites such as fumarate or succinate can lead to the inactivation of PDH/fatiga and the subsequent stabilization of HIF-1α/sima (Kaelin & Ratcliffe, 2008). In addition, HIF-1α/sima can be induced under aerobiosis by cytokines, growth factors, energy-metabolism intermediates such as pyruvate, lactate and oxaloacetate, reactive oxygen species and nitric oxide.

Inactivation of PHD enzymes may be promoted by ROS due to oxidation of the central Fe(II) to Fe(III), especially if the antioxidant capacity of the cell is low. In *Drosophila,* NO promotes the stabilization of Sima by inhibitng protein hydroxylation of HIF-1α/sima (Hagen *et al.*, 2003; Callier & Nijhout, 2014).-

As exposed above, Notch-PI3K/Akt tumors display high levels of ROS and Nos. Therefore, we examined the role of HIF-1α/sima in this particular tumorigenic context. As expected, we observed sima protein is stabilized in tumors compared to wild type. Hemocytes also express elevated levels of sima protein in both wild type and tumors (data not shown), explained by its physiological role in hematopoietic development, as already published (Mukherjee *et al.*, 2011). Moreover, knockdown of *sima* with RNA

interference led to a reduction in tumor incidence although not completely stalled, as happens in other tumors (Sutphin *et al.*, 2004).

Lactate dehydrogenase (*Ldh*) upregulation and the subsequent increase in Ldh enzymatic activity is a hallmark of aerobic glycolysis. Sima is one of the key inducers of Ldh expression in tumors (Dang & Semenza, 1999). Therefore, as expected, expression levels of *Ldh* are increased in tumor eye discs. Moreover, sima induces the expression of some glycolytic enzymes in several tumors (Semenza, 2012). Here we observed that *Pgi* and *Pfk* were upregulated, but strikingly the other glycolytic enzymes remained unchanged. Furthermore, contrary to expectations, inhibition or overexpression of *Ldh* did not affect tumor incidence, indicating that the tumorigenic process is Ldh-independent.

These results reflect the complexity of the metabolic landscape of tumors under *in vivo* conditions. While cancer cells mostly rely on glucose and glutamine for survival and growth *in vitro,* tumors display a high cell and temporal heterogeneity accompanied by different metabolic phenotypes even in a single tumor mass (Gatenby *et al.*, 2007; Migneco *et al.*, 2010; Ertel *et al.*, 2012; Lee & Yoon, 2015). Therefore, it is overly reductive to assume that 'the Warburg effect' is a general feature of all cancer cells (Fu *et al.*, 2017).

Pten loss drives a whole-body metabolic shift towards Glycolysis and the Pentose Phosphate Pathway

In cancer, interactions not only occur within cancer-containing tissues and the microenvironment, but also within normal cells in distant tissues, with or without metastases. Consequently, having a cancer affects other tissues/organs of the host in manners that are not fully understood and, whereas metabolic reprogramming of cancer cells and their microenvironment has been widely studied over the last decades, our knowledge about how malignant cells communicate with distant tissues and the subsequent impact in the host metabolism is still very limited.

Here we evaluated the carbohydrate metabolism of Notch-PI3K/Akt tumors since it is commonly altered in cancer cells. We have demonstrated that Notch-PI3K/Akt-driven tumors rely on glucose catabolism. However, we provide evidence that cancer also causes alterations in whole-body metabolism. Particularly, the loss of Pten in eye disc tumors reprograms the host metabolism towards upregulation of glycolysis and the pentose phosphate pathway.

It has been previously published that the "greedy" behavior of cancer cells results in the deprivation of vital metabolites for the surrounding cells, such as the immune cells, which must compete for nutrients also by reprogramming their metabolism to robust aerobic glycolysis and glutaminolysis (Wang *et al.*, 2014). In *Drosophila*, the link between metabolism and immunity is integrated in the fat body, since this organ not only responds to dietary signals, but also is involved in the immune response. We observed that the fat body is the main source of the metabolic changes that occur in the whole animal. This tissue exhibits dramatically high levels of glycolytic and PPP enzymes in tumor-bearing larvae and also a high consumption of intermediates of both pathways. Indeed, systemic glucose levels are low in tumor-bearing larvae, indicating that is being highly consumed. Our results reveal that the presence of the tumor in the eye imaginal disc tumors is remotely accelerating the host energy/glucose metabolism, particularly in the fat body. This may reflect an attempt of the immune cells from the fat body to boost immune defense, since it has a high energetic cost (Lazzaro & Galac, 2006).

Pten-deficient tumors reprogram whole-body metabolism and inflammation via the tryptophan-kynurenine pathway

The mechanisms by which cancer cells negative influence the host metabolism are largely unknown. We performed large-scale and tissue-specific metabolomics to better characterize the systemic metabolic changes that occur in tumor-bearing larvae, further revealing major alterations in the tryptophan-kynurenine pathway brought about by the *Pten* deficiency.

This pathway is the main route for tryptophan catabolism and the starting point for the synthesis of NAD(H) in mammals and, in *Drosophila,* is implicated in eye color pigmentation and brain plasticity (Tearle, 1991; Savvateeva *et al.*, 2000). The KP has received greater attention in recent years due to its important role in inflammation, immunomodulation and central nervous system disorders. In agreement with this, the fruit fly has provided a useful model for studies linking the KP with the modulation of neurodegeneration, memory and courtship (Campesan *et al.*, 2011; Campesan *et al.*, 2012).

Several kynurenine metabolites are neuroactive; 3-hydroxykynurenine (3-HK), and quinolinic acid (QA) are neurotoxic via generation of free radicals and oxidative stress (Okuda *et al.*, 1996; Okuda *et al.*, 1998). Besides this, QA induces exocitotoxicity by activation of N-methyl-D-aspartate (NMDA) receptors (Stone,& Perkins, 1981; Schwarcz *et al.*, 1983) and induces the production of proinflammatory mediators which potentiates the inflammatory response (Guillemin *et al.*, 2003). Conversely, kynurenic acid (KA) is neuroprotective through its antioxidant properties, antagonism of both the α7 nicotinic acetylcholine receptor and the NMDA receptor (Foster *et al.*, 1984; Goda *et al.*, 1999; Lugo-Huitrón *et al.*, 2011) and suppression of several inflammatory pathways (Wirthgen *et al.*, 2017). Levels of these metabolites are regulated at two critical points: (*i*) the initial, rate-limiting conversion of Trp into *N*-formylkynurenine by either TDO or IDO enzymes and (*ii*) the synthesis of 3-HK from kynurenine by KMO (Amaral *et al.*, 2013). *Drosophila* has a single TDO encoded by the *vermilion* gene (Searles & Voelker, 1986; Walker *et al.* 1986) and a KMO homologue encoded by the gene *cinnabar* (Warren *et al.*, 1996).

Our metabolomics analysis in tumor-bearing larvae revealed a dramatic increase in the levels of 3-HK, especially in the fat body. This might explain the hyperactivation of the PPP in this organ as an attempt to counteract the high oxidative stress state of the animal by generating NADPH, which has an antioxidant function (Wood *et al.*, 2003). Accordingly, treatment with NADPH tetrasodium salt strongly reduces tumor incidence (Villegas *et al.*, 2018). Although 3-HK is a natural breakdown product of tryptophan, this metabolite is oxidized easily under physiological conditions, producing reactive oxygen species (Okuda *et al.*, 1996, Okuda *et al.*, 1998; Wei *et al.*, 2000) and when accumulated in cells it leads to apoptosis (Wei *et al.*, 2000). Insects maintain physiological conditions by preventing the accumulation of this reactive compound by converting 3-HK into xanthurenic acid (Han *et al.*, 2007). Therefore, as expected, we found that circulating levels of xanthurenic acid were also increased, acting as a protective response to dampen the toxic levels of 3-HK.

In humans, xanthurenic acid has a diabetogenic effect and high plasma levels are associated with insulin resistance **(**Reginaldo *et al.,* 2015), which is characterized by an increase in insulin production and secretion associated with an increased glycemia (Pasco & Leopold, 2012). Contrary to expectations, the expression of *InR* and *4EBP* was markedly down-regulated in the fat body from tumor-bearing larvae. This indicates that fat body cells have an increased capacity to activate the signaling cascade downstream of InR and have therefore become insulin sensitive. This condition allows the fat body cells to use glucose more effectively, reducing glucose levels. Consistent with these results, the amount of systemic glucose is lower in tumor-bearing larvae. However, expression levels of *4E-BP* are higher in the whole larva, suggesting that the fat body might be insulin sensitive, whereas insulin signaling is reduced at systemic levels. It remains to be established directly whether this systemic insulin resistance is a consequence of the elevated XanA levels.

As expected, the expression levels of TDO/*v* and KMO/*cn*, the KP key enzymes, are increased in the fat body of Notch-PI3K/Akt larvae, albeit there is a mild but significant up-regulation of KMO/*cn* in the eye tumors. In mammals, the overproduction of TDO and/or IDO enzymes has long been postulated to lead to diminished availability of tryptophan (Badawy, 2017). Consequently, the huge

increment in the activity of the pathway in the fat body correlates with the elevated levels of kynurenine metabolites and the systemic tryptophan depletion observed.

It is important to notice that kynurenine can be metabolized along two distinct routes competing for it as a substrate, one produces kynurenic acid and the other NAD+. Interestingly, kynurenic acid remained unchanged, which indicates that the pathway is shifted towards the production of 3-HK, QA and finally NAD+.

Our large-scale analysis in tumor-bearing larvae also confirms the presence of tumor-derived inflammatory factors identified by Villegas *et al.* in the host. We observed lower levels of arginine, indicating that this aminoacid is being used to produce nitric oxide. In addition, our study also revealed low levels of arachidonic acid, and the subsequent increase in the leukotriene LTB4 (Suppl. Fig. 4), together with high levels of histamine and acetylhistamine (Jutel *et al.*, 2009), further indicating a systemic inflammation (Suppl. Table 1). Under inflammatory conditions, activated immune cells need a lot of energy and hence large amounts of NAD+ (Moffett & Namboodiri, 2003). Thus, it is reasonable to expect an increased metabolism down the QA branch of the KP. Accordingly, we found unaltered levels of NAD+, meaning that is not accumulated and therefore is being consumed. The major precursor for NAD+ is the compound niacin, also known as nicotinic acid/nicotinamide or vitamin B3 (Murray, 2003; Bogan & Brenner, 2008) which can be either obtained by the diet or synthesized *de novo* through the kynurenine pathway (Fukuwatari & Shibata, 2013; Bogan & Brenner, 2008). The systemic depletion of niacin found in tumor-bearing larvae suggests that this metabolite is being used for the generation of NAD+, but also might reflect a dietary deficiency of this essential vitamin (Suppl. Table 1).

The significant upregulation of tryptophan metabolites is of particular importance in the context of cancer and inflammation, since the different tryptophan catabolic pathways have become one of the most critical checkpoints in immunity (Grohmann & Bronte, 2010; Murray, 2016; Grohmann *et al.* 2017). In humans and mice, both gene and protein expression of TDO and IDO are well-documented in cancer and these enzymes are known to shape the immunosuppressive environment (Badawy *et al.,* 2016) and tumor tolerance (Muller *et al.*, 2005; Munn & Mellor, 2007). TDO is constitutively expressed in some type of cancers, being able to suppress antitumor

immune responses (Platten *et al.*, 2012). In turn, there is emerging evidence that excessive KMO activity stimulates tumor growth (Jin *et al.*, 2015) and KMO overexpression is a marker of poor prognosis (Chiu *et al.*, 2019). Similarly, TDO/*v* and KMO/*cn* are up-regulated in Notch-PI3K/Akt/Pten tumors and tumor-specific knockdown of these KP enzymes was clearly antineoplastic. However, halving gene dosage of TDO/*v* or KMO/*cn* using endogenous mutations that affect the whole animal resulted in a more drastic reduction of tumor incidence. In line with these findings, diet supplementation with 3-HK or in tumor-bearing larvae lacking KMO/*cn* rescued the tumor phenotype. Notably, XanA supplementation was lethal to *ey>Dl>Pten*-RNAi hosts due to vehicle toxicity (Suppl. Fig. 5).

Furthermore, tumor-specific downregulation of the tryptophan transporters *white* and *scarlet* reduced tumor incidence, unveiling the need for tryptophan and fat body-derived kynurenine metabolites in Notch-PI3K/Akt cancer cells to grow. Notably, some kynurenine metabolites activate IDO via AhR, which dampens the immune response to prevent excessive inflammation and autoimmunity. Nevertheless, the downside is that IDO activation leads to an immunosuppressive state and the immune escape of tumor cells in the context of human cancer (Litzenburger *et al.*, 2014). Here we downregulated AhR/*spineless* using both tumor-specific RNAi and endogenous mutations, resulting in a reduced tumor incidence. These results support the notion that the KP has a dual role in Pten-driven tumorigenesis, since the hyperactivation of the pathway promotes tumor growth not only by up-regulating the TDO/*v* and KMO/*cn* in the tumor tissue, but also by rewiring the host tryptophan-kynurenine metabolism, towards aberrant production of inflammatory/immunosuppressive metabolites, such as 3-HK.

Recent studies have highlighted the therapeutic potential of inhibiting the critical KP regulatory enzymes. Constitutive IDO expression has been reported in most human tumors and systemic pharmacological inhibition of IDO has been shown to reverse immune resistance mechanisms in several animal models (Uyttenhove *et al.*, 2003). In fact, IDO inhibitors (Prendergast *et al.*, 2017) have entered clinical trials with the aim to dampen tumour immune escape (Sheridan *et al.,* 2015). In addition, overactivation of liver-specific TDO in cancer (Cheong & Sun, 2018) suggests that this enzyme also contributes to drive immune escape. Consistently, systemic TDO inhibition restored tumor rejection in a preclinical model (Opitz *et al.,* 2011; Pilotte *et al.*, 2012). KMO is

also considered to be an important pharmaceutical target for the development of drugs for neurodegenerative diseases (Pellicciari *et al.* 2003; Samadi *et al.*, 2005; Moroni *et al.*, 2005). Much evidence indicates that the efficacy of KMO inhibition arises from normalizing the imbalance between neurotoxic/pro-inflammatory 3-HK/QA and neuroprotective/anti-inflammatory KA, thereby enhancing anti-tumor immune function (Adams *et al.*, 2012).

Hence, we administered a TDO/IDO/vermilion and KMO/cinnabar drug inhibitors to tumor-bearing hosts. Whereas TDO/v inhibitor did not have an effect at the tested doses, treatment with the KMO inhibitor is robustly protective in this cancer model. These data provide proof-of-concept evidence that KMO inhibitors block tumorigenesis by dampening the tryptophan-kynurenine metabolism not only in tumor cells, but also in the whole organism. Consequently, our work strongly supports targeting the critical steps of the kynurenine pathway as a potential treatment strategy for Pten-deficient cancers.

Finally, we demonstrated that NOS enzyme overexpression is able to trigger TDO/IDO/*vermilion* gene activation in the fat body (Suppl. Fig 7). This result might represet indirect evidence that excessive nitric oxide produced by the tumor (Villegas *et al.*, 2018) could potentially induce the activation of the KP in a distal organ, the fat body. Such interesting and striking results demonstrate for the first time that cancer cells are not only able to reprogram their own metabolism or the microenvironment, but also can produce signals that impact in distal organs and shift the host metabolism for profit-making purposes.

Notch-PI3K/Akt-driven tumors impact in brain serotonin synthesis and tryptophan degradation by gut microbiota

The KP contributes for the great majority of tryptophan degradation. Nevertheless, this essential amino acid can be also converted into serotonin (also known as 5-hydroxytryptamine, 5-HT) or degraded by gut microbiota through the indole pathway. Serotonin is an important neurotransmitter that modulates numerous neuropsychological processes including mood, reward, anger, anxiety and cognition (Canli & Lesch, 2007). In *Drosophila* and other insects, modulates circadian rhythm (Yuan *et al.,* 2005), feeding (Novak & Rowley 1994; Novak *et al.,* 1995), locomotion (Kamyshev *et al.,* 1983), reproduction (Barreteau *et al.,* 1991) and heart rate (Dasari & Cooper, 2006). Tryptophan hydroxylase (Trh) is the enzyme that functions as the first and rate-limiting step in the synthesis of serotonin, since it converts Trp to 5-hydroxytryptophan (5-HTP), the immediate precursor of serotonin. We previously reported that tumor-specific silencing of the serotonin receptor 5HT1B reduces Notch-PI3K/Akt tumors (Villegas *et al.*, 2018). In line with these results, halving the amount of serotonin production by inhibiting the Trh enzyme using a pBacTRH null mutation (Neckameyer *et al.*, 2007) yielded reduced tumor incidence, further highlighting that these tumors rely on serotonin through an unknown mechanism.

Earlier works have demonstrated that Trp breakdown along the KP leads to decreased availability of Trp for cerebral serotonin synthesis (Badawy & Evans, 1983). Serotonin is implicated in the pathophysiology of depression, a common comorbidity in nearly 20% of cancer patients (Mitchell *et al.*, 2011; Ng *et al.*, 2011; Linden *et al.*, 2012). The development of depression in cancer patients is not only due to emotional distress, since immune activation and the subsequent enchancement of Trp breakdown and has been proposed to play an important role (Kurz *et al.*, 2011; Barreto *et al.*, 2018; Sforzini *et al.*, 2019). In addition, it has been demonstrated that depressive- like behavior related to immune activation is associated with an upregulation of IDO (O'Connor *et al.*, 2009; Norden *et al.*, 2015; Doolin *et al.*, 2018) as well as KMO enzymes in several animal models (Savitz *et al.*, 2015; Meier *et al.*, 2016; Parrot *et al.*, 2016). However, contrary to our expectations, brain serotonin synthesis was increased in tumor-bearing larvae, albeit the diminished Trp availability. Furthermore, systemic levels of the serotonin precursor 5-HTP were significantly higher in these animals.

All together, these interesting results support the notion that Notch-PI3K/Akt-driven tumors can impact brain serotonin production either direct or indirectly and benefit from it. It remains to be studied the specific mechanism by which serotonin is implicated in the tumorigenic process, how the tumor bypasses the Trp depletion associated to an enhanced breakdown towards KP to synthesize more serotonin in the brain and the behavioral outcome of these animals, such as a depression-like phenotype.

In addition, tryptophan from degradation of dietary proteins is also converted into various indole metabolites by the gut microbiota. Growing evidence suggests that these catabolites play an important role in host-microbial cross-talk, and may contribute to intestinal and systemic homeostasis. In addition, indoles produced by commensal bacteria have been found to improve the health of a range of different animal models including *C. elegans, Drosophila melanogaster* and mice via ligand activation of the aryl hydrocarbon receptor (AhR), which is found in intestinal immune cells (Whitehead *et al.*, 2008; Zelante *et al.*, 2013; Cheng *et al.*, 2015; Hubbard *et al.*, 2015; Sonowal *et al.*, 2017). Several studies have underlined that indole-induced AhR activation may contribute to mucosal homeostasis by increasing expression of genes involved in maintenance of intestinal epithelial barrier function (Bansal *et al.*, 2010; Shimada *et al.*, 2013). Microbial tryptophan metabolites affect the immune system in the gut, but also the host physiology, since they can be absorbed in the gut and enter the bloodstream (Wikoff *et al.*, 2009). A recent study found that indoleacrylic acid (IA) had anti-inflammatory and antioxidative effects in human PBMCs. Similarly, indoleacetic acid (IAA) attenuated pro-inflammatory responses in murine macrophage and hepatocyte cultures in an AhR-dependent way (Krishnan *et al.*, 2018), suggesting that microbial indole catabolites could influence inflammatory responses in the liver as well. This raises the intriguing possibility that gut microbiota-derived tryptophan catabolites may reduce frailty and improve health also in humans. The concept of frailty is of particular importance in patients with cancer and is defined as “a state of extreme vulnerability to stressors that leads to adverse health outcomes” (Ethun *et al.*, 2017).

Our metabolomics analysis revealed reduced levels of IA and IAA in tumor-bearing larvae, probably as a consequence of high Trp degradation by other pathways or by gut dysbiosis. Here we supplemented the diet with IA at different doses. However, since the vehicle is DMSO, which has a high toxicity at these doses, it remains

unresolved if IA supplementation could potentially benefit tumor hosts at the tested doses. Thus, although targeting the gut microbial metabolism is an area that still remains to be explored, it holds the promise for developing alternative strategies to prevent and treat cancer. Furthermore, our findings confirm for the first time that tumors lacking Pten not only have metabolic alterations in a cell autonomous manner, but also communicate with distal tissues to induce a multi-organ metabolic reprogramming.

Dietary tryptophan supplementation is sufficient to prevent tumor and overcome lethality associated with Pten loss under caloric restriction

Certain dietary modulations impact host metabolism and cancer outcomes. Previous studies have shown that modulating the amino acid composition of the diet can influence cancer growth (Maddocks *et al.*, 2013) and the immune response through complex mechanisms. It is described that tumor cells compete with host cells for essential nutrients such as glucose, lipids and amino acids (Gupta *et al.*, 2017). However, how the tumor communicates its nutritional requirements to the host and how the host influences tumor growth by bidirectional crosstalk remains an open question. Here we have observed that Trp catabolism is shifted towards overproduction of kynurenine metabolites and serotonin synthesis, which contributes to tumorigenesis and consequently results in a systemic Trp depletion. Therefore, we added a Trp supplement to the standard food, which was sufficient to drastically reduce the tumor phenotype. This result can be explained because the excess of Trp inhibits the kynurenine pathway through reverse binding sequence (Badawy, 2017) and also because more Trp might be available for the gut microbiota to produce healthy metabolites.

On the other hand, dietary restriction delays the incidence of certain cancers, whereas hypercaloric diets can increase tumorigenesis via the activation of the PI3K/AKT pathway (Baumann *et al.,* 1939; Tannenbaum & Silverstone, 1953; Hirabayasi *et al.*, 2013). The high prevalence of metabolic alterations in cancer cells and the ability of diet starvation to modulate host immunity (Kritchevsky, 2001; Lien & Vander Heiden, 2019) has prompted clinical investigations on caloric restriction as an intervention to reduce cancer incidence in part by modulation/inhibition of the IGF-1/PI3K/AKT signalling (Lu *et al.,* 2019).

Particularly, amino acid reduction enhances the proliferative potential of tumor cells with overactive PI3K/Akt pathway, which in turn has a detrimental effect in the whole animal through an unknown non-autonomous mechanism (Nowak *et al.*, 2013). Here we corroborate this idea by rearing larvae with Notch-PI3K/Akt/Pten tumors in a low-protein diet. In addition, to rescue the host lethality associated to Pten inactivation, we supplemented the low-protein food with tryptophan, further revealing that this

amino-acid is essential to overcome caloric restriction resistance. Moreover, this intervention also dramatically reduced the tumor phenotype, inducing wild type-like eyes. It has been previously described that partial starvation produces higher amounts of vermilion enzyme (Beadle *et al*., 1938). We hypothesize that dietary restriction of *Pten* loss-bearing hosts with already high levels of KP might induce a toxic level of kynurenine metabolites, which may explain the death of the whole organism. This hypothesis awaits more experimental evidence and is part of our future perspectives for continuing research.

These results have particular relevance, since malnutrition is a common accompaniment of cancer patients, and therefore it is important to determine which dietary interventions can constitute an improvement to the patient's quality of life.

2. Conclusions

Section 1. PI3K/Akt cooperates with oncogenic Notch by inducing Nitric Oxide-dependent inflammation

1. A drug screen selectively targeting Notch-PI3K/Akt cooperative oncogenesis identified 90 compounds that strongly suppressed (61) or enhanced (29) tumorigenesis.
2. Tumor-specific RNAi downregulation of candidate target genes mimicked the action of the corresponding compounds, thus validating the drug screen results.
3. The drug screen revealed numerous anti-inflammatory agents targeting the NO/NOS and LOX signaling pathways.
4. PI3K/Akt fuels Notch-driven tumorigenesis through NOS. The top hit compound of the screen, the drug BW B70C, dampens a tumor formation process orchestrated by inflammatory NOS.
5. LOX pathway inhibition blocks Notch-PI3K/Akt-driven tumorigenesis.
6. Protumorigenic immune inflammation underlies Notch- PI3K/Akt cooperation.
7. Genetic depletion of prophenoloxidase in immune cells fuels Notch-mediated tumorigenesis.
8. The antitumor effect of BW B70C was validated in human T Cell Acute Lymphoblastic Leukemia cells that depend on NOTCH1 and PI3K/AKT signaling via suppression of the aberrant eNOS.

Section 2. PI3K/Akt/Pten-induced mitochondrial dysfunction cooperates with Notch in tumorigenesis

1. Notch-PI3K/Akt combination triggers downstream phosphorylation of ATP synthase β subunit.
2. ATP synthase deficiency results in mitochondrial dysfunction and generation of ROS, which cooperates with Notch to promote tumorigenesis. The amount of ROS is increased in human T-ALL cells from patients and BW B70C treatment induces toxic levels of ROS.

3. Tumor-specific hyperactivation of the ROS-scavenging system avoids tumor formation.
4. Notch-PI3K/AKT-induced JNK signaling triggers apoptosis as an anti-tumor response.
5. Mitochondria induce apoptosis through cytochrome *c* oxidase hyperactivation in Notch-PI3K/Akt tumors.
6. Notch-PI3K/Akt tumors rely on enhanced glucose uptake.
7. Hipoxia inducible factor 1α (HIF1α) is stabilized in Notch-PI3K/Akt tumors, but there are not major changes in glycolysis or PPP.

Section 3. Notch-PI3K/Akt/Pten tumors reprogram whole-body metabolism via the Tryptophan-Kynurenine pathway

1. Dietary restriction is detrimental to host bearing Pten-deficient tumors and tryptophan diet supplementation rescues tumorigenesis and lethality.
2. Loss of *Pten* drives whole-body metabolic shift towards upregulation of Glycolysis and Pentose Phosphate Pathway. The fat body is the origin of major metabolic changes observed in tumor-bearing larvae.
3. The tryptophan-kynurenine pathway is increased towards production of proinflammatory and toxic 3-HK in tumor-bearing larvae.
4. Overexpression of Kynurenine 3-monooxygenase (KMO/*cinnabar*) is the main contributor to *Pten* tumorigenesis. Genetic inhibition of the kynurenine pathway suppresses tumorigenesis. Pharmacologic inhibition of KMO/cinnabar exerts an antineoplastic effect.
5. Tumor-specific inhibition of Trp/K cellular uptake reduces tumor incidence, indicating that tryptophan and/or fat body-derived kynurenine metabolites are necessary for the Notch-PI3K/Akt cancer cells to grow.
6. High levels of kynurenine metabolites found in tumor-bearing hosts trigger an immunosuppressive effect through binding to AhR and the subsequent activation of TDO/IDO/vermilion, generating a loop that reinforces tumor cell immune escape.
7. Notch-PI3K/Akt-driven tumors trigger higher brain serotonin synthesis.
8. Notch-PI3K/Akt-driven tumors impact in tryptophan degradation by gut microbiota.

Conclusiones

Sección 1. PI3K/Akt coopera con Notch Oncogénico induciendo una inflamación dependiente de Óxido Nítrico.

1. Una prueba de detección de fármacos dirigida selectivamente a la oncogénesis cooperativa de Notch-PI3K/Akt identificó 90 compuestos que suprimieron fuertemente (61) o mejoraron (29) la tumorigénesis.
2. La regulación negativa específica de los genes diana candidatos en el tumor usando ARNi imitó la acción de los compuestos correspondientes, validando así los resultados del cribado de fármacos.
3. El cribado de fármacos reveló numerosos agentes antiinflamatorios dirigidos a las vías de señalización NO/NOS y LOX.
4. PI3K/Akt estimula e incrementa la tumorigénesis impulsada por Notch a través de NOS. El fármaco con más éxito del cribado, BW B70C, amortigua el proceso formación del tumor orquestado por NOS inflamatorio.
5. La inhibición de la vía de LOX bloquea la tumorigénesis impulsada por Notch-PI3K/Akt.
6. La inflamación inmunitaria protumorigénica subyace a la cooperación Notch-PI3K/Akt.
7. El bloqueo genético de la profenoloxidasa en las células inmunitarias estimula la tumorigénesis mediada por Notch.
8. El efecto antitumoral de BW B70C se validó en células humanas procedentes de leucemia linfoblástica aguda (T-ALL), que dependen de NOTCH1 y PI3K/AKT, mediante la supresión de la expresión aberrante de eNOS.

Sección 2. La disfunción mitocondrial inducida por PI3K /Akt/Pten coopera con Notch en tumorigénesis

1. La combinación Notch-PI3K/Akt desencadena la fosforilación de la subunidad β de la ATP sintasa.

2. La deficiencia de la ATP sintasa da como resultado una disfunción mitocondrial y la generación de ROS, que coopera con Notch para promover la tumorigénesis. La cantidad de

1. ROS es elevada en células T-ALL humanas de pacientes y el tratamiento con BW B70C induce niveles tóxicos de ROS.
2. La hiperactivación específica del sistema de eliminación de ROS en el disco de ojo evita la formación del tumor.
3. La señalización de JNK inducida por Notch-PI3K / AKT desencadena la apoptosis como respuesta antitumoral.
4. Las mitocondrias inducen la apoptosis a través de la hiperactivación de la enzima citocromo c oxidasa en tumores Notch-PI3K/Akt.
5. Los tumores Notch-PI3K/Akt dependen de una mayor captación de glucosa.
6. El factor inducible por hipoxia 1α (HIF1α) se estabiliza en tumores Notch-PI3K/Akt, pero no hay cambios importantes en la glucólisis o la vía de PPP.

Sección 3. Los tumores Notch-PI3K/Akt/Pten reprograman el metabolismo de todo el cuerpo a través de la vía triptófano-quinurenina

1. La restricción dietética es perjudicial para el hospedador portador de tumores deficientes en Pten y la suplementación con triptófano rescata la tumorigénesis y la letalidad.
2. La pérdida de Pten impulsa el cambio metabólico de todo el cuerpo hacia el aumento de las vías de glucólisis y pentosas fosfato. El cuerpo graso es el origen de la mayoría de los cambios metabólicos importantes observados en larvas portadoras de tumores.
3. La vía triptófano-quinurenina aumenta hacia la producción de 3-HK proinflamatorio, el cual es tóxico en larvas portadoras de tumores.
4. La sobreexpresión de quinurenina 3-monooxigenasa (KMO/cinnabar) es la principal contribuyente a la tumorigénesis de Pten. La inhibición genética de la vía quinurenina suprime la tumorigénesis. La inhibición farmacológica de KMO/cinnabar ejerce un efecto antineoplásico.
5. La inhibición tumoral específica de la captación celular de Trp/K reduce la incidencia de tumores, indicando que el triptófano y/o los metabolitos de

quinurenina derivados del cuerpo graso son necesarios para que crezcan las células cancerosas Notch-PI3K/Akt.

6. Los altos niveles de metabolitos de quinurenina encontrados en hospedadores con tumores desencadenan un efecto inmunosupresor mediante la unión a AhR y la activación posterior de TDO/IDO/vermilion, generando un bucle que refuerza el escape de las células tumorales de la respuesta inmunitaria.
7. Los tumores impulsados por Notch-PI3K/Akt desencadenan una mayor síntesis de serotonina cerebral.
8. Los tumores impulsados por Notch-PI3K/Akt impactan en la degradación del triptófano por parte de la microbiota intestinal.

3. Supplementary figures

Supplementary Figure 1. Antioxidant capacity is unaltered in Notch-PI3K/Akt tumors.

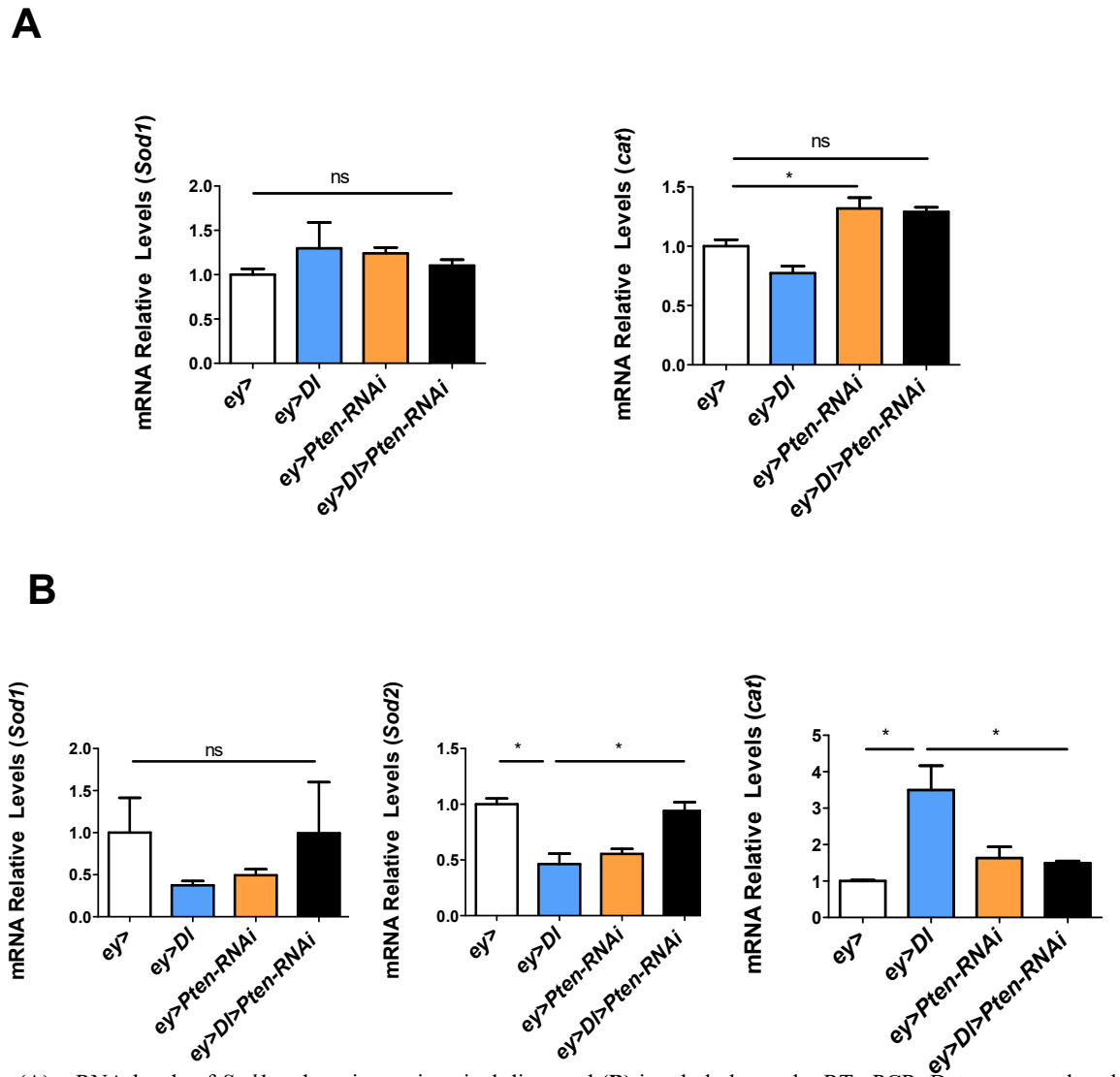

(A) mRNA levels of *Sod1* and *cat* in eye imaginal discs and **(B)** in whole larvae by RT-qPCR. Data were analyzed by a two-tailed unpaired t-test and values represent the mean ± SD of three independent repeates.$p<0.05$

Supplementary Figure 2. Glucose uptake in Notch or PI3K/Akt is not altered.

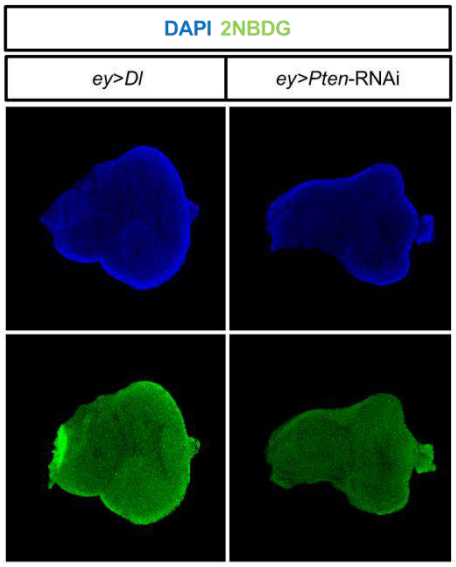

2NBDG assays to monitor glucose consumption *in vivo* in *ey>Dl* and *ey>Pten*-RNAi.

Supplementary Figure 3. KP metabolites production is increased in tumor-bearing hosts.

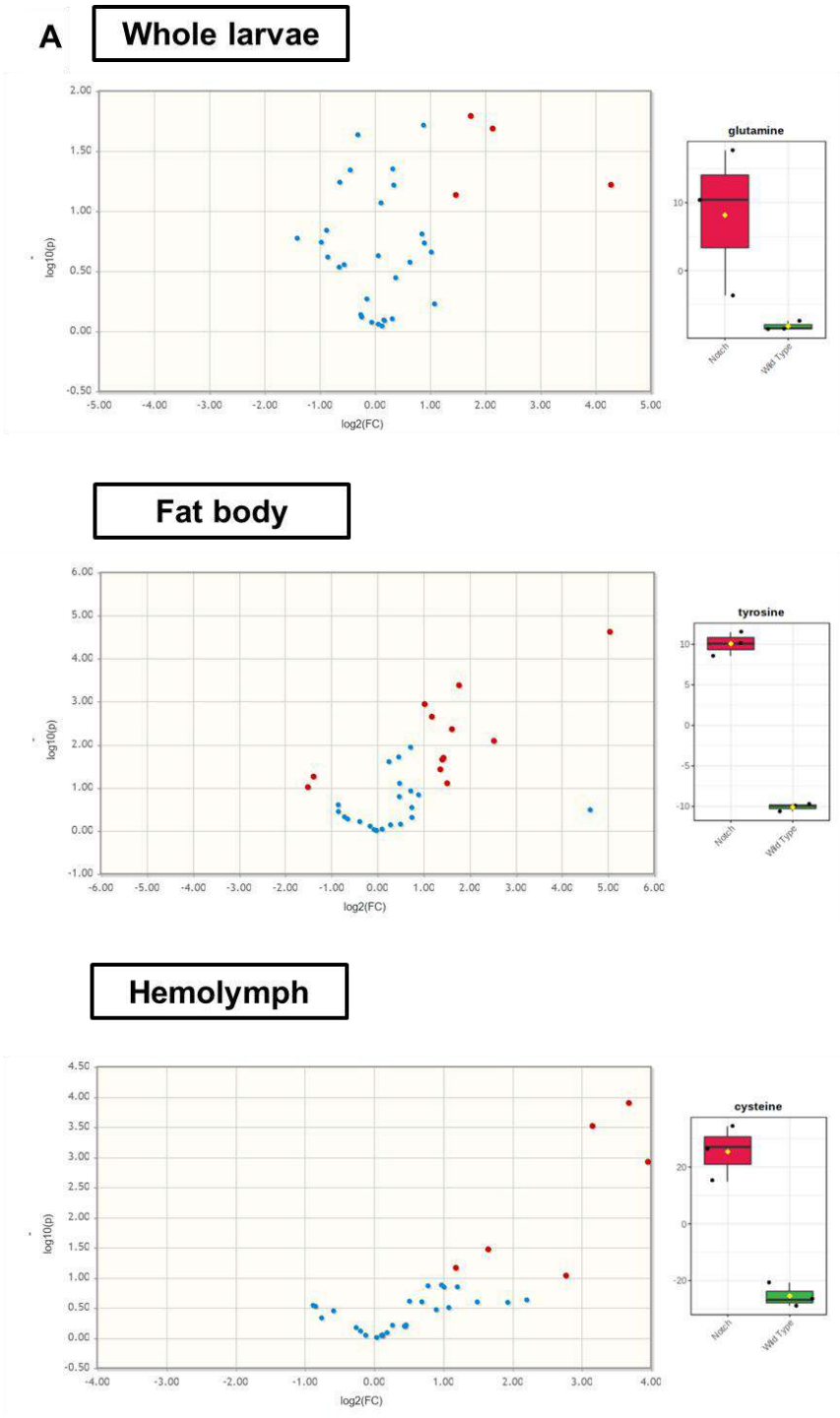

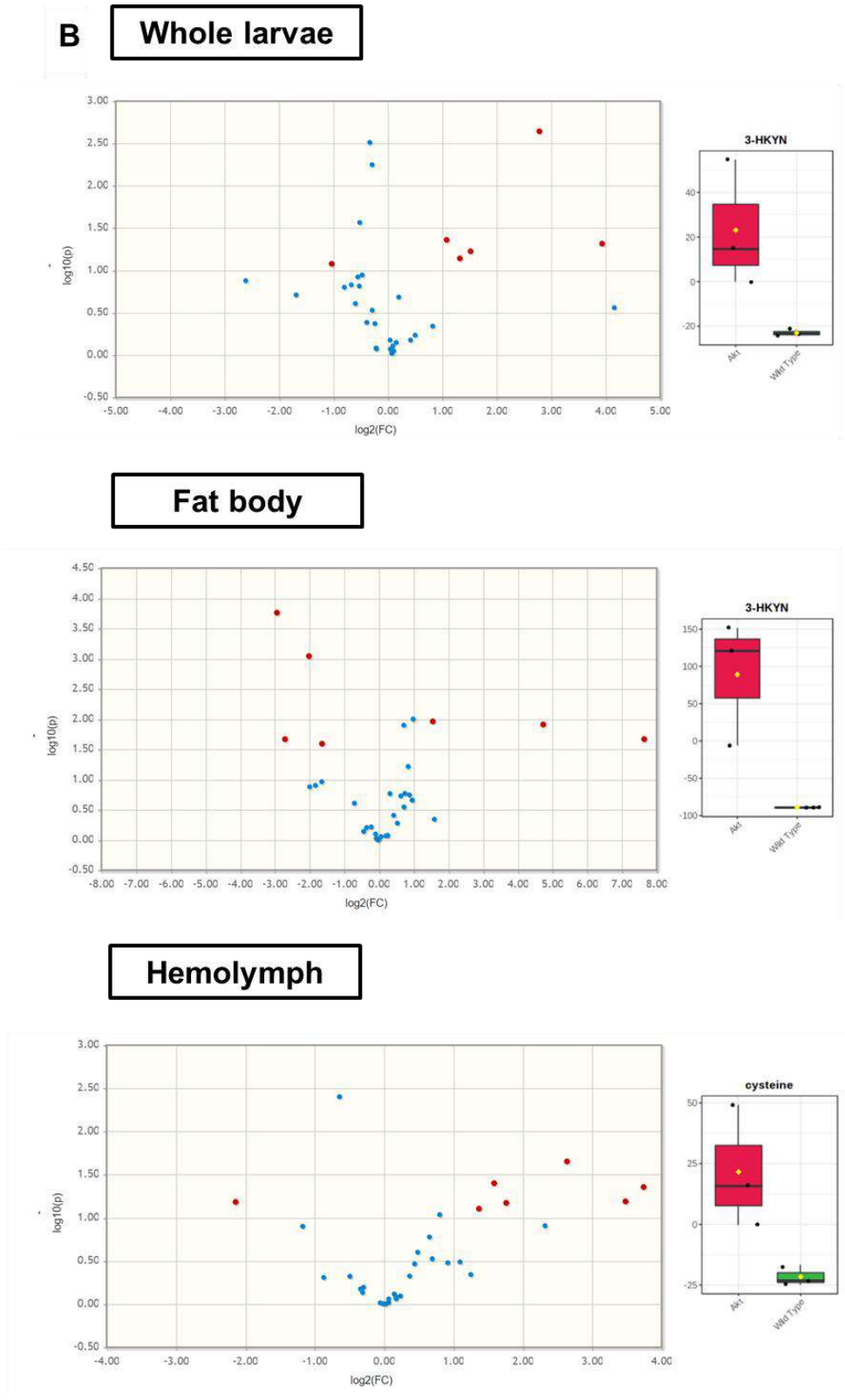

Volcano plot representing GC-MS quantification of metabolites identified between whole larvae, fat bodies and hemolymph of **(A)** *ey>Dl* versus wild type larvae and **(B)** *ey>Pten*-RNAi vs wild type larvae. Y-axis indicates −log10 (p value) while the horizontal axis indicates base 2 logarithmic value of mean metabolite abundance ratio (Notch^{+} or Pten^{-}/Wild type). The horizontal dashed line represents the Benjamini-Hochberg FDR threshold of significance assigned for subsequent analysis of metabolites. Compounds that show significant changes are indicated in red.

Supplementary table 1. Second analysis of of compounds identified by LC-MS with statistical significance ($p < 0.05$).

Tentative ID	Fold Change (Tumor/WT)	p. adjusted	Biological process
3-hydroxykynurenine	209,83	0,0042326	Tryptophan metabolite from kynurenine pathway
Xanthurenic acid	23,62	0,00085097	Tryptophan metabolite from kynurenine pathway
5-hydroxy-L-tryptophan	23,332	0,010531	Serotonin precursor
LTB4, PGA1	3,7364	0,064789	Leukotriene
Kynurenine	2,7426	0,07906	Tryptophan metabolite from kynurenine pathway
Glutamate	1,752	0,12844	Amino acid
Nicotinamide adenine dinucleotide NAD	1,4451	0,65876	Coenzyme. Redox power.
Kynurenic acid	1,3987	0,42589	Tryptophan metabolite from kynurenine pathway
Proline	0,9762	0,74501	Amino acid
Pyruvate	0,81252	0,040363	Glycolysis product
Arginine	0,76527	0,0060274	Amino acid
Arachidonic acid	0,76485	0,42996	Membrane phospholipid
Succinate	0,67571	0,18445	TCA metabolite
Sedoheptulose-7-P	0,66346	0,056621	PPP metabolite
Tryptophan	0,60538	0,013381	Amino acid
Alanine	0,51749	0,00027846	Amino acid
Nicotinic acid/niacin/vit b3/picolinic acid	0,38668	0,0057359	Vitamin, coenzyme
Glucose	0,20687	0,00077921	Carbohydrate, monosaccharide. Energy source
Indole acetic acid	0,11099	7,90E-05	Tryptophan metabolite from microbiota

In orange: metabolites more abundant in the tumor-bearing larvae (Fold Change > 1). In blue: metabolites less abundant in the tumor-bearing larvae (Fold Change < 1).

Supplementary Figure 4. Tumor-derived inflammatory factors in the host.

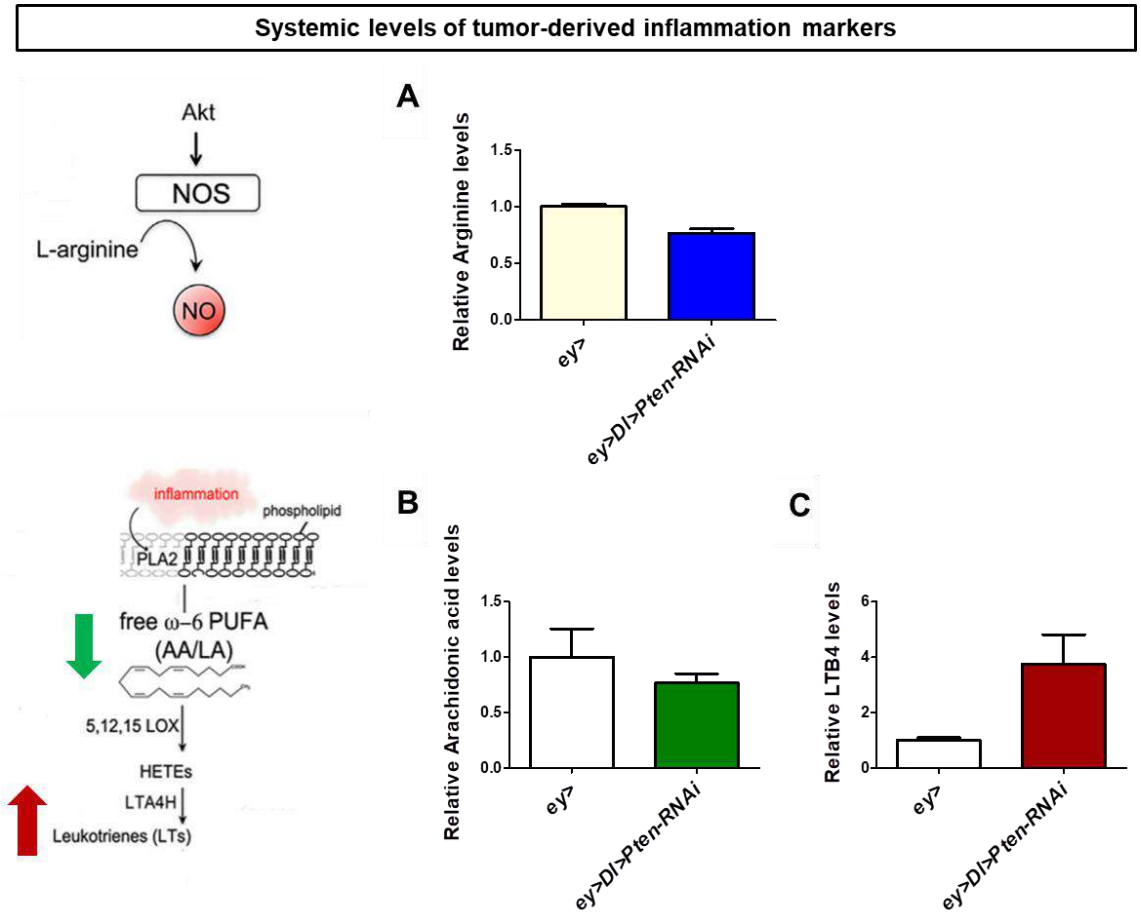

LC-MS quantification of **(A)** arginine, **(B)** arachidonic acid and LTB4 levels in Notch-PI3K/Akt/Pten tumor-bearing larvae versus wild type larvae.

Supplementary Figure 5. Diet supplementation with xanthurenic acid at different doses in tumor-bearing hosts.

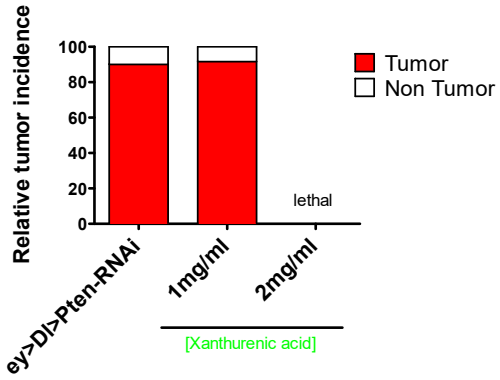

Supplementary figure 6. Pten-deficient tumor hosts are hypersensitive to dietary restriction.

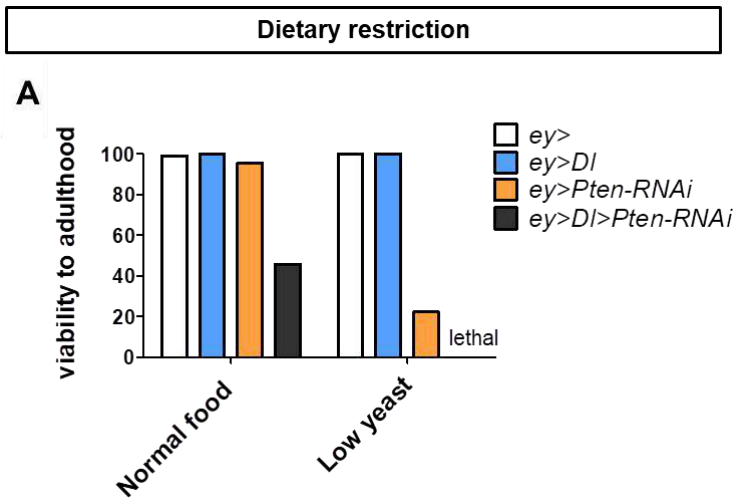

(A) Relative viability to adulthood in standard food (control) or in low yeast diet.

Supplementary figure 7. Nos induces the expression of TDO/vermilion.

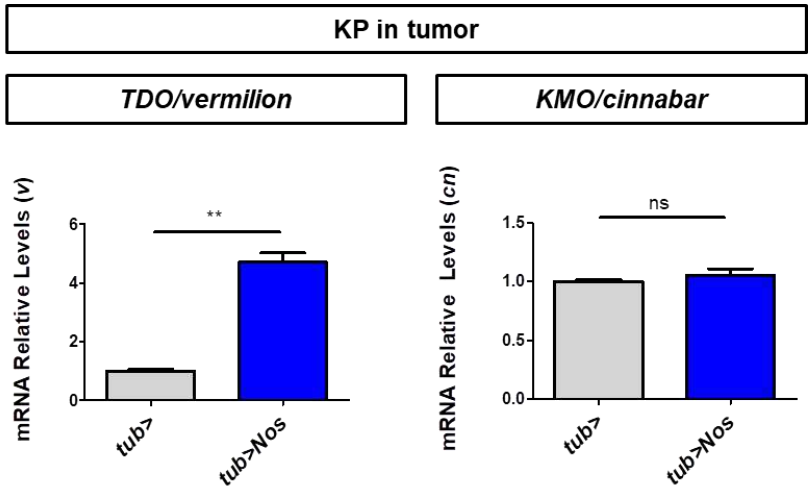

mRNA levels of *vermilion* and *cinnabar* in whole larvae by RT-qPCR. Data were analyzed by a two-tailed unpaired t-test and values represent the mean ± SD of three independent repeates.$p<0.05$

4. References

1. Adams, S., Braidy, N., Bessede, A., Brew, B. J., Grant, R., Teo, C., & Guillemin, G. J. (2012). The kynurenine pathway in brain tumor pathogenesis. Cancer research, 72(22), 5649–5657.
2. Ahn, H. M., Lee, K. S., Lee, D. S., & Yu, K. (2012). JNK/FOXO mediated PeroxiredoxinV expression regulates redox homeostasis during Drosophila melanogaster gut infection. Developmental and comparative immunology, 38(3), 466–473.
3. Ahn, Y.H., Yang, Y., Gibbons, D.L., Creighton, C.J., Yang, F., Wistuba, I.I., Lin, W., Thilaganathan, N., Alvarez, C.A., Roybal, J., Goldsmith, E.J., Tournier, C., Kurie, J.M. (2011). Map2k4 functions as a tumor suppressor in lung adenocarcinoma and inhibits tumor cell invasion by decreasing peroxisome proliferator-activated receptor γ2 expression. Mol Cell Biol. 31(21):4270-85
4. Altomare, D.A., Testa, J.R. (2005). Perturbations of the AKT signaling pathway in human cancer. Oncogene 24:7455–64.
5. Amaral, M., Outeiro, T. F., Scrutton, N. S., & Giorgini, F. (2013). The causative role and therapeutic potential of the kynurenine pathway in neurodegenerative disease. Journal of molecular medicine (Berlin, Germany), 91(6), 705–713.

   Andersson, E.R., and Lendahl, U. (2014). Therapeutic modulation of Notch signalling—are we there yet? Nat. Rev. Drug Discov. 13, 357–378.
6. Ashida, M. and Brey, P.T. (1997). Recent advances in research on the insect prophenoloxidase cascade. Molecular Mechanisms of Immune Response in Insects 135–172.
7. Artavanis-Tsakonas, S., Matsuno, K., & Fortini, M. E. (1995). Notch signaling. Science (New York, N.Y.), 268(5208), 225–232.
8. Asri, R.M., Salim, E., Nainu, F., Hori, A., Kuraishi, T. (2019). Sterile induction of innate immunity in Drosophila melanogaster. Frontiers In Bioscience, Landmark, 24, 1390-1400
9. Ayres, J.S. and Schneider, D.S. (2009). The role of anorexia in resistance and tolerance to infections in Drosophila. PLoS Biol 7, e1000150

10. Badawy A. A. (2017). Tryptophan availability for kynurenine pathway metabolism across the life span: Control mechanisms and focus on aging, exercise, diet and nutritional supplements. Neuropharmacology, 112(Pt B), 248–263.
11. Badawy, A.A. (2002). Tryptophan metabolism in alcoholism. Nutr Res Rev. 1:123–152.
12. Badawy, A.A., Namboodiri, A. M., & Moffett, J. R. (2016). The end of the road for the tryptophan depletion concept in pregnancy and infection. Clinical science, 130(15), 1327–1333.
13. Badawy, A.A. (2017) Kynurenine Pathway of Tryptophan Metabolism: Regulatory and Functional Aspects. International Journal of Tryptophan Research. 10: 1–20
14. Badawy, A.A., Evans, M. (1983). Opposite effects of chronic administration and subsequent withdrawal of drugs of dependence on the metabolism sand disposition of endogenous and exogenous tryptophan in the rat. Alcohol Alcohol.18:369–382
15. Balkwill, F. and Mantovani, A. (2001). Inflammation and cancer: back to Virchow? Lancet 357, 539–545
16. Bansal, T., Alaniz, R. C., Wood, T. K., & Jayaraman, A. (2010). The bacterial signal indole increases epithelial-cell tight-junction resistance and attenuates indicators of inflammation. Proceedings of the National Academy of Sciences of the United States of America, 107(1), 228–233.
17. Baron, J. A. and Sandler, R. S. (2000). Nonsteroidal anti-inflammatory drugs and cancer prevention. Annu. Rev. Med. 51, 511–523
18. Barreteau, H., Perrière, C., Brousse-Gaury, P., Gayral, P., Jacquot, C., & Goudey-Perrière, F. (1991). Indolamines in the cockroach Blaberus craniifer Burm nervous system--I Fed and crowded young females. Comparative biochemistry and physiology. Comparative pharmacology and toxicology, 99(3), 567–571.
19. Barreto, F.S., Chaves Filho, A.J., de Araujo, M., de Moraes, M.O., de Moraes, M.E., Maes, M, (2018) Tryptophan catabolites along the indoleamine 2,3-dioxygenase pathway as a biological link between depression and cancer. Behav Pharmacol. 29:165–80.
20. Baumann, C.A., Jacobi, H.P. and Rusch, H.P (1939). The effect of diet on experimental tumor production. Am. J. Hygiene. 30: 1-6. 3.
21. Beadle, G. W., Tatum, E.L. & Clancy, C. W. (1938). Food Level in Relation to Rate of Development and Eye Pigmentation in Drosophila Melanogaster. Biological Bulletin, Vol. 75, No. 3, pp. 447-462

22. Bender, D.A. (1983). Biochemistry of tryptophan in health and disease. Mol Aspects Med.6:1–97.
23. Bergantinos, C., Corominas, M., Serras, .F (2010) Cell death-induced regeneration in wing imaginal discs requires JNK signalling. Development 137: 1169–1179
24. Bertolin, A. P., Katz, M. J., Yano, M., Pozzi, B., Acevedo, J. M., Blanco-Obregón, D., Gándara, L., Sorianello, E., Kanda, H., Okano, H., Srebrow, A., & Wappner, P. (2016). Musashi mediates translational repression of the Drosophila hypoxia inducible factor. Nucleic acids research, 44(16), 7555–7567.
25. Bijur, G.N. and Jope. R.S. (2003). Rapid accumulation of Akt in mitochondria following phosphatidylinositol 3-kinase activation. J. Neurochem., 87: 1427-1435
26. Bilder, D., Li, M. and Perrimon, N. (2000). Cooperative regulation of cell polarity and growth by Drosophila tumor suppressors. Science 289, 113-116.
27. Bjordal, M., Arquier, N., Kniazeff, J., Pin, J.P., Léopold, P. (2014). Sensing of amino acids in a dopaminergic circuitry promotes rejection of an incomplete diet in Drosophila.Cell. 156(3):510-21.
28. Bogan, K.L., Brenner, C. (2008). Nicotinic acid, nicotinamide, and nicotinamide riboside: A molecular evaluation of NAD+ precursor vitamins in human nutrition. Annu Rev Nutr.;28:115–30.
29. Boros, L. G., Lee, W. N., & Go, V. L. (2002). A metabolic hypothesis of cell growth and death in pancreatic cancer. Pancreas, 24(1), 26–33.
30. Boroughs, L. K., DeBerardinis, R. J., (2015). Metabolic pathways promoting cancer cell survival and growth. Nat. Cell Biol. 17, 351–359
31. Brand, M. D., (2010). The sites and topology of mitochondrial superoxide production. Exp. Gerontol. 45, 466–472
32. Bray, S.J. (2006). Notch signalling: a simple pathway becomes complex.Nat Rev Mol Cell Biol. 7(9):678-89.
33. Britton, J. S., Lockwood, W. K., Li, L., Cohen, S. M., & Edgar, B. A. (2002). Drosophila's insulin/PI3-kinase pathway coordinates cellular metabolism with nutritional conditions. Developmental cell, 2(2), 239–249.
34. Broughton, S.J., Piper, M.D., Ikeya, T., Bass, T.M., Jacobson, J., Driege, Y., Martinez, P., Hafen, E., Withers, D.J., Leevers, S.J., Partridge, L. (2005). Longer lifespan, altered metabolism, and stress resistance in Drosophila from ablation of cells making insulin-like ligands. Proc. Natl Acad. Sci. USA 102, 3105–3110

35. Brown, G.C. & Borutaite, V. (2008). Regulation of apoptosis by the redox state of cytochrome c. Biochimica et Biophysica Acta (BBA) - Bioenergetic (7-8) 877-881
36. Bruick, R.K., McKnight, S.L. (2001). A conserved family of prolyl-4-hydroxylases that modify HIF. Science. 294(5545):1337-1340
37. Brumby, A. M. and Richardson, H. E. (2003). Scribble mutants cooperate with oncogenic Ras or Notch to cause neoplastic overgrowth in Drosophila. EMBO J. 22, 5769-5779.
38. Brumby, A.M., and Richardson, H.E. (2005). Using Drosophila melanogaster to map human cancer pathways. Nature reviews Cancer 5: 626-639
39. Buchon, N., Silverman, N., and Cherry, S. (2014). Immunity in Drosophila melanogaster--from microbial recognition to whole-organism physiology. Nature reviews. Immunology, 14(12), 796–810
40. Buzzai, M., Bauer, D., Jones, R. (2005). The glucose dependence of Akt-transformed cells can be reversed by pharmacologic activation of fatty acid β-oxidation. Oncogene 24, 4165–4173
41. Callier, V., Nijhout, H.F. (2014). Plasticity of insect body size in response to oxygen: Integrating molecular and physiological mechanisms. Current Opinion in Insect Science. 1: 59-65
42. Campesan, S., Green, E. W., Breda, C., Sathyasaikumar, K. V., Muchowski, P. J., Schwarcz, R., Kyriacou, C. P., & Giorgini, F. (2011). The kynurenine pathway modulates neurodegeneration in a Drosophila model of Huntington's disease. Current biology. CB, 21(11), 961–966.
43. Canli, T., & Lesch, K. P. (2007). Long story short: the serotonin transporter in emotion regulation and social cognition. Nature neuroscience, 10(9), 1103–1109.
44. Cantor, J. R., Sabatini, D. M., (2012). Cancer cell metabolism: One hallmark, many faces. Cancer Discov. 2, 881–898
45. Caussinus, E. and Gonzalez, C. (2005). Induction of tumor growth by altered stem-cell asymmetric division in Drosophila melanogaster. Nat. Genet. 37, 1125-1129.
46. Centanin, L., Ratcliffe, P.J. and Wappner, P. (2005). Reversion of lethality and growth defects in Fatiga oxygen-sensor mutant flies by loss of Hypoxia-Inducible Factor-α/Sima Lázaro. EMBO Rep. 6(11): 1070–1075.
47. Chambers, J. W., & LoGrasso, P. V. (2011). Mitochondrial c-Jun N-terminal kinase (JNK) signaling initiates physiological changes resulting in amplification of

reactive oxygen species generation. The Journal of biological chemistry, 286(18), 16052–16062.

48. Chandel, N. S., Tuveson D. A., (2014). The promise and perils of antioxidants for cancer patients. N. Engl. J. Med. 371, 177–178
49. Chang, S., Bray, S.M., Li, Z. (2008) Identification of small molecules rescuing fragile X syndrome phenotypes in Drosophila. Nat Chem Biol 4: 256–263
50. Chen, Y., Hu, Y., Zhang, H., Peng, C., and Li, S. (2009). Loss of the Alox5 gene impairs leukemia stem cells and prevents chronic myeloid leukemia. Nat Genet. 41, 783–792.
51. Cheng, Y., Jin, U. H., Allred, C. D., Jayaraman, A., Chapkin, R. S., & Safe, S. (2015). Aryl Hydrocarbon Receptor Activity of Tryptophan Metabolites in Young Adult Mouse Colonocytes. Drug metabolism and disposition: the biological fate of chemicals, 43(10), 1536–1543. https://doi.org/10.1124/dmd.115.063677
52. Cheong, J. E., & Sun, L. (2018). Targeting the IDO1/TDO2-KYN-AhR Pathway for Cancer Immunotherapy - Challenges and Opportunities. Trends in pharmacological sciences, 39(3), 307–325.
53. Chia, S., Gandhi, S., Joy, A.A., Edwards, S., Gorr, M., Hopkins, S., Kondejewski, J., Ayoub, J.P., Califaretti, N., Rayson, D., and Dent, S.F. (2015). Novel agents and associated toxicities of inhibitors of the pi3k/Akt/mtor pathway for the treatment of breast cancer. Curr. Oncol. 22, 33–48.
54. Chiu, Y. H., Lei, H. J., Huang, K. C., Chiang, Y. L., & Lin, C. S. (2019). Overexpression of Kynurenine 3-Monooxygenase Correlates with Cancer Malignancy and Predicts Poor Prognosis in Canine Mammary Gland Tumors. Journal of oncology, 2019, 6201764.
55. Cho, E.S., Cha, Y.H., Kim, H.S., Kim, N.H., Yook, J.I.(2018). The Pentose Phosphate Pathway as a Potential Target for Cancer Therapy. Biomol Ther (Seoul) 26(1): 29–38.
56. Colotta, F., Allavena, P., Sica, A., Garlanda, C., and Mantovani, A. (2009).Cancer-related inflammation, the seventh hallmark of cancer: links to genetic instability. Carcinogenesis 30, 1073–1081.
57. Commisso, C., Davidson, S. M., Soydaner-Azeloglu, R. G., Parker, S. J., Kamphorst, J. J., Hackett, S., Grabocka, E., Nofal, M., Drebin, J. A., Thompson, C. B., Rabinowitz, J. D., Metallo, C. M., Vander Heiden, M. G., Bar-Sagi, D., (2013).

Macropinocytosis of protein is an amino acid supply route in Ras-transformed cells. Nature 497, 633–637

58. Cotran, Kumar, Collins, Robbins (1998). Pathologic Basis of Disease. Philadelphia: W.B Saunders Company. ISBN 978-0-7216-7335-6.
59. Coussens, L.M and Werb, Z. (2002). Inflammation and cancer. Nature 420: 860–867
60. Crabtree, H.G. (1929). Observations on the carbohydrate metabolism of tumours. Biochem J.; 23(3):536-45.
61. Cross, C.E., Halliwell, B., Borish, E.T., Pryor, W.A., Ames, B.N., Saul, R.L., McCord, J.M., Harman, D. (1987). Oxygen radicals and human disease. Ann Intern Med 107: 526-545
62. Cross, D., Alessi, D., Cohen, P., Andjelkovich, M., Hemmings, B. (1995). Inhibition of glycogen synthase kinase-3 by insulin mediated by protein kinase B. Nature, 378: 785–789.
63. Cullion, K., Draheim, K.M., Hermance, N., Tammam, J., Sharma, V.M., Ware, C., Nikov, G., Krishnamoorthy, V., Majumder, P.K., Kelliher, M.A. (2009). Targeting the Notch1 and mTOR pathways in a mouse T-ALL model. Blood. 11;113(24):6172-81.
64. Dang, T. P. (2012). Notch, apoptosis and cancer. Advances in experimental medicine and biology, 727, 199–209.
65. Dang, C. V., (2012). Links between metabolism and cancer. Genes Dev. 26, 877–890
66. Dang, C.V., Semenza, G.L. (1999). Oncogenic alterations of metabolism. Trends in Biochemical Sciences. 24(2):68-72
67. Dar, A. C., Das, T. K., Shokat, K. M. and Cagan, R. L. (2012). Chemical genetic discovery of targets and anti-targets for cancer polypharmacology. Nature 486, 80-84.
68. Dasari, S., & Cooper, R. L. (2006). Direct influence of serotonin on the larval heart of Drosophila melanogaster. Journal of comparative physiology. B, Biochemical, systemic, and environmental physiology, 176(4), 349–357.
69. De Gregorio, E., Spellman, P.T., Tzou, P., Rubin, G.M., Lemaitre, B. (2002). The Toll and Imd pathways are the major regulators of the immune response in Drosophila. EMBO J;21: 2568–2579.

70. De Palma, M., and Lewis, C. E. (2013). Macrophage regulation of tumor responses to anticancer therapies. Cancer Cell 23, 277–286.
71. Deangelo, D., Stone, R., Silverman, L. (2006). A phase I clinical trial of the notch inhibitor MK-0752 in patients with T-cell acute lymphoblastic leukemia/lymphoma (T-ALL) and other leukemias. Journal of Clinical Oncology 24:6585
72. DeBerardinis, R. J., Mancuso, A., Daikhin, E., Nissim, I., Yudkoff, M., Wehrli, S., Thompson, C. B., (2007). Beyond aerobic glycolysis: Transformed cells can engage in glutamine metabolism that exceeds the requirement for protein and nucleotide synthesis. Proc. Natl. Acad. Sci. U.S.A. 104, 19345–19350
73. DeBerardinis, R.J., Cheng, T. (2010). Q's next: the diverse functions of glutamine in metabolism, cell biology and cancer. Oncogene 29: 313-324,
74. Dekanty, A., Lavista-Llanos, S., Irisarri, M., OLdham, S., Wappner, P.(2005). The insulin-PI3K/TOR pathway induces a HIF-dependent transcriptional response in Drosophila by promoting nuclear localization of HIF-alpha/Sima. J Cell Sci. 2005 Dec 1;118(Pt 23):5431-41
75. Dennis, E.A., and Norris, P.C. (2015). Eicosanoid storm in infection and inflammation. Nat. Rev. Immunol. 15, 511–523.
76. Dexter, J.S. (1914). The analysis of a case of continuous variation in Drosophila by a study of its linkage relationships. The American Naturalist. 1914:712–758.
77. Dhanasekaran, D. N., & Reddy, E. P. (2008). JNK signaling in apoptosis. Oncogene, 27(48), 6245–6251.
78. Di Cristofano, A., Pesce, B., Cordon-Cardo, C., Pandolfi, P.P. (1998). Pten is essential for embryonic development and tumour suppression. Nat Genet. 19(4):348-55.
79. DiAngelo, J.R., Bland, M.L., Bambina, S., Cherry, S. and Birnbaum, M.J . (2009).The immune response attenuates growth and nutrient storage in Drosophila by reducing insulin signaling. Proc. Natl Acad. Sci. USA 106, 20853–20858
80. Dibble, C. C., & Manning, B. D. (2013). Signal integration by mTORC1 coordinates nutrient input with biosynthetic output. Nature cell biology, 15(6), 555–564.
81. Dimmeler, S., Fleming, I., Fisslthaler, B., Hermann, C., Busse, R., & Zeiher, A. M. (1999). Activation of nitric oxide synthase in endothelial cells by Akt-dependent phosphorylation. Nature, 399(6736), 601–605.

82. Dionne, M. S., & Schneider, D. S. (2008). Models of infectious diseases in the fruit fly Drosophila melanogaster. Disease models & mechanisms, 1(1), 43–49.
83. Domínguez, M. (2014). Oncogenic programmes and Notch activity: An ‘organized crime’? Seminars in Cell and Developmental Biology 28:78-85
84. Doolin, K., Allers, K.A., Pleiner, S., Liesener, A., Farrell, C., Tozzi, L. (2018) Altered tryptophan catabolite concentrations in major depressive disorder and associated changes in hippocampal subfield volumes. Psychoneuroendocrinology. 95:8–17.
85. Dorn, G.W. and Kitsis, R.N. (2015). The mitochondrial dynamism–mitophagy–cell death interactome: multiple roles performed by members of a mitochondrial molecular ensemble. Circ Res 116: 167-182
86. Dudzic, J.P., Kondo, S., Ueda, R., Bergman, C.M., Lemaitre, B. (2015). Drosophila innate immunity: regional and functional specialization of prophenoloxidases. BMC Biol. 2015; 13: 81.
87. Duronio, R. J., O'Farrell, P. H., Sluder, G. and Su, T. T. (2017). Sophisticated lessons from simple organisms: appreciating the value of curiosity-driven research. Dis. Model. Mech. 10, 1381-1389.
88. Dvorak, H. F. (1986). Tumors: wounds that do not heal. Similarities between tumor stroma generation and wound healing. N. Engl. J. Med. 315, 1650–1659
89. Edgar, B. A. and Lehner, C. F. (1996). Developmental control of cell cycle regulators: a fly's perspective. Science 274, 1646-1652.
90. Efstratiadis, A., Szabolcs, M. and Klinakis, A. (2007) Notch, Myc and breast cancer. Cell Cycle 6: 418–429
91. Eichenlaub, T., Villadsen, R., Freitas, F.C.P. (2018). Warburg Effect Metabolism Drives Neoplasia in a Drosophila Genetic Model of Epithelial Cancer. Curr Biol. 28(20):3220-3228.
92. Eliasz, S., Liang, S., Chen, Y., De Marco, M.A., Machek, O., Skucha, S., Miele, L. and Bocchetta, M. (2010) Notch-1 stimulates survival of lung adenocarcinoma cells during hypoxia by activating the IGF-1R pathway. Oncogene 29: 2488–2498
93. Ellisen, L.W., Bird, J., West, D.C. (1991) TAN-1, the human homolog of the Drosophila notch gene, is broken by chromosomal translocations in T lymphoblastic neoplasms. Cell, 66 (4) pp. 649-661

94. Eming, S. A., Krieg, T., Davidson, J. M. (2007). Inflammation in wound repair: molecular and cellular mechanisms. Journal of Investigative Dermatology. 127 (3): 514–525.
95. Ertel, A., Tsirigos, A., Whitaker-Menezes, D., Birbe, R. C., Pavlides, S., Martinez-Outschoorn, U. E., Pestell, R. G., Howell, A., Sotgia, F., & Lisanti, M. P. (2012). Is cancer a metabolic rebellion against host aging? In the quest for immortality, tumor cells try to save themselves by boosting mitochondrial metabolism. Cell cycle (Georgetown, Tex.), 11(2), 253–263.
96. Fan, J., Ye, J., Kamphorst, J. J., Shlomi T., Thompson C. B., Rabinowitz J. D., (2014). Quantitative flux analysis reveals folate-dependent NADPH production. Nature 510, 298–302
97. Fernández-Hernández, I., Scheenaard, E., Pollarolo, G., and Gonzalez, C. (2016). The translational relevance of Drosophila in drug discovery. EMBO reports, 17(4), 471–472.
98. Ferrero-Miliani, L., Nielsen, O.H., Andersen, P.S., Girardin, S.E.; Girardin, A. (2007). Chronic inflammation: importance of NOD2 and NALP3 in interleukin-1beta generation. Clin. Exp. Immunol. 147 (2): 061127015327006
99. Ferres-Marco, D., Gutierrez-Garcia, I., Vallejo, D. M., Bolivar, J., Gutierrez-Aviño, F. J. and Dominguez, M. (2006). Epigenetic silencers and Notch collaborate to promote malignant tumours by Rb silencing. Nature 439, 430-436.
100. Foster, A.C., Vezzani, A., French, E.D., Schwarcz, R. (1984). Kynurenic acid blocks neurotoxicity and seizures induced in rats by the related brain metabolite quinolinic acid. Neurosci Lett 48(3):273–278.
101. Franke, T.F., Kaplan, D.R., Cantley, L.C. (1997). PI3K: Downstream AKTion blocks apoptosis. Cell: 88: 435–437.
102. Fruman, D.A., and Rommel, C. (2014). PI3K and cancer: lessons, challenges and opportunities. Nat Rev Drug Discov. 13(2):140-56.
103. Fu, Y., Liu, S., Yin, S., Niu, W., Xiong ,W., Tan, M., Li, G., Zhou, M. (2017). The reverse Warburg effect is likely to be an Achilles' heel of cancer that can be exploited for cancer therapy. Oncotarget. 8: 57813-57825
104. Fukumura, D., Kashiwagi, S., and Jain, R.K. (2006). The role of nitric oxide in tumour progression. Nat. Rev. Cancer 6, 521–534.
105. Fukuwatari, T., Shibata, K. (2013). Nutritional aspect of tryptophan metabolism. Int J Tryptophan Res.;6:3–8.

106. Fulton, D., Gratton, J. P., McCabe, T. J., Fontana, J., Fujio, Y., Walsh, K., Franke, T. F., Papapetropoulos, A., & Sessa, W. C. (1999). Regulation of endothelium-derived nitric oxide production by the protein kinase Akt. Nature, 399(6736), 597–601.

107. Galluzzi, L., Morselli, E., Kepp, O., Vitale, I., Rigoni, A., Vacchelli, E., Michaud, M., Zischka H., Castedo, M., Kroemer, G. (2010). Mitochondrial gateways to cancer. Mol Aspects Med 31: 1-20

108. Galluzzi, L., Pietrocola, F., Bravo-San Pedro, J. M., Amaravadi, R. K., Baehrecke, E. H., Cecconi, F., Codogno, P., Debnath, J., Gewirtz, D. A., Karantza, V., Kimmelman, A., Kumar, S., Levine, B., Maiuri, M. C., Martin, S. J., Penninger, J., Piacentini, M., Rubinsztein, D. C., Simon, H. U., Simonsen, A., Kroemer, G. (2015). Autophagy in malignant transformation and cancer progression. The EMBO journal, 34(7), 856–880.

109. Gao, G., Chen, L., Huang, C. (2014) Anti-cancer drug discovery: update and comparisons in yeast, Drosophila, and Zebrafish. Curr Mol Pharmacol 7: 44–51

110. Garcia, A., and Kandel, J. J. (2012). Notch: a key regulator of tumor angiogenesis and metastasis. Histology and histopathology, 27(2), 151–156. doi:10.14670/HH-27.151

111. Garcia-Rodriguez, L. A. and Huerta-Alvarez, C. (2001). Reduced risk of colorectal cancer among long-term users of aspirin and nonaspirin nonsteroidal antiinflammatory drugs. Epidemiology 12, 88–93

112. Gateff, E. and Schneiderman, H. A. (1967). Developmental studies of a new mutation of Drosophila melanogaster: lethal malignant brain tumor 1(2)gl4. Am. Zool. 7, 760.

113. Gateff, E. and Schneiderman, H. A. (1969). Neoplasms in mutant and cultured wild-tupe tissues of Drosophila. Natl. Cancer Inst. Monogr. 31, 365-397.

114. Gateff, E. and Schneiderman, H. A. (1974). Developmental capacities of benign and malignant neoplasms of Drosophila. Wilhelm Roux Arch. Entwickl. Mech. Org. 176, 23-65.

115. Gatenby, R. A., Smallbone, K., Maini, P. K., Rose, F., Averill, J., Nagle, R. B., Worrall, L., & Gillies, R. J. (2007). Cellular adaptations to hypoxia and acidosis during somatic evolution of breast cancer. British journal of cancer, 97(5), 646–653.

116. Georgescu, M.M. (2010). PTEN tumor suppressor network in PI3K-Akt pathway control. Genes Cancer 1:1170–7.

117. Gladstone, M., Frederick, B., Zheng, D. (2012). A translation inhibitor identified in a Drosophila screen enhances the effect of ionizing radiation and taxol in mammalian models of cancer. Dis Models Mech 5: 342–350

118. Goda, K., Hamane, Y., Kishimoto, R., Ogishi, Y. (1999). Radical scavenging properties of tryptophan metabolites. Estimation of their radical reactivity. Adv Exp Med Biol 467:397–402.

119. Gonzalez-Garcia, S., Garcia-Peydro, M., Alcain, J. and Toribio, M.L. (2012) Notch1 and IL-7 Receptor Signalling in Early T-cell Development and Leukaemia. In Notch Regulation of the Immune System, Radtke F (ed) pp 47–73

120. Gore, L., DeGregori, J. and Porter, C.C. (2013) Targeting developmental pathways in children with cancer: what price success? The lancet oncology. 14(2), e70–e78. doi:10.1016/S1470-2045(12)70530-2

121. Grabher, C., Von Boehmer, H., Look, A.T.. (2006). Notch 1 activation in the molecular pathogenesis of T-cell acute lymphoblastic leukemia. Nat Rev Cancer 6:347–59.

122. Grandison, R. C., Piper, M. D., & Partridge, L. (2009). Amino-acid imbalance explains extension of lifespan by dietary restriction in Drosophila. Nature, 462(7276), 1061–1064. https://doi.org/10.1038/nature08619

123. Green, E. W., Campesan, S., Breda, C., Sathyasaikumar, K. V., Muchowski, P. J., Schwarcz, R., Kyriacou, C. P., & Giorgini, F. (2012). Drosophila eye color mutants as therapeutic tools for Huntington disease. Fly, 6(2), 117–120.

124. Greene, E.R., Huang, S., Serhan, C.N., and Panigrahy, D. (2011). Regulation of inflammation in cancer by eicosanoids. Prostaglandins Other Lipid Mediat. 96, 27–36.

125. Grifoni, D., Garoia, F., Schimanski, C. C., Schmitz, G., Laurenti, E., Galle, P. R., Pession, A., Cavicchi, S. and Strand, D. (2004). The human protein Hugl-1 substitutes for Drosophila lethal giant larvae tumour suppressor function in vivo. Oncogene 23, 8688-8694.

126. Grivennikov, S. I., Greten, F. R., and Karin, M. (2010). Immunity, inflammation, and cancer. Cell 140, 883–899.

127. Grohmann, U., Bronte, V. (2010) Control of immune response by amino acid metabolism. Immunol Rev. 236:243–64.

128. Grohmann, U., Mondanelli, G., Belladonna, M. L., Orabona, C., Pallotta, M. T., Iacono, A., Puccetti, P., & Volpi, C. (2017). Amino-acid sensing and degrading pathways in immune regulation. Cytokine & growth factor reviews, 35, 37–45.

129. Grönke, S., Clarke, D.F., Broughton, S., Andrews, T.D. and Partridge, L. (2010). Molecular evolution and functional characterization of Drosophila insulin-like peptides. PLoS Genet 6, e1000857

130. Guertin, D. A. and Sabatini, D. M. (2007). Defining the role of mTOR in cancer. Cancer Cell 12, 9-22

131. Guillemin, G.J., Croitoru-Lamoury, J., Dormont, D., Armati, P.J., Brew, B.J. (2003). Quinolinic acid upregulates chemokine production and chemokine receptor expression in astrocytes. Glia.41:371–81.

132. Gupta, S., Roy, A., & Dwarakanath, B. S. (2017). Metabolic Cooperation and Competition in the Tumor Microenvironment: Implications for Therapy. Frontiers in oncology, 7, 68.

133. Gutierrez, A., Sanda, T., Grebliunaite, R., Carracedo, A., Salmena, L., Ahn, Y., Dahlberg, S., Neuberg, D., Moreau, L.A., Winter, S.S., Larson, R., Zhang, J., Protopopov, A., Chin, L., Pandolfi, P.P., Silverman, L.B., Hunger, S.P., Sallan, S.E. and Look, A.T. (2009) High frequency of PTEN, PI3K, and AKT abnormalities in T-cell acute lymphoblastic leukemia. Blood 114: 647–650

134. Shen, H., Kreisel, D., Goldstein, D. R. (2013). Processes of Sterile Inflammation. J Immunol 191, 2857–2863

135. Hagen, T., Taylor, C. T., Lam, F., & Moncada, S. (2003). Redistribution of intracellular oxygen in hypoxia by nitric oxide: effect on HIF1alpha. Science (New York, N.Y.), 302(5652), 1975–1978.

136. Hales, E.C., Taub, J.W. and Matherly, L.H. (2014) New insights into Notch1 regulation of the PI3K-AKT-mTOR1 signaling axis: targeted therapy of γ-secretase inhibitor resistant T-cell acute lymphoblastic leukemia. Cellular Signalling 26: 149–161

137. Han, Q., Beerntsen, B. T., & Li, J. (2007). The tryptophan oxidation pathway in mosquitoes with emphasis on xanthurenic acid biosynthesis. Journal of insect physiology, 53(3), 254–263.

138. Hanahan, D. and Weinberg, R.A. (2000). The Hallmarks of Cancer [Review]. Cell 100:57-70

139. Hanahan, D. and Weinberg, R.A. (2011). Hallmarks of cancer: the next generation. Cell 144(5):646-74

140. Hensley, C.T., Faubert, B., Yuan, Q., Lev-Cohain, N., Jin, E., Kim, J., Jiang, L., Ko B, Skelton, R., Loudat, L. (2016). Metabolic Heterogeneity in Human Lung Tumors. Cell 164:681–694.

141. Hernandez Tejada, F.N., Galvez Silva, J.R. and Zweidler-McKay, P.A. (2014) The challenge of targeting notch in hematologic malignancies. Front Pediatr 2: 54

142. Herranz, D., Ambesi-Impiombato, A., Sudderth, J., Sánchez-Martín, M., Belver, L., Tosello, V., Xu, L., Wendorff, A. A., Castillo, M., Haydu, J. E., Márquez, J., Matés, J. M., Kung, A. L., Rayport, S., Cordon-Cardo, C., DeBerardinis, R. J., & Ferrando, A. A. (2015). Metabolic reprogramming induces resistance to anti-NOTCH1 therapies in T cell acute lymphoblastic leukemia. Nature medicine, 21(10), 1182–1189.

143. Herrington, S. (2014). Muir's Textbook of Pathology (15th ed.). CRC Press. p. 59. ISBN 978-1444184990.

144. Hielscher, A., & Gerecht, S. (2015). Hypoxia and free radicals: role in tumor progression and the use of engineering-based platforms to address these relationships. Free radical biology & medicine, 79, 281–291.

145. Hielscher, A., Gerecht, S. (2015). Hypoxia and free radicals: role in tumor progression and the use of engineering-based platforms to address these relationships. Free Radic Biol Med 79: 281-291

146. Hirabayashi, S., Baranski, T. J., & Cagan, R. L. (2013). Transformed Drosophila cells evade diet-mediated insulin resistance through wingless signaling. Cell, 154(3), 664–675. https://doi.org/10.1016/j.cell.2013.06.030

147. Højlund, K., Wrzesinski, K., Larsen, P.M., Fey, S.J., Roepstorff, P., Handberg, A., Dela, F., Vinten, J., McCormack, J.G., Reynet, C., Beck-Nielsen, H. (2003). Proteome Analysis Reveals Phosphorylation of ATP Synthase β-Subunit in Human Skeletal Muscle and Proteins with Potential Roles in Type 2 Diabetes. The Journal of Biological Chemistry 278, 10436-10442.

148. Hollander, M.C., Blumenthal, G.M., Dennis, P.A. (2011). PTEN loss in the continuum of common cancers, rare syndromes and mouse models. Nat Rev Cancer 11(4):289-301

149. Homey, B., Muller, A. and Zlotnik, A. (2002). Chemokines: agents for the immunotherapy of cancer? Nature Rev. Immunol. 2, 175–184

150. Hoxhaj, G., Manning, B.D. (2020). The PI3K–AKT network at the interface of oncogenic signalling and cancer metabolism. Nat Rev Cancer 20, 74–88

151. Hubbard, T. D., Murray, I. A., Bisson, W. H., Lahoti, T. S., Gowda, K., Amin, S. G., Patterson, A. D., & Perdew, G. H. (2015). Adaptation of the human aryl hydrocarbon receptor to sense microbiota-derived indoles. Scientific reports, 5, 12689. https://doi.org/10.1038/srep12689

152. Hübner, A., Mulholland, D. J., Standen, C. L., Karasarides, M., Cavanagh-Kyros, J., Barrett, T., Chi, H., Greiner, D. L., Tournier, C., Sawyers, C. L., Flavell, R. A., Wu, H., & Davis, R. J. (2012). JNK and PTEN cooperatively control the development of invasive adenocarcinoma of the prostate. Proceedings of the National Academy of Sciences of the United States of America, 109(30), 12046–12051.

153. Hucke, C., MacKenzie, C.R. , Adjogble, K.D., Takikawa, O., Daubener, W. (2004) Nitric oxide-mediated regulation of gamma interferon-induced bacteriostasis: inhibit ion and degradation of human indoleamine 2,3-diox ygenase. Infect Immun. 72:2723–2730.

154. Hunter, T. (1991). Cooperation between oncogenes. Cell. 64(2):249-70.

155. Hursting, S.D., Smith, S.M., Lashinger, L.M., Harvey, A.E., Perkins, S.N. (2010). Calories and carcinogenesis: Lessons learned from 30 years of calorie restriction research. Carcinogenesis 31: 83–89.

156. Igaki, T., Pagliarini, R. A. and Xu, T. (2006). Loss of cell polarity drives tumor growth and invasion through JNK activation in Drosophila. Curr. Biol. 16, 1139-1146.

157. Irving, P., Troxler, L., Heuer, T.S., Belvin M., Kopczynski, C. and Charles Hetru (2001). A genome-wide analysis of immune responses in Drosophila. Proc Natl Acad Sci USA 98: 15119–15124.

158. Israelsen, W. J., Dayton, T. L., Davidson, S. M., Fiske, B. P., Hosios, A. M., Bellinger, G., Li, J., Yu, Y., Sasaki, M., Horner, J. W., Burga, L. N., Xie, J., Jurczak, M. J., DePinho, R. A., Clish, C. B., Jacks, T., Kibbey, R. G., Wulf, G. M., Di Vizio, D., Mills, G. B., Cantley L. C., Vander Heiden M. G., (2013). PKM2 isoform-specific deletion reveals a differential requirement for pyruvate kinase in tumor cells. Cell 155, 397–409

159. Iurlaro, R., León-Annicchiarico, C.L., Muñoz-Pinedo, C. (2014). Regulation of cancer metabolism by oncogenes and tumor suppressors. Methods Enzymol 542: 59-80

160. Ivan, M., Kondo, K., Yang, H., Kim, W., Valiando, J., Ohh, M., Salic, A., Asara, J. M., Lane, W. S., & Kaelin , W. G., Jr (2001). HIFalpha targeted for VHL-mediated destruction by proline hydroxylation: implications for O2 sensing. Science (New York, N.Y.), 292(5516), 464–468.

161. Janeway, C. (1989) Evolution and revolution in immunology. Cold Spring Harb Symp Quant Biol 54: 1–13.

162. Janiszewska, M., and Polyak, K. (2015). Clonal evolution in cancer: a tale of twisted twines. Cell Stem Cell 16, 11-12.

163. Jiang, P., Du, W., & Wu, M. (2014). Regulation of the pentose phosphate pathway in cancer. Protein & cell, 5(8), 592–602. https://doi.org/10.1007/s13238-014-0082-8

164. Jiang, W., Zhu, Z. and Thompson, H. J. (2008). Dietary energy restriction modulates the activity of AMPactivated protein kinase, Akt, and mammalian target of rapamycin in mammary carcinomas, mammary gland, and liver. Cancer Res 68, 5492-9

165. Jin, H., Zhang, Y., You, H., Tao, X., Wang, C., Jin, G., Wang, N., Ruan, H., Gu, D., Huo, X., Cong, W., & Qin, W. (2015). Prognostic significance of kynurenine 3 monooxygenase and effects on proliferation, migration, and invasion of human hepatocellular carcinoma. Scientific reports, 5, 10466.

166. Jone, L.H. and Bunnage, M.E. (2017). Applications of chemogenomic library screening in drug discovery. Nat Rev Drug Discov. (4):285-296.

167. Jones, W., Bianchi, K. (2015) Aerobic glycolysis: beyond proliferation. Front Immunol 6: 227

168. Julliard, W., Fechner, J.H., Mezrich, J.D. (2014). The aryl hydrocarbon receptor meets immunology: friend or foe? A little of both. Front Immunol. 5:458.

169. Jutel, M., Akdis, M., & Akdis, C. A. (2009). Histamine, histamine receptors and their role in immune pathology. Clinical and experimental allergy: journal of the British Society for Allergy and Clinical Immunology, 39(12), 1786–1800.

170. Kaeberlein, M., Powers, R.W., Steffen, K.K., Westman, E.A., Hu, D., Dang, N., Kerr, E.O., Kirkland, K.T., Fields, S., Kennedy, B.K. (2005). Regulation of yeast replicative life span by TOR and Sch9 in response to nutrients. Science 310, 1193-6

171. Kaelin Jr, W.G., Ratcliffe, P.J. (2008). Oxygen sensing by metazoans: The central role of the HIF hydroxylase pathway. Molecular Cell. 30(4):393-402

172. Kalaany, N.Y., Sabatini, D.M.. (2009). Tumours with PI3K activation are resistant to dietary restriction. Nature. 2 9;458(7239):725-31.

173. Kamphorst, J. J., Nofal, M., Commisso, C., Hackett, S. R., Lu W., Grabocka, E., Vander Heiden, M. G., Miller, G., Drebin, J. A., Bar-Sagi, D., Thompson, C. B., Rabinowitz, J. D., (2015). Human pancreatic cancer tumors are nutrient poor and tumor cells actively scavenge extracellular protein. Cancer Res. 75, 544–553

174. Kamyshev, N. G., Smirnova, G. P., Savvateeva, E. V., Medvedeva, A. V., & Ponomarenko, V. V. (1983). The influence of serotonin and p-chlorophenylalanine on locomotor activity of Drosophila melanogaster. Pharmacology, biochemistry, and behavior, 18(5), 677–681.

175. Kannan, K. and Fridell, Y-WC (2013). Functional implications of Drosophila insulin-like peptides in metabolism, aging, and dietary restriction. Front. Physiol 4, 288

176. Kantner, H.P., Warsch, W., Delogu, A., Bauer, E. (2013). ETV6/RUNX1 Induces Reactive Oxygen Species and Drives the Accumulation of DNA Damage in B Cells. Neoplasia 15(11): 1292–1300

177. Kapahi, P., Zid, B.M., Harper, T., Koslover, D., Sapin, V., Benzer, S. (2004). Regulation of lifespan in Drosophila by modulation of genes in the TOR signaling pathway. Curr Biol 14, 885-90

178. Karim, F. D. and Rubin, G. M. (1998). Ectopic expression of activated Ras1 induces hyperplastic growth and increased cell death in Drosophila imaginal tissues. Development 125, 1-9.

179. Karpac, J., Younger, A. and Jasper, H. (2011). Dynamic coordination of innate immune signaling and insulin signaling regulates systemic responses to localized DNA damage. Dev. Cell 20, 841–854

180. Keda S, Kotake Y. (1986). Urinary excretion of xanthurenic acid and zinc in diabetes: Occurrence of xanthurenic acid-Zn2+ complex in urine of diabetic patients and of experimentally-diabetic rats. Ital J Biochem.35:232–241.

181. Khandekar, M.J., Cohen, P., Spiegelman, B.M. (2011). Molecular mechanisms of cancer development in obesity. Nat Rev Cancer 11: 886–895.

182. Kim, R., Emi, M., Tanabe, K. (2006). The role of apoptosis in cancer cell survival and therapeutic outcome. Cancer Biol Ther 5: 1429-1442

183. Kim, S., Mateo, R., Yin, Y., Wu, G. (2007). Functional Amino Acids and Fatty Acids for Enhancing Production Performance of Sows and Piglets. Asian-Australas J Anim Sci 20(2):295-306.

184. Kim, S.K. and Rulifson, E.J. (2004). Conserved mechanisms of glucose sensing and regulation by Drosophila corpora cardiaca cells. Nature 431, 316–320

185. Kim, Y. J., Borsig, L., Varki, N. M. and Varki, A. (1998). P-selectin deficiency attenuates tumor growth and metastasis. Proc. Natl Acad. Sci. USA 95, 9325–9330

186. Knoechel, B. and Aster, J.C. (2015). Metabolic Mechanisms of Drug Resistance in Leukemia. Cell Metab. 22(5):759-60. doi: 10.1016/j.cmet.2015.10.005.

187. Knoechel, B., Roderick, J. E., Williamson, K. E., Zhu, J., Lohr, J. G., Cotton, M. J., Gillespie, S. M., Fernandez, D., Ku, M., Wang, H., Piccioni, F., Silver, S. J., Jain, M., Pearson, D., Kluk, M. J., Ott, C. J., Shultz, L. D., Brehm, M. A., Greiner, D. L., Gutierrez, A., Bernstein, B. E. (2014). An epigenetic mechanism of resistance to targeted therapy in T cell acute lymphoblastic leukemia. Nature genetics, 46(4), 364–370.

188. Kopan, R. and Ilagan, M.X. (2009). The canonical Notch signaling pathway: unfolding the activation mechanism. Cell. 137(2):216-33.

189. Koppenol, W.H., Bounds, P.L, Dang, C.V. (2011). Otto Warburg's contributions to current concepts of cancer metabolism. Nat Rev Cancer. 11(5):325-37.

190. Krishnan, S., Ding, Y., Saedi, N., Choi, M., Sridharan, G. V., Sherr, D. H., Yarmush, M. L., Alaniz, R. C., Jayaraman, A., & Lee, K. (2018). Gut Microbiota-Derived Tryptophan Metabolites Modulate Inflammatory Response in Hepatocytes and Macrophages. Cell reports, 23(4), 1099–1111. ¡

191. Kritchevsky, D. Caloric restriction and cancer. J. Nutr. Sci. Vitaminol. (Tokyo) 47, 13–19 (2001)

192. Kumar, R., Clermont, G., Vodovotz, Y., Chow, C.C. (2004). The dynamics of acute inflammation. Journal of Theoretical Biology. 230 (2): 145–155.

193. Kurz, K., Schroecksnadel, S., Weiss, G., Fuchs, D. (2011) Association between increased tryptophan degradation and depression in cancer patients. Curr Opin Clin Nutr Metab Care. 14:49–56.

194. Laird, P. W. (2005). Cancer epigenetics. Hum Mol Genet 14 Spec No 1, R65-76.

195. Laplante, M., Sabatini, D.M. (2012). mTOR signaling in growth control and disease. Cell 149, 274–293

196. Lawlor, M.A., Alessi, D.R. (2001). PKB/Akt: A key mediator of cell proliferation, survival and insulin responses? J Cell Sci: 114: 2903–2910.

197. Lazzaro, B.P. and Galac, M.R. (2006). Disease pathology: wasting energy fighting infection. Curr. Biol 16, R964–R965

198. Leclerc, V., Reichhart, J.M. (2004). The immune response of Drosophila melanogaster. Immunol Rev. Apr;198:59-71.

199. Lee, H. W., Choi, H. J., Ha, S. J., Lee, K. T., and Kwon, Y. G. (2013b). Recruitment of monocytes/macrophages in different tumor microenvironments. Biochim. Biophys. Acta 1835, 170–179.

200. Lee, J.I., Soria, J.C., Hassan, K.A. (2001). Loss of PTEN expression as a prognostic marker for tongue cancer. Arch Otolaryngol Head Neck Surg; 127; 1441–1445.

201. Lee, K.S., Kwon, O.Y., Lee, J.H., Kwon, K., Min, K.J., Jung, S.A., Kim, A.K., You, K.H., Tatar, M., Yu, K. (2008). Drosophila short neuropeptide F signalling regulates growth by ERK-mediated insulin signalling. Nature Cell Biol 10, 468–475

202. Lee, M., & Yoon, J. H. (2015). Metabolic interplay between glycolysis and mitochondrial oxidation: The reverse Warburg effect and its therapeutic implication. World journal of biological chemistry, 6(3), 148–161.

203. Lemaitre, B., Reichhart, J.M., Hoffmann, J.A. (1997). Drosophila host defense: differential induction of antimicrobial peptide genes after infection by various classes of microorganisms. Proc Natl Acad Sci USA 94: 14614–14619.

204. Lewis, C. A., Parker, S. J., Fiske, B. P., McCloskey, D., Gui, D. Y., Green, C. R., Vokes, N. I., Feist, A. M., Vander Heiden M. G., Metallo C. M., (2014). Tracing compartmentalized NADPH metabolism in the cytosol and mitochondria of mammalian cells. Mol. Cell 55, 253–263

205. Li, H., Tennessen, J.M. (2018).Preparation of Drosophila Larval Samples for Gas Chromatography-Mass Spectrometry (GC-MS)-based Metabolomics. J. Vis. Exp. (136):57847. doi: 10.3791/57847.

206. Li, Y., Padmanabha, D., Gentile, L. B., Dumur, C. I., Beckstead, R. B., & Baker, K. D. (2013). HIF- and non-HIF-regulated hypoxic responses require the estrogen-related receptor in Drosophila melanogaster. PLoS genetics, 9(1), e1003230.

207. Lien, E.C. & Vander Heiden, M.G. (2019). A framework for examining how diet impacts tumour metabolism. Nature Reviews Cancer 19(11), 651–661.

208. Linden, W., Vodermaier, A., Mackenzie, R., Greig, D. (2012) Anxiety and depression after cancer diagnosis: prevalence rates by cancer type, gender, and age. J Affect Disord. 141:343–51.

209. Litzenburger, U. M., Opitz, C. A., Sahm, F., Rauschenbach, K. J., Trump, S., Winter, M., Ott, M., Ochs, K., Lutz, C., Liu, X., Anastasov, N., Lehmann, I., Höfer, T., von Deimling, A., Wick, W., & Platten, M. (2014). Constitutive IDO expression in human cancer is sustained by an autocrine signaling loop involving IL-6, STAT3 and the AHR. Oncotarget, 5(4), 1038–1051.

210. Lobry, C., Oh, P., and Aifantis, I. (2011). Oncogenic and tumor suppressor functions of Notch in cancer: it's NOTCH what you think. The Journal of experimental medicine, 208(10), 1931–1935. doi:10.1084/jem.20111855

211. Locasale, J. W., Grassian, A. R., Melman, T., Lyssiotis, C. A., Mattaini, K. R., Bass, A. J., Heffron, G., Metallo, C. M., Muranen, T., Sharfi, H., Sasaki, A. T., Anastasiou, D., Mullarky, E., Vokes, N. I., Sasaki, M., Beroukhim, R., Stephanopoulos, G., Ligon, A. H., Meyerson, M., Richardson, A. L., Chin, L., Wagner, G., Asara, J. M., Brugge, J. S., Cantley, L. C., Vander Heiden, M. G., (2011). Phosphoglycerate dehydrogenase diverts glycolytic flux and contributes to oncogenesis. Nat. Genet. 43, 869–874

212. Longo, V.D., Fontana, L. (2010). Calorie restriction and cancer prevention: Metabolic and molecular mechanisms. Trends Pharmacol Sci 31: 89–98.

213. Louvi A, Artavanis-Tsakonas S. (2012) Notch and disease: a growing field.Semin Cell Dev Biol. 23(4):473-80.

214. Lugo-Huitrón, R., Blanco-Ayala, T., Ugalde-Muñiz, P., Carrillo-Mora, P., Pedraza-Chaverrí, J., Silva-Adaya, D., Maldonado, P. D., Torres, I., Pinzón, E., Ortiz-Islas, E., López, T., García, E., Pineda, B., Torres-Ramos, M., Santamaría, A., & La Cruz, V. P. (2011). On the antioxidant properties of kynurenic acid: free radical scavenging activity and inhibition of oxidative stress. Neurotoxicology and teratology, 33(5), 538–547.

215. Lunt, S. Y., Vander Heiden, M. G., (2011). Aerobic glycolysis: Meeting the metabolic requirements of cell proliferation. Annu. Rev. Cell Dev. Biol. 27, 441–464

216. Luo, Z., Saha, A. K., Xiang, X. and Ruderman, N. B. (2005). AMPK, the metabolic syndrome and cancer. Trends Pharmacol Sci 26, 69-76

217. Mackenzie SM, Brooker MR, Gill TR, Cox GB, Howells AJ, Ewart GD. (1999). Mutations in the white gene of Drosophila melanogaster affecting ABC transporters that determine eye coloration. Biochim Biophys Acta. 1419:173–185.

218. Maddocks, O.D., Berkers, C.R., Mason, S.M., Zheng, L., Blyth, K., Gottlieb, E., Vousden, K.H. (2013). Serine starvation induces stress and p53-dependent metabolic remodelling in cancer cells. Nature 493:542–546.

219. Manalo, D. J., Rowan, A., Lavoie, T., Natarajan, L., Kelly, B. D., Ye, S. Q., Garcia, J. G., & Semenza, G. L. (2005). Transcriptional regulation of vascular endothelial cell responses to hypoxia by HIF-1. Blood, 105(2), 659–669.

220. Mantovani, A., Allavena, P., Sica, A., and Balkwill, F. (2008). Cancer-related inflammation. Nature 454, 436–444.

221. Marin-Valencia, I., Yang, C., Mashimo, T., Cho, S., Baek, H., Yang, X.L., Rajagopalan, K.N., Maddie, M., Vemireddy, V., Zhao, Z.,. (2012). Analysis of tumor metabolism reveals mitochondrial glucose oxidation in genetically diverse human glioblastomas in the mouse brain in vivo. Cell Metab.15:827–837

222. Markstein, M., Dettorre, S., Cho, J. (2014) Systematic screen of chemotherapeutics in Drosophila stem cell tumors. Proc Natl Acad Sci USA 111: 4530–4535

223. Martínez-Reyes, I. and Cuezva, J.M. (2014). The H+-ATP synthase: A gate to ROS-mediated cell death or cell survival. Biochimica et Biophysica Acta (BBA) 1837 (7): 1099-1112

224. Martinez-Reyes, I., Diebold, L. P., Kong, H., Schieber, M., Huang, H., Hensley, C. T., Mehta, M. M., Wang, T., Santos, J. H., Woychik, R., Dufour, E., Spelbrink, J. N., Weinberg, S. E., Zhao, Y., DeBerardinis, R. J., Chandel, N. S., (2016). TCA cycle and mitochondrial membrane potential are necessary for diverse biological functions. Mol. Cell 61, 199–209

225. Meier, T.B., Drevets, W.C., Wurfel, B.E., Ford, B.N., Morris, H.M., Victor, T.A. (2016) Relationship between neurotoxic kynurenine metabolites and reductions in right medial prefrontal cortical thickness in major depressive disorder. Brain Behav Immun. 53:39–48.

226. Meister, M., Lagueux, M. (2003). Drosophila blood cells. Cell Microbiol. 5: 573–580

227. Merlo, L. M., Pepper, J. W., Reid, B. J., and Maley, C. C. (2006). Cancer as an evolutionary and ecological process. Nat Rev Cancer 6, 924-935.

228. Micchelli, C.A., Esler, W.P., Kimberly, W.T., Jack, C., Berezovska, O., Kornilova, A., Hyman, B.T., Perrimon, N. and Wolfe, M.S. (2003). Gamma-secretase/presenilin inhibitors for Alzheimer's disease phenocopy Notch mutations in Drosophila. FASEB Journal (Federation of American Societies for Experimental Biology) 17: 79–81

229. Miele, L., Golde, T., & Osborne, B. (2006). Notch signaling in cancer. Current molecular medicine, 6(8), 905–918Palomero, T., Lim, W. K., Odom, D. T., Sulis, M. L., Real, P. J., Margolin, A., Barnes, K. C., O'Neil, J., Neuberg, D., Weng, A. P., Aster, J. C., Sigaux, F., Soulier, J., Look, A. T., Young, R. A., Califano, A., & Ferrando, A. A. (2006). NOTCH1 directly regulates c-MYC and activates a feed-forward-loop transcriptional network promoting leukemic cell growth. Proceedings of the National Academy of Sciences of the United States of America, 103(48), 18261–18266.

230. Migneco, G., Whitaker-Menezes, D., Chiavarina, B., Castello-Cros, R., Pavlides, S., Pestell, R. G., Fatatis, A., Flomenberg, N., Tsirigos, A., Howell, A., Martinez-Outschoorn, U. E., Sotgia, F., & Lisanti, M. P. (2010). Glycolytic cancer associated fibroblasts promote breast cancer tumor growth, without a measurable increase in angiogenesis: evidence for stromal-epithelial metabolic coupling. Cell cycle (Georgetown, Tex.), 9(12), 2412–2422.

231. Milán, M., Campuzano, S. and García-Bellido, A. (1996). Cell cycling and patterned cell proliferation in the wing primordium of Drosophila. Proc. Natl. Acad. Sci. USA 93, 640-645.

232. Milán, M., Campuzano, S. and García-Bellido, A. (1997). Developmental parameters of cell death in the wing disc of Drosophila. Proc. Natl. Acad. Sci. USA 94, 5691-5696.

233. Mitchell, A.J., Chan, M., Bhatti, H., Halton, M., Grassi, L., Johansen, C., (2011) Prevalence of depression, anxiety, and adjustment disorder in oncological, haematological, and palliative-care settings: a meta-analysis of 94 interview-based studies. Lancet Oncol. 12:160–74.

234. Moffett, J.R., Namboodiri, M.A. (2003). Tryptophan and the immune response. Immunol Cell Biol. 81:247–65.

235. Moroni, F., Cozzi, A., Carpendo, R., Cipriani, G., Veneroni, O., & Izzo, E. (2005). Kynurenine 3-mono-oxygenase inhibitors reduce glutamate concentration

in the extracellular spaces of the basal ganglia but not in those of the cortex or hippocampus. Neuropharmacology, 48(6), 788–795.

236. Muellner, M.K., Uras, I.Z, Gapp, B.V., Kerzendorfer, C., Smida, M., Lechtermann, H., Craig-Mueller, N., Colinge, J., Duernberger, G. and Nijman, S.M.B. (2011) A chemical-genetic screen reveals a mechanism of resistance to PI3K inhibitors in cancer. Nat Chem Biol 7: 787–793

237. Mukherjee, T., Kim, W. S., Mandal, L., & Banerjee, U. (2011). Interaction between Notch and Hif-alpha in development and survival of Drosophila blood cells. Science (New York, N.Y.), 332(6034), 1210–1213.

238. Muller, A. J., Malachowski, W. P., & Prendergast, G. C. (2005). Indoleamine 2,3-dioxygenase in cancer: targeting pathological immune tolerance with small-molecule inhibitors. Expert opinion on therapeutic targets, 9(4), 831–849.

239. Muller, A.J., DuHadaway, J.B., Donover, P.S., Sutanto-Ward, E., Prendergast, G.C. (2005). Inhibition of indoleamine 2,3-dioxygenase, an immunoregulatory target of the cancer suppression gene Bin1, potentiates cancer chemotherapy. Nat Med. 11:312–319.

240. Munn, D. H., & Mellor, A. L. (2007). Indoleamine 2,3-dioxygenase and tumor-induced tolerance. The Journal of clinical investigation, 117(5), 1147–1154.

241. Murphy M. P., (2009). How mitochondria produce reactive oxygen species. Biochem. J. 417, 1–13

242. Murray, M.F. (2003). Nicotinamide: An oral antimicrobial agent with activity against both mycobacterium tuberculosis and human immunodeficiency virus. Clin Infect Dis.36:453–60.

243. Murray, P.J. (2016) Amino acid auxotrophy as a system of immunological control nodes. Nat Immunol. 17:132–9. 10.

244. Nam, S.Y., Lee HS, Jung GA. (2003). Akt/PKB activation in gastric carcinomas correlates with clinicopathologic variables and prognosis. APMIS: 111: 1105–1113.

245. Nave, B.T., Ouwens, M., Withers, D.J., Alessi, D.R., Shepherd, P.R. (1999). Mammalian target of rapamycin is a direct target for protein kinase B: Identification of a convergence point for opposing effects of insulin and amino-acid deficiency on protein translation. Biochem J; 344: 427–431.

246. Navrotskaya, V., Wnorowski, A., Turski, W. (2018). Effect of Kynurenic Acid on Pupae Viability of Drosophila melanogaster cinnabar and cardinal Eye Color

Mutants with Altered Tryptophan-Kynurenine Metabolism. Neurotox Res 34, 324–331

247. Neckameyer, W. S., Coleman, C. M., Eadie, S., & Goodwin, S. F. (2007). Compartmentalization of neuronal and peripheral serotonin synthesis in Drosophila melanogaster. Genes, brain, and behavior, 6(8), 756–769.

248. Nemoto, S., Finkel, T. (2002). Redox regulation of forkhead proteins through a p66shc-dependent signaling pathway. Science 295: 2450–2452, 2002.

249. Ng, C.G., Boks, M.P., Zainal, N.Z., de Wit, N.J. (2011). The prevalence and pharmacotherapy of depression in cancer patients. J Affect Disord. 131:1–7.

250. Norden, D.M., Devine, R., Bicer, S., Jing, R., Reiser, P.J., Wold, L.E. (2015) Fluoxetine prevents the development of depressive-like behavior in a mouse model of cancer related fatigue. Physiol Behav. 140:230–5.

251. Novak, M. G., & Rowley, W. A. (1994). Serotonin depletion affects blood-feeding but not host-seeking ability in Aedes triseriatus (Diptera: Culicidae). Journal of medical entomology, 31(4), 600–606.

252. Novak, M. G., Ribeiro, J. M., & Hildebrand, J. G. (1995). 5-hydroxytryptamine in the salivary glands of adult female Aedes aegypti and its role in regulation of salivation. The Journal of experimental biology, 198(Pt 1), 167–174.

253. Nowak, K., Seisenbacher, G., Hafen, E., Stocker, H. (2013). Nutrient restriction enhances the proliferative potential of cells lacking the tumor suppressor PTEN in mitotic tissues. elife 2:e00380

254. Ntziachristos, P., Lim, J.S., Sage, J. and Aifantis, I. (2014) From Fly Wings to Targeted Cancer Therapies: A Centennial for Notch Signaling. Cancer Cell 25: 318–334

255. O'Connor, J.C., Lawson, M.A., André, C., Moreau, M., Lestage, J., Castanon, N. (2009) Lipopolysaccharide-induced depressive-like behavior is mediated by indoleamine 2,3-dioxygenase activation in mice. Mol Psychiatry. 14:511–22.

256. Okuda, S., Nishiyama, N., Saito, H., & Katsuki, H. (1998). 3-Hydroxykynurenine, an endogenous oxidative stress generator, causes neuronal cell death with apoptotic features and region selectivity. Journal of neurochemistry, 70(1), 299–307.

257. Okuda, S., Nishiyama, N., Saito, H., Katsuki, H. (1996). Hydrogen peroxide-mediated neuronal cell death induced by an endogenous neurotoxin, 3-hydroxykynurenine. Proc Natl Acad Sci USA 93(22):12553–12558

258. Opitz, C. A., Litzenburger, U. M., Sahm, F., Ott, M., Tritschler, I., Trump, S., Schumacher, T., Jestaedt, L., Schrenk, D., Weller, M., Jugold, M., Guillemin, G. J., Miller, C. L., Lutz, C., Radlwimmer, B., Lehmann, I., von Deimling, A., Wick, W., & Platten, M. (2011). An endogenous tumour-promoting ligand of the human aryl hydrocarbon receptor. Nature, 478(7368), 197–203.

259. Opitz, C. A., Litzenburger, U. M., Sahm, F., Ott, M., Tritschler, I., Trump, S., Schumacher, T., Jestaedt, L., Schrenk, D., Weller, M., Jugold, M., Guillemin, G. J., Miller, C. L., Lutz, C., Radlwimmer, B., Lehmann, I., von Deimling, A., Wick, W., & Platten, M. (2011). An endogenous tumour-promoting ligand of the human aryl hydrocarbon receptor. Nature, 478(7368), 197–203.

260. Osaki, M., Oshimura, M., Ito, H. (2004). The PI3K-Akt pathway: Its functions and alterations in human cancer. Apoptosis. 9 (6): 667-676.

261. Oudot, C., Auclerc, M.F, Levy, V., Porcher, R., Piguet, C., Perel, Y., Gandemer, V., Debre, M., Vermylen, C., Pautard, B., Berger, C., Schmitt, C., Leblanc, T., Cayuela, J.M., Socie, G., Michel, G. Leverger, G., Baruchel, A.. (2008). Prognostic factors for leukemic induction failure in children with acute lymphoblastic leukemia and outcome after salvage therapy: the FRALLE 93 study. J Clin Oncol. 26(9):1496–1503

262. Owusu-Ansah, E., Banerjee, U. (2009). Reactive oxygen species prime Drosophila haematopoietic progenitors for differentiation. Nature 24;461(7263):537-41.

263. Oxenkrug GF. (2015). Increased plasma levels of xanthurenic and kynurenic acids in type 2 diabetes. Mol Neurobiol. 52:805–810.

264. Palomero, T., Sulis, M.L., Cortina, M., Real, P.J., Barnes, K., Ciofani, M., Caparros, E., Buteau, J., Brown, K., Perkins, S.L., *et al.* (2007). Mutational loss of PTEN induces resistance to NOTCH1 inhibition in T-cell leukemia. Nature medicine 13:1203-1210

265. Palomero, T., and Ferrando, A. (2008). Oncogenic NOTCH1 control of MYC and PI3K: challenges and opportunities for anti-NOTCH1 therapy in T-cell acute lymphoblastic leukemias and lymphomas. Clinical cancer research: an official journal of the American Association for Cancer Research, 14(17), 5314–5317.

266. Pandey, U.B., Nichols, C.D. (2011) Human disease models in Drosophila melanogaster and the role of the fly in therapeutic drug discovery. Pharmacol Rev 63: 411–436

267. Parrott, J.M., Redus, L., Santana-Coelho, D., Morales, J., Gao, X, O'Connor, J.C. (2016). Neurotoxic kynurenine metabolism is increased in the dorsal hippocampus and drives distinct depressive behaviors during inflammation. Transl Psychiatry. 6:e918.

268. Pasco, M. Y., & Léopold, P. (2012). High sugar-induced insulin resistance in Drosophila relies on the lipocalin Neural Lazarillo. PloS one, 7(5), e36583.

269. Pastor-Pareja, J. C., Wu, M., and Xu, T. (2008). An innate immune response of blood cells to tumors and tissue damage in Drosophila. Dis. Model Mech. 1, 144–154.

270. Pavlova, N.N., Thompson, C.B. (2016). The emerging hallmarks of cancer metabolism. Cell Metab 23:27–47.10.

271. Pearson, A.M., Baksa, K., Rämet, M., Protas, M., McKee, M., Brown, D., Ezekowitz, R.A. (2003). Identification of cytoskeletal regulatory proteins required for efficient phagocytosis in Drosophila. Microbes Infect. 5: 815–824.

272. Pellicciari, R., Amori, L., Costantino, G., Giordani, A., Macchiarulo, A., Mattoli, L., Pevarello, P., Speciale, C., & Varasi, M. (2003). Modulation of the kynurine pathway of tryptophan metabolism in search for neuroprotective agents. Focus on kynurenine-3-hydroxylase. Advances in experimental medicine and biology, 527, 621–628.

273. Pendse, J., Ramachandran, P. V., Na, J., Narisu, N., Fink, J. L., Cagan, R. L., Collins, F. S., & Baranski, T. J. (2013). A Drosophila functional evaluation of candidates from human genome-wide association studies of type 2 diabetes and related metabolic traits identifies tissue-specific roles for dHHEX. BMC genomics, 14, 136.

274. Perez-Garijo, A., Shlevkov, E., Morata, G. (2009). The role of Dpp and Wg in compensatory proliferation and in the formation of hyperplastic overgrowths caused by apoptotic cells in the Drosophila wing disc. Development 136: 1169–1177

275. Perez-Tenorio, G., Stal, O. (2002). Activation of AKT/PKB in breast cancer predicts a worse outcoming among endocrine treated patients. Br J Cancer; 86: 540–545.

276. Petkau, K., Ferguson, M., Guntermann, S., and Foley, E. (2017). Constitutive immune activity promotes tumorigenesis in Drosophila intestinal progenitor cells. Cell Rwp. 20(8):1784-1793.

277. Phan, L.M., Yeung, S.C., Lee, M.H. (2014). Cancer metabolic reprogramming: importance, main features, and potentials for precise targeted anti-cancer therapies. Cancer Biol Med. Mar; 11(1): 1–19.

278. Pilotte, L., Larrieu, P., Stroobant, V., Colau, D., Dolusic, E., Frédérick, R., De Plaen, E., Uyttenhove, C., Wouters, J., Masereel, B., & Van den Eynde, B. J. (2012). Reversal of tumoral immune resistance by inhibition of tryptophan 2,3-dioxygenase. Proceedings of the National Academy of Sciences of the United States of America, 109(7), 2497–2502.

279. Platten, M., Wick, W., Van den Eynde, B.J. (2012). Tryptophan catabolism in cancer: beyond IDO and tryptophan depletion. Cancer Res. 72:1–6.

280. Platten, M., von Knebel Doeberitz, N., Oezen, I., Wick, W., Ochs, K. (2014). Cancer Immunotherapy by Targeting IDO1/TDO and Their Downstream Effectors. Front Immunol. 5:673.

281. Possemato, R., Marks, K. M., Shaul, Y. D., Pacold, M. E., Kim, D., Birsoy, K., Sethumadhavan, S., Woo, H.-K., Jang, H. G., Jha, A. K., Chen, W. W., Barrett, F. G., Stransky, N., Tsun, Z.-Y., Cowley, G. S., Barretina, J., Kalaany, N. Y., Hsu, P. P., Ottina, K., Chan, A. M., Yuan, B., Garraway, L. A., Root, D. E., Mino-Kenudson, M., Brachtel E. F., Driggers E. M., Sabatini D. M., (2011). Functional genomics reveal that the serine synthesis pathway is essential in breast cancer. Nature 476, 346–350

282. Powers, R. W., Kaeberlein, M., Caldwell, S. D., Kennedy, B. K. and Fields, S. (2006). Extension of chronological life span in yeast by decreased TOR pathway signaling. Genes Dev 20, 174-84

283. Prendergast, G. C., Malachowski, W. P., DuHadaway, J. B., & Muller, A. J. (2017). Discovery of IDO1 Inhibitors: From Bench to Bedside. Cancer research, 77(24), 6795–6811. https://doi.org/10.1158/0008-5472.CAN-17-2285

284. Pugh, T.D., Oberley, T.D., Weindruch, R. (1999). Dietary intervention at middle age: caloric restriction but not dehydroepiandrosterone sulfate increases lifespan and lifetime cancer incidence in mice. Cancer Res. 59:1642–1648.

285. Rajan, A. and Perrimon, N. (2013). Of flies and men: insights on organismal metabolism from fruit flies. BMC Biol 11, 38

286. Razzell, W., Wood, W., Martin, P. (2011). Swatting flies: modelling wound healing and inflammation in Drosophila. Disease Models and Mechanisms 4: 569-574

287. Read, R. D., Bach, E. A. and Cagan R. L. (2004). Drosophila C-terminal Src kinase negatively regulates organ growth and cell proliferation through inhibition of the Src, Jun N-terminal kinase, and STAT pathways. Mol. Cell. Biol. 24, 6676-6689.

288. Reginaldo C, Jacques P, Scott T, Oxenkrug G, Selhub J, Paul L. Xanthurenic acid is associated with higher insulin resistance and higher odds of diabetes. FASEB J. 2015;29:20

289. Rizzo P, Osipo C, Foreman K, Golde T, Osborne B, Miele L. (2008). Rational targeting of Notch signaling in cancer. Oncogene. Sep 1;27(38):5124-31.

290. Romero-Garcia, S., Lopez-Gonzalez, J.S., Báez-Viveros, J.L., Aguilar-Cazares, D., Prado-Garcia, H. (2011). Tumor cell metabolism: an integral view. Cancer Biol Ther 12: 939-948

291. Rous P. (1914). THE INFLUENCE OF DIET ON TRANSPLANTED AND SPONTANEOUS MOUSE TUMORS. The Journal of experimental medicine, 20(5), 433–451.

292. Roy, J., Galano, J.M., Durand, T., Le Guennec, J.Y., Lee, J.C.. (2017). Physiological role of reactive oxygen species as promoters of natural defenses. FASEB J. 31(9):3729-3745.

293. Rubin, G.M., Yandell, M.D., Wortman, J.R. *et al* (2000) Comparative genomics of the eukaryotes. Science 287: 2204–2215

294. Ryoo, H.D., Gorenc, T., Steller, H. (2004) Apoptotic cells can induce compensatory cell proliferation through the JNK and the Wingless signaling pathways. Dev Cell 7: 491–501

295. Saito, Y., Chapple, R. H., Lin, A., Kitano, A., Nakada, D. (2015). AMPK protects leukemia-initiating cells in myeloid leukemias from metabolic stress in the bone marrow. Cell Stem Cell 17, 585–596

296. Sakurai, T., Maeda, S., Chang, L., Karin, M. (2006). Loss of hepatic NF-kappa B activity enhances chemical hepatocarcinogenesis through sustained c-Jun N-terminal kinase 1 activation. Proc Natl Acad Sci U S A. 2006;103:10544-51

297. Salmena, L., Carracedo, A., Pandolfi, P.P. (2008). Tenets of PTEN tumor suppression. Cell 2;133(3):403-14

298. Samadi, P., Grégoire, L., Rassoulpour, A., Guidetti, P., Izzo, E., Schwarcz, R., & Bédard, P. J. (2005). Effect of kynurenine 3-hydroxylase inhibition on the dyskinetic and antiparkinsonian responses to levodopa in Parkinsonian

monkeys. Movement disorders: official journal of the Movement Disorder Society, 20(7), 792–802.

299. Sato, Y., Ohshima, T., Kondo, T. (1999). Regulatory role of endogenous interleukin-10 in cutaneous inflammatory response of murine wound healing. Biochem Biophys Res Commun. 265 (1): 194–9.

300. Savitz, J., Drevets, W.C., Wurfel, B.E., Ford, B.N., Bellgowan, P.S., Victor, T.A. (2015) Reduction of kynurenic acid to quinolinic acid ratio in both the depressed and remitted phases of major depressive disorder. Brain Behav Immun. 46:55–9.

301. Savvateeva, E., Popov, A., Kamyshev, N., Bragina, J., Heisenberg, M., Senitz, D., Kornhuber, J., & Riederer, P. (2000). Age-dependent memory loss, synaptic pathology and altered brain plasticity in the Drosophila mutant cardinal accumulating 3-hydroxykynurenine. Journal of neural transmission (Vienna, Austria : 1996), 107(5), 581–601.

302. Sawicki, R., Singh, S.P., Mondal, A.K., Benes, H., Zimniak, P. (2003). Cloning, expression and biochemical characterization of one Epsilon-class (GST-3) and ten Delta-class (GST-1) glutathione S-transferases from Drosophila melanogaster, and identification of additional nine members of the Epsilon class. Biochem J. 370:661–669.

303. Schoppmann, S.F., Birner, P., Stöckl, J., Kalt, R., Ullrich, R., Caucig, C., Kriehuber, E., Nagy, K., Alitalo, K., Kerjaschki, D. (2002). Tumor-associated macrophages express lymphatic endothelial growth factors and are related to peritumoral lymphangiogenesis. Am. J. Pathol. 161, 947–956

304. Schramek, D., Kotsinas, A., Meixner, A., Wada, T., Elling, U., Pospisilik, J.A., Neely, G.G., Zwick, R.H., Sigl, V., Forni, G., Serrano, M., Gorgoulis, V.G., Penninger, J.M. (2011). The stress kinase MKK7 couples oncogenic stress to p53 stability and tumor suppression. Nat Genet. 43(3):212-9.

305. Schug, Z. T., Peck, B., Jones, D. T., Zhang, Q., Grosskurth, S., Alam, I. S., Goodwin, L. M., Smethurst, E., Mason, S., Blyth, K., McGarry, L., James, D., Shanks, E., Kalna, G., Saunders, R. E., Jiang, M., Howell, M., Lassailly, F., Thin, M. Z., Spencer-Dene, B., Stamp, G., van den Broek, N. J. F., Mackay, G., Bulusu V., Kamphorst, J. J., Tardito, S., Strachan, D., Harris, A. L., Aboagye, E. O., Critchlow, S. E., Wakelam, M. J. O., Schulze, A., Gottlieb, E., (2015). Acetyl-CoA synthetase 2 promotes acetate utilization and maintains cancer cell growth under metabolic stress. Cancer Cell 27, 57–71

306. Schwarcz, R., Whetsell, W.O. Jr, Mangano, R.M. (1983). Quinolinic acid: An endogenous metabolite that produces axon-sparing lesions in rat brain. Science 219(4582):316–318.

307. Schwartsburd. P. (2019). Cancer-Induced Reprogramming of Host Glucose Metabolism: "Vicious Cycle" Supporting Cancer Progression. Front Oncol. 9: 218.

308. Searles, L. L., & Voelker, R. A. (1986). Molecular characterization of the Drosophila vermilion locus and its suppressible alleles. Proceedings of the National Academy of Sciences of the United States of America, 83(2), 404–408.

309. Sekulic, A., Hudson, C.C., Homme, J.L. (2000). A direct linkage between the phosphoinositide 3-kinase-AKT signaling pathway and the mammalian target of rapamycin in mitogenstimulated and transformed cells. Cancer Res 60: 3504– 3513.

310. Sell, C. (2003). Caloric restriction and insulin-like growth factors in aging and cancer. Horm Metab Res. 35:705–711.

311. Semenza, G.L. (2012). Hypoxia-inducible factors in physiology and medicine. Cell 148, 399–408

312. Semenza, G.L. (2010). HIF-1: upstream and downstream of cancer metabolism. Curr Opin Genet Dev.20(1):51-56)

313. Serhan, C.N., Savill, J. (2005). Resolution of inflammation: the beginning programs the end. Nat. Immunol. 6 (12): 1191–7.

314. Sforzini, L., Nettis, M.A., Mondelli, V., Pariante, C.M. (2019) Inflammation in cancer and depression: a starring role for the kynurenine pathway. Psychopharmacology. 236:2997–3011.

315. Shaw, R.J. (2006). Glucose metabolism and cancer. Curr Opin Cell Biol 18: 598-608

316. Sheridan C. (2015). IDO inhibitors move center stage in immuno-oncology. Nature biotechnology, 33(4), 321–322.

317. Shimada, Y., Kinoshita, M., Harada, K., Mizutani, M., Masahata, K., Kayama, H., & Takeda, K. (2013). Commensal bacteria-dependent indole production enhances epithelial barrier function in the colon. PloS one, 8(11), e80604.

318. Shlevkov, E., Morata, G. (2012) A dp53/JNK-dependent feedback amplification loop is essential for the apoptotic response to stress in Drosophila. Cell Death Differ 19: 451–460

319. Silva, A., Jotta, P.Y., Silveira, A.B. and Ribeiro, D. , Brandalise, S.R., Yunes, J.A., Barata, J.T. (2009) Regulation of PTEN by CK2 and Notch1 in primary T-cell

acute lymphoblastic leukemia: rationale for combined use of CK2-and gamma-secretase inhibitors. Haematologica. 95(4):674-8

320. Sjölund, J., Manetopoulos, C., Stockhausen, M.T., Axelson, H. (2005). The Notch pathway in cancer: Differentiation gone awry. European Journal of Cancer 41 (17) 2620-2629

321. Smith-Bolton, R.K., Worley, M.I., Kanda, H., Hariharan, I.K. (2009) Regenerative growth in Drosophila imaginal discs is regulated by Wingless and Myc. Dev Cell 16: 797–809

322. Soderhall, K., Cerenius, L. (1998). Role of the prophenoloxidase-activating system in invertebrate immunity. Curr Opin Immunol 10: 23–28.

323. Song, M.S., Salmena, L., Pandolfi, P.P. (2012). The functions and regulation of the PTEN tumour suppressor. Nat Rev Mol Cell Biol. 13(5):283-96

324. Song, M.S., Carracedo, A., Salmena, L., Song, S.J., Egia, A., Malumbres, M., Pandolfi, P.P. (2011). Nuclear PTEN regulates the APC-CDH1 tumor suppressive complex in a phosphatase-independent manner. Cell 144(2): 187–199

325. Sonowal, R., Swimm, A., Sahoo, A., Luo, L., Matsunaga, Y., Wu, Z., Bhingarde, J. A., Ejzak, E. A., Ranawade, A., Qadota, H., Powell, D. N., Capaldo, C. T., Flacker, J. M., Jones, R. M., Benian, G. M., & Kalman, D. (2017). Indoles from commensal bacteria extend healthspan. Proceedings of the National Academy of Sciences of the United States of America, 114(36), E7506–E7515.

326. Stambolic, V., Suzuki, A., de la Pompa, J.L., Brothers, G.M., Mirtsos, C., Sasaki, T., Ruland, J., Penninger, J.M., Siderovski, D.P., Mak, T.W. (1998). Negative regulation of PKB/Akt-dependent cell survival by the tumor suppressor PTEN. Cell. 95(1):29-39.

327. Stark, M. B. (1918). An hereditary tumor in the fruit fly, Drosophila. Am. Assoc. Cancer Res. J. 3, 279-301.

328. Stark, M. B. (1919b). An hereditary tumor. J. Exp. Zool. 27, 509-529.

329. Steinhilber, D., Fischer, A.S., Metzner, J., Steinbrink, S.D., Roos, J., Ruthardt, M., and Maier, T.J. (2010). 5-lipoxygenase: underappreciated role of a proinflammatory enzyme in tumorigenesis. Front. Pharmacol. 1, 143.

330. Stevens, E.A., Mezrich, J.D., Bradfield, C.A. (2009). The aryl hydrocarbon receptor: a perspective on potential roles in the immune system. Immunology. 127:299–311.

331. Stincone, A., Prigione, A., Cramer, T., Wamelink, M. M. C., Campbell, K., Cheung, E., Olin-Sandoval, V., Grüning, N.-M., Krüger, A., Tauqeer Alam, M., Keller, M. A., Breitenbach, M., Brindle, K. M., Rabinowitz, J. D., Ralser, M., (2014). The return of metabolism: Biochemistry and physiology of the pentose phosphate pathway. Biol. Rev. Camb. Philos. Soc. 90, 927–963

332. Stocker, H., & Hafen, E. (2000). Genetic control of cell size. Current opinion in genetics & development, 10(5), 529–535.

333. Stone, T. W., & Perkins, M. N. (1981). Quinolinic acid: a potent endogenous excitant at amino acid receptors in CNS. European journal of pharmacology, 72(4), 411–412.

334. Stratton, M. R., Campbell, P. J., and Futreal, P. A. (2009). The cancer genome. Nature 458, 719-724.

335. Sulis ML, Parsons R. (2003) PTEN: from pathology to biology. Trends Cell Biol. 13:478–83.

336. Sullivan, D.T., Bell, L.A., Paton, D.R., Sullivan, M.C. (1980). Genetic and functional analysis of tryptophan transport in Malpighian tubules of Drosophila. Biochem Genet. 18:1109–1130.

337. Sullivan, L.B., Chandel, N.S. (2014). Mitochondrial reactive oxygen species and cancer. Cancer Metab 2: 17

338. Sutphin, P.D., Chan, D.A., Giaccia, A.J.. (2004). Dead cells don't form tumors: HIF-dependent cytotoxins. Cell Cycle.3(2):160-163

339. Sykiotis, G.P. and Bohmann, K. (2008). Keap1/Nrf2 signaling regulates oxidative stress tolerance and lifespan in Drosophila. Dev Cell. 14(1): 76–85.

340. Tannenbaum A, Silverstone H. (1953). Effect of limited food intake on survival of mice bearing spontaneous mammary carcinoma and on the incidence of lung metastases. Cancer Res. 13:532–536.

341. Tannenbaum a. (1954). Dietary factors in carcinogenesis. Acta - Unio Internationalis Contra Cancrum, 10(3), 117–122.

342. Tannenbaum, A. and Silverstone, H. (1953). Nutrition in Relation to Cancer. Advances in Cancer Research 1: 451-501

343. Tannenbaum, A., Silverstone, H. (1949). The influence of the degree of caloric restriction on the formation of skin tumors and hepatomas in mice. Cancer Res. 9:724–727.

344. Tearle R. (1991). Tissue specific effects of ommochrome pathway mutations in Drosophila melanogaster. Genetical research, 57(3), 257–266.

345. Thompson HJ, Zhu Z, Jiang W. (2003). Dietary energy restriction in breast cancer prevention. J Mammary Gland Biol Neoplasia. ;8:133–142.

346. Toba, G., Ohsako, T., Miyata, N., Ohtsuka, T., Seong, K. H., & Aigaki, T. (1999). The gene search system. A method for efficient detection and rapid molecular identification of genes in Drosophila melanogaster. Genetics, 151(2), 725–737.

347. Tomas, S.R., Terentis, A.C., Cai, H (2007) Post-tra nslational regulation of human indoleamine 2,3-dioxygenase activit y by nitric oxide. J Biol Chem. 282:23778–23787.

348. Tournier, C. (2013). The 2 Faces of JNK Signaling in Cancer. Genes & cancer,4(9-10), 397–400.

349. Trachootham, D., Alexandre, J., Huang, P. (2009). Targeting cancer cells by ROS-mediated mechanisms: a radical therapeutic approach? Nat Rev Drug Discov.. 8(7):579-91

350. Trachootham, D., Lu, W., Ogasawara, M.A., Nilsa, R.D., Huang, P. (2008). Redox regulation of cell survival. Antioxid Redox Signal 10: 1343-1374

351. Uyttenhove, C., Pilotte, L., Théate, I., Stroobant, V., Colau, D., Parmentier, N., Boon, T., & Van den Eynde, B. J. (2003). Evidence for a tumoral immune resistance mechanism based on tryptophan degradation by indoleamine 2,3-dioxygenase. Nature medicine, 9(10), 1269–1274.

352. Van Es, J.H., van Gijn, M.E., Riccio, O., van den Born, M., Vooijs, M., Begthel, H., Cozijnsen, M., Robine, S., Winton, D.J., Radtke, F and Clevers H. (2005). Notch/γ-secretase inhibition turns proliferative cells in intestinal crypts and adenomas into goblet cells. Nature. 435(7044):959-63.

353. Van Vlierberghe, P. and Ferrando, A. (2012). The molecular basis of T cell acute lymphoblastic leukemia. The Journal of clinical investigation 122: 3398-3406

354. Vander Heiden, M.G., DeBerardinis, R.J. (2017) Understanding the intersections between metabolism and cancer biology. Cell 168:657–69.

355. Vellai, T., Takacs-Vellai, K., Zhang, Y., Kovacs, A.L., Orosz, L., Müller, F. (2003). Genetics: influence of TOR kinase on lifespan in C. elegans. Nature 426, 620

356. Vidal, M., and Cagan, R. L. (2006). Drosophila models for cancer research. Curr Opin Genet Dev 16, 10-16.

357. Villegas, S. N., Gombos, R., García-López, L., Gutiérrez-Pérez, I., García-Castillo, J., Vallejo, D. M., Da Ros, V. G., Ballesta-Illán, E., Mihály, J., & Dominguez, M. (2018). PI3K/Akt Cooperates with Oncogenic Notch by Inducing Nitric Oxide-Dependent Inflammation. Cell reports, 22(10), 2541–2549

358. Villegas, S.N. (2019). One hundred years of Drosophila cancer research: no longer in solitude. Dis. Model. Mech 12(4): dmm039032

359. Villegas, S.N., Ferres-Marco, D., Domínguez, M. (2019). Using Drosophila Models and Tools to Understand the Mechanisms of Novel Human Cancer Driver Gene Function. The Drosophila Model in cancer, Advances in experimental medicine and biology 1167. Springer Nature.

360. Vyas, S., Zaganjor, E., & Haigis, M. C. (2016). Mitochondria and Cancer. Cell, 166(3), 555–566.

361. Walker, A., Howells, A.J., Tearle, R.G. (1986). Cloning and characterization of the vermilion gene of Drosophila melanogaster. Mol. Gen. Genet. 202: 102--107.

362. Wang, C., Youle, R.J. (2009).The role of mitochondria in apoptosis. Annu Rev Genet 43: 95-118

363. Wang, D., and Dubois, R.N. (2010). Eicosanoids and cancer. Nat. Rev. Cancer 10, 181–193.

364. Wang, G.L., Semenza, G.L. (1995). Purification and characterization of hypoxia-inducible factor 1.The Journal of Biological Chemistry. 270(3):1230-1237

365. Wang, L., Kounatidis, I. and Ligoxygakis, P. (2014). Drosophila as a model to study the role of blood cells in inflammation, innate immunity and cancer. Front. Cell. Infect. Microbiol. 3: 113.

366. Wang, Q., Somwar, R., Bilan, P.J. (1999). Protein kinase /Akt participates in GLUT4 translocation by insulin in L6 myoblasts. Mol Cell Biol; 19: 4008–4018.

367. Wang, T., Liu, G., Wang, R. (2014). The Intercellular Metabolic Interplay between Tumor and Immune Cells.Front Immunol. 5:358.

368. Warburg, O. (1925). The metabolism of carcinoma cells. The Journal of Cancer Research. 9(1):148–163.

369. Warburg, O. (1956). On the origin of cancer cells. Science 123:309-314

370. Warren, W.D., Palmer, S., Howells, A.J. (1996). Molecular characterization of the cinnabar region of Drosophila melanogaster: identification of the cinnabar transcription unit. Genetica 98(3): 249--262.

371. Wei, H., Leeds, P., Chen, R. W., Wei, W., Leng, Y., Bredesen, D. E., & Chuang, D. M. (2000). Neuronal apoptosis induced by pharmacological concentrations of 3-hydroxykynurenine: characterization and protection by dantrolene and Bcl-2 overexpression. Journal of neurochemistry, 75(1), 81–90.

372. Weinberg, F., Chandel, N.S. (2009). Mitochondrial metabolism and cancer. Ann NY Acad Sci 1177: 66-73

373. Weinberg, F., Hamanaka, R., Wheaton, W. W., Weinberg, S., Joseph, J., Lopez, M., Kalyanaraman, B., Mutlu, G. M., Budinger, G. R. S., Chandel, N. S., (2010). Mitochondrial metabolism and ROS generation are essential for Kras-mediated tumorigenicity. Proc. Natl. Acad. Sci. U.S.A. 107, 8788–8793

374. Weindruch R, Walford RL. (1982). Dietary restriction in mice beginning at 1 year of age: effect on life-span and spontaneous cancer incidence. Science. ;215:1415–1418

375. Weinstein, I.B., Joe, A.K. (2006). Mechanisms of disease: Oncogene addiction--a rationale for molecular targeting in cancer therapy. Nat Clin Pract Oncol. (8):448-57.

376. Whitehead, T. R., Price, N. P., Drake, H. L., & Cotta, M. A. (2008). Catabolic pathway for the production of skatole and indoleacetic acid by the acetogen Clostridium drakei, Clostridium scatologenes, and swine manure. Applied and environmental microbiology, 74(6), 1950–1953.

377. Whitmarsh, A.J., Davis, R.J. (2007). Role of mitogen- activated protein kinase kinase 4 in cancer. Oncogene. 26:3172-84

378. Wikoff, W. R., Anfora, A. T., Liu, J., Schultz, P. G., Lesley, S. A., Peters, E. C., & Siuzdak, G. (2009). Metabolomics analysis reveals large effects of gut microflora on mammalian blood metabolites. Proceedings of the National Academy of Sciences of the United States of America, 106(10), 3698–3703.

379. Williams, C. S., Mann, M. and DuBois, R. N. (1999). The role of cyclooxygenases in inflammation, cancer, and development. Oncogene 18, 7908–7916

380. Willoughby, L.F., Schlosser, T,, Manning, S.A., Parisot, J.P., Street, I.P., Richardson, H.E., Humbert, P.O., Brumby, A.M. (2013). An in vivo large-scale

chemical screening platform using Drosophila for anti-cancer drug discovery. Disease Models and Mechanisms 6: 521-529

381. Wirthgen, E., Hoeflich, A., Rebl, A., Gunther, J. (2017). Kynurenic acid: the Janus-faced role of an immunomodulatory tryptophan metabolite and its link to pathological conditions. Front Immunol.8: 1957

382. Wlodarska, M., Luo, C., Kolde, R., d'Hennezel, E., Annand, J. W., Heim, C. E., Krastel, P., Schmitt, E. K., Omar, A. S., Creasey, E. A., Garner, A. L., Mohammadi, S., O'Connell, D. J., Abubucker, S., Arthur, T. D., Franzosa, E. A., Huttenhower, C., Murphy, L. O., Haiser, H. J., Vlamakis, H., Xavier, R. J. (2017). Indoleacrylic Acid Produced by Commensal Peptostreptococcus Species Suppresses Inflammation. Cell host & microbe, 22(1), 25–37.e6.

383. Wood, Z. A., Poole, L. B., & Karplus, P. A. (2003). Peroxiredoxin evolution and the regulation of hydrogen peroxide signaling. Science. 300(5619), 650–653.

384. Wood, W., Faria, C. and Jacinto, A. (2006). Distinct mechanisms regulate hemocyte chemotaxis during development and wound healing in Drosophila melanogaster. J. Cell Biol. 173, 405–416

385. Wu, Y., and Zhou, B. P. (2009). Inflammation: a driving force speeds cancer metastasis. Cell Cycle 8, 3267–3273.

386. Yamamoto, S., Tomita, Y., Hoshida, Y. (2004). Prognostic significance of activated Akt expression in pancreatic ductal adenocarcinoma. Clin Cancer Res 10: 2846–2850.

387. Yang, M., Soga, T., Pollard, P. J., (2013). Oncometabolites: Linking altered metabolism with cancer. J. Clin. Invest. 123, 3652–3658

388. Yeung, S.J., Pan, J., Lee, M.H. (2008). Roles of p53, MYC and HIF-1 in regulating glycolysis - the seventh hallmark of cancer. Cell Mol Life Sci 65: 3981-3999

389. Yoo, H., Stephanopoulos, G., Kelleher, J. K., (2004). Quantifying carbon sources for de novo lipogenesis in wild-type and IRS-1 knockout brown adipocytes. J. Lipid Res. 45, 1324–1332

390. Youle, R.J., Narendra, D.P. (2011). Mechanisms of mitophagy. Nat Rev Mol Cell Biol. 12(1):9-14.

391. Yuan, Q., Lin, F., Zheng, X., & Sehgal, A. (2005). Serotonin modulates circadian entrainment in Drosophila. Neuron, 47(1), 115–127.

392. Yuan, T. L., & Cantley, L. C. (2008). PI3K pathway alterations in cancer: variations on a theme. Oncogene, 27(41), 5497–5510.

393. Zelante, T., Iannitti, R. G., Cunha, C., De Luca, A., Giovannini, G., Pieraccini, G., Zecchi, R., D'Angelo, C., Massi-Benedetti, C., Fallarino, F., Carvalho, A., Puccetti, P., & Romani, L. (2013). Tryptophan catabolites from microbiota engage aryl hydrocarbon receptor and balance mucosal reactivity via interleukin-22. Immunity, 39(2), 372–385.

394. Zerofsky, M., Harel, E., Silverman, N. and Tatar, M. (2005).Aging of the innate immune response in Drosophila melanogaster. Aging Cell 4, 103–108

395. Zhang, W., Thompson, B.J., Hietakangas, V. and Cohen, S.M. (2011). MAPK/ERK signaling regulates insulin sensitivity to control glucose metabolism in Drosophila. PLoS Genet 7, e1002429

396. Zheng, J. (2012). Energy metabolism of cancer: Glycolysis versus oxidative phosphorylation. Oncol Lett 4: 1151-1157

397. Zhu Z, Haegele AD, Thompson HJ. (1997). Effect of caloric restriction on pre malignant and malignant stages of mammary carcinogenesis. Carcinogenesis. 18:1007–1012.

398. Zwaans, B.M., Lombard, D.B. (2014). Interplay between sirtuins, MYC and hypoxia-inducible factor in cancer-associated metabolic reprogramming. Dis Model Mech 7: 1023-1032

5. Agradecimientos

Mientras escribo estas palabras, una de las etapas más importantes de mi vida está a punto de concluir. Me miro al espejo y veo a la mujer que de niña soñaba con ser astrónoma y que anotaba en un cuaderno la posición de la luna cada noche y el número de cráteres que observaba con los viejos prismáticos de mi padre. Me quedaba entonces por delante mucho tiempo para descubrir mi verdadera vocación y, al final, no fui astrónoma, pero entendí que mi verdadera pasión era la biología. En todas y cada una de las etapas de mi vida he ido evolucionando y quizá ya no queda tanto de aquella niña, aunque en esencia sea la misma. El doctorado ha sido, sin duda, el periodo en el que mayor crecimiento personal he experimentado, al fin y al cabo, seis años dan para mucho.

Dedicarse a la investigación no siempre es fácil, a menudo tienes que enfrentarte a grandes dosis de frustración. Sin embargo, uno aprende a tolerar y a relativizar todo eso con el tiempo, y cuando por fin ves que avanzas o que descubres algo nuevo te sientes muy satisfecho.

Seré sincera. Tener un título está bien, tener algún *paper* también, sentirse realizado académica y laboralmente, y todo eso. Pero, para mí, lo que realmente vale la pena de llegar hasta aquí es haberme topado con las personas más maravillosas, que no sólo me han facilitado todo el proceso, sino que han sacado lo mejor de mí y que muchos formarán parte de mi vida, espero, ya para siempre.

Todo esto no hubiera sido posible sin que María me diera la oportunidad de entrar en su laboratorio. Pero María no es sólo la puerta de entrada. Gracias por confiar en mí, incluso cuando ni yo misma lo hacía. Gracias por comprenderme en mis momentos más duros y por ser tan humana.

Tengo la suerte de poder afirmar que todas las personas que están y estuvieron en este laboratorio hacen que estar ahí adentro durante muchas horas y muchos años sea casi como estar en familia. Y es que en ese sentido me he sentido tan querida y apoyada por vosotros, que no tengo más que agradecer…

A Laura, por darme siempre un punto de vista optimista. Eres un ser de luz, sin maldad, siempre amable y confiable. Para alguien como yo, que a veces soy un poco gris, tenerte al lado pasando moscas ha sido una verdadera suerte.

A Rosa, porque sin ti el laboratorio se cae. Eres una auténtica profesional y nosotros un poco "tonticos" con los papeleos a veces, menos mal que estás siempre para ayudarnos. Y como persona, qué decir, eres un trocito de pan de pueblo, de Elda por ejemplo.

A Irene Oliveira, una de las mujeres más sabias que he conocido nunca. Me has dado siempre buenos consejos, te has preocupado por mí y sabes que el cariño es mutuo.

A Mari, que simplemente yo quiero ser como tú de mayor. Un ejemplo de templanza y de saber disfrutar de la vida.

A Javier, porque siempre hemos tenido buena relación y por aceptar ser parte de mi tribunal de tesis. Además, el surtido de ibéricos que me regalaste está en mi top 1 de regalos del amigo invisible.

A Isabel, porque honestamente, eres una tía ~~de p*** madre~~ genial. Coincidimos en muchas cosas y da gusto poder compartir ideas contigo y nutrirme también de ese positivismo y espíritu emprendedor.

A Dolors, por ser una fuente de conocimiento. Gracias por compartirlo con nosotros los mortales, eso es algo que solo alguien con un gran corazón como tú puede hacer y es un honor tenerte en el lab.

A Dianilla, porque si Dolors es la reina de la genética, tú directamente ¿hay alguna técnica de molecular que no sepas hacer? Eres otro ejemplo a seguir, por tu perseverancia y por la amabilidad con que tratas a los que vamos a preguntarte cual moscas cansinas cada dos por tres. No me olvido del tiempo en el que hemos colaborado juntas y trabajado codo con codo. Y aunque no me salía casi ningún experimento de ese proyecto, aprendí mucho a tu lado.

A Nahuel, por enseñarme tanto y por confiar en mis capacidades. Por las conversaciones sobre todo tipo de temáticas en tu despacho, los consuelos y los chistes de Zuperhéroes. Todo el mundo querría tener a un guía como tú. Me alegro mucho de que hayas llegado tan lejos y de que tu trabajo sea reconocido, te lo mereces.

Y a Esther, gracias simplemente por ser tú. Confío mucho en ti, me da mucha paz hablar contigo porque siempre me siento mejor después, porque tenemos una forma de pensar muy parecida y encima a las dos nos flipan los fenómenos paranormales. Cuando tengo el día regulero me escuchas y me aconsejas, aunque estés súper liada. Espero mantenerte por mucho tiempo en mi vida.

También por este laboratorio han pasado otros estudiantes de doctorado. Con ellos se crea una gran complicidad, se comparten penas y alegrías y se crean vínculos, algunos de ellos, casi indestructibles.

A Roberto, porque no sólo eres un genio, sino que transmites muy buen rollo y paz. Me alegro mucho de haber compartido estos años contigo, sé que vas a llegar muy lejos.

A Ernesto, por tener la iniciativa de aprender y por soportarme como "jefa chunga". También por las divagaciones y los salseos a las seis de la tarde, que no todo va a ser trabajar. Te auguro un gran futuro en la ciencia, así que sigue trabajando así de bien.

A Juan, porque tienes mucho coco, niño. Y porque solemos tener formas de ver las cosas muy parecidas, siempre es un gusto tener una charlita contigo. Te deseo mucha suerte en todo.

Quizá por la dificultad de los inicios, a estos tres que van ahora les tengo un especial cariño.

Te doy gracias, Irenilla, pues eres la persona a la que más admiraba y admiro. Fuiste siempre un ejemplo para mí y no sabes cuánto me alegra haber sido testigo de tu historia de superación y verte ahora en la más plena felicidad. Además sé que puedo contar siempre contigo, amiga.

A Pol, porque además de ser una de las personas más nobles que conozco, todos queríamos tener tu templanza y tu filosofía para conllevar las penurias del doctorado, pero también porque ves siempre el lado bueno de las cosas y tener a un amigo como tú es todo un privilegio.

A Sergio, joder, es que a ti te quiero un montonazo. Es que hasta nos fuimos de viaje por Nueva York y nos tomamos una cerveza de lata en un rascacielos de lujo. No solo has sido uno de los pilares fundamentales durante mi estancia en el laboratorio, sino que a día de hoy sigues siendo una de esas personas a las que nunca dejaría marchar. Sé que

conseguirás todo lo que te propongas (porque soy medio brujilla) y yo espero estar ahí para verlo.

A Dani, aunque no has estado desde mi principio, yo sí he estado desde el tuyo. Me acuerdo de cuando eras apenas un bebé. Te he visto crecer y hacer tu propio camino. La vida nos dio un golpe demasiado duro, pero tú nunca te has detenido. Eres extraordinario y estoy orgullosa de ti, te mereces todo lo bueno que la vida te ofrezca, yo siempre voy a estar ahí. Y él también.

Uno de los varios puntos de inflexión de mi tesis fue irme a Estados Unidos de estancia. A las personas que más me ayudaron allí les estoy inmensamente agradecida.

Thank you Jason for give me the opportunity of learning and staying in your lab, for being always kind and helpful with me. Being alone in a foreign country can be very hard sometimes, so thanks to Madhulika, Zoher and Yasaman, because they worried about me and helped me a lot, something that I will never acknowledge enough. Thanks also to Nader, Kylie, Vicky, Dr. Jon and all the people there for helping me with all the technical issues and for teaching me how to perform metabolomics.

La suerte de estar aquí no sólo me ha llevado a conocer a gente maravillosa en el laboratorio, también fuera de él en otros laboratorios. Allá por 2014 empezaba todo esto, en el máster de neurociencias. Qué geniales eran todos y cada uno de mis compañeros, cuántos momentos épicos compartimos…

Algunos se quedaron y otros se fueron, y aunque para todos tengo lugar en mi memoria y en mi corazón, algunos ocupan un lugar especial en mi vida.

Gracias a Andrea, porque tienes un gran corazón y todo lo necesario para alcanzar todas tus metas en la vida, nunca dudes de ello.

Gracias a Fran Quiles, eres la alegría de la huerta, sensato, sensible y sencillamente un amor de persona.

Gracias a Marta, por ser un soplo de aire fresco y movernos para ir tachando los planes y restaurantes de la lista. Y tremendamente adorable, espero que no cambies nunca.

También a Carla, Elena, Sergio Cano, Sandy Brownie, Juan Medrano, Chrysa, Nerea, Mine… A todos vosotros gracias por haber formado o formar parte de esta etapa. Hacéis todo más fácil y me habéis brindado muchos buenos momentos.

Gracias a mis amigos Fran y Ainara, juntos los tres desde principio a fin. Os admiro y os quiero tanto, para vosotros sobran las palabras, el tiempo y las experiencias que hemos vivido hablan por sí solas.

Gracias a Noemi, eres una mujer increíble, puedes llegar a donde tú quieras. Estaré a tu lado siempre que me necesites y si hace falta pondré "la cara de digna" para recordarte lo valiosa que eres. I love you bebé.

Gracias a mi canaria favorita, Aysha, porque haber pasado una cuarentena juntas y conocerte mejor ha sido lo mejor de este odioso 2020. Desde el primer día que hablamos por teléfono cuando estabas buscando piso sentí como si te conociera de toda la vida, y ya ves, al final te has convertido en alguien muy importante para mí. Espero tenerte siempre, amiga.

Gracias a Irene. Tú literalmente has sido capaz de sacar lo mejor de mí misma. Gracias a ti estoy cumpliendo uno de mis sueños, poder tener mi propio grupo de música. Un proyecto que comenzamos juntas y que crece cada día más. Eres admirable como científica y como persona, y te quiero mucho.

Gracias a mi mejor amiga Karen, porque eres como una hermana. Mi más fiel apoyo, sabes todo de mí. Hasta ahora y los que nos quede por delante, juntas. Gracias a mi amigo Jaime, porque sé que pase lo que pase siempre podemos contar el uno con el otro.

Por último, aunque no menos importante, gracias a mi familia. A mi madre, padre, hermano y hermana. Sé que os sentís orgullosos de mí, pero sin vosotros yo no sería quien soy. Me habéis apoyado toda mi vida en cada decisión que he tomado y habéis creído en mí, algo que no siempre he sido capaz de hacer ni yo misma. Sois mi refugio y los que me devolvéis a la realidad si alguna vez veo todo un poco negro.

Qué suerte la mía, después de tantos años, que entre todos me habéis pintado la mente de color. Termino mi doctorado siendo mejor de lo que era cuando empecé, con más a autoestima y confianza, siendo más optimista y, en definitiva, con muchas más luces que sombras. Gracias a todos, que la fuerza os acompañe.